

# Journal of Energy

ISSN 1849-0751 (On-line)  
ISSN 0013-7448 (Print)  
UDK 621.31

**VOLUME 64 Number 1–4 | 2015 Special Issue**

- 03** I. Kuzle  
Department of Energy and Power Systems – 80 years of success in science, teaching and cooperation with industry
- 29** S. Krajcar, P. Ilak, I. Rajšl  
Hydropower plant simultaneous bidding in electricity market and ancillary services markets
- 52** D. Feretić, Ž. Tomšić  
Multi-criteria evaluation of nuclear option
- 62** B. Franc, I. Uglešić, S. Piliškić  
Lightning data utilization in power system control
- 78** Ž. Tomšić, I. Gašić, G. Čačić  
Energy management in the public building sector – ISGE/ISEMIC model
- 90** D. Grgić, S. Šadek, V. Benčik, D. Konjarek  
Decay heat calculation for spent fuel pool application
- 102** M. Brezovac, I. Kuzle, M. Krpan  
Detailed mathematical and simulation model of a synchronous generator
- 130** J. Kajić, H. Pirić, F. Rendulić, M. Cerjan, M. Delimar  
Impact of various hydro power generation scenarios on energy balance and power markets in SEE region
- 148** S. Krajcar, I. Rajšl, P. Ilak  
Risk-averse approach for assessment of investment in a run-of-the-river power plants while considering reduced water availability
- 163** S. Šadek, D. Grgić  
NPP Krško containment modelling with the ASTEC code
- 178** Ž. Tomšić  
From market uncertainty to policy uncertainty for investment in power generation: real options for NPP on electricity market
- 198** V. Benčik, D. Grgić, N. Čavlina, S. Šadek  
Optimization of OPDT protection for overcooling accidents
- 217** Ž. Tomšić, T. Galić  
Analysis of fuel cell technologies for micro-cogeneration devices in the households and service sector
- 245** V. Milardić, I. Pavić  
Analysis of surge arresters failures in the installation of broadcasting transmitter
- 258** J. Havelka, A. Marušić, I. Kuzle, H. Pandžić, T. Capuder  
Hands-on experience with power systems laboratory upgrade
- 275** I. Pavić, F. Tomašević, I. Damjanović  
Application of artificial neural networks for external network equivalent modeling
- 285** Z. Zbunjak, H. Bašić, H. Pandžić, I. Kuzle  
Phase shifting autotransformer, transmission switching and battery energy storage systems to ensure n-1 criterion of stability

# Journal of Energy

Scientific Professional Journal Of Energy, Electricity, Power Systems

Online ISSN 1849-0751, Print ISSN 0013-7448, VOL 64

## Published by

HEP d.d., Ulica grada Vukovara 37, HR-10000 Zagreb

HRO CIGRÉ, Berislavićeva 6, HR-10000 Zagreb

## Publishing Board

Robert Krklec, (president) HEP, Croatia,

Božidar Filipović-Grčić, (vicepresident), HRO CIGRÉ, Croatia

## Editor-in-Chief

Goran Slipac, HEP, Croatia

## Associate Editors

Helena Božić HEP, Croatia

Stjepan Car Končar-Electrical Engineering Institute, Croatia

Tomislav Gelo University of Zagreb, Croatia

Davor Grgić University of Zagreb, Croatia

Mićo Klepo Croatian Energy Regulatory Agency, Croatia

Stevo Kolundžić Croatia

Vitomir Komen HEP, Croatia

Marija Šiško Kuliš HEP, Croatia

Dražen Lončar University of Zagreb, Croatia

Goran Majstrovic Energy Institute Hrvoje Požar, Croatia

Tomislav Plavšić Croatian Transmission system Operator, Croatia

Dubravko Sabolić Croatian Transmission system Operator, Croatia

Mladen Zeljko Energy Institute Hrvoje Požar, Croatia

## International Editorial Council

Anastasios Bakirtzis University of Thessaloniki, Greece

Eraldo Banovac J.J. Strossmayer University of Osijek, Croatia

Frano Barbir University of Split, Croatia

Tomislav Barić J.J. Strossmayer University of Osijek, Croatia

Frank Bezzina University of Malta

Srećko Bojić Power System Institute, Zagreb, Croatia

Tomislav Capuder University of Zagreb, Croatia

Ante Elez Končar-Generators and Motors, Croatia

Dubravko Franković University of Rijeka, Croatia

Hrvoje Glavaš J.J. Strossmayer University of Osijek, Croatia

Mevludin Glavić University of Liege, Belgium

Božidar Filipović Grčić University of Zagreb, Croatia

Dalibor Filipović Grčić Končar-Electrical Engineering Institute, Croatia

Josep M. Guerrero Aalborg Universitet, Aalborg East, Denmark

Dirk Van Hertem KU Leuven, Faculty of Engineering, Belgium

Žarko Janić Siemens-Končar-Power Transformers, Croatia

Igor Kuzle University of Zagreb, Croatia

Niko Malbaša Ekoner, Croatia

Matislav Majstrovic University of Split, Croatia

Zlatko Maljković University of Zagreb, Croatia

Predrag Marić J.J. Strossmayer University of Osijek, Croatia

Viktor Milardić University of Zagreb, Croatia

Srete Nikolovski J.J. Strossmayer University of Osijek, Croatia

Damir Novosel Quanta Technology, Raleigh, USA

Hrvoje Pandžić University of Zagreb, Croatia

Milutin Pavlica Power System Institute, Zagreb, Croatia

Robert Sitar Končar-Electrical Engineering Institute, Croatia

Damir Sumina University of Zagreb, Croatia

Elis Sutlović University of Split, Croatia

Zdenko Šimić Joint Research Centre, Petten, The Netherlands

Damir Šljivac J.J. Strossmayer University of Osijek Croatia

Darko Tipurić University of Zagreb, Croatia

Bojan Trkulja University of Zagreb, Croatia

Nela Vlahinić Lenz University of Split, Croatia

Mario Vražić University of Zagreb, Croatia

## INTRODUCTION

This special issue of the Journal of Energy is dedicated to the establishment of today the **Department for Energy and Power Systems (ZVNE)**, University of Zagreb Faculty of Electrical Engineering and Computing in 1934. In that time the High Voltage Department as part of the Technical Faculty. For this reason, the history of the **Department for Energy and Power Systems** is presented in the introductory article, while the other articles are part of a broad scientific and professional work of the employees of the Department and some of the articles were created in wide cooperation with experts from the companies, that graduated from the Department.

Journal of Energy special issue: present 17 papers selected for publication in Journal of Energy after having undergone the peer review process. We would like to thank the authors for their contributions and the reviewers who dedicated their valuable time in selecting and reviewing these papers. We hope this special issue will provide you valuable information of some achievements at Department of Energy and Power Systems, Faculty of Electrical Engineering and Computing.

Short introduction of scientific and expert work of the **Department for Energy and Power Systems (ZVNE)**:

Besides educational energy related programmes for undergraduate, graduate and postgraduate students, **DEPARTMENT OF ENERGY AND POWER SYSTEMS** has been actively involved for many years in many scientific and expert studies. Studies on scientific projects include collaboration with industry, national institutions, electric utilities, and many foreign universities.

The Department has developed valuable international cooperation with many research institutions around the world, either directly or through inter-university cooperation.

The Department is the leading institution in the field of electrical power engineering in the region, it has a long lasting cooperation with the economic sector, and it is recognized for its scientific activities and a large number of published scientific papers in globally relevant journals, as well as numerous national and international scientific projects.

Main Department areas of activities are:

- a) Power Engineering and Power Technologies,**
- b) Energy, Environment, Energy Management and**
- c) Nuclear Power Engineering**

In **Power Systems Engineering** the research is focused to development of both fundamental knowledge and applications of electrical power engineering. The research is generally directed to increasing the availability and the reliability of a power system with an emphasis on the adjustment to the open market environment. Specific goals include: improving models and methodologies for power system analysis, operation and control; development, production and application of models and methodologies for power systems planning, maintenance and development; application of soft-computing (artificial intelligence, meta-heuristics, etc.), information technologies (web-oriented technologies, geographic information systems, enterprise IT solutions, etc.) and operational research in improving processes of planning, development, exploitation and control of power systems; investigation on applications for coordinated control of power system devices and exploring the power system stability, security and economic operation; integration of intelligent devices and agents in energy management systems and distribution management systems equipment and software; advanced modelling of dynamics, disturbances and transient phenomena in transmission and distribution networks (in particular regarding distributed generation); advances in fault detection, restoration and outage management. The researches also cover high voltage engineering. At time of global changes in the energy sector, with emphasis on sustainable development, significant efforts are devoted to liberalization efforts, facilities revitalization, improved legislation and adoption of new standards.

In area of **Power Technologies, Energy and Environment, Energy Management** the main framework for the research are: sustainable electricity generation on a liberalized market, modelling ETS and electricity market; energy security and climate change; power system optimization with emission trading; rational use of energy and energy savings; energy management in industry and buildings; energy conservation and energy auditing in industry and buildings. General objective of the research is to develop methodologies for quantitative assessment of the environmental impact of applicable energy technologies (electric power producing plants and their technology chains), as a base for estimating optimal long-term development strategy of the Croatian power system. Research work includes new strategies of energy sector and power system development; preparing medium and long-term electricity generation expansion plan for power system; comparison of energy, economic and environmental characteristics of different options for electric

power generation; studies for rational use of energy and energy savings, assuming a centralized structure of the electricity market. Research work also includes renewable energy sources and its role in power sector, as well as electricity production considering cap on CO2 emissions. Research covers development of new models for power system generation optimization and planning under uncertainties on the open electricity market. The goal of that research is to create analytical and software tools which will enable a successful transition to liberalized electricity market and ensure healthy and efficient power system operation in compliance with environmental requirements.

In the **Nuclear Energy Field** research cover nuclear physics reactor theory, nuclear power plants, fuel cycles and reactors materials and general objective of the research is to develop methodologies for reliable assessment of nuclear power plants operational safety. In the nuclear energy field the specific analysis cover calculations of transients and consequences of potential accidents in NPP Krško. In the field of safety analyses of nuclear power plants the research activities are oriented to the mathematical modelling of nuclear power plant systems and components.

## Guest Editors

prof. dr. sc. Željko Tomšić

prof. dr. sc. Igor Kuzle

Department of Energy and Power Systems

University of Zagreb Faculty of Electrical Engineering and Computing

**IGOR KUZLE**

[igor.kuzle@fer.hr](mailto:igor.kuzle@fer.hr)

**University of Zagreb Faculty of Electrical Engineering  
and Computing**

## **DEPARTMENT OF ENERGY AND POWER SYSTEMS – 80 YEARS OF SUCCESS IN SCIENCE, TEACHING AND COOPERATION WITH INDUSTRY**

### **SUMMARY**

The Department of Energy and Power Systems of the Faculty of Electrical Engineering and Computing, University of Zagreb was founded in 1934 and celebrated its 80th anniversary in 2014. In its long history, many well-known experts, members of the Department, have left their mark on the power engineering activity in Croatia. The Department has been studying and creating improvements in the fields of production, transmission, distribution and final use of electricity, renewable energy sources, advanced power grids, electricity management problems, electricity trading and markets problems and usage of other forms of energy.

Throughout the years, the Department has become the leading institution in the field of electrical power engineering in the region, maintaining long-term cooperation with the industry sector and has been recognized for scientific activity since the time of professor Požar and his establishment principles of the Zagreb School of Energy. Determined to remain a respectable research institution, the Department undertakes scientific research at the highest international levels through which valuable international cooperation with many research institutions around the world has been established.

**Key words:** Department of Energy and Power Systems; Electrical engineering; Energy; Power systems; Faculty; Anniversary; Curriculum

## 1. INTRODUCTION

The Department of Energy and Power Systems studies and brings improvements in the fields of generation, transmission, distribution and the use of electrical energy, energy efficiency, high voltage engineering, renewable energy sources, smart grids, problems of power systems management, nuclear engineering and safety, electricity markets etc.. The Department has been the leading institution in the field of electrical power engineering in the region, with the long lasting cooperation with the utilities and industry, and has been recognized for its scientific activities and a large number of published scientific papers in globally relevant journals, as well as numerous national and international scientific projects. In parallel, during the years the Department continued its development with a commitment to the permanent improvement of its curriculum.

This article describes the history of the Department of Energy and Power Systems, its current infrastructure and plans for the future. It mentions the most important people contributing to the development of the Department, describes the curriculum modifications and provides insights into the less known historic facts from the 80 years long Department history. At the end, the paper shows the ongoing project of the transition of the existing Power systems laboratory to a modern Smart Grids Laboratory (SGLab) serving within a Bologna Declaration compliant curriculum.

## 2. HISTORY OF THE DEPARTMENT

### 2.1. The Department establishment and High-Voltage Current study profile.

The Technical College in Zagreb was founded by the decree of the State Commissioners' Council on 10<sup>th</sup> of December 1918 and welcomed its first students on 1<sup>st</sup> of October 1919. It was one of the first technical high education schools in the South-east Europe. Among other departments, the College had the Department of Electrical Engineering. On 31<sup>st</sup> of March 1926 the Technical College was transformed into a faculty, joined with University of Zagreb and renamed to College of Engineering [1]. Already in academic year 1921/22. the first power engineering subjects appeared when honorary teachers Ing. **Edgar Montina** lectured the subject “Decree of the Electrical Centers and the Network”, and in the academic year 1926/27. Ing **Miroslav Plohl** lectured the subject “Transmission and Distribution of Electricity and High-Voltage Techniques”. It is interesting to mention that from the beginning of the studies until the early 60s, under the influence of the German study methodology, the study programme was divided into two basic profiles: the High-Voltage Current profile and the Low-Voltage Current profile.

Professor **Juro Horvat**, associate professor at the University of Ljubljana, who came to the College of Engineering in Zagreb in the summer semester of year 1932/33., was employed as the first permanent lecturer in the field of power

engineering as a full professor. When Juro Horvat joined the College of Engineering, the course “Power Engineering” was introduced, followed by “Electric Energy Production” in the academic year 1933/1934 and by “Transient Processes in Electrical Devices” in the academic year 1935/1936. After the tragic death of Professor Miroslav Plohl in late 1939, **Anton Dolenc** took over the duty of part-time lecturer in the subjects of High-Voltage Techniques.

	<p>Juro Horvat, dipl. ing, was born on 17<sup>th</sup> of April 1882 in Gospić, where he finished elementary school. He finished high school in Vinkovci in 1900 and electromechanical engineering graduate studies at the Graz Technical High School in 1904. After graduating, he worked in factories around Stuttgart, Geneva and eventually as director of the company "Energos" in Vienna. He worked on the first Slovenian HPP "Fala" on Drava river. From 1924 he was a lecturer at the Faculty of Engineering in Ljubljana and from 1932 at the Faculty of Engineering in Zagreb. He was the founder of the High voltage department in 1934. He in parallel dealt with problems of electrification and published papers in the respected journals of that time such as <i>Electrotechnik und Maschinenbau</i>. He was one of the founders of the Banovinski Electrical Engineering Company in 1937 in Zagreb. He retired in 1947 and passed away in Zagreb on 18<sup>th</sup> April 1954.</p>
---	---

The arrival of prof. Horvat fulfilled the preconditions for establishment of The Department of Energy and Power Systems, which was established by the Faculty council of the Technical College on its 129<sup>th</sup> regular session held on June 26<sup>th</sup>, 1934. Under item 13 of the agenda (Figure 1) the proposal of prof. ing. Jure Horvat to establish a Laboratory for High voltage engineering was accepted, which today's Department of Energy and Power Systems originates from. As a Head of the Chair of Electricity Generation, Transmission and Distribution prof. Horvat founded the Department to enable laboratory work for the students, as well as to enable scientific research and professional work of the staff. He was the first Head of the Department (Table I). Through his work, some of the instruments and equipment were acquired, together with technical magazines and books, which were the foundation for the establishment of the Department's laboratories and libraries.

Table I Department's Heads

	Head of the Department	Mandate	
1.	Prof. ing. Juro Horvat	1934.-1943.	<ul style="list-style-type: none"> <li>• Since its establishment, the Department has been led by 14 Department Heads</li> <li>• The founder of the Department and its first Head was prof. ing. Juro Horvat.</li> <li>• The longest mandate as a Head of the Department belongs to prof. dr. sc. Božidar Stefanini who led the Department for 24 years. In ac. year 1958/59. at the same time he served as the Faculty Dean and as the Head of the Department</li> <li>• In ac. year 2002/03 the function of Head's assistant was introduced. Four lecturers have been performing this function so far.</li> </ul>
2.	Prof. ing. Vladimir Žepić	1948.-1952.	
3.	Prof. dr. sc. Božidar Stefanini	1952.-1976.	
4.	Academician dr. sc. Hrvoje Požar	1976.-1978.	
5.	Prof. dr. sc. Mario Padelin	1978.-1982.	
6.	Doc. Željko Zlatar	1982.-1986.	
7.	Prof. dr. sc. Danilo Feretić	1986.-1990.	
8.	Prof. dr. sc. Vladimir Mikuličić	1990.-1994.	
9.	Prof. dr. sc. Vjekoslav Filipović	1994.-1998.	
10.	Prof. dr. sc. Zdravko Hebel	1998.-2002.	<b>Head's assistant</b>
11.	Prof. dr. sc. Slavko Krajcar	2002.-2006.	Prof. dr. sc. Nenad Debrecin
12.	Prof. dr. sc. Nenad Debrecin	2006.-2010.	Prof. dr. sc. Tomislav Tomiša
13.	Prof. dr. sc. Tomislav Tomiša	2010.-2014.	Prof. dr. sc. Igor Kuzle
14.	Prof. dr. sc. Igor Kuzle	2014.- today	Prof. dr. sc. Davor Grgić

P O Z I V

na 129 redovnu sjednicu Savjeta Tehničkog fakulteta Univerziteta  
Kraljevine Jugoslavije u Zagrebu za utorak dne 26 juna 1934 u 16 sati.

Dnevni red:

- 1/ Čitanje zapisnika 128 redovne sjednice.
- 2/ Izvještaj dekana.
- 3/ Izvještaji starješina.
- 4/ Izbor dekana za 1934/35 školsku godinu.
- 5/ Predlog prof. dra Njegovana i dra ing. Hanamana da se univ. docent dr ing. Krajinović Matija postavi za vanrednog profesora za katedru za Organsku kemijsku tehnologiju / II čitanje/.
- 6/ Predlog prof. ing. Plohla i ing. Horvat Jure da se univ. docent Dr Lončar Josip postavi za vanrednog profesora za katedru za Osnove elektro tehnike i električna mjerenja /Teorijsku elektrotehniku i električna mjerenja/ /II čitanje/.
- 7/ Predlog prof. dra Njegovana i dra Plotnikova da se dr. ing. Prelog Vladimir postavi za univerzitetskog docenta za katedru za Organske hemiju. /II čitanje/.
- 8/ Predlog Arhitektonsko-inženjerskog otdjeka da se predavanja iz Uredjenja gradova /Urbanizma/ 2 i 2 u zimskom semestru i 2 i 4 u ljetnom semestru povjere arh. Hribar Stjepanu kao honorarnom nastavniku uz propisani honorar po održanom času /II čitanje/.
- 9/ Predlog Gradjevno-inženjerskog otdjeka da se predavanja iz Arhitekture za gradjevinare 2 i 0 u zimskom i 2 i 2 u ljetnom semestru povjere ing. Denzler Juraju kao honorarnom nastavniku uz propisani honorar po održanom času /II čitanje/.
- 10/ Predlog prof. dr ing. Hanamana i prof. ing. Stipetića da se vanredni profesor ing. Sahazarov Artemij izabere i postavi za redovnog profesora na katedri za Mehaničku tehnologiju /I čitanje/.
- 11/ Predlog Arhitektonsko-inž. otdjeka i Gradjevno-inž. otdjeka da se raspise Stečaj za popunjenje jednog mjesta vanrednog profesora na katedri za Statiku konstrukcija.
- 12/ Predlog prof. ing. Plohla da se osnuje Laboratorij za slabu struju.
- 13/ Predlog prof. ing. Horvat Jure da se osnuje Laboratorij za visoki napon.
- 14/ Izvještaj Kuratorija, izbor članova Kuratorija zaklada Dra Jurja Žerjavića i za unutarnje uređenje.
- 15/ Izbor pretstavnika Tehničkog fakulteta u Odbor Univerzitetske biblioteke.
- 16/ Kventuslija.

U Zagrebu, dne 23 juna 1934.

Prodekan:

Dr. Njegovan, v. r.



Figure 1. Agenda of the 129<sup>th</sup> regular session of the Technical College on which the Department foundations were set

The beginning of the 2<sup>nd</sup> World War marks the beginning of the stagnation of Department activities. Prof. Horvat travels abroad, for which he was unwillingly retired later in 1943. After the end of the War, he returned to Zagreb, attempted to re-activate at the Faculty, but did not succeed and finally retired at the beginning of 1947.

After the 2<sup>nd</sup> World War the Department was consequently left with only two honorary lecturers: **Mladen Dokmanić**, dipl. ing., from academic year 1945/46, and **Fedor Jelušić**, dipl.ing. from academic year 1946/47. Everything had to be reinitiated from the start at a time when large number of students entered University and when the need for engineers was rapidly increasing in the developing country.

In academic year 1948/49 as a permanent teacher in the position of the associate professor **Vladimir Žepić**, dipl. ing. was selected. Vladimir Žepić later also becomes the Head of the Department.

Vladimir Žepić was born in 1894 in Zagreb, and before being admitted to the Department, he worked as an engineer at the municipal power station and was a prominent member of Rotary Club Zagreb. In 1945 he became the first technical manager of the Electrical Company of Croatia (ELPOH). He became the member of the Department in 1948. He was forced from the Faculty as a politically unsuited by the government at the end of the winter semester 1951/52. He died in 1971.

At the end of the 1940s new members come to the Department, members that will later be the bearers of development and will bring the Department international recognition. At the beginning of the summer semester 1949/50 the position of assistant professor in the Department was trusted to **Božidar Stefanini**, dipl. ing., and in academic year 1950/51. **Hrvoje Požar**, dipl. ing. was elected as the assistant and honorary professor. After the forced departure of prof. Žepić from the Faculty, Head of the Department at the beginning of ac. year



*Božidar Stefanini, PhD was born in Split on October 18, 1913. He graduated in 1937 at the Technical College of Zagreb. Until 1950 he worked on high voltage network implementation in Yugoslavia's power utility company and then moved to the Technical Faculty of Zagreb where he obtained his PhD in 1954. He was elected full professor in 1959 at the Faculty of Electrical Engineering. He was the head of the High-Voltage Department (from 1952 to 1976) and Dean of Faculty in 1958/59. He is one of the founders of the University Computing Center (SRCE) and the most prominent person for procurement, installation and implementation of IBM1130, first Computing System at the Faculty of Electrical Engineering. He taught the courses of Electric Power Transmission, High Voltage Engineering and Power System Stability. He wrote the first books on Fortran IV programming language and co-authored book "Matrix methods in power system network analysis" (1975). He received "Nikola Tesla" award for scientific work in 1972. He died in Zagreb in March 1991.*

1952/53 becomes Božidar Stefanini.

Since the beginning of the 1950's, the Departments intensive development has begun, which was enabled by more available laboratory space. The Department was first located in one, and later in two rooms at Rooswelt Square no. 6. In 1950 it moved to the first floor of the building in Vukotinovićeve Street no. 2, where it got

enough space for laboratories, from which the most important is the High-voltage laboratory established in 1954. The great credit for that goes to **Boris Markovčić**, dipl. ing. As the laboratory was established practicum for students was introduced in a form of 6 experimental exercises. In 1953, a photo-laboratory for slides production was installed at the Department, which were used for lectures. The study of High-voltage currents was nine- semester long and elective courses were introduced with the purpose of more focused student specialization.

As part of the study of High-Voltage Currents in the academic year 1950/51 two study profiles were established: Electro-industrial profile and Electric Power profile. The Department for High Voltage becomes the bearer of teachings in the



*Hrvoje Požar, PhD was born in Knin on July 5, 1916. He graduated in 1939 at the Technical Faculty of Zagreb. He started his career as power systems designer and dispatcher (1946-51) and then moved to Electrical department on the Technical Faculty (that later became Faculty of Electrical Engineering) where he obtained his PhD in 1955. He was elected full professor in 1960 and performed duty of a Dean in 1960/1962 and 1968/1970. He was the head of Department for High Voltage and Energy and the founder of the Zagreb Energy School. He was Yugoslavian Academy of Science and Arts associate member from 1965, full member from 1975 and secretary-General from 1978. From 1970 to 1972 he was the Vice-Rector of the University of Zagreb. Since 1976 he was Editor-in-Chief for Technical Encyclopedia (volumes V-XII). He also worked at the Institute for Electric Power from which today's Energy Institute "Hrvoje Požar" originates. He was a member of Croatian Constitutional Commission in 1990. He received numerous awards and acknowledgments. He received "Nikola Tesla" award for scientific work in 1963.*

Electric Power profile (Appendix I).

Special attention was also given to the professional work, which was carried out with extensive cooperation with the economy and industry sectors. At that time, scientific work was done not only by individual members of the Department but also by the Department as a whole with the extensive usage of expanding laboratory equipment and libraries. At that time **Branko Jermić**, long-term director of the TEŽ factory, joins the Department as a honorary professor of the subject "Electric Lighting".

## 2.2. 1956: Faculty of Electrical Engineering (ETF)

By the decision of the Parliament of the People's Republic of Croatia, on 26<sup>th</sup> of April 1956, the former College of Engineering of the University of Zagreb was divided into four new faculties, one of them becoming the Faculty of Electrical Engineering, which started its independent existence on 1<sup>st</sup> of July 1956.

This was the start of the third, modern stage in the development of electrical engineering in Croatia, characterized by a turbulent development in electronics, electrical power engineering, automation, communication technology and computing. First independent curriculum (ETF-1) started its application from academic year 1959/60 in which profiles of High-voltage currents and Low-voltage currents are still present. The most significant change is reduction of direct lectures

student engagement from 40 hours/week (according to curriculum from 1950/51) to 30 hours/week. The average student engagement of 30 hours/week has not changed till today which serves as a confirmation of forethought of professors of that time who managed to recognize the right amount of weekly student obligations already 60 years ago.

*In order to respond to fundamental goals of academic education and social requirements Faculty changed its curriculum seven times from its beginnings. The 8th change of curriculum is now planned for academic year 2018/19 (FER-3). All curriculums with according subjects of the Power engineering profile are listed in the appendix section (Appendix I).*

After the gain of independency of the Faculty the working conditions for the Department improved significantly, especially after the transfer to the 6<sup>th</sup> floor of the newly built Faculty building “C”. The Faculty buildings "A", "B" and "C" at the present location (Unska 3, Zagreb) were completed and equipped by the year 1965 (building “A” in 1961, building “C” in 1963. and building “B” in 1965) and were fully operational.

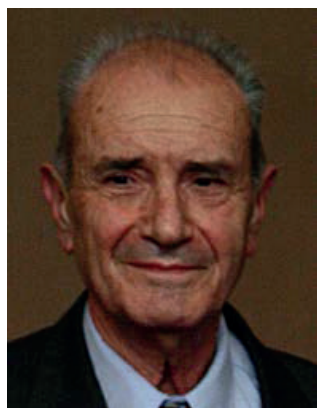
In that time (after 1965.) the Department equipped, alongside already mentioned high-voltage laboratory, power facilities laboratory, electric lighting laboratory and relay protection laboratory. The high-voltage laboratory and power facilities laboratory were been located in adequately large facilities in the newly built building “B” (High-voltage laboratory on 300 m<sup>2</sup> and Power facilities laboratory on 200 m<sup>2</sup>). Furthermore, available space in the Department premises was used for establishment of well-equipped Department library. Library contained more than 2000 books and was monthly receiving more than 40 different technical journals and magazines. Furthermore, at that time the Department already utilizes digital computers for solving problems in power engineering. Therefore, the installation of IBM 1130 computer in the University computing center had an even further positive impact both on the computer aided teaching and professional and scientific activities. The biggest contribution in that regard goes to prof. Božidar Stefanini and prof. Hrvoje Požar who were both constantly improving the curriculum with the latest international scientific achievements.

Postgraduate studies (Master of Science (Mr. sc.) degree) started from the academic year 1964/65. In the initial part of High-current postgraduate studies Department had lectures: “Machine operation”, “Frequency and voltage control”, “Power system scheduling”, “Power system construction”, “High voltage network construction and design”, “Power network analysis”, “Relay protection”, “Transmission stability”, “Overhead lines”, “Power network overvoltage”, “High voltage impulse testing”, “Hydro power plant operation” and “Thermal power plant operation”.

In academic year 1967/68 Faculty introduced new curriculum (ETF-2) with three-way studies: Power engineering, Electronics and Electrical machines and automation. Study duration was four years with initial two years the same for all the students. Courses were divided in lectures and exercises. New curriculum reduced lectures from professors from Faculty of mechanical engineering and naval architecture and increased number of lectures in the field of electrical engineering.

New courses held by the Department include: “Overvoltage protection” and “Relay protection”. “Electrical grids and installations” course changed the name to “Electric power distribution”. There were also various new elective courses established and taught by Department members. New department professors were **Marko Padelin**, **Milan Šodan** and **Željko Zlatar**.

After only three years of application of ETF-2 the new curriculum change followed in academic year 1970/71 (ETF-3). Power engineering became one of the 3 study profiles. There was an increase in number of required courses held by Department. New courses were: “Energy fundamentals” and “Electric power systems” while the course “Electric power transmission” was divided into “Electrical power lines” and “High voltage networks” courses. “Low voltage grids and installations” became required course of the study profile and “Nuclear power engineering” became the new elective course. With other three elective courses on nuclear power engineering they were the foundation of future Nuclear Power Engineering sub-profile. Number of elective courses in the field of electric power networks also increased. Basic (required) courses were lectured by aforementioned professors and by new professors: **Vjekoslav Filipović**, **Srđan Babić**, **Mirjana Urbija-Feuerbach** and **Vjekoslav Srb** (honorary professor) who were all representative of the new generation of Department members. ETF-3 separated laboratory and auditorium exercises and introduced practical student projects.



*Danilo Feretić, PhD was born in Omišalj on October 13, 1930. He graduated in 1954 at the Technical Faculty of Zagreb. He finished postgraduate studies in England and received his PhD in 1967. at the Faculty of Electrical Engineering in Belgrade. He worked at the Power Engineering Institute in Zagreb, 1954-55, Institute for Nuclear Science "Boris Kidrič" in Vinča 1959-63, Energoinvest in Sarajevo 1963-67, Institute for Nuclear Research in Egypt 1967-74, in Zagreb Electric Power Utility 1974 -82. He was the Technical director of Krško nuclear power plant under construction. In 1968 he worked at the Faculty of Mechanical Engineering and Naval Architecture in Zagreb, where he became a full professor in 1979. In the same year he moved to the Faculty of Electrical Engineering (now Faculty of Electrical Engineering and Computing) where he served as a Dean for the 1992-1994 mandate and became Professor emeritus in 2002. He is engaged in nuclear power and the influence of nuclear power plants on the environment and power plant construction and design. He worked as an expert for the International Atomic Energy Agency. He has published several books and won many awards, some of which are: "Nikola Tesla" (1991), "Fran Bošnjaković" (1997), "Ruder Bošković" (1998), and the State Lifetime Achievement Award (2007).*

### 2.3. 1978: Department of Power Systems (ZVNE)

In 1978, the department changed its name from High-voltage Department to the Department of Energy and Power Systems (in Croatian: *Zavod za visoki napon i energetiku*). The research work at the Department was significantly improved with the acquisition of an electronic computer in 1980. The computer was regularly used in three shifts according to its usage schedule.

In ac. year 1978/79. a new ETF-4 curriculum was introduced, where Power Engineering became one out of eight study profiles. It is important to emphasize that Nuclear Power Engineering profile was introduced to the Faculty's curriculum for the purpose of education of engineers in nuclear energy field, as the NPP Krško was under the construction. Professor **Danilo Feretić** was highly creditable for the development of this profile. In the Power Engineering profile a new course "Energy Processes" was introduced. Power engineering study profile on the fourth year was branched into three specialization programs:

- Power System Construction and Operation
- Power System Management and Control
- General Electric Power Engineering

Profile Power System Construction and Operation varies the least from the previous ETF-3 curriculum. In profile Power System Management and Control several new courses from the field of regulation, automatization and digital electronics were introduced: "Regulation in Electric Power System", "Control in Electric Power System" and "Digital Control". General Power Engineering profile introduced subjects which studied matter that is not only related to electricity issues but also to all forms of energy: "Energy Sources", "Energy Systems and Balance", "Economy in Energy". Nuclear Power Engineering profile was transformed into Energy Technology profile in ac. year 1990/91.

During the 80s, the Department developed with the increase in the number of young teachers who took over the courses: **Zdravko Hebel, Vladimir Tuk, Vladimir Mikuličić, Sejid Tešnjak, Slavko Krajcar, Nikola Čavlina** and **Ivo Uglešić**. The development is particularly reflected in more extensive professional and scientific work, cooperation with the industry sector and international professional and scientific cooperation. International exchanges and visits of expert, especially with regard to the expansion of activities in the field of nuclear energy further increase the relevance of the Department. All these activities also resulted in a considerable increase in the number of staff members, most of whom have achieved scientific their titles in the Department.

With the support of the industry and government new building (building "D") was built and inaugurated in 1989 where Department of Energy and Power moved in and stayed up to today. Building construction was led by ex-Dean and Department employee Professor Milan Šodan. During year 1991 significant number of modern software packages for electric power system analysis and measurement equipment have been acquired, which significantly improved Department scientific work capabilities and enabled introduction of modern teaching techniques. Since then, every member of the Department had a computer, and thanks to that, more diversified collaboration with the economy was established. This led to further acquisition of new and modern computers, which contributed to further advancements in the work of the Department. The Department library of that time had more than 5,000 books and was receiving over 50 different journals.

During the Croatian War of Independence (1991-1995) there were difficulties in performing the work and teaching, primarily due to frequent danger alarms. Despite the hardship, during this period a new curriculum was formed which

received the name FER-1 after (1995) the Faculty changed its name to Faculty of Electrical Engineering and Computing.

#### 2.4. 1995: Faculty of Electrical Engineering and Computing (FER)

The Faculty of Electrical Engineering (ETF - *Elektrotehnički fakultet*, in Croatian) existed under this name until 7 March 1995 when it was renamed to Faculty of Electrical Engineering and Computing (FER - *Fakultet elektrotehnike i računarstva*, in Croatian). Faculty was renamed to follow the global trends characterized by the rapid development in the field of computing.

The first generation of students enrolled FER-1 curriculum in the academic year 1994-95. The general characteristic of this curriculum is a significantly higher choice of courses (in the study profile Power Engineering students had to engage 40 hours of courses instead of the previous 13 hours of elective courses). A certain number of elective subjects were from other study profiles. In the organizational sense, the following changes have been made - instead of the previous profiles Power Engineering and Energy Technologies, which were chaired by the Department of Energy and Power Systems, a unique study of Power Engineering with two profiles was introduced: profile Energy Systems and profile Energy Technologies, while the ETF-4 curriculum profiles mentioned before was abolished.

The Department staff was significantly expanded by employing new associates: **Ante Marušić, Tomislav Tomiša, Davor Škrlec, Nenad Debrecin and Ivica Pavić.**

The Department continued its development with a commitment to the permanent improvement of its curriculum. Soon, the curriculum was changed again (to be named FER-2) due to the Bologna declaration. The Bologna Declaration was signed by 29 European countries in 1999, adopting the new three-step university education system: bachelor, master, and doctoral studies. Today, the Bologna Process is implemented in national qualification frameworks of 47 European countries, including Croatia. At the Faculty of Electrical Engineering and Computing (FER), University of Zagreb, this involves a 3-year bachelor program, followed by a 2-year master program and a 3-year doctoral program. The master program at FER covers three fields: Electrical Engineering and Information Technologies, Information and Communication Technologies, and Computer Science. Each field was divided to profiles, and Power Systems was a study profile within the Electrical Engineering and Information Technologies field [8].

Since the individualization of the classes that students attend is one of the main objectives of the Bologna reform, each profile consisted of five mandatory courses, one laboratory course, and a minimum of 13 elective courses (Appendix I). Additional motivation for introducing this laboratory-only course is to increase the importance of laboratory exercises in master studies. When laboratory exercises were just a part of theoretical courses, the students were mostly focused on the theory-based exams since these accrued most points towards the overall grade. The low amount of points students could accumulate at laboratory exercises marginalized their significance.

Introduction of the laboratory-only course rectified this shortcoming of the previous master program FER-1 and recognized three shortcomings of today's engineering education: a need for more general engineering technical knowledge, a need for more hands-on experience, and a need for higher level of professional awareness.

The main goal of laboratory focused teaching is to enable students to apply and test theoretical knowledge they mastered in previous years of studies. The laboratory courses enable them to develop practical skills in various fields of power engineering in a controlled environment. Furthermore, students are provided with the possibility of performing experiments and tests that would otherwise be either too expensive or nearly impossible to carry out in a real power system.

The Department, within the curriculum FER-2, introduced a number of new subjects for the study profile of Electrical Power Engineering. Furthermore, transversal subjects serving the educational needs of the whole Faculty were also introduced and included: "Sustainable Development and Environment", "Economics and Managerial Decision Making" (in joint organization with ZOEM), "Management in Engineering" (in joint organization with ZOEM and ZTEL) and "Risk Management". For all students of Electrical Engineering and Information Technology there is also the subject "Energy Technology" being taught on the second year of bachelor study.

### 3. THE DEPARTMENT TODAY

After the year 2000 the Department staff number continued to grow with **Zdenko Šimić, Željko Tomšić, Davor Grgić, Igor Kuzle, Marko Delimar, Viktor Milardić and Juraj Havelka**, being accepted as young teachers. All of these teachers, responsible not only for teaching, contributed to professional and scientific development of the Department by means of improved cooperation with the industry sector and improved international academic cooperation. The Department facilities were continually upgraded with equipment and software acquired from funds earned by industry cooperation projects or from domestic and international scientific projects. These projects enabled further staff growth by employing doctoral students, postgraduate students and expert associates who all together represented Department's future potential.

Today, the Department has five research laboratories that include:

- Smart Grid Laboratory (SGLab)
- Laboratory for Energy and Environmental Markets and Exchanges (LEEMaE)
- Power System Protection Laboratory (PSP Lab)
- Atmospheric Phenomena Laboratory (APPLY)
- Laboratory for Nuclear Energy and Safety (LNES)

whose Heads are : **Igor Kuzle** (SGLab), **Željko Tomšić** (LEEMaE), **Juraj Havelka** (PSP Lab), **Ivo Uglešić** (APPLY) and **Nikola Čavlina** (LNES).

Today, the Department is the leading national and regional research and higher education institution, with excellent teachers and students, closely linked with the industry sector, excellently organized and internationally recognized.

Our mission is:

- to educate students capable of carrying out the technological and social development of Croatia through education and research in the fields of electrical power engineering and energy systems, using scientific background from applied mathematics and applied physics;
- to create new knowledge by internationally acknowledged research and by development of safe, clean and efficient energy sources;
- to innovatively develop the economy and public services, hence contributing to the overall development of the society;
- to be an institution of high academic values and ethical principles, a site of critical thinking and questioning, and of equality for all its members;
- to be the driving force of the power sector in the Croatia.

The Department staff was also involved in the organization of important international conferences, of which most significant were:

- International Conference on the Nuclear Option in Countries with Small and Medium Electricity Grids which so far had 10 editions, biannually, located each time in different Croatian city
- International Conference on Power Systems Transients (IPST 2015), Dubrovnik, Croatia, 15-18 June 2015
- IEEE International Energy Conference (IEEE ENERGYCON 2014), Dubrovnik, Croatia, 13-16 May 2014
- EUROCON 2013 - The International Conference on "Computer as a tool" (IEEE EuroCon 2013), Zagreb, Croatia, 1-4 July 2013
- 8th International Conference on the European Energy Market (EEM11), Zagreb, Croatia, 25-27 May 2011

The Department is also the holder of a specialist postgraduate study of Railway Electrical Engineering Systems (study head **Ivo Uglešić**) which is being carried out since 2012. The underlying reason for launching a specialist study program is to improve the development, design, production and maintenance of railway electrical systems components, which requires application of modern methods and interdisciplinary knowledge.

Regarding the teaching curriculum development, the Department has always has a rich history and has always followed world trends in the development of power engineering and related sectors that are of the scientific interest to the Department. The curriculum development continues today with the preparation of the eighth curriculum change, for which introduction is planned by the academic year 2018/19.

A large number of employees of the Department are actively involved in the shaping of a newly-introduced dislocated undergraduate program of the University of Zagreb titled "Energy Efficiency and Renewable Energy study program" located in Šibenik, which is planned to start in the academic year 2015/16.

#### 4. DISTINGUISHED MEMBERS OF THE DEPARTMENT

Several Department members made a significant contribution to the development of the academic community in Croatia. The position of the Dean of Faculty of Electrical Engineering was held by five professors (figure 2) from the Department for High Voltage and Energy, and several of them had additional significant functions at University of Zagreb level (Table II).



Figure 12. Distinguished members of the department serving as Deans of the Faculty

Apart from the university duties, certain staff members of the Department were engaged in socio-political activities, especially professor **Željko Tomšić**, who served as Assistant Minister for Energy and Mining in the period 2004-2008, and professor **Davor Škrlec**, who was elected as a Croatian representative in the European Parliament on 1<sup>st</sup> of July 2014.

Some staff members have left an indelible mark in sports activities like long-time professor and former Head of the Department professor **Zdravko Hebel** who won the gold waterpolo medal at the 1968 Olympics in Mexico. In addition to the aforementioned medal, professor Hebel was also the President of the Croatian Olympic Committee in the period 2000-2002.

In the field of professional organizations activities, significant work was done by professor **Hrvoje Požar** as the President of JUGO CIGRE 1968-1972, and recently professor **Ante Marušić**, who was the Vice-president of HRO CIGRE, professor **Marko Delimar** and professor **Igor Kuzle**, who have been active in the IEEE association and serving prominent positions: Marko Delimar as the Director of IEEE Region 8 and IEEE Secretary and Igor Kuzle as Vice-President for Technical Activities in IEEE Region 8 and as the President of the Croatian Section of IEEE. Professors **Nikola Čavlin**, **Zdenko Šimić** and **Davor Grgić** were the Presidents of the Croatian Nuclear Society.

Table II. List of distinguished Department members and their functions

1.	Prof. Božidar Stefanini, PhD	<i>1956.-1957. vice-dean</i>
		<i>1958.-1959. dean</i>
		<i>1959.-1962. vice-dean</i>
		<i>1971.-1979. director of the University Computing Centre (SRCE)</i>
2.	Academic prof. Hrvoje Požar, PhD	<i>1960.-1962. dean</i>
		<i>1962.-1966. vice-dean</i>
		<i>1968.-1970. dean</i>
		<i>1970.-1972. vice-rector</i>
3.	Prof. Milan Šodan, PhD	<i>1980.-1982. vice-dean</i>
		<i>1982.-1984. dean</i>
4.	Prof. Sejid Tešnjak, PhD	<i>1988.-1990. vice-dean</i>
5.	Prof. Danilo Feretić, PhD	<i>1990.-1992. vice-dean</i>
		<i>1992.-1994. dean</i>
6.	Prof. Slavko Krajcar, PhD	<i>1990.-1996. dean assistant</i>
		<i>1996.-1998. vice-dean</i>
		<i>1998.-2002. dean</i>
7.	Prof. Vladimir Mikuličić, PhD	<i>1994.-1996. vice-dean</i>
8.	Prof. Nenad Debrecin, PhD	<i>1998.-2000. vice-dean</i>
9.	Prof. Tomislav Tomiša, PhD	<i>2002.-2006. vice-dean</i>
10.	Prof. Marko Delimar, PhD	<i>2014.- today vice-dean</i>

## 5. PUBLICATIONS

Department's publishing activity has been continuously improved since its establishment. Significant footprint was left by the books by prof. Hrvoje Požar which have been used by many generations of students and experts. Besides numerous university textbooks, Department members published more than 30 books (Appendix II). After Croatian War for Independence, publishing activities were slowed down but in recent years they have been on a gradual increase.

Significant improvements have been made in scientific research as more and more papers are published in prestigious international journals. Also, considerable investments obtained by international projects are channeled into improvement of the laboratories.

## **6. FUTURE DEVELOPMENT**

Future development is based on improving laboratory capacities.

### **6.1. Transformation from Power system laboratory to Smart grid laboratory**

Power system laboratory was neglected for many years due to its size and lack of funds needed for the refurbishment. Laboratory started with operation on 4<sup>th</sup> of January 1969 when small hydro power plant model became operational. Shortly after that small thermal power plant model was also completed. They were unified into the interconnected power system. The laboratory can provide students and researchers with valuable ability to test and apply theoretical knowledge on real machines in controlled environment. Further laboratory improvements and investments are oriented towards renewable energy sources integration following mandatory European Union guidelines for all member countries. Current power system concept based on centralized generation is moving towards Smart Grid concepts which integrate centralized and distributed generation with new control capabilities and technologies. The output of the renewable energy sources is variable and of stochastic nature, which requires changes in the current practices of the power system operation. On the other hand, growing environmental awareness and strong political impetus have promoted new technologies that help reduce the emissions (e.g. electric vehicles).

In order to provide the students with the necessary knowledge of advanced and smart grid technologies, the decision to modernize the current laboratory and transform it into Smart Grid Laboratory (SGLab) was reached. Along with the existing AC microgrid, a new DC microgrid is being developed. It will comprise of different renewable energy sources and energy storage devices, different batteries types being used to run electric vehicles, different demand-responsive loads, as well as multiple AC/DC converters and DC/AC inverters to allow interaction between the AC and DC microgrids. Therefore, the existing miniature electric power system in the Laboratory that resembles Croatian electric power system (Figure 1) will be drastically expanded to better include the transition power system is undergoing.

Addition of different renewable energy sources and DC microgrid will enable research in the field of RES integration and demand flexibility. Following activities and investments are planned for the SGLab:

- Hydro power plant reconstruction;
- Thermal power plant reconstruction;
- PV generation installation (60 various technology and installation PV modules);

- Li-ion batteries for electric vehicle simulation acquisition;
- Battery energy storage installation;
- AC/DC and DC/AC converters installation;
- AC and DC controllable loads introduction;
- Various distributed generation models connection;
- Modern power system protection completion;
- Modern SCADA system installation.



Figure 1. Miniature power system (1—thermal turbine; 2—hydro turbine; 3—transmission network).

## 7. CONCLUSION

During the past 80 years since the founding of the Department as a component of the College of Engineering of the University of Zagreb (1934-1956), the Faculty of Electrical Engineering (1956-1995) and the Faculty of Electrical Engineering and Computing (from 1996 until today) a wide range of great historical and scientific events have occurred connected with the Department. States and social systems have been swapped, wars have passed, economic and international relations have changed, new curricula and study programs have been introduced, organizations of the University and faculties have changed. Locations, buildings, lectures, laboratories, cabinets and people changed, but the most significant changes were in the development of new technologies and the creation of opportunities for scientific research and improvement of overall teaching at the Faculty. There were also many other less significant changes that marked the past and affected the present life of the Department. The Department, as one of the oldest institutions in the field of technical sciences at the University of Zagreb,

participated in all this in a very specific way and left many significant results that are relevant even today.

The paper presents the development of the Department since its establishment in 1934 to the present days. The Department's intensive development began in 1950 with the introduction of the new courses in accordance to the new curricula (High-voltage current study profile). Throughout the years laboratories as well as scientific and professional work were developed. This paper, in addition to the historical overview of the Department activities and the most prominent employees gives a review of the study curriculum development and changes. Furthermore, guidelines for the future development of the Department were given through the plans for improvement of practical teaching with students within a Bologna Declaration compliant curriculum as a part of a modern power system laboratory that is currently under reconstruction.

## 8. REFERENCES

- [1] History of FER, <http://www.fer.unizg.hr/en/about/history>, accessed December 1, 2017
- [2] Stefanini, Božidar. The fiftieth anniversary of the Power System Department of the Electrical Engineering Faculty Zagreb (in Croatian: Pedeset godina Zavoda za visoki napon i energetiku Elektrotehničkog fakulteta u Zagrebu), *Elektrotehnika*, Vol. 28, No. 1-2, January/April 1985, pp. 3-6
- [3] Šodan, Milan. Study of the Electrical Power Engineering and its development in Zagreb (in Croatian: Studij elektroenergetike i njegov razvoj u Zagrebu), *Elektrotehnika*, Vol. 28, No. 1-2, January/April 1985, pp. 7-10
- [4] Spomenica 1919. – 1969., 50 godina studija elektrotehnike u Hrvatskoj, Tehnička knjiga, Zagreb, 1969.
- [5] Spomenica, Tehnički fakulteti 1919.-1994. : monografija u povodu 75. obljetnice osnutka tehničke visoke škole u Zagrebu, Sveučilište u Zagrebu, Zagreb, 1994.
- [6] Ban, Drago. 90 godina Zavoda za elektrostrojarstvo i automatizaciju, 1925-2015, FER, Zagreb, 2015.
- [7] Šodan, Milan; Filipović, Vjekoslav; Tešnjak, Sejid; Marušić, Ante; Tomiša, Tomislav; Kuzle, Igor; Dizdarević, Nijaz; Erceg, Romina; Zelić, Radoslav; Skok, Srđan; Havelka, Juraj. Management, Control and Protection of Electric Power Systems (in Croatian: Upravljanje, regulacija i zaštita elektroenergetskog sustava), *EGE: energetika, gospodarstvo, ekologija, etika*, vol. 7, no. 2, March/April 1999, pp. 91-93
- [8] Kuzle, Igor; Havelka, Juraj; Pandžić, Hrvoje; Capuder, Tomislav. Hands-On Laboratory Course for Future Power System Experts, *IEEE Transactions on Power Systems*, vol. 29, no. 4, July 2014, pp. 1963-1971
- [9] Kuzle, Igor; Jurković, Kristina; Pandžić, Hrvoje. Development of the Power System Simulations Laboratory (in Croatian: Razvoj laboratorija za električna postrojenja), 12. session of the HRO CIGRÉ, Šibenik, Croatia, 8–11 November 2015, pp. 1-9 – accepted for publication

## APPENDIX I - CURRICULUMS

Study profile: High-voltage Current – Electric Power Engineering, academic year 1951/52

Third year			Fourth year		
Required courses	Semester		Required courses	Semester	
	Winter	Summer		Winter	Summer
Heat Machines	4+2	-	Heat Machines	2+1	-
Hydraulic Machines	-	3+1	Hydraulic Machines	3+1	-
Theory of El. Engineering	3+2	3+2	Electrical Machines Testing	2+4	2+4
Electrical Measurements	1+3	1+3	Electric Power Transmission	4+3	4+3
Electric Materials Technology	3+1	-	Electric Power Stations	2+2	3+2
Electrical Facilities	2+2	-	Fundamentals of El. Economy	2+0	-
El. Grids and Installations	4+4	4+3	Electrical Machines	4+4	-
Electrical Machines	3+3	3+3	Encyc. of High-frequency Tech.	-	3+0
Industrial Buildings	-	2+1	High Voltage Engineering	-	2+1
Encyc. of Wired-comm. Tech.	-	3+0	Organization of Power Utilities	-	2+1
Power Routers	-	2+0	Geodesy in Power Utilities	-	1+1
Pre-military Training	2+0	2+0	Pre-military Training	2+0	2+0
			<b>Elective course</b>	<i>min 6 hours</i>	
			Theory of Electrical Engineering	-	2+2
			Economics in Power System	-	2+1
			Electrical Machines	-	3+5
			Construction of El. Devices	-	3+1
			Motor Drives	-	3+1
			Power Transmission Stability	-	2+0
			Electrical Lighting	-	2+2
			Electrical Railways	-	2+1
			Electric Power Dispatch	-	2+1
			Exploitation of Water Resources	-	2+0

Study profile: High-voltage Current – ETF-1, academic year 1959/60

Third year			Fourth year		
Required courses	Semester		Required courses	Semester	
	Winter	Summer		Winter	Summer
Heat Machines	3+1	2+2	Theory of El. Engineering	3+2	-
Hydraulic Machines	2+1	2+1	Electrical Machines	4+4	-
Electrical Measurements	2+3	2+3	Electrical Facilities	2+3	-
El. Grids and Installations	4+2	-	Electrical Machines Testing	2+3	1+3
Electrical Machines	3+2	2+4	Electric Power Transmission	4+3	-
Low-voltage Current	3+2	-	Power Routers	2+0	-
Theory of El. Engineering	-	3+2	High Voltage Engineering	-	2+3
Electrical Facilities	-	2+3	Organization	-	2+0
			<b>Elective course</b>	<i>min 13 hours</i>	
			El. Grids and Installations	-	3+2
			Electrical Facilities, Sel. Chap.	-	3+2
			El. Power Transm., Sel. Chap.	-	3+2
			Electrical Machines, Sel. Chap.	-	3+2
			Theory of Electrical Engineering	-	3+2
			Motor Drives	-	3+2
			Regulation Techniques	-	3+2
			Construction of El. Devices	-	2+1
			Economy of Electrical Energy	-	2+1
			Power Routers, Sel. Chap.	-	2+1
			Electrical Lighting	-	2+1
			Electric Traction	-	2+1
			Electric Power Dispatch	-	2+1
			Electrothermy	-	2+1
			Power Transmission Stability	-	2+1

## Study profile: Electrical Power Engineering – ETF-2, academic year 1967/68

Third year			Fourth year		
Required courses	Semester		Required courses	Semester	
	Winter	Summer		Winter	Summer
Theory of El. Engineering	2+2	4+2	Electrical Facilities	2+3	3+2
Electrical Machines	4+2	3+2	Electric Power Transmission	4+4	4+2
Electronic Circuits	2+2	-	High Voltage Engineering	2+2	-
Hydraulic Machines	3+1	-	Electrical Machines	2+2	-
Mechanical Technology	2+0	-	Regulation Techniques	3+2	-
Machine Elements	3+3	-	Fundamentals of Economy	2+0	2+0
Fundamentals of Sociology	2+2	2+2	Overvoltage Protection	-	2+2
Electronic Computers	2+2	-	Relay Protection	-	2+1
Electrical Facilities	-	2+3	<b>Elective course</b>	<i>min 12 hours</i>	
Electric Power Distribution	-	4+2	Potential Fields	-	2+1
Heat Machines	-	4+2	Measuring Techniques	-	2+3
			Motor Drives	-	2+1
			Regulation in Power Plants	-	2+1
			Organization Methods	-	2+1
			Electrothermy	-	2+1
			Electrical Devices	-	4+2
			Laboratory of El. Machines	-	2+4
			Construction of Rot.Machines	-	4+2
			Power Routers	-	4+0
			Nuclear Power Plants	-	3+2
			Load Distribution in EPS	-	2+1
			Overhead Lines	-	2+1
			Operational Safety	-	2+1
			Bulk Energy Transfer	-	2+1
			Power Grid Regulation	-	2+1
			Aux. Devices in Power Plants	-	2+1
			Electrical Lighting	-	2+1
			Networks and Installations	-	2+1
			Impulse and Digital Electronic	-	2+2

## Study profile: Electrical Power Engineering – ETF-3, academic year 1970/71.

Third year			Četvrta godina		
Required courses	Semester		Required courses	Semester	
	Winter	Summer		Winter	Summer
Energy Fundamentals	2+0+0+0	-	Electrical Energy Production	4+2+2+0	-
Power Transf. and Machines	4+2+0+0	-	Electrical Energy Production	0+0+0+1	-
Electrical Power Lines	3+0+1+0	-	High Voltage Networks	4+0+1+0	-
Electrical Power Lines	0+0+0+2	-	High Voltage Networks	0+0+0+1	-
Electrical Fields and Circuits	4+4+0+0	-	Electric Motors	2+0+0+0	-
Electrical Circuits	2+1+2+0	-	High Voltage Engineering	4+0+2+0	-
Electronic Computers	2+0+2+0	-	Regulation Techn. and Automation	2+1+0+0	2+1+1+0
El. Facilities and Devices	-	4+1+3+0	Electric Power Systems	-	2+0+1+0
El. Facilities and Devices	-	0+0+0+1	Relay and Measuring Techn.	-	3+0+2+0
Synch. Machines and Routers	-	3+1+0+0	Relay and Measuring Techn.	-	0+0+0+1
Synch. Machines and Routers	-	0+0+0+1	Construction program	-	0+0+5+0
LV Grids and Installations	-	4+0+1+0	Fund. of Ind. Sociology	2+0+0+0	-
LV Grids and Installations	-	0+0+0+2	Fundamentals of Economy	2+0+0+0	-
Fund. of Mechanical Construct.	-	2+1+0+0	<b>Elective course</b>	<i>min 12 hours</i>	
Fund. of Mechanical Construct.	-	2+0+0+0	Remark: Because of their large number elective courses are not listed.		
Fundamentals of Ind. Sociology	-	2+0+0+0			
Fundamentals of Economy	-	2+0+0+0			
Industrial Practices	-	yes			

Study profile: Electrical Power Engineering – ETF-4, academic year 1980/81

Third year			Fourth year: Construction and Operation of EPS		
Required courses	Semester		Required courses	Semester	
	Winter	Summer		Winter	Summer
Theory of El. Engineering	3+3+0+0	-	Selected Chap. of Mathematics	3+2+0+0	-
Energy processes	4+3+0+0	-	Power Plants	2+0+2+0	-
Power Transformers	2+2+0+0	-	Power Plants	0+0+0+1	-
Fund. of Mech. Constructions	2+1+0+0	-	Electric Power Networks I	0+0+0+1	-
Electronic Circuits	3+1+1+0	-	Synchronous Machines	0+0+0+1	-
Economics in Engineering	2+0+0+0		Electric Power Networks II	3+1+1+0	-
Foreign Language	2+0+0+0	2+0+0+0	Electric Power Networks II	0+0+0+1	-
Electrical Facilities	-	4+1+3+0	High Voltage Engineering	3+0+2+0	-
Electrical Facilities	-	0+0+0+1	Electric Motors	2+0+1+0	-
Power Electronics		2+0+1+0	Electric Power Systems	3+0+1+0	-
Synchronous Machines	-	3+1+0+0	Electric Power Systems	0+0+0+1	-
Electric Power Networks I	-	4+1+1+0	Electric Power Networks III	-	4+0+1+0
Regulation Techniques	-	4+2+1+0	Relay Protection	-	3+1+2+0
Industrial Practices	-	da	Construction program	-	0+0+5+0
			<b>Elective course</b>	<i>min 13 hours</i>	

Fourth year: Control of EPS		
Selected Chap. of Mathematics	3+2+0+0	-
Power Plants	2+0+2+0	-
Power Plants	0+0+0+1	-
High Voltage Engineering	3+0+2+0	-
Electric Power Networks I	0+0+0+1	-
Synchronous Machines	0+0+0+1	-
Electric Motors	2+0+1+0	-
Digital Control	3+2+2+0	-
Regulation in EPS	2+0+1+0	-
Control in EPS	-	3+0+2+0
Control in EPS	-	0+0+0+1
Relay Protection	-	3+1+2+0
Construction program	-	0+0+5+0
<b>Elective course</b>	<i>min 13 hours</i>	

Fourth year: Power Engineering		
Selected Chapters of Mathematics	3+2+0+0	-
Power Plants	2+0+2+0	-
Power Plants	0+0+0+1	-
High Voltage Engineering	3+0+2+0	-
Electric Power Networks I	0+0+0+1	-
Synchronous Machines	0+0+0+1	-
Electric Motors	2+0+1+0	-
Electric Power Systems	3+0+1+0	-
Electric Power Systems	0+0+0+1	-
Nuclear Physics Introduction	2+2+0+0	-
Energy Sources	-	3+2+0+0
Energy Sources	-	0+0+0+1
Energy Systems and Balance	-	3+2+0+0
Energy Systems and Balance	-	0+0+0+1
Operations Research	-	2+2+0+0
Economics of Energy	-	2+2+0+0
Energy and Environment	-	2+1+0+0
Construction program	-	0+0+7+0

Study profile: Nuclear Power Engineering – ETF-4, academic year 1980/81

Third year			Fourth year		
Required courses	Semester		Required courses	Semester	
	Winter	Summer		Winter	Summer
Nuclear Physics Introduction	2+2+0+0	-	Sel. Chap. of Mathematics	3+2+0+0	-
Theory of Electrical Engineering	3+3+0+0	-	Electronic Circuits	3+1+1+0	-
Energy processes	4+3+0+0	-	Lab. of Nuclear Engineering	0+0+2+0	-
Power Transformers	2+2+0+0	-	Reactor Heat Processes	3+2+0+0	-
Fund. of Mech. Constructions	2+1+0+0	-	Power Plants	2+0+2+0	-
Reactor Kinetics and Dynamics	3+1+0+0	3+2+0+0	Power Plants	0+0+0+1	-
Foreign Language	2+0+0+0	2+0+0+0	Nuclear fuel Cycles	2+1+0+0	-
Electrical Facilities	-	4+1+3+0	Reactor Materials	2+1+0+0	-
Electrical Facilities	-	0+0+0+1	Economics in Engineering	2+0+0+0	-
Synchronous Machines	-	3+1+0+0	Power Electronics	-	2+0+1+0
Lab. of Nuclear Engineering	-	0+0+3+0	Motor Drives	-	3+0+1+0
Regulation Techniques	-	4+2+1+0	Safety and Regulation	-	4+2+0+0
Industrial Practices	-	yes	Nuclear Power Plants	-	3+1+0+0
			Nuclear Power Plants	-	0+0+0+1
			Control and Regulat. in NPP	-	3+0+2+0
			Radiation Eff. and Protection	-	2+0+2+0
			Nuclear Reactor Safety	-	2+0+1+0

Study profile: Electrical Power Engineering (module Energy Systems) – FER-1, academic year 1994/95.

Undergraduate study – third year			Graduate study – first year		
Required courses (ECTS)	Semester		Required courses (ECTS)	Semester	
	Winter	Summer		Winter	Summer
Energy processes (6)	4+2+0	-	Electrical Facilities (7)	4+1+1	-
Electrical Mach. and Transf. (7)	4+1+1	-	Electric Power Networks (6)	4+1+0	-
Nuclear Power Eng. Intro. (5)	4+0+0	-	Numerical Analysis. of Electric Power Systems (7)	4+1+1	-
Theory of El. Engineering (6)	3+2+0	-	High-voltage Engineering (5)	3+0+1	-
Social course (2+2)	2+0+0	2+0+0	Social skills course (2)	2+0+0	-
Power Electronics Princip. (5)	-	2+1+1	Power Plants (5)	-	2+1+1
Regulation Techniques (7)	-	3+1+1	Power System Control (5)	-	2+1+1
Fund. of Mechatronics (7)	-	3+1+1	Power Syst. Protect. and Automatization (5)	-	2+1+1
Electric Power Transmis. (5)	-	3+1+0	Economics (2)	-	2+0+0
<b>Selection of elective courses (at least 8 ECTS)</b>			Seminar (7)	-	1+0+3
			<b>Selection of elective courses (at least 9 ECTS)</b>		
<b>Graduate study – second year</b>					
Required courses (ECTS)	Semester		<i>Remark: Because of their large number elective courses are not listed.</i>		
	Winter	Summer			
Electric Power System Operation and Control (6)	3+0+2	-			
Graduation Thesis (18)	1+0+14	-			
<b>Selection of elective courses (at least 6 ECTS)</b>					

Study profile: Electrical Power Engineering (module Energy Technology) – FER-1,  
academic year 1994/95.

Undergraduate study – third year			Graduate study – first year		
Required courses (ECTS))	Semester		Required courses (ECTS)	Semester	
	Winter	Summer		Winter	Summer
Energy processes (6)	4+2+0	-	Electrical Facilities (7)	4+1+1	-
El. Machines and Trans. (7)	4+1+1	-	Electric Power Networks (6)	4+1+0	-
Nucl. Power Eng. Intro. (5)	4+0+0	-	Rad. Effects and Protection (6)	3+1+1	-
Renew. Energy Resources (6)	3+0+1	-	Nuclear fuel Cycles and Reactor Materials (6)	3+1+0	-
Social course (2+2)	2+0+0	2+0+0	Social skills course (2)	2+0+0	-
Princ. of Power Electronics (5)	-	2+1+1	Power Plants (5)	-	2+1+1
Regulation Techniques (7)	-	3+1+1	Energy and Environment (4)	-	2+1+0
Fund. of Mechatronics (7)	-	3+1+1	Nuclear Power Plants (6)	-	4+1+0
Heat transfer (5)e	-	3+1+0	Economics (2)	-	2+0+0
<b>Elective courses selection of at least 8 ECTS</b>			Seminar (7)	-	1+0+3
<b>Graduate study – second year</b>			<b>Elective courses selection of at least 9 ECTS</b>		
Required courses (ECTS)	Semester		<i>Remark:</i> <i>Because of their large number all elective courses are not listed.</i>		
	Winter	Summer			
Safety of Nuclear Plants (6)	3+1+0	-			
Graduation Thesis (18)	1+0+14	-			
<b>Elective courses selection of at least 6 ECTS</b>					

Study profile and module: Electrical Power Engineering – FER-2,  
academic year 2005/06.

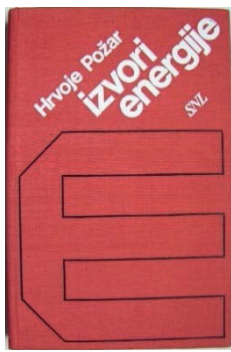
Undergraduate study module – third year electrical Power Engineering			Graduate study module – first year Electrical Power Engineering		
Required courses (ECTS)	Semester		Required courses (ECTS)	Semester	
	Winter	Summer		Winter	Summer
Automatic Control (5)	4+0+1	-	Power Systems Analysis (5)	3+2+0	-
Electric Facilities (4)	3+2+1	-	Power Sys. Dyn. and Con. (5)	3+1+0,4	-
Electromech. and El. Conv. (4)	3+1,3+1	-	Energy Conversion (5)	3+1+0	-
Electronic Communications (5)	4+0+1	-	Economics of Energy (5)	-	3+0,3+0
Sust. Develop. and Environ.(2)	2+0+0	-	High Voltage Engineering (5)	-	2,6+0,4+0
Project (6)	0+0+0	-	<b>Required courses (ECTS)</b>	<b>Winter</b>	<b>Summer</b>
Information Theory (4)	3+0+1	-	Lab. of El. Power Eng. 1 (5)	-	2+0+4
BSc Thesis (12+12)	0+0+0	0+0+0	Seminar (3)	-	2+0+0
Trans. and Dist. of El. Power (4)	-	3+2+0,8	Lab. of El. Power Eng. 2 (3)	-	1+0+2
Commercial Law (2)	-	2+0+0	<b>Specialization courses 12 ECTS</b>		
<b>Selection of elective courses of at least 12 ECTS</b>			<b>Mathematics and science 8 ECTS</b>		
<b>Graduate study module – second year Electrical Power Engineering</b>			<b>Humanistic or social courses 4 ECTS</b>		
Required courses (ECTS)	Semester		<i>Remark:</i> <i>Because of their large number elective courses, specialization courses, courses of mathematics and science and humanistic or social courses are not listed.</i>		
	Winter	Summer			
Project (8)	0+0+0	-			
Graduation Thesis (30+30)	0+0+0	0+0+0			
<b>Selection of elective courses (at least 12 ECTS)</b>					
<b>Specialization courses of total 8 ECTS</b>					
<b>Humanistic or social skills courses 2 ECTS</b>					

## APPENDIX II – LIST OF PUBLISHED BOOKS

1. Hrvoje Požar. “*Economic dispatch in power system: foundations for a practical work of power system operators*” (original in Croatian: Ekonomična raspodjela opterećenja u elektroenergetskom sistemu: osnovi za praktičan rad elektroenergetskih dispečera), Školska knjiga, Zagreb, 1953.
2. Hrvoje Požar. “*Power and energy in composite power systems*” (original in German: Leistung und Energie in Verbundsystemen, Springer-Verlag), Wien, Austria, 1963.
3. Hrvoje Požar. “*Power and energy in power systems*” (original in Croatian: Snaga i energija u elektroenergetskim sistemima), Zajednica jugoslavenske elektroprivrede, Beograd, 1966.
4. Hrvoje Požar. “*High-voltage electric facilities*” (original in Croatian: Visokonaponska rasklopna postrojenja), Tehnička knjiga, Zagreb, 1967.
5. Milan Šodan. “*Automation using logic circuits*” (Original in Croatian: Automatizacija logičkim sklopovima, Školska knjiga), Zagreb, 1973.
6. Hrvoje Požar. “*High-voltage electric facilities – 2nd edition*” (Original in Croatian: Visokonaponska rasklopna postrojenja, Drugo izdanje), Tehnička knjiga, Zagreb, 1973.
7. Božidar Stefanini. “*Fortran – programming course book*” (Original in Croatian: Fortran - udžbenik programiranja), Tehnička knjiga, Zagreb, 1973.
8. Božidar Stefanini, Srđan Babić, Mirjana Urbiha-Feuerbach. “*Matrix methods in power system network analysis*” (Original in Croatian: Matrične metode u analizi električnih mreži), Školska knjiga, Zagreb, 1975.
9. Božidar Stefanini. “*Fortran V – fundamentals*” (Original in Croatian - Fortran V, osnovni tečaj), Školska knjiga, Zagreb, 1975.
10. Hrvoje Požar. “*Power engineering fundamentals – Volume 1*” (Original in Croatian – Osnove energetike, Prvi svezak), Školska knjiga, Zagreb, 1976.
11. Hrvoje Požar. “*Power engineering fundamentals – Volume 2*” (Original in Croatian – Osnove energetike, Drugi svezak), Školska knjiga, Zagreb, 1978.
12. Hrvoje Požar. “*High-voltage electric facilities – 3rd edition*” (Original in Croatian: Visokonaponska rasklopna postrojenja, Treće popravljeno izdanje), Tehnička knjiga, Zagreb, 1978.
13. Hrvoje Požar. “*Energy sources*” (Original in Croatia: Izvori energije), Sveučilišna naklada Liber, Zagreb, 1980.
14. Hrvoje Požar. “*Power and energy in electric power systems – Volume 1 - 2nd edition*” (Original in Croatian: Snaga i energija u elektroenergetskim sistemima, Svezak 1, Drugo prošireno i potpuno prerađeno izdanje), Informator, Zagreb, 1983.
15. Hrvoje Požar. “*High-voltage electric facilities – 4th edition*” (Original in Croatian: Visokonaponska rasklopna postrojenja, Četvrto popravljeno izdanje), Tehnička knjiga, Zagreb, 1984.
16. Hrvoje Požar. “*Power and energy in electric power systems – Volume 2 - 2nd edition*” (Original in Croatian: Snaga i energija u elektroenergetskim sistemima, Drugi svezak, Drugo prošireno i potpuno prerađeno izdanje), Informator, Zagreb, 1985.
17. Mario Padelin. “*Lightning protection*” (Original in Croatian: Zaštita od groma), Školska knjiga, Zagreb, 1987.
18. Hrvoje Požar. “*Power engineering fundamentals 1, 2nd edition*” (Original in Croatian: Osnove energetike 1, Drugo dopunjeno i izmjenjeno izdanje), Školska knjiga, Zagreb, 1992.
19. Hrvoje Požar. “*Power engineering fundamentals 2, 2nd edition*” (Original in Croatian: Osnove energetike 2, Drugo dopunjeno i izmjenjeno izdanje), Školska knjiga, Zagreb, 1992.
20. Hrvoje Požar. “*Power engineering fundamentals 3, 2nd edition*” (Original in Croatian: Osnove energetike 3, Drugo dopunjeno i izmjenjeno izdanje), Školska knjiga, Zagreb, 1992.
21. Danilo Feretić. “*Nuclear power engineering introduction*” (Original in Croatia: Uvod u nuklearnu energetiku), Školska knjiga, Zagreb, 1992.
22. Danilo Feretić, Nikola Čavlina, Nenad Debrecin. “*Nuclear power plants*” (Original in Croatian: Nuklearne elektrane), Školska knjiga, Zagreb, 1995.
23. Danilo Feretić, Željko Tomšić, Dejan Škanata, Nikolna Čavlina, Damir Subašić. “*Power plants and environment*” (Original in Croatian: Elektrane i okoliš), Element, Zagreb, 2000.
24. Srđan Skok. “*Uninterruptable power supply*” (Original in Croatian: Besprekidni izvori napajanja), Kigen, Zagreb, 2002.

25. Zoran Vukić, Ljubomir Kuljača, Dali Donlagić, Sejid Tešnjak. "Nonlinear Control Systems", Marcel Dekker, Inc., New York-Basel, 2003.
26. Srđan Skok. "DC systems and circuits in power facilities" (Original in Croatian: Sustavi istosmjernih razvoda u elektroenergetskim postrojenjima), Kigen, Zagreb, 2007.
27. Vladimir Mikuličić, Zdenko Šimić. "Reliability, availability and risk assessment models in power systems" (Original in Croatian: Modeli pouzdanosti, raspoloživosti i rizika u elektroenergetskom sustavu), Kigen, Zagreb, 2008.
28. Sejid Tešnjak, Eraldo Banovac, Igor Kuzle. "Electricity market" (Original in Croatian: Tržište električne energije), Graphis, Zagreb, 2009.
29. Danilo Feretić, Željko Tomšić, Dejan Škanata, Nikolna Čavlina, Damir Subašić, "Power plants and environment – 2<sup>nd</sup> edition" (Original in Croatian: Elektrane i okoliš, Drugo izdanje), Element, Zagreb, 2009.
30. Danilo Feretić. "Nuclear power engineering introduction – 2<sup>nd</sup> expended edition" Uvod u nuklearnu energetiku, Drugo dopunjeno izdanje, Školska knjiga, Zagreb, 2010.
31. Ivo Uglešić, Milivoj Mandić. "Electric Traction Power Supply" (Original in Croatian: Napajanje električne vuče), Graphis, Zagreb, 2014.
32. Amir Tokić, Viktor Milardić. "Quality of electric power supply" (Original in Bosnian: Kvalitet električne energije), Printcom, Tuzla, 2015.

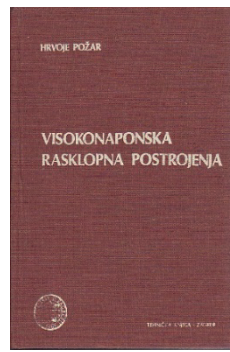




1  
9  
8  
0



1  
9  
8  
3



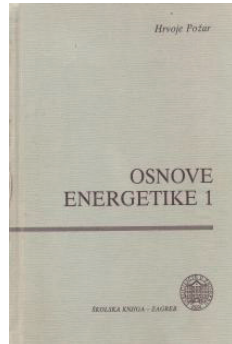
1  
9  
8  
4



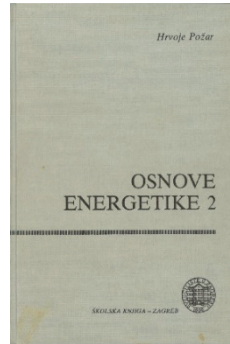
1  
9  
8  
5



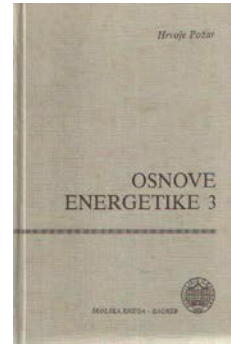
1  
9  
8  
7



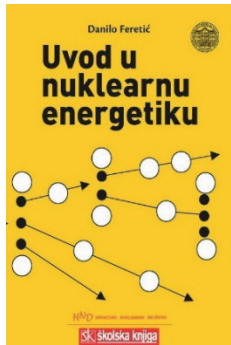
1  
9  
9  
2



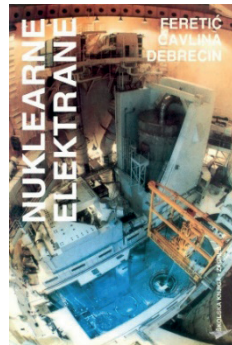
1  
9  
9  
2



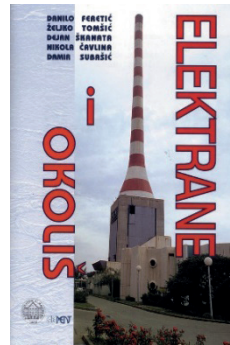
1  
9  
9  
2



1  
9  
9  
2



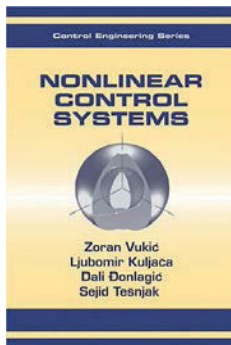
1  
9  
9  
5



2  
0  
0  
0



2  
0  
0  
2



2  
0  
0  
3



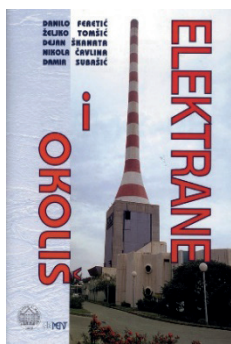
2  
0  
0  
7



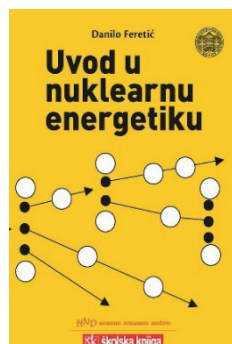
2  
0  
0  
8



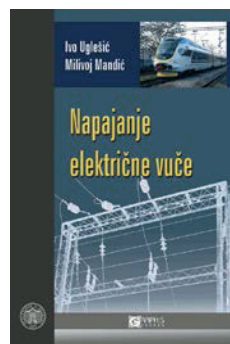
2  
0  
0  
9



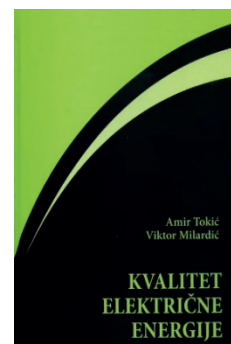
2  
0  
0  
9



2  
0  
1  
0



2  
0  
1  
4



2  
0  
1  
5

### APPENDIX III – LIST OF THE DEPARTMENT LECTURERS AND PROFESORS

NAME	TITLE	PERIOD	FILED
Dr. sc. Srđan Babić (1935)	associate professor	1961-2000	transmission networks, power system stability
Dr. sc. Nikola Čavlina (1950)	full professor	1975-2017	nuclear power plant safety and control
Dr. sc. Nikola Čupin (1938)	associate professor	1964-1973	electrical facility design
Dr. sc. Nenad Debrecin (1953)	full professor	1975	nuclear power plants, heat transfer
Dr. sc. Marko Delimar (1974)	associate professor	1997	transmission networks, power system analysis
Mladen Dokmanić, dipl. ing. (1908-1980)	associate professor	1952-1978	transmission networks, el. grids and installations
Dr. sc. Danilo Feretić (1930)	professor emeritus	1982-2002	nuclear power plants, heat transfer
Dr. sc. Vjekoslav Filipović (1935-2012)	full professor	1961-2005	electrical facilities, power system optimisation
Dr. sc. Davor Grgić (1959)	associate professor	1990	nuclear power plants safety
Dr. sc. Juraj Havelka (1974)	assistant professor	1998	power system protection, SCADA
Dr. sc. Zdravko Hebel (1943-2017)	full professor	1966-2013	transmission networks, power system analysis
ing. Juro Horvat (1882-1954)	professor	1932-1947	electricity generation, transients in el. devices
Dr. sc. Ivo Hrs (1937-1998)	assistant professor	1960-1966	high voltage engineering
Slavko Krajcar (1951)	full professor	1974	electrical facility design, distribution networks
Igor Kuzle (1967)	professor	1992	power systems dynamics and control, smart grids
Toussaint Levičnik, dipl.ing. (1903-1984)	senior associate	1958-1974	electrical facilities
Boris Markovčić, dipl. ing. (1915-2006)	senior lecturer	1952-1957	high voltage engineering, bulk power transmission
Dr. sc. Ante Marušić (1952)	full professor	1977	power system protection and local control
Dr. sc. Vladimir Mikuličić (1944)	full professor	1970-2014	energy conversion, el. power system reliability
Dr. sc. Viktor Milardić (1971)	associate professor	1998	high voltage engineering, electromag. compatibility
Dr. sc. Zoran Morvaj (1957)	assistant professor	1981-1992	energy efficiency, expert systems
Dr. sc. Mario Padelin (1922-1984)	full professor	1957-1984	high voltage techniques, high voltage protection
Dr. sc. Ivica Pavić (1962)	professor	1987	transmission networks, power system analysis
Academician Dr. sc. Hrvoje Požar (1916-1991)	full professor	1951-1984	Electric power systems, electric power engineering
Dr. sc. Božidar Stefanini (1913-1991)	full professor	1950-1984	transmission networks, power system stability
Dr. sc. Zdenko Šimić (1964)	associate professor	1988-2015	electric power engineering, power systems reliability
Dr. sc. Davor Škrlec (1963)	full professor	1987-2014	el. distribution systems, GIS
Dr. sc. Milan Šodan (1927)	full professor	1965-1996	power system control, automation
Dr. sc. Sejid Tešnjak (1949)	full professor	1973-2017	power plants, power system dynamics and control
Dr. sc. Tomislav Tomiša (1954)	full professor	1977	power system automation
Dr. sc. Željko Tomšić (1957)	associate professor	1991	energy management, power system generation planning
Mr. sc. Vladimir Tuk (1943-1997)	assistant	1967-1997	high voltage engineering
Dr. sc. Ivo Uglešić (1952)	full professor	1976	high voltage engineering, electrical railways
Mr. sc. Mirjana Urbiha-Feuerbach (1926-2010)	scientific assistant	1960-1986	power system analysis, overhead lines
Željko Zlatar (1925-2006)	assistant professor	1959-1995	power system protection
Vladimir Žepić (1894-1971)	associate professor	1948-1952	generation, transmission networks

SLAVKO KRAJCAR    PERICA ILAK    IVAN RAJŠL

[perica.ilak@fer.hr](mailto:perica.ilak@fer.hr)    [slavko.krajcar@fer.hr](mailto:slavko.krajcar@fer.hr)    [ivan.rajšl@fer.hr](mailto:ivan.rajšl@fer.hr)

University of Zagreb Faculty of Electrical Engineering and Computing

## HYDROPOWER PLANT SIMULTANEOUS BIDDING IN ELECTRICITY MARKET AND ANCILLARY SERVICES MARKETS

### SUMMARY

In a traditional environment, hydropower plant owners seek for minimum cost while in today deregulated environment goal function is profit maximization. Besides electricity only market, power producers can offer their services also in ancillary services markets. By doing so, it is possible to increase expected profit. This paper focuses on simultaneous hydropower plant bidding in electricity and ancillary services markets, and purpose is to examine and verify effects of the proposed method on expected profit of hydropower plant owner. A mathematical model based on mixed integer programming approach is used. Head effect is also taken into account with price-wise linear performance curves. Prices from real electricity markets and ancillary markets are used, and real hydropower system Lokve-Bayer in Croatia, with focus on hydropower plant Vinodol, is modelled. Obtained results show that there is a notable improvement in expected profit of hydropower plant if presented market bidding approach is used. It is also shown that hydropower plant Vinodol is capable for simultaneous bidding in different power markets.

**Keywords:** multimarket bidding; reservoir head effects; mixed integer programming; hydropower plant scheduling;

# 1. NOMENCLATURE

## Sets

$T$	Set of indices of the steps of the optimization period, planning horizon, $T = \{1, 2, \dots, T_{\max}\}, t \in T, T_{\max} \in N$
$I$	Set of indices of the reservoirs/plants, $I = \{\text{“Križ”}, \text{“Lokve”}, \text{“Lepenica”}, \text{“Bajer”}\}, i \in I.$
$J$	Set of indices of the perf. curves $J = \{1\text{-high lvl.}, 2\text{-middle lvl.}, 3\text{-low lvl.}\}, j \in J.$
$U_i$	Set of upstream reservoirs of plant $i$ .
$B$	Set of indices of the blocks of the piecewise linearization of the unit performance curve $B = \{1, 2, 3\}, b \in B.$
$N$	Set of indices of the profit tolerances $N = \{1, 2, \dots, N_{\max}\}, n \in N.$

## Parameters

$M$	Conversion factor equal to $3600 \text{ (m}^3 \cdot \text{s} \cdot \text{m}^{-3} \cdot \text{h}^{-1}\text{)}.$
$X_{\max}(i)$	Maximal content of the reservoir $i \text{ (m}^3\text{)}.$
$X_l(i)$	$l$ -th discrete level of the content of the reservoir $i, l \in \{1,2,3,4\} \text{ (m}^3\text{)}.$
$X_{\min}(i)$	Minimal content of the reservoir $i \text{ (m}^3\text{)}.$
$X(i, 0)$	Initial water content of the reservoir $i \text{ (m}^3\text{)}.$
$X(i, 24)$	Final water content of the reservoir $i \text{ (m}^3\text{)}.$
$W(i, t)$	Forecasted natural water inflow of the reservoir $i$ in time step $t \text{ (m}^3/\text{s}\text{)}.$
$\Pi_{\text{spot}}(t)$	Forecasted price of real-time electricity market in time step $t \text{ (\$/MWh)}.$
$\Pi_e(t)$	Forecasted price of day ahead electricity market in time step $t \text{ (\$/MWh)}.$
$\Pi_r(t)$	Forecasted price of day ahead regulation market in time step $t \text{ (\$/MWh)}.$
$\Pi_{sr}(t)$	Forecasted price of day-ahead 10 minute spinning reserve market in time step $t \text{ (\$/MWh)}.$
$Q_{\min}(i)$	Minimum water discharge of plant $i \text{ (m}^3/\text{s}\text{)}.$
$Q_{\max}(i)$	Maximum water discharge of plant $i \text{ (m}^3/\text{s}\text{)}.$
$Q_{\max}(i, b)$	Maximum water discharge of block $b$ of plant $i \text{ (m}^3/\text{s}\text{)}.$
$B_{\min}(i)$	Ecological minimum of plant $i \text{ (m}^3/\text{s}\text{)}.$
$P0_n(i)$	Minimum power output of plant $i$ for performance curve $n, n \in \{1,2,3,4,5\} \text{ (MW)}.$
$P_{\max}(i)$	Capacity of plant $i \text{ (MW)}.$
$\rho_j(i, b)$	Slope of the block $b$ of the performance curve $j$ of plant $i \text{ (MW/m}^3\text{)}.$
$\rho^{-1}(i, t)$	Conversion factor used for converting $\text{(m}^3\text{)}$ to $\text{(MWh)}$ for reservoir $i$ in particular time step $t$ . Meaning calculation of reservoir energy potential $\text{(MWh/m}^3\text{)}$ in time step $t$ .
$p_{\text{rup}}(t)$	Probability of being in Regulation-up state in time step $t$ .
$p_{\text{rdown}}(t)$	Probability of being in Regulation-down state in time step $t$ .
$p_{\text{del}}(t)$	Probability of spinning reserve to be activated in time step $t$ .

$MSR(i)$	Maximum sustain ramp rate of plant $i$ (MW/min).
$UP(i)$	Ramping up limit of plant $i$ (MW/h).
$DR(i)$	Ramping down limit of plant $i$ (MW/h).
$\Delta_l(i)$	Difference between maximal values of two neighboring perf. curves of plant $i$ , $l \in \{1,2,3,4\}$ (MW).
$\delta_l(i)$	Difference between minimal values of two neighboring perf. curves of plant $i$ , $l \in \{1,2,3,4\}$ (MW).
<b>Variables</b>	
$X(i, t)$	Water content of the reservoir $i$ at the end of time step $t$ (m <sup>3</sup> ).
$X_{avg}(i, t)$	Average water content of the reservoir $i$ in time step $t$ (m <sup>3</sup> ).
$q(i, t)$	Water discharge of plant $i$ in time step $t$ (m <sup>3</sup> /s).
$q_u(i, t, b)$	Water discharge of block $b$ of plant $i$ in time step $t$ (m <sup>3</sup> /s).
$s(i, t)$	Spillage of the reservoir $i$ in time step $t$ (m <sup>3</sup> /s).
$d_k(i, t)$	0/1 variable used for discretization of performance curves, $k \in \{1, 2, 3, 4\}$ .
$w(i, t, 0)$	0/1 variable which is equal to 1 if plant $i$ is on-line in time step $t$ .
$w(i, t, b)$	0/1 variable which is equal to 1 if water discharged by plant $i$ has exceeded block $b$ in time step $t$ .
$P(i, t)$	Total power output of the performance curve of plant $i$ in time step $t$ (MW).
$P_e(i, t)$	Power output of plant $i$ committed to energy market in time period $t$ (MW).
$P_r(i, t)$	Regulation service capacity of plant $i$ in time period $t$ (MW).
$P_{sr}(i, t)$	10 min spinning reserve of plant $i$ available for increase of output power in time period $t$ (MW).
$P_{tr}(i, t)$	Tertiary reserve of plant $i$ available for increase of output power in time period $t$ (MW).
$E(i, t)$	Total electricity produced for the energy, regulation and spinning reserve market.
$E_e(i, t)$	Electricity produced for energy market by plant $i$ in time period $t$ (MWh).
$E_r(i, t)$	Electricity produced for regulation service by plant $i$ in time period $t$ (MWh).
$E_{sr}(i, t)$	Electricity produced for spinning reserve service by plant $i$ in time period $t$ (MWh).
$E_{tr}(i, t)$	Electricity produced for tertiary regulation service by plant $i$ in time period $t$ (MWh).

## 2. INTRODUCTION

Water is a scarce resource with uncertain availability. It is therefore complicated to find economically optimal hydropower plant schedule. In a traditional environment, goal function is usually cost minimization [1], [2] and [3] while in the deregulated environment goal function is profit maximization [4] and

[5]. In this paper that is based on [6], hydropower plant (HPP) operation in a deregulated environment is considered. Optimization purpose is to find maximum profit with simultaneous bidding on a day-ahead auction market (DAAM) and ancillary services markets. Model is set by *mixed* integer linear programming (MILP) approach with HPP maximum profit as a goal function. In a short-term planning, most of the parameters can be considered as known, and short-term models are called therefore deterministic [7] and [8]. Model in this paper is also deterministic. Some stochastic models are presented in [9], [10] and [11], [12], [13]. Short-term planning also considers effects of water levels in reservoirs on HPP power output. It is, therefore, necessary to model these dependencies between reservoir water levels, turbine discharge and power outputs as described in [14]. This paper is focused on the real hydropower system (HPS), HPS Vinodol, also called HPS Lokve-Bajer because it utilizes water power from Lokvarka and Ličanka basins and some other minor connected basins. Particular attention is given to HPP Vinodol as core building part of HPS Vinodol which data is presented in Figure 1.

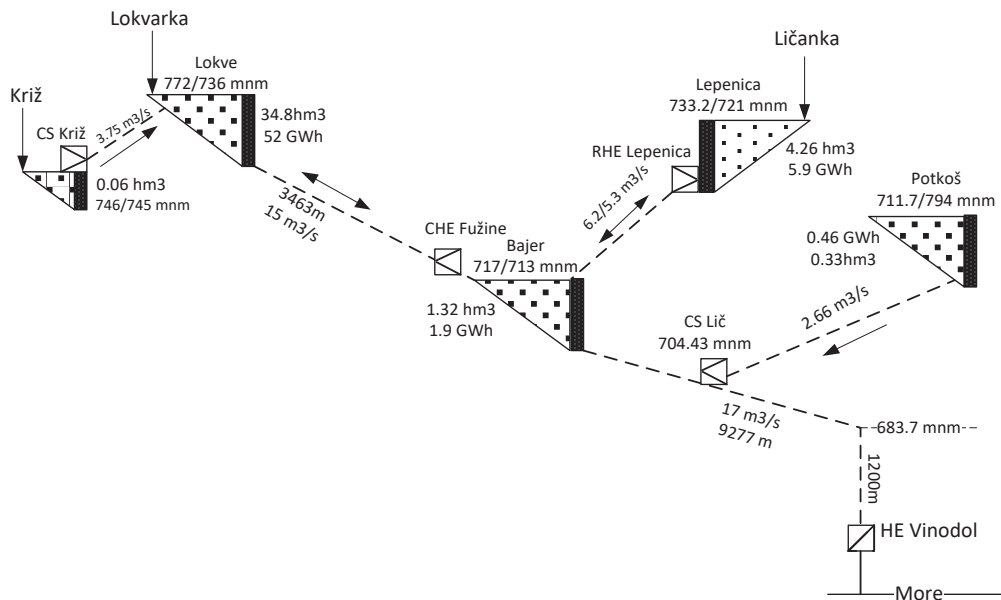


Figure 1. The depiction of HPS Vinodol

Data on electrical assets in HPS Vinodol are taken from [15]. Ramp-up and ramp-down speed of power plant is of great importance regarding their role in ancillary services markets. Ramping constraints in thermal power plants are due to the mechanical and thermodynamic stress of turbines, and typical values are 0,03-0,6 p.u.MW/min (0,0005-0,01 p.u.MW/s) [16], [17] and [18]. On the other hand, technical characteristics of HPPs allow fast ramping in both directions. Ramping constraints in hydropower plants are defined by primary regulators, and therefore HPPs have faster ramping in comparison to thermal power plants with typical values of 2,7 p.u.MW/min (0,045 p.u.MW/s) for ramp-up and -3,6 p.u.MW/min (-0,06 p.u.MW/s) for ramp-down [17]. HPP Vinodol can increase power output from zero to nominal power  $P_{max}$  in 22 seconds. It can also decrease power output from nominal power to zero in 17 seconds. Maximum sustain ramp rate for HPP Vinodol in this paper is set to: MSR = 2.7 /-3,6 [p.u.MW/min] and falls into typical value range for

HPP. It is obvious that HPP owners may find some benefits from bidding also on ancillary services markets, in addition to bidding on just electricity markets.

A modelled day ahead electricity market (DAAM) is similar to those deregulated markets such as New England Power Pool, California Market, Australia Electricity Market and New Zealand Electricity Market, where production plan of each power producer or generating company – GENCO is its responsibility in search for maximum profit. GENCO uses PBUC price based unit commitment [19] optimization model for optimal power schedule.

### 3. PROBLEM DESCRIPTION AND FORMULATION

Model of simultaneous participation of HPP in DAAM and ancillary services markets requires a definition of multilayer problem, namely hydraulic layer, electrical layer and economic layer. Goal function is the profit of HPP Vinodol expressed in (1):

$$\text{Profit}(t) = \sum_{i \in I} [\Pi_e(t) \cdot E_e(i, t) + \Pi_{\text{spot}}(t) \cdot E_r(i, t) + \Pi_r(t) \cdot P_r(i, t) + \Pi_{\text{spot}}(t) \cdot E_{sr}(i, t) + \Pi_{sr}(t) \cdot P_{sr}(i, t)] \quad (1)$$

where variables and parameters are defined in the nomenclature above.

A mathematical model, analysis and results will be based on a model of real HPS Lokve-Bajer (HPS Vinodol). But since HPP Vinodol is by far largest and most dominant HPP in system optimization criterion is set to be a maximum profit of HPP Vinodol.

### 4. HPS Lokve-Bajer/ HPS Vinodol

HPS Lokve-Bajer consists of 5 reservoirs (Križ, Lokve, Bajer, Lepenica, Potkoš), two pumped stations (PS) (PS Križ, PS Lič) and 3 HPPs (PHPP Fužine, PHPP Lepenica, HPP Vinodol). Technical characteristics of HPPs and reservoirs are given in table 1. Natural inflows and reservoir seepages are given in table 2.

Table I Technical characteristics of HPPs and reservoirs, \*turbine/pump

Reservoir	Volume [hm <sup>3</sup> ]	HPP/PS	Discharge [m <sup>3</sup> /s]	Power [MW]
Križ	0.06	PS Križ	1.1	0.34
Lokve	34.8	PHPP Fužine	10/9*	4.6/4.8*
Bajer	1.32	HPP Vinodol	18.6	94.5
Lepenica	4.26	PHPP Lepenica	6.2/5.3*	1.14/1.25*
Potkoš	0.33	PS Lič	0.45	0.36

Table II. Natural inflow of reservoirs, \*inflow/seepage

Reservoir	Križ	Lokve	Bajer	Lepenica	Potkoš
Natural inflow	4	4	8/1*	4	4

A mathematical model of HPS Lokve-Bajer consists among other of water balances [14] that describe the relationship between reservoirs in each time step  $t$ . HPP Vinodol is modelled by power output curves in more details for already stated reasons while rest HPPs and pumped stations are modelled with a simple linear relationship between turbine discharge and power output.

## 5. Reservoirs

Five reservoirs in HPS Bajer-Lokve are mutually interconnected with pipelines. Reservoir water level (volume) in time step  $t$  is determined by reservoir water level (volume) in time step  $t - 1$ , natural inflow, turbine discharges and overflows of upstream HPPs connected with a reservoir of interest, and also own turbine discharge and overflow in step  $t$ . This linear relationship (2) is called reservoir water balance. In this model time delays are neglected.

$$X(i, t) = X(i, t - 1) + M \cdot W(i, t) + M \cdot \sum_{j \in U} [q(j, t) + s(j, t)] - M \cdot [q(i, t) + s(i, t)] \quad (2)$$

$$\forall i \in I, \forall t \in T$$

## 6. HPPs and pumped stations

Data for the model of HPPs and pumped stations are given in table 3.

Table III. Technical characteristics of HPPs and pumped stations of HPS Lokve-Bajer<sup>1</sup>

HPP/PS	Q <sub>t</sub> /Q <sub>c</sub> (m <sup>3</sup> /s)	P <sub>t</sub> /P <sub>c</sub> (MW)	H <sub>b</sub> (m)	H <sub>n</sub> (m)
PS Križ	NA/1.1	NA/0.34	8.5	8
PS Lič	NA/0.45	NA/0.36	NA	NA
PHPP Fužine	10.0/9.0	4.6/4.8	NA	37
HPP Vinodol	18.6/NA	94.5/NA	658.5	623

## 7. Power output curves for HPP Vinodol

The power output of HPP Vinodol is modelled by five piecewise linear power output curves. Each curve is used to describe appropriate discrete reservoir part in reservoir Bajer (connected to HPP Vinodol). This nonlinear relationship is called Hill chart [20]. It is set of nonlinear curves called performance curves each defined for the specific water content of reservoir. According to [14] and [20], it is possible to linearize these curves by using binary (0/1) variables and mixed integer linear

<sup>1</sup> Source: Hrvatska elektroprivreda

programming approach to precisely model performance curves. The same approach is used in this paper. HPP Vinodol linearized performance curves are shown in figure 2.

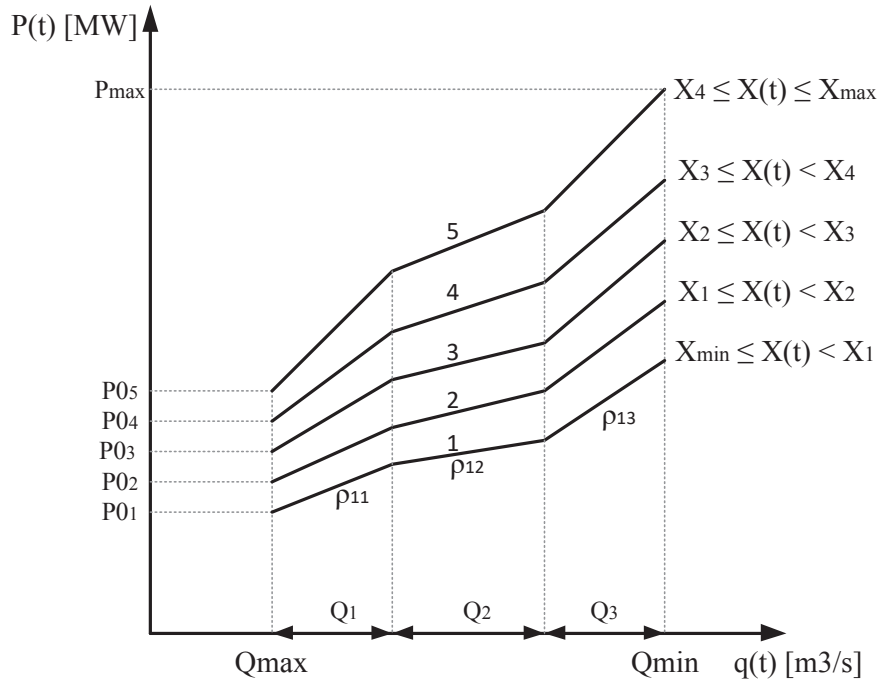


Figure 2 The depiction of HPS Vinodol

Activation of appropriate power output curve  $P(t)$  in time step  $t$  depends on water level (volume) of reservoir  $X(t)$  in time step  $t$ . It is, therefore, necessary to divide reservoir Bajer into discrete levels as shown in table 4. This activation is presented in [14] and upgraded in [21]. Expressions (3) - (13) are used to model this activation:

Table IV. Discrete levels of reservoir Bajer

Reservoir	Xmin	X1	X2	X3	X4	Xmax
Bajer	1.0hm <sup>3</sup>	1.1hm <sup>3</sup>	1.20hm <sup>3</sup>	1.25hm <sup>3</sup>	1.30hm <sup>3</sup>	1.32hm <sup>3</sup>

$$X_{avg}(i, t, k) = \frac{X(i, t, k) + X(i, t - 1, k)}{2}, \quad \forall i \in I, \forall t \in T, \forall k \in K \quad (3)$$

$$X_{avg}(i, t, k) \geq X_1(i) \cdot [d_1(i, t, k) - d_2(i, t, k)] + X_2(i) \cdot [d_2(i, t, k) - d_3(i, t, k)] \\ + X_3(i) \cdot [d_3(i, t, k) - d_4(i, t, k)] + X_4(i) \cdot d_4(i, t, k), \\ \forall i \in I, \forall t \in T, \forall k \in K \quad (4)$$

$$X_{avg}(i, t, k) \leq X_{max}(i) \cdot d_4(i, t, k) + X_1(i) \cdot [1 - d_1(i, t, k)] + X_2(i) \\ \cdot [d_1(i, t, k) - d_2(i, t, k)] + X_3(i) \cdot [d_2(i, t, k) - d_3(i, t, k)] + X_4(i) \\ \cdot [d_3(i, t, k) - d_4(i, t, k)], \forall i \in I, \forall t \in T, \forall k \in K \quad (5)$$

$$d_1(i, t, k) \geq d_2(i, t, k), \quad (6)$$

$$d_2(i, t, k) \geq d_3(i, t, k),$$

$$d_3(i, t, k) \geq d_4(i, t, k), \quad \forall i \in I, \forall t \in T, \forall k \in K$$

$$X(i, t, k) \leq X_{max}(i), \quad (7)$$

$$X(i, t, k) \geq X_{min}(i), \quad \forall i \in I, \forall t \in T, \forall k \in K$$

Each of five power output curves is defined with unique combination of binary decision variables  $d1, d2, d3, d4$  shown in table 5.

Table V. Combinations of binary decision variables  $d_1, d_2, d_3, d_4$

Combination	0000	1000	1100	1110	1111
Curve	1	2	3	4	5

For example, when water content  $X(t)$  of reservoir is between levels  $X_1$  and  $X_2$ , expressions (3) to (7) sets the binary variables  $d1, d2, d3, d4$  to values 1, 0, 0, 0 and, therefore, activates performance curve 2 using expressions (8) to (13).

$$P(i, t, k) - P0_1(i) \cdot v(i, t, k) - \sum_{blok=1}^3 q(i, t, k, blok) \cdot \rho(i, blok) - 10 \cdot P_{max}(i) \cdot [d_1(i, t, k) + d_2(i, t, k) + d_3(i, t, k) + d_4(i, t, k)] \leq 0,$$

$$P(i, t, k) - P0_1(i) \cdot v(i, t, k) - \sum_{blok=1}^3 q(i, t, k, blok) \cdot \rho(i, blok) + 10 \cdot P_{max}(i) \cdot [d_1(i, t, k) + d_2(i, t, k) + d_3(i, t, k) + d_4(i, t, k)] \geq 0, \quad (8)$$

$$\forall i \in I, \forall t \in T, \forall k \in K$$

$$P(i, t, k) - P0_2(i) \cdot v(i, t, k) - \sum_{blok=1}^3 q(i, t, k, blok) \cdot \rho(i, blok) - 10 \cdot P_{max}(i) \cdot [1 - d_1(i, t, k) + d_2(i, t, k) + d_3(i, t, k) + d_4(i, t, k)] \leq 0,$$

$$P(i, t, k) - P0_2(i) \cdot v(i, t, k) - \sum_{blok=1}^3 q(i, t, k, blok) \cdot \rho(i, blok) + 10 \cdot P_{max}(i) \cdot [1 - d_1(i, t, k) + d_2(i, t, k) + d_3(i, t, k) + d_4(i, t, k)] \geq 0, \quad (9)$$

$$\forall i \in I, \forall t \in T, \forall k \in K$$

$$P(i, t, k) - P0_3(i) \cdot v(i, t, k) - \sum_{blok=1}^3 q(i, t, k, blok) \cdot \rho(i, blok) - 10 \cdot P_{max}(i) \cdot [2 - d_1(i, t, k) - d_2(i, t, k) + d_3(i, t, k) + d_4(i, t, k)] \leq 0,$$

$$P(i, t, k) - P0_3(i) \cdot v(i, t, k) - \sum_{blok=1}^3 q(i, t, k, blok) \cdot \rho(i, blok) + 10 \cdot P_{max}(i) \cdot [2 - d_1(i, t, k) - d_2(i, t, k) + d_3(i, t, k) + d_4(i, t, k)] \geq 0, \quad (10)$$

$$\forall i \in I, \forall t \in T, \forall k \in K$$

$$P(i, t, k) - P0_4(i) \cdot v(i, t, k) - \sum_{blok=1}^3 q(i, t, k, blok) \cdot \rho(i, blok) - 10 \cdot P_{max}(i) \cdot [3 - d_1(i, t, k) - d_2(i, t, k) - d_3(i, t, k) + d_4(i, t, k)] \leq 0,$$

$$P(i, t, k) - P0_4(i) \cdot v(i, t, k) - \sum_{blok=1}^3 q(i, t, k, blok) \cdot \rho(i, blok) + 10 \cdot P_{max}(i) \cdot [3 - d_1(i, t, k) - d_2(i, t, k) - d_3(i, t, k) + d_4(i, t, k)] \geq 0, \quad (11)$$

$$P(i, t, k) - P0_4(i) \cdot v(i, t, k) - \sum_{blok=1}^3 q(i, t, k, blok) \cdot \rho(i, blok) + 10 \cdot P_{max}(i) \cdot [3 - d_1(i, t, k) - d_2(i, t, k) - d_3(i, t, k) + d_4(i, t, k)] \geq 0,$$

$$\forall i \in I, \forall t \in T, \forall k \in K$$

$$P(i, t, k) - P_{04}(i) \cdot v(i, t, k) - \sum_{blok=1}^3 q(i, t, k, blok) \cdot \rho(i, blok) - 10 \cdot P_{max}(i) \cdot [4 - d_1(i, t, k) - d_2(i, t, k) - d_3(i, t, k) - d_4(i, t, k)] \leq 0,$$

$$P(i, t, k) - P_{04}(i) \cdot v(i, t, k) - \sum_{blok=1}^3 q(i, t, k, blok) \cdot \rho(i, blok) + 10 \cdot P_{max}(i) \cdot [4 - d_1(i, t, k) - d_2(i, t, k) - d_3(i, t, k) - d_4(i, t, k)] \geq 0,$$

$$\forall i \in I, \forall t \in T, \forall k \in K$$

$$q(i, t, 1', k) \leq Q_1(i) \cdot v(i, t, k),$$

$$q(i, t, 1', k) \geq Q_1(i) \cdot w(i, t, 1', k),$$

$$q(i, t, 2', k) \leq Q_2(i) \cdot w(i, t, 1', k),$$

$$q(i, t, 2', k) \geq Q_2(i) \cdot w(i, t, 2', k),$$

$$q(i, t, 3', k) \leq Q_3(i) \cdot w(i, t, 2', k),$$

$$q(i, t, 3', k) \geq Q_3(i) \cdot w(i, t, 3', k), \quad \forall i \in I, \forall t \in T, \forall k \in K$$

Expressions (8) to (13) define performance curves shown in figure 2. Performance curves are linearized form of Hill chart. Conversion coefficients  $\rho$  [MW / m<sup>3</sup>/s] in (9) to (13) define the efficiency of transformation of water energy (1m<sup>3</sup> in a reservoir) into electrical energy (MWh).

## 8. Ancillary services

Ancillary service that will be provided by HPP in this paper is service of frequency control. That can be achieved by primary, secondary or tertiary regulation for which provision is responsible transmission system operator (TSO) [22]. Criteria that provider must comply with are defined by conditions for connection to transmission grid [23].

### 8.1.1. The primary regulation

Methods of modelling reserve of active power for the primary regulation presented in [24] and [19] are modified to a suite to model of HPS in this paper.

- Regulation-up: In this case, power output must increase. HPP makes a profit based on an available amount of primary reserve  $P_r(t)$  [MW] with a price  $\lambda_r(t)$  [€/MW] in time step  $t$  and delivered electricity for regulation  $E_r(t)$  [MWh] with electricity spot price  $\lambda_e(t)$  [€/MWh] while providing regulation in time step  $t$ .  $p_{r,up}$  is a probability that HPP will be in the Regulation-up state.
- Regulation-down: In this case, power output must increase. HPP makes a profit based on an available amount of primary reserve  $P_r(t)$  [MW] with a price  $\lambda_r(t)$  [€/MW] in time step  $t$ . Due to the decrease in delivered electricity during regulation-down ( $E_r(t)$  [MWh] < 0), HPP does not receive electricity spot price  $\lambda_e(t)$  [€/MWh] for an amount  $E_r(t)$ .  $p_{r,down}$  is a probability that HPP will be in the Regulation-down state.

- No-regulation: In this case, power output does not change. HPP makes a profit based on an available amount of primary reserve  $P_r(t)$  [MW] with a price  $\lambda_r(t)$  [€/MW]. The probability that HPP will be in No-regulation state is  $(1 - p_{r,up} \cdot p_{r,down})$ .

The probability for Regulation-up and Regulation-down are 40% and 35% respectively. This assumption is taken from [25] and presented in table 6.

Table VI. Combinations of binary decision variables  $d_1, d_2, d_3, d_4$

$p_{r,up}$	$p_{r,down}$	$(1 - p_{r,up} \cdot p_{r,down})$
0.40	0.35	0.25

In comparison to primary regulation modelling in [24], where mixed integer non-linear programming - MINLP was used, in this paper primary regulation is modelled using mixed integer linear programming – MILP. Piecewise linear performance curves are suitable for the additional description of primary regulation, and it is used in figure 3 (performance curve number 5).

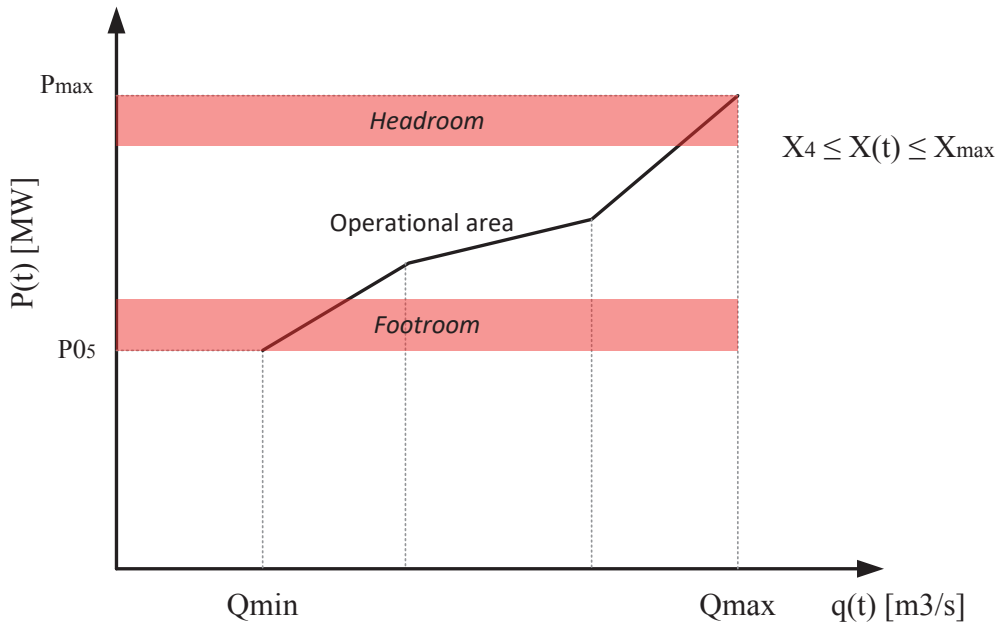


Figure 3 Operational area of HPP while providing primary regulation

The operational area of HPP for producing electricity  $P_e(t)$  becomes narrower if some amount of primary regulation  $P_r(t)$  is provided (Figure 3.). HPP, therefore, must operate below nominal power, and this restricted part is called headroom and defined by (14). Bottom restricted operational area, called foot room, considers that HPP must operate above its minimum power output  $P0$ , to be able to provide some regulation-down service. This part is defined by (15). Following expressions define previously stated restricted areas:

$$P_e(t) \leq P_{max} - P_r(t) \quad [\text{MW}], \forall t \in T \quad (14)$$

$$P_e(t) \geq P_0 + P_r(t) \text{ [MW]}, \forall t \in T \quad (15)$$

Expressions (14) and (15) are actually simplified versions of expressions used in the model. Those more complex expressions for an operational area are following:

$$P_e(t) \leq P_{max} + \Delta_1 \cdot (d_1(t) - 1) + \Delta_2 \cdot (d_2(t) - 1) + \Delta_3 \cdot (d_3(t) - 1) + \Delta_4 \cdot (d_4(t) - 1) - P_r(t) \text{ [MW]}, \forall t \in T \quad (16)$$

$$P_e(t) \geq P_{05} + \delta_1 \cdot (d_1(t) - 1) + \delta_2 \cdot (d_2(t) - 1) + \delta_3 \cdot (d_3(t) - 1) + \delta_4 \cdot (d_4(t) - 1) + P_r(t) \text{ [MW]}, \forall t \in T \quad (17)$$

Where symbols  $\Delta_i, i \in \{1,2,3,4\}$  denote difference between maximum values of two neighboring power output curves, and symbols  $\delta_i, i \in \{1,2,3,4\}$  denote a difference between maximum values of two neighboring power output curves (Figure 4).

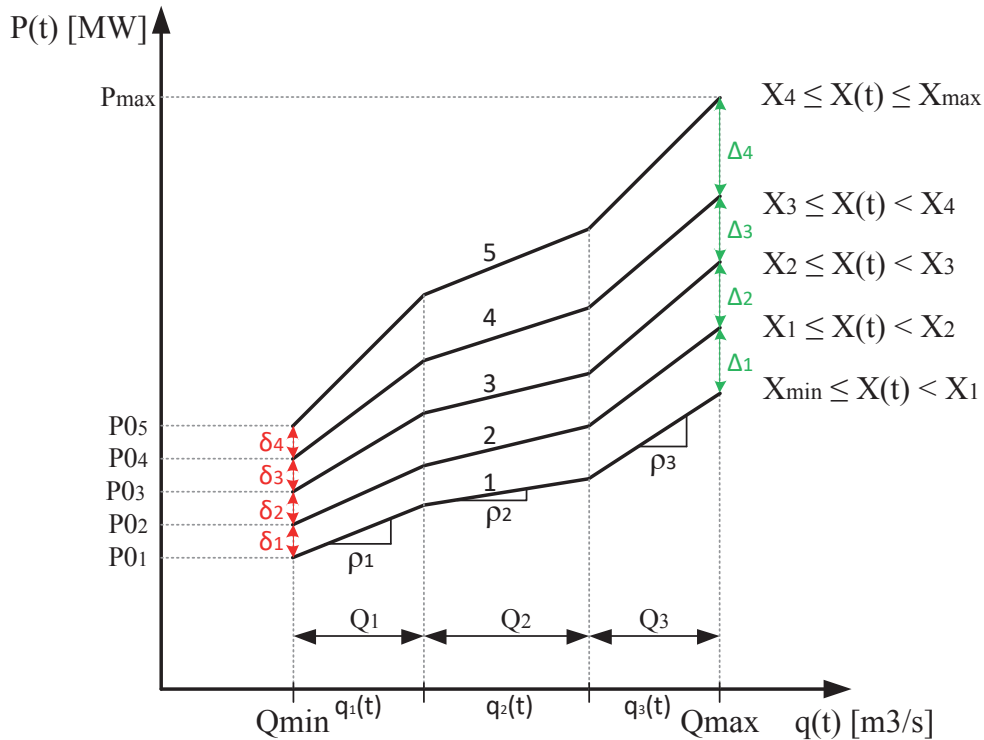


Figure 4 Performance curves for HPP Vinodol

Each  $E(t)$  represents performance curve  $P(t)$  for (expected) power output in [MW], and is defined by (18). Time step  $t$  is 1h, and therefore (18) in step  $t$  can also be considered as (expected) produced electricity  $E(t)$  in [MWh] and is defined by (19).

$$P(t) := E(t) = P_e(t) + (p_{r,up} - p_{r,down}) \cdot P_r(t) \text{ [MW]} \text{ or} \quad (18)$$

$$E(t) = E_e(t) + E_r(t) \text{ [MWh]} \quad (19)$$

Like method presented in [24], top and bottom constraint on primary regulation for HPP are modelled by (20). In this case, a top constraint is equal to a half value of nominal power output of HPP:

$$0 \leq P_r(t) \leq P_{max}/2 \text{ [MW]}, \forall t \in T \quad (20)$$

### 8.1.2. Spinning reserve

According to [26], secondary regulation is ancillary service related to secondary control that tries to minimize Area Control Error (ACE). The range of secondary regulation is an interval of active power that is available for remote control by automatic generation control (ACG) within 10 minutes from secondary control activation. The amount of secondary-up or secondary-down regulation is an amount for which active power can be increased or decreased considering an operational state of HPP at the moment of activation of the secondary control. Spinning reserve is modelled similarly to methods presented in [24] and [19]. There are no time constraints regarding the response of the secondary reserve of HPP in [24]. On the other hand, in [19] those temporal constraints are taken into account in the form of maximum sustain ramp rate (MSR) [MW/min] parameter that is defined by the manufacturer. MSR represents maximum stable ramp rate of power plant and is a very important parameter for frequency control. According to [27] for needs of the primary regulation, an available primary reserve should have following characteristics: the power plant must be able to change power output for 1,5% of nominal power in less than 15 seconds for frequency variations up to 100 mHz and linearly change power output for 3% of nominal power in less than 30 seconds for frequency variations up to 200 mHz. For this paper time constraints, regarding power output changes, in other words, MSR parameter, is set to  $MSR = 5.67$  MW/min. According to [19] the secondary regulation available in time step  $t$  is:

$$P_{sr}(t) \leq \min\{15 \cdot MSR, P_{max} - P_e(t)\} \quad (21)$$

and considering also both primary reserve and secondary-up and down reserve:

$$P_{sr, up}(t) \leq \min\{15 \cdot MSR, P_{max} - P_e(t) - P_r(t)\} \quad (22)$$

$$P_{sr, down}(t) \leq \min\{15 \cdot MSR, P_e(t) - P_0 - P_r(t)\} \quad (23)$$

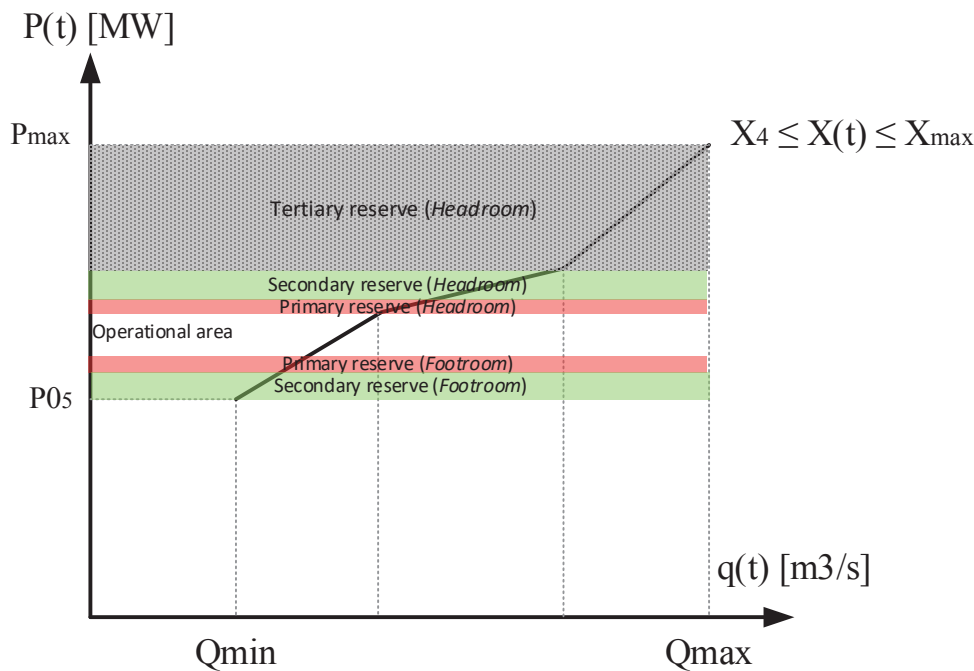


Figure 5. Footroom and headroom for primary and secondary reserve

Footroom for both primary and secondary reserve is shown in figure 5. The ramp rate of HPP Vinodol (MSR) is several times larger than nominal power, and therefore there are no restrictions on secondary regulation ( $15[\text{min}] \cdot \text{MSR}[\frac{\text{MW}}{\text{min}}]$ ) except required headroom and footroom for the secondary reserve. Ramping constraints for HPP are defined by expressions (24) and (25):

$$P_{sr,up}(t) \leq \min\{15 \cdot \text{MSR}, P_{max} - P_e(t) - P_r(t)\} \quad (24)$$

$$P_{sr,down}(t) \leq \min\{15 \cdot \text{MSR}, P_e(t) - P_0 - P_r(t)\} \quad (25)$$

Same assumption. as in the example from [31]. is made. Therefore, HPP Vinodol can change power output very fast, from minimum power  $P_0$  to nominal power  $P_{max}$  within 17 seconds. Expressions (26) and (27), taken from [24], define an amount of the power output changes between two consecutive time steps (hours) that cannot be greater than parameters UP and DR stated in table 7.

$$P(t) - P(t - 1) \leq UP \quad (26)$$

$$P(t - 1) - P(t) \leq DR \quad (27)$$

Table VII. Combinations of binary decision variables  $d_1, d_2, d_3, d_4$

HPP	MSR Up [p.u.MW/min]	MSR Down [p.u.MW/min]	15·MSR up [MW/min]	15·MSR Down [MW/min]	UR [MW]	DR [MW]
Vinodol	2.7	-3.6	94.5	-94.5	94.5	-94.5

Expressions (28) and (29) define an operational area for HPP power output regarding electricity production:

$$P_e(t) \leq P_{max} - P_r(t) - P_{sr}(t) \quad [\text{MW}], \forall t \in T \quad (28)$$

$$P_e(t) \geq P_0 + P_r(t) + P_{sr}(t) \quad [\text{MW}], \forall t \in T \quad (29)$$

Expressions (28) and (29) are actually simplified versions of expressions used in model in order to define operational area. Those more complex expressions for operational area are following:

$$P_e(t) \leq P_{max} + \Delta_1 \cdot (d_1(t) - 1) + \Delta_2 \cdot (d_2(t) - 1) + \Delta_3 \cdot (d_3(t) - 1) + \Delta_4 \cdot (d_4(t) - 1) - P_r(t) - P_{sr}(t) \quad [\text{MW}], \forall t \in T \quad (30)$$

$$P_e(t) \geq P_0 + \delta_1 \cdot (d_1(t) - 1) + \delta_2 \cdot (d_2(t) - 1) + \delta_3 \cdot (d_3(t) - 1) + \delta_4 \cdot (d_4(t) - 1) + P_r(t) + P_{sr}(t) \quad [\text{MW}], \forall t \in T \quad (31)$$

Where symbols  $\Delta_i, i \in \{1,2,3,4\}$  denote a difference between maximum values of two neighboring power output curves, and symbols  $\delta_i, i \in \{1,2,3,4\}$  denote difference between maximum values of two neighboring power output curves. When HPP participate in ancillary services market in particular time step  $t$ , HPP makes a profit from that market and also from electricity market. If HPP participates in the secondary regulation market following situations can occur:

- HPP also participate in electricity market: in this state, HPP also makes a profit from electricity market besides the secondary reserve market. The probability of this state is  $p_{del}$ .
- HPP does not participate in electricity market: in this state, HPP makes a profit just from secondary reserve market. The probability of this state is  $(1 - p_{del})$ .

In order to calculate HPP profit it is necessary to determine amount of electricity that HPP has produced for needs of secondary regulation  $E_{sr}(t)[MWh]$ . Therefore  $p_{del} \cdot E_{sr}(t)$  is used in expression (33) that defines total produced electricity in time step  $t$ . It is important to note that this is actually expected value.

$$P(t) := E(t) = P_e(t) + p_{del} \cdot P_{sr}(t) \quad [MW] \quad \text{or} \quad (32)$$

$$E(t) = E_e(t) + E_{sr}(t) \quad [MWh] \quad (33)$$

Expected power output,  $p_{del} \cdot P_{sr}(t)$ , ( $p_{del} \cdot E_{sr}(t)$ ) and water discharge  $q(t)$  from HPP Vinodol in time step  $t$  are shown in figure 6.

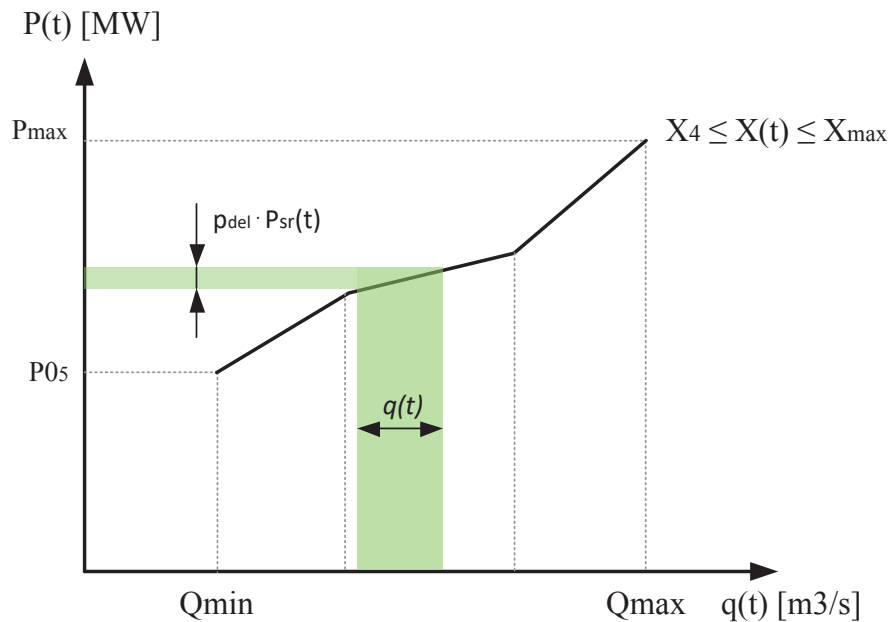


Figure 6 Expected power output and water discharge from HPP Vinodol

### 8.1.3. The tertiary (cold) reserve

The tertiary reserve can be divided into fast and slow. The fast tertiary reserve is activated for necessary secondary reserve backup. It is also called minute backup and must mitigate effects of an outage of a largest producing power plant in the system [28]. The slow tertiary reserve is needed for an optimization of power flows and electricity production in the system [29]. The tertiary reserve can also be used for congestion management by the rescheduling of production in one regulation area. The operational area of HPP, that offers tertiary reserve, is shown on figure 5 and defined by expressions (34) and (35) and additionally (36) and (37):

$$P_{tr}(t) \leq P_{max} \quad [MW], \forall t \in T \quad (34)$$

$$P_{tr}(t) \geq P0 \text{ [MW]}, \forall t \in T \quad (35)$$

Expressions (35) and (36) are more complex and are used in this model. They define cold reserve and its range:

$$P_{tr}(t) \leq P_{max} + \Delta_1 \cdot (d_1(t) - 1) + \Delta_2 \cdot (d_2(t) - 1) + \Delta_3 \cdot (d_3(t) - 1) + \Delta_4 \cdot (d_4(t) - 1) \text{ [MW]}, \forall t \in T \quad (36)$$

$$P_{tr}(t) \geq P0_5 + \delta_1 \cdot (d_1(t) - 1) + \delta_2 \cdot (d_2(t) - 1) + \delta_3 \cdot (d_3(t) - 1) + \delta_4 \cdot (d_4(t) - 1) \text{ [MW]}, \forall t \in T \quad (37)$$

To calculate HPP profit, it is necessary to determine an amount of electricity that HPP has produced for needs of the tertiary regulation  $E_{tr}(t)[MWh]$ . Therefore,  $p_{tr,del} \cdot P_{tr}(t)$  is used in expressions (38).

- Probability that HPP will be chosen for tertiary reserve in time step  $t$  is  $p_{tr,del}$ . That probability is used to determine expected produced electricity in time step  $t$  using expression (38). In this case, HPP makes a profit both from participation on the tertiary reserve market and delivered electricity during provision of tertiary reserve.

$$E_{tr}(t) = p_{tr,del} \cdot P_{tr}(t) \text{ [MW]} \quad (38)$$

#### 8.1.4. About electricity market and ancillary services markets

HPP Vinodol is assumed to be price taker. Ancillary services markets modelled in this paper are previously mentioned primary, secondary and tertiary reserves. Due to issues of sequentially performed market clearings of electricity market and ancillary services markets discussed in [30] in this paper simultaneous clearing of all markets is assumed in like presented in [31]. Furthermore, model of market structure is assumed to be based on PBUC [31] (price based unit commitment) approach. Electricity producer makes decision on activating power plant unit according to his risk analysis. In this approach GENCO takes all risk of unit scheduling and commitment. In this paper same GENCO owns power plant units from HPS Lokve-Bajer. Goal function is therefore maximum profit of the HPS considering PBUS approach. In order to make optimal power plant schedule it is required to predict day ahead market prices (for electricity market, primary, secondary and tertiary reserve market) as accurate as possible. Day-ahead power plant schedule is submitted the day before and consists of:

- Vertical bidding curve  $C_{ee}(P(t))$  with point in  $P_{ee}(t)$  for every time step  $t$  for electricity market:  $P_{ee}(t)[MW], \forall t \in T$
- Vertical bidding curve  $C_{pr}(P(t))$  with point in  $P_{pr}(t)$  for every time step  $t$  for primary reserve market:  $P_{pr}(t)[MW], \forall t \in T$
- Two vertical bidding curves  $C_{sr,up}(P(t))$  with point in  $P_{sr,up}(t)$  and  $C_{sr,down}(P(t))$  with point in  $P_{sr,down}(t)$  for every time step  $t$  for secondary reserve market:  $P_{sr}(t)[MW], \forall t \in T$  and
- Vertical bidding curve  $C_{tr}(P(t))$  with point in  $P_{tr}(t)$  for every time step  $t$  for tertiary reserve market:  $P_{tr}(t)[MW], \forall t \in T$

According to assumption that GENCO Lokve-Bajer is price-taker electricity producer, it will be sufficient to create just vertical bidding curves since bids will be accepted with forecasted marginal clearing price (MCP) regardless of submitted quantity. In deterministic model that is presented in this paper, electricity price and also ancillary services prices are not forecasted. Instead, hourly prices for electricity only market and also ancillary services markets are taken from day ahead electricity market and day ahead ancillary services market on NYISO pool for day 09.6.2012.

## 9. CASE STUDY AND RESULTS

Prices of electricity (electric energy day-ahead – EE DA), the primary regulation, the secondary regulation, 10-minute spinning reserve and cold (the tertiary) reserve are taken from day-ahead auction market. Real-time electricity price (electric energy real-time – EE RT) is taken from real-time electricity market where hourly prices are equal to pondered average prices during that hour. All data is taken from NYISO electricity market and ancillary services markets on 09.06.2012 and are shown in figure 7.

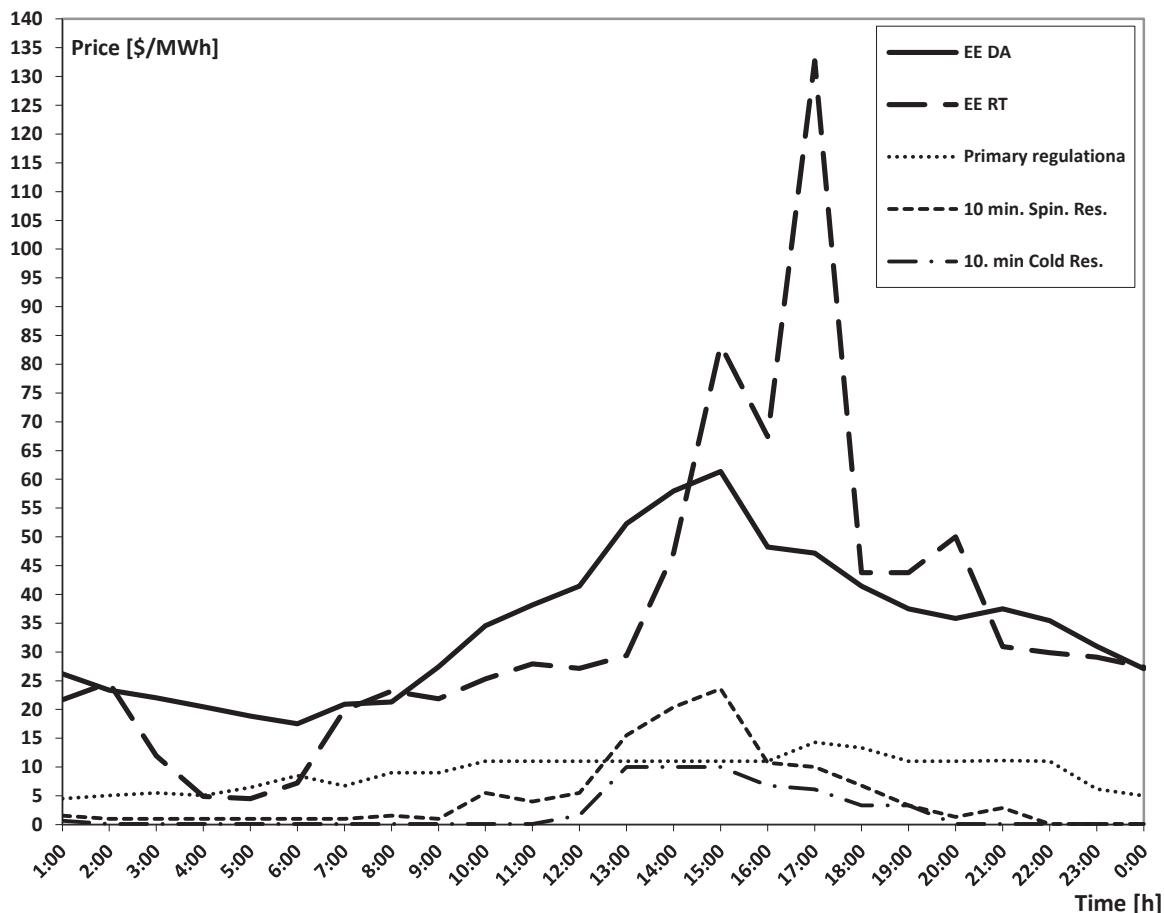


Figure 7 Hourly prices taken from NYISO on 09.06.2012. for zone N.Y.C. (New York City).

Acquired results from optimization runs have shown that HPP Vinodol has by far largest role in HPS Lokve-Bajer and therefore has the largest effect on profit of HPS Lokve-Bajer as a whole. Profit, when HPP Vinodol participated only in the

electricity market and only HPP Vinodol profit is maximized, is equal to 72 629 \$. If profit of HPS Lokve-Bayer is maximized then it reaches 76 580 \$. It is obvious that HPP Vinodol share of total profit is around 95% and consequently decided to optimize only HPP Vinodol profit has been made. This simplification has positive effects on calculation and optimization process. Case study data are presented in table 8 and table 9.

Table VIII. Average natural inflows during day in reservoirs

Reservoir	Križ	Lokve	Bajer	Lepenica	Potkoš
[m <sup>3</sup> /s]	2	8	6	2	2

Table IX. Parameters of HPP/PS\* and reservoirs in HPS Lokve-Bajer

Reservoir	Volume [hm <sup>3</sup> ]	HPP/PS	Discharge [m <sup>3</sup> /s]	Power [MW]
Križ	0.06	PS Križ	1.1	0.34
Lokve	34.8	PHPP Fužine	10/9*	4.6/4.8*
Bajer	1.32	HPP Vinodol	18.6	94.5
Lepenica	4.26	PHPP Lepenica	6.2/5.3*	1.14/1.25*
Potkoš	0.33	PS Lič	0.45	0.36

On figure 8 HPP Vinodol schedule while participating only in the electricity market is shown. If HPP Vinodol additionally participated in the primary regulation its daily profit is increased by 5,17% and is equal to 79430 \$. HPP Vinodol schedule in this new environment is shown in figure 9.  $P_{ee}(t)$  represents HPP Vinodol part of capacity for electricity production and  $P_{reg}(t)$  represents HPP Vinodol part of capacity intended for primary regulation. The probability that HPP Vinodol will participate in the primary regulation market is shown in table 10.

Table X. Probability that HPP Vinodol will participate in primary regulation

$p_{r,up}$	$p_{r,down}$	$(1 - p_{r,up} - p_{r,down})$
0.40	0.35	0.25

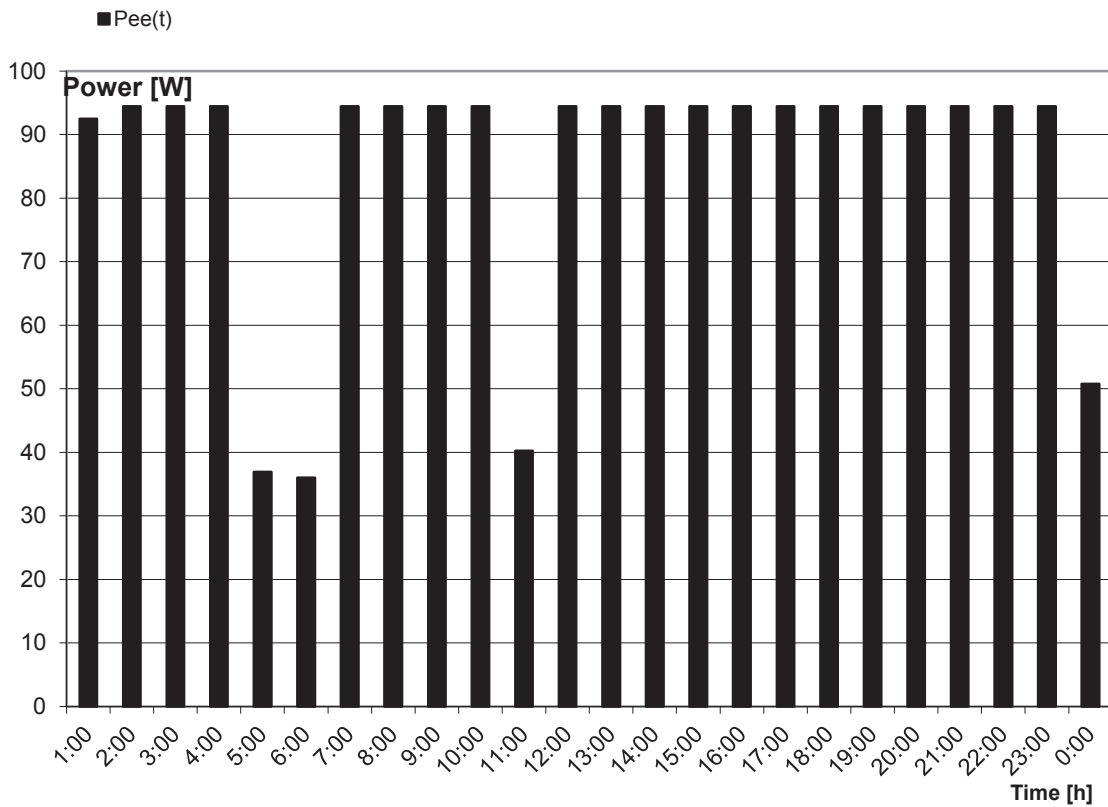


Figure 8 HPP Vinodol schedule while participating only in electricity market

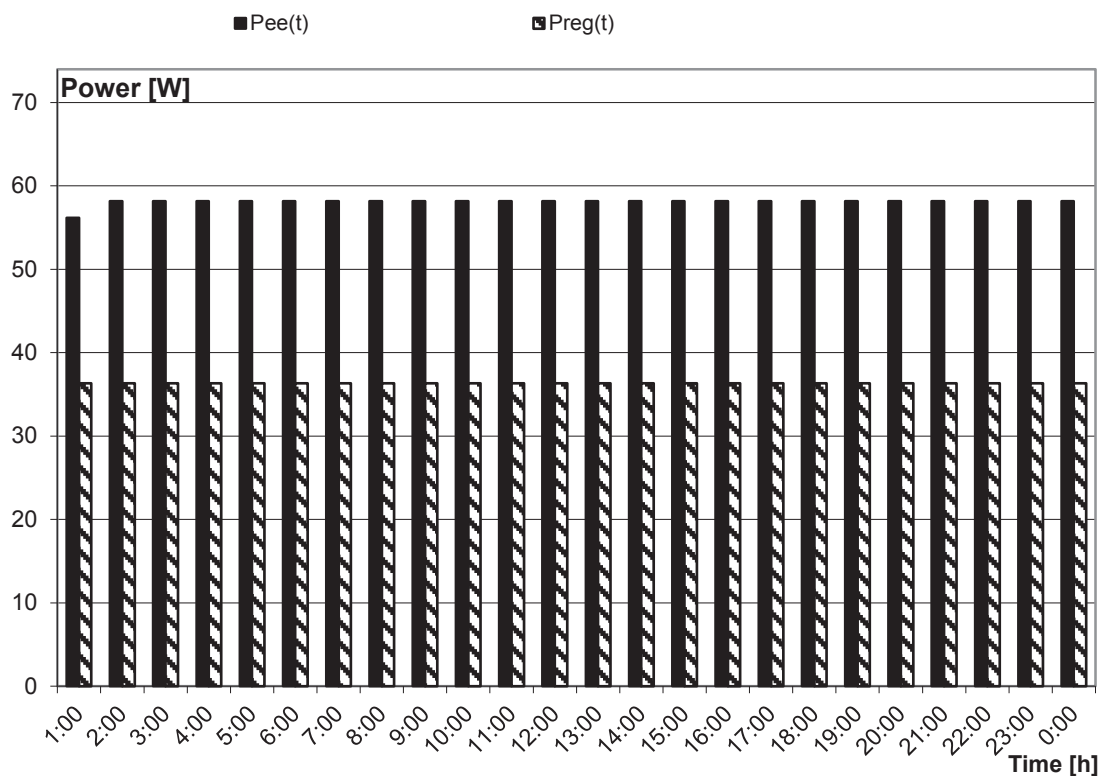


Figure 9 Available capacity and schedule of HPP Vinodol while participating in electricity market and primary regulation market

On figure 10 HPP Vinodol schedule while participating in electricity market and spinning reserve market is shown. If HPP Vinodol additionally participate in spinning reserve its daily profit is equal to 74731 \$.

On figure 11 HPP Vinodol schedule while participating in the electricity market, the primary regulation, the spinning reserve market and the cold reserve market is shown. If HPP Vinodol additionally participated in the primary regulation, the spinning reserve market and the cold reserve market its daily profit is equal to 81643 \$.  $P_{ee}(t)$  represents HPP Vinodol part of the capacity for electricity production and  $P_{reg}(t)$  represents HPP Vinodol part of the capacity intended for the primary regulation.  $P_{rot,up}(t)$  represents HPP Vinodol part of the capacity for the secondary-up regulation.  $P_{rot,down}(t)$  represents HPP Vinodol part of the capacity for secondary-down regulation.  $P_{cold}(t)$  represents HPP Vinodol part of the capacity for the tertiary regulation.

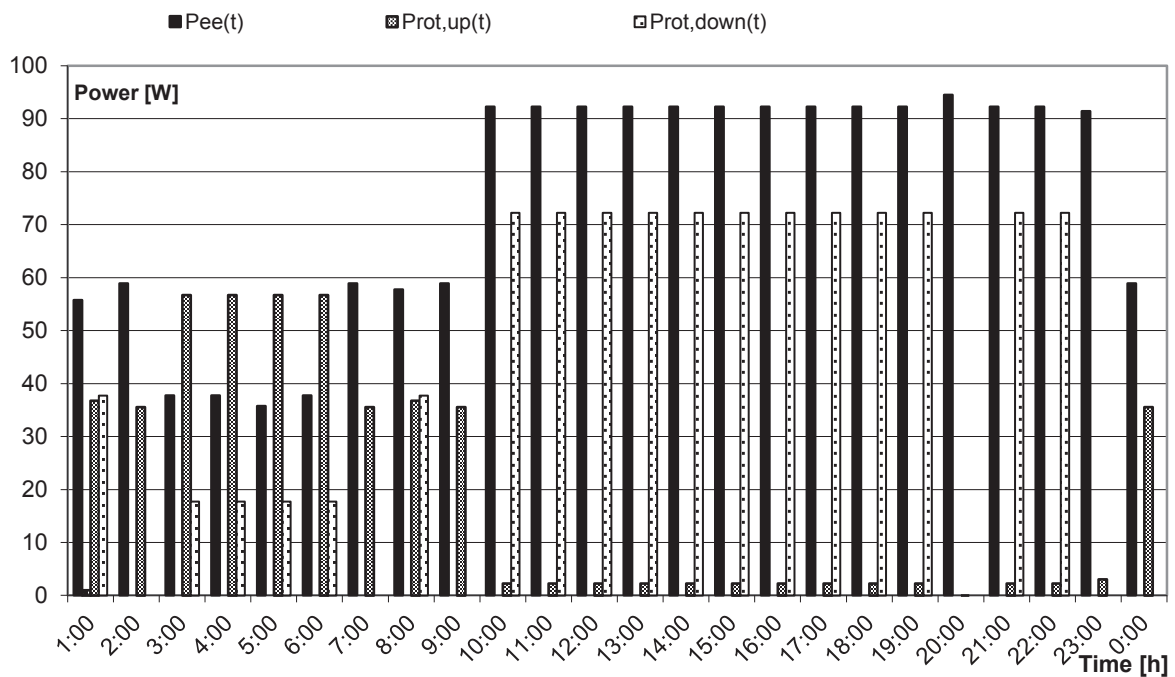


Figure 10 Available capacity and schedule of HPP Vinodol while participating in electricity market and spinning reserve market.

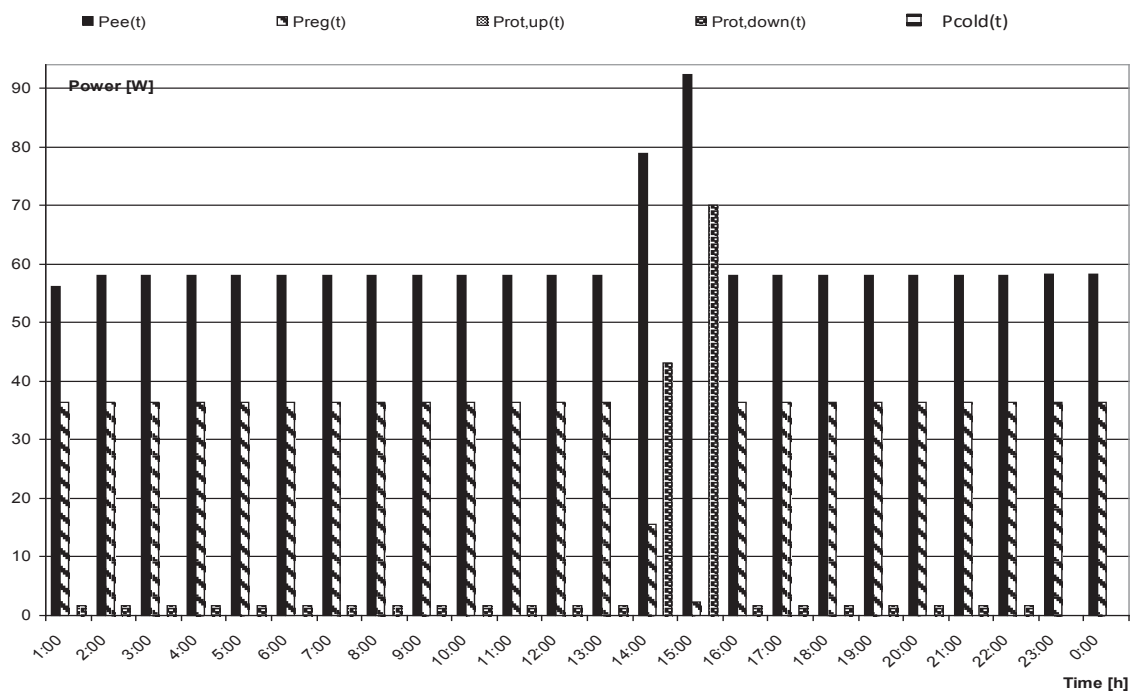


Figure 11 Available capacity and schedule of HPP Vinodol while participating in electricity market, primary regulation, spinning reserve market and cold reserve market.

## 10. CONCLUSION

In this paper, it has been elaborated and shown that due to their high flexibility and robustness hydropower plants are capable of providing all sorts of ancillary services, from primary control to providing a cold reserve in a system. Assumptions that hydropower owners can increase expected profit by bidding on several markets at the same time have been proven right. Results have shown by additional bidding on primary regulation market HPP Vinodol can increase expected profit by approximately 5% in comparison to the case where it only bids to the electricity market. If bids are also submitted to the spinning reserve and the cold reserve market this increase can reach 8%. This simultaneous bidding imposes a certain new risk to the owners of hydropower plants due to exposure to a wider range of market risks. But at the same time opportunities for an additional profit and to economic flexibility are increased. This paper shows that in near deterministic environment such as day-ahead markets it is possible to boost expected profit notably. It is of course almost impossible to utilize these opportunities without certain adequate support tool. One such tool is presented in this paper. Although rather simple due to computing limitations, presented model is efficiently found an optimum schedule of different services besides just bidding on the electricity market. Presented results are based on one specific case study of hydropower system Lokve-Bajer and therefore cannot be treated as a general estimate of the presented method. But at the same time, the model is flexible

enough to be adjusted to different specific locations to apply a similar analysis as presented in this paper.

## 11. REFERENCES

### 12.

- [1] D. Zhang, P. B. Luh and Y. Zhang, "A Bundle Method for Hydrothermal Scheduling," *IEEE Transactions on Power Systems*, vol. 14, no. 4, pp. 1355-1361, 1999.
- [2] A. George, C. Reddy and A. Y. Sivaramakrishnan, "Multi-objective, short-term hydro thermal scheduling based on two novel search techniques," *International Journal of Engineering Science and Technology*, vol. 2, no. 12, pp. 7021-7034, 2010.
- [3] J. S. Dhillon and D. P. kothari, "Multi-Objective Short-Term Hydrothermal Scheduling Based on Heuristic Search Technique," *Asian Journal of Information Technology*, vol. 6, no. 4, pp. 447-454, 2007.
- [4] J. L. Zhang and K. Ponnambalam, "Hydro energy management optimization in a deregulated electricity market," *Optimization in Engineering*, vol. 7, no. 1, pp. 47-61, 2006.
- [5] A. Horsley and A. G. Wrobel, "Profit-maximizing operation and valuation of hydroelectric plant: A new solution to the Koopmans problem," *Journal of Economic Dynamics and Control*, vol. 31, no. 3, pp. 938-970, 2007.
- [6] P. Ilak, Istovremeno participiranje hidroelektrane na tržištu električne energije i tržištima pomoćnih usluga, Zagreb: Sveučilište u Zagrebu Fakultet elektrotehnike i računarstva, diplomski rad, 2012.
- [7] J. Garcia-Gonzalez, E. Parrilla and M. A., "Risk-averse profit-based optimal scheduling of a hydro-chain in the day-ahead electricity market," *European Journal of Operational Research*, vol. 181, no. 3, pp. 1354-1369, 2007.
- [8] J. Garcia-Gonzalez, E. Parrilla, A. Mateo and R. Moraga, "Building optimal generation bids of a hydro chain in the day-ahead electricity market under price uncertainty," in *International Conference on Probabilistic Methods Applied to Power Systems 2006. PMAPS*, Stockholm, 2006.
- [9] D. De Ladurantaye, M. Gendreau and J. Potvin, "Optimizing profits from hydroelectricity production," *Elsevier*, October 2007.

- [10] P. Coulibaly and F. Anctil, "Real-time short-term natural water inflows forecasting using recurrent natural networks," in *Proc. Of IJCNN '99, International joint conference on neural networks*, 1999.
- [11] D. Druce, "Insights from a history of seasonal inflow forecasting with conceptual hydrologic model," *Journal of Hydrology*, 2001.
- [12] A. Franco, E. Lobato and L. Rouco, "Optimization of the Spanish Market Sequence by a Price-Taker Generating Firm," in *IEEE Bologna Power Tech Conference*, 2003.
- [13] A. Baillo, M. Ventosa, M. Rivier and A. Ramos, "Strategic Bidding Uncertainty in a Competitive Electricity Market," in *Presented on the 6th International Conference on Probabilistic Methods Applied to Power Systems*, Madeira, 2000.
- [14] A. Conejo, J. Arroyo, J. Contreras and F. Villamor, "Self-Scheduling of a Hydro Producer in a Pool-Based Electricity Market," *IEEE Transactions on Power Systems*, vol. 17, no. 4, 2002.
- [15] HEP. [Online]. Available at [www.hep.hr](http://www.hep.hr).
- [16] J. Nanda, A. Mangla and S. Suri, "Some new findings on automatic generation control of an interconnected hydrothermal system with conventional controllers," *IEEE Transaction on Energy Conversion*, vol. 21, no. 1, pp. 187-194, 2006.
- [17] K. Vrdoljak and P. N., "Primjena optimalnog kliznog režima upravljanja u sekundarnoj regulaciji frekvencije i djelatne snage razmjene regulacijskim hidroelektranama," *Automatika*, vol. 51, no. 1, pp. 3-18, 2010.
- [18] Y. H. Moon, H. S. Ryu, K. B. Song and M. C. Shin, "Extended integral control for loadfrequency control with the consideration of generation-rate constraints," *Journal of Electrical Power & Energy Systems*, vol. 24, no. 4, 2002.
- [19] H. Y. Yamin, "Review on methods of generation scheduling in electric power systems," *Science Direct*, 2003.
- [20] R. A. Ponrajah, J. Witherspoon and F. D. Galiana, "Systems to optimize conversion efficiencies at Ontario Hydro's hydroelectric plants," *IEEE Trans. Power Syst.*, vol. 14, pp. 1044-1050, 1998.
- [21] I. Rajšl, P. Ilak, M. Delimar and S. Krajcar, "Dispatch Method for Independently owned Hydro Power Plants in the Same River Flow," *Energies*, 2012.

- [22] V. Gruić, "Pomoćne usluge u elektroenergetskom sustavu," Zagreb.
- [23] V. Gruić and N. Mandić, "Regulacija frekvencije u uvjetima otvorenog tržišta električne energije," *Energija*, vol. 51, no. 2, 2002.
- [24] S. J. Kazempour, M. Hosseinpour and M. P. Moghaddam, "Self-Scheduling of a Joint Hydro and Pumped-Storage Plants in Energy, Spinning Reserve and Regulation Markets," *IEEE Xplore*, 2010.
- [25] S. E. Fleten and E. Pettersen, , "Construction bidding curves for a price-taking retailer in the Norwegian market," *IEEE Trans. Power Syst.*, vol. 20, pp. 701-708, 2005.
- [26] P. Andrianesis, P. Biskas and G. Liberopoulos, "An overview of Greece's wholesale electricity market with emphasis on ancillary services," *Electric Power System Research*, 2011.
- [27] E. L. Miguelez and I. E. Cortes, "An overview of ancillary services in Spain," *Science Direct*, 2008.
- [28] M. Mehmedović, M. Stojsavljević, D. Nemeč, A. Černicki , B. Horvat and B. Premer, "Sustav sekundarne regulacije frekvencije i snage razmjene hrvatskog EES -Idejno rješenje".
- [29] "Current state of balance management in south east europe - document for the 8th Athens forum," 2006.
- [30] S. S. Oren, "Auction design for ancillary reserve products," 2002.
- [31] D. Kirchen and G. Strbac, *Fundamentals of Power System Economics*, John Wiley & Sons, 2004.

DANILO FERETIĆ

ŽELJKO TOMŠIĆ

[danilo.feretic@fer.hr](mailto:danilo.feretic@fer.hr)

[zeljko.tomsic@fer.hr](mailto:zeljko.tomsic@fer.hr)

University of Zagreb Faculty of Electrical Engineering and Computing

Department of Energy and Power Systems

## MULTI-CRITERIA EVALUATION OF NUCLEAR OPTION

### SUMMARY

When evaluating power system expansion scenarios there is a need to take into consideration a range of measurable and non-measurable impacts. Measurable impacts are fixed and variable production costs and, recently, external costs. Non-measurable impacts include public attitude to a certain energy technology and investor's risk in achieving the expected profit. Public attitude has a large, and sometimes essential impact on decision-making and can be divided in objective and subjective part.

Investor's risk in achieving the expected profit is mostly associated with possible changes of domestic or foreign regulations or policy that can influence power plant operation and long-term fuel availability and price.

The objective of multi-criteria evaluation, after weighting and quantification of all impacts, is to determine the most acceptable power system expansion option.

In the article a simplified quantification was made of measurable and non-measurable elements that affect future investment decision. For that purpose possible relative values of non-measurable impacts of different options will be determined (their weights and impact on relative increase of annual costs).

Four possible technologies will be compared: nuclear power plant, coal power plant, combined cycle gas plant and wind power plant in combination with gas plant.

The expected change of non-measurable impacts on investment decision in the period 2010-2030 was analysed as well as the influence of those changes on future investment decisions.

**Key words:** Multi-criteria evaluation; Power Plant; Nuclear option; Investment cost; Competiveness

## 1. INTRODUCTION

Inadequate power system expansion plan can lead to great difficulties in system operation or large expenses in the future. Therefore it is a very serious and responsible task where all the possible different impacts should be included in decision-making process. For many years the most important and sometimes the only criterion in planning were costs. It is not possible to make an expansion plan only on the basis of least-cost planning any more. Many other criteria become important, and will be more important in the future and multi-criteria methods are essential in evaluation of different options.

The multi-criteria decision making (MCDM) process should be made in several steps [1]. Different methods of MCDM define different steps but we will use a simple five-steps method:

1. Attributes (criteria) selection
2. Definition of options (alternatives)
3. Weighting the attributes
4. Quantifying impacts
5. Amalgamation

The first step in MCDM is attribute selection. Selecting issues to be included in planning may be one of the most difficult tasks. Selected attributes (criteria) often reflect who participates in the decision making process, they reflect perception about what is important. When evaluating power system expansion scenarios there is a need to take into consideration a range of impacts but here will hold on four groups: costs, environmental impacts, public attitude and risk.

The objective of MCDM is to choose the "best" option among all possible options. As "all possible options" can be a huge number of them the next step is to make a set of reasonable number of options to choose from. In this paper we evaluate nuclear option against some other energy options.

Weights of attributes show how much certain criterion is important for decision maker. They show for example if environmental issues are of a great concern or the public opinion is more important. Quantifying impacts of different options should be done very carefully and as much objective as it can be done.

A difficult and sometimes controversial task in MCDM is to amalgamate different impacts into a single value. But expressing different impacts with the same unit of measure and aggregate impacts

## 2. IDENTIFICATION OF ATTRIBUTES AND OPTIONS

The major objective in power system expansion planning is to minimize costs. Years ago it was realized that cost minimization does not take into consideration other impacts of energy production that should be considered, primarily the environmental impact. All energy technologies produce some negative impact to the environment but the problem was how to evaluate it. One often used method for evaluation of environmental impact is the method of external costs where the damage to the environment and human health is monetary valued. Extern costs are shown to be a quite good method although monetary valuation of environmental impact is still a controversial issue and there is no generally acceptable method of evaluation. The emissions from thermal power plants can be determined precisely, their impact to human health not so precisely, but the major problem is the valuation of human health. On the other hand extern costs don't take into consideration other impacts and they are shown to be inadequate as a power system expansion planning method and multi criteria decision making can be considered as a step forward in planning methods.

As the result of democratization process public opinion have more and more importance and its impact to decision making becomes greater, sometimes essential. This impact can be divided in objective and subjective part. Objective part, which is in proportion with scientifically approved environmental impact of energy options (inversely proportional to external costs) is relatively small, while the other, subjective category which is not proportional with the actual environmental impact (especially in the case of nuclear power), is much larger.

The electricity sector in many countries is in some kind of restructuring (deregulation, privatization, liberalization etc.). Regulation and "rules of the game" are changing and that brings uncertainties for investors of new power plants. Another uncertainty is the future fuel prizes and their availability. All those institutional, political or economic uncertainties bring the risk for investor's expected profit and should be included in the decision making process.

There are also other attributes that can be consider (between five and fifteen attributes are typical for energy sector applications) but in this paper we will hold on these four:

1. Costs (direct and indirect)
2. Environmental impact (external costs)
3. Public impact (objective and subjective)
4. Investor's risk (change of regulation, availability and cost of fuel)

Costs are "measurable" impacts, we can calculate them. Environmental impact became "measurable" through the method of external costs. But many other impacts are not measurable and cannot be easily monetarily expressed. We call them "non-measurable impacts". Quantifying different non-measurable impacts needs expert judgment on the importance of certain impact and determines the specific MCDM model. Monetary valuation of different impacts is quite a controversial issue but it's still the best and the most used method in MCDM. This method aggregates all the impacts into the single number, enabling an easy comparison of different options.

### 3. WEIGHTING THE ATTRIBUTES AND QUANTIFYING IMPACTS

A method for evaluating the environmental impact through external costs is used in this paper. However the external costs are weighted with the factor of 0.5 that means that external costs impact is weighted as 50% of direct costs impact. Sum of internal costs and 50% of external costs are called the total costs. In this paper we use the ratios of different impacts, and then compare them to the total costs as the basic criterion (relative impact set to 1). Total cost impact is valued as 50% of total impact, and for example the investor's risk concerning change of regulations 15%. That leads us to relative impact of 0.3. All the attributes with their weights are shown in Table I.

This step does not yet present the evaluation of options because they are not yet determined. The table just shows the decision-maker's attitude to different attributes in decision-making process. Decision-maker determines those weights and they show how much certain criterion is important to him.

Table I. Weights of attributes

Attribute		Percentage of impact	Weight
Direct costs		40%	1
External costs		20% $\times$ 0,5=10%	
Public impact	Objective	2%	0,04
	Subjective	18%	0,36
Investor's risk	Changes of regulations	15%	0,30
	Availability and cost of fuel	15%	0,30

In every decision making process there are different options to choose from. Important step is to define well a reasonable number of options that shows meaningful difference in type of option and its impacts. Evaluation of nuclear option is done in comparison with other energy technology options. Those options are coal power plant, combined cycle gas power plant and combination of wind and gas (CC) power plants. This should be a reasonable number of reasonable options for the purpose of this paper but in the real evaluation of energy options the number of options (and criteria) should be larger.

Impacts of different options are quantified relatively to the largest impact. Subjective public impact is the largest in nuclear option and it is set to be 1. Weights for other energy technology options are evaluated in comparison with that one. Subjective public impact is large also in coal option (weighted as 0,9) and it is significantly lower in gas (0,3) and wind+gas (0,2) option. Prizes and availability of gas are the most uncertainly among examined options, while for nuclear and coal fuel that risk is weighted as 10% of risk in gas option. All weights are shown in the Table II.

Table II Quantification of impacts of different energy options

Power Plant Technology		Coal	Gas	Nuclear	Wind + Gas
Public impact	Rational	1,0	0,5	0,1	0,2
	Non-rational	0,9	0,3	1,0	0,2
Investor's risk	Change of regulations	0,7	0,2	1,0	0,4
	Availability and cost of fuel	0,1	1,0	0,1	0,7

When attributes are weighted and impacts are quantified we can calculate the total relative values of non-measurable impacts as the product of those two values. As we weighted impacts in comparison with total costs these values represents relative increase of total costs and they are presented in Table III.

Table III. Relative increase of total costs

Power Plant Technology		Coal	Gas	Nuclear	Wind + Gas
Public impact	Rational	0,040	0,020	0,004	0,008
	Non-rational	0,324	0,108	0,360	0,072
	Total public impact	0,364	0,128	0,364	0,080
Investor's risk	Change of regulations	0,210	0,06	0,300	0,120
	Availability and cost of fuel	0,030	0,30	0,030	0,210
	Total investor's risk	0,240	0,360	0,330	0,330
Total increase of annual costs		0,604	0,488	0,694	0,410

Investor's risk and the public impact will increase costs of new coal power plant for 60,4%, gas plant for 48,8%, nuclear power plant for 69,4% and new gas and wind power plants for 41%. It is important to notice that these cost increments are not the real costs, it is just the measure of what we called "non-measurable" impacts in the decision making process. Cost increments for all options with shares of different impacts are shown in the Figure 1.

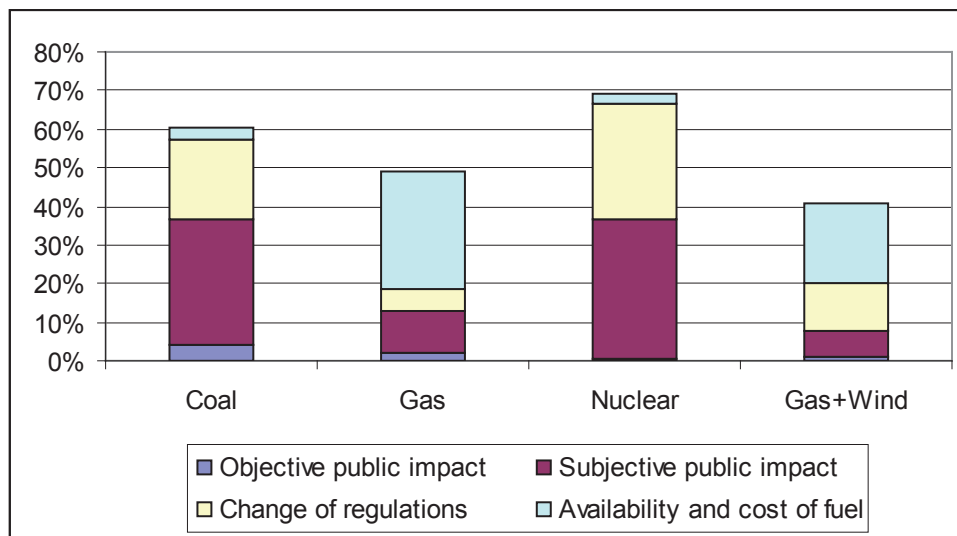


Figure 1. Cost increments

In Table IV a calculation for four candidate 600 MW power plants is presented [2]. When only direct costs are evaluated the gas option is shown to be the cheapest. If we include the extern costs (50% of them) that represent the environmental impact the best option is nuclear. But, when all the non-measurable impacts are included, nuclear option loses its first position and gas is again taking it. The most expensive option (wind+gas) in this case is very near to coal option although direct costs are almost 80% higher. Both options are more than 40% worst than the nuclear option.

The construction period of a new power plant is long, from several years up to seven or even more, depending on technology and other circumstances than can occur during the construction. The lifetime of new power plants is usually 40 or more years and the return of investment is usually from 15 to 30 years. The factor of time is therefore very important in evaluating the projects in energy sector and it has to be taken into the consideration during the decision making process.

In a long-time period different impacts in MCDM will not preserve the same importance. A time period until 2030 is analyzed here and it is divided in three subperiods. Different weights of attributes and impacts of different options are assumed in each subperiod. It is expected that the objective public impact will increase due to spread of knowledge and better understanding of the matter in the public. On the contrary, the subjective impact will decrease. This can be expected because the general public is becoming more concerned and involved in the energy policy matters.

As mentioned above, the electricity sector in many countries is in some kind of restructuring and uncertainties caused by the change of regulations are high. It can be expected that in the next decades when this process will be finished and the liberalized electricity market completely established and functioning, this impact will decrease. On the other hand the risk concerning the availability and cost of fuel in the future will significantly increase.

Table IV. Investments, annual O&M costs, fuel costs and indirect costs of power plants

Power Plant Technology	Coal	Gas	Nuclear	Wind + Gas
Capacity (MW)	2x300	3x200	600	600x1+3x200
Investment costs (USD/kW)	1500	600	2000	2800+600=3400
Fixed O&M costs (USD/kW-year)	35	12	100	wind 24, gas 12, average 18
Investment rate (percent, number of years)	7%, 20yr	7%, 15yr	7%, 20yr	7%, 15yr
Life time (years)	30	30	40	30
Annual capital costs (USD/kW)	141,59	65,87	188,78	373,30
Total annual fixed costs (USD/kW-year)	176,59	77,87	288,78	391,30
Fixed Costs (USD/MWh-year)	23,6	10,4	38,8	52,6
Fuel cost (USD/MWh)	16	31	5	0,65/0,85x31=23,7 (for wind LF=0,2)
Variable O&M costs (USD/MWh)	4	2	2	1
Total variable costs (USD/MWh)	20	33	7	24,7
Total annual direct costs (USD/MWh)	43,6	43,4	45,8	77,3
Extern costs (USD/MWh)	60	20	7	2/3x20+1/3x3= 14,3
Total costs (direct+50% extern) (USD/MWh)	73,6	53,4	49,3	84,45
Increase factor of total costs	1,604	1,488	1,694	1,410
Increased total costs (USD/MWh)	118,1	79,5	83,5	119,1
Relative costs (NPP=1)	1,414	0,952	1,000	1,426

Total annual costs are weighted as 50% of total impacts in all subperiods. All impacts to power plant investment decision and their relative increase of total costs in period until 2030 are shown in Table V.

Table V. Expected change of attribute weights until 2030

Period		until 2010	2010-2020	2020-2030	
Public impact	Objective	Impact	2%	4%	7%
		Weight	0,04	0,08	0,14
	Subjective	Impact	18%	11%	8%
		Weight	0,36	0,22	0,16
Investor's risk	Change of regulations	Impact	15%	10%	5%
		Weight	0,30	0,20	0,10
	Availability and cost of fuel	Impact	15%	25%	30%
		Weight	0,30	0,50	0,60

In Table VI we quantified impacts of different technology in three subperiods. Subjective public attitude toward nuclear option it is assumed to be slightly better in the next decades and therefore the impact factor is lower. Risk of change of regulation in all options is lower in the next decades.

Table VI. Expected change of non-measurable impact factor to power plant costs until 2030

Technology	Coal			Gas			Nuclear			Wind + Gas		
Period	until 2010	2010-2020	2020-2030									
Public impact												
Objective public impact												
Impact factor	1	1	1	0,5	0,5	0,5	0,1	0,1	0,1	0,2	0,25	0,3
Cost Increase Factor	0,04	0,08	0,14	0,02	0,04	0,07	0,004	0,008	0,014	0,008	0,020	0,042
Subjective public impact												
Impact factor	0,9	0,9	1	0,3	0,3	0,3	1	0,8	0,7	0,2	0,2	0,2
Cost Increase Factor	0,324	0,198	0,16	0,108	0,066	0,048	0,36	0,176	0,112	0,072	0,044	0,032
Investor's risk												
Change of regulations												
Impact factor	0,7	0,5	0,3	0,2	0,15	0,1	1	0,8	0,6	0,4	0,3	0,2
Cost Increase Factor	0,21	0,1	0,03	0,06	0,03	0,01	0,3	0,16	0,06	0,12	0,06	0,02
Availability and cost of fuel												
Impact factor	0,1	0,1	0,15	1	1	1	0,1	0,15	0,2	0,7	0,8	0,9
Cost Increase Factor	0,03	0,05	0,09	0,3	0,5	0,6	0,03	0,075	0,12	0,21	0,4	0,54

Total costs of different technologies are calculated in Table IV and in Table VII we can see the influence of non-measurable impacts to those costs.

Table VII. Costs of different power plants until 2030

Technology	Coal			Gas			Nuclear			Wind + Gas		
Period	until 2010	2010-2020	2020-2030									
Total costs (USD/MWh)	73,6			53,4			49,3			84,45		
Increase factor of total costs	1,604	1,428	1,420	1,488	1,636	1,728	1,694	1,419	1,306	1,410	1,524	1,634
Increased total costs (USD/MWh)	118,1	105,1	104,5	79,5	87,4	92,3	83,5	70,0	64,4	119,1	128,7	138,0
Relative costs (NPP=1 in the first subperiod)	1,414	1,259	1,251	0,952	1,047	1,105	1,000	0,838	0,771	1,426	1,541	1,653

How much will total increments of costs due to the measurable impacts change for different energy technologies can be seen in the Figure 2. Although these non-measurable factors have the greatest impact on nuclear option it is expected that they will decrease the most in next decades what will make the nuclear option much more competitive.

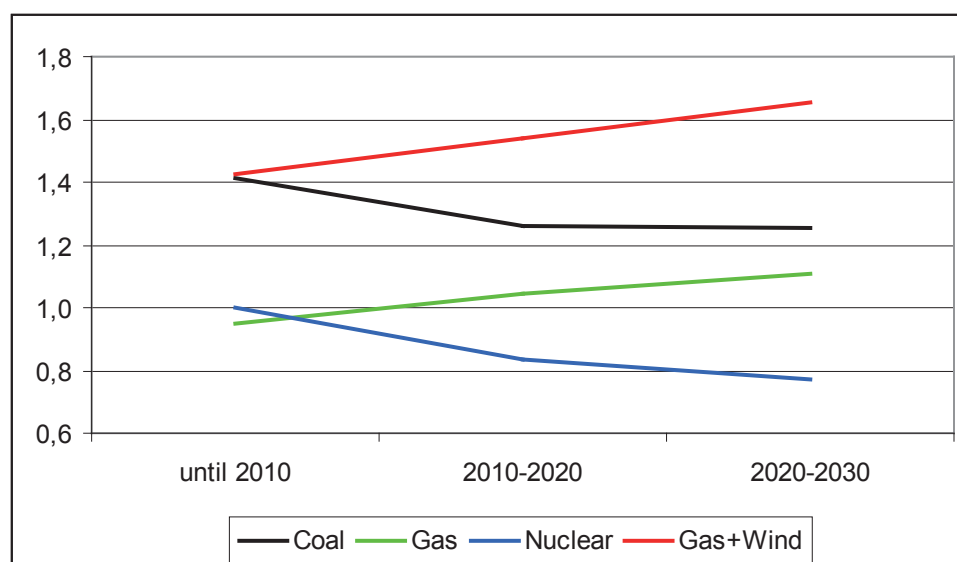


Figure 2 Relative acceptance indicators of different power plants up to 2030

The long-term competitiveness evaluation shows decrease of gas power plants competitiveness, mostly caused by investor's risk due to possible change of fuel availability and price. It also shows an increase of NPP competitiveness caused by

expected decrease of public disagreement and decrease of investors risk concerning change of regulations.

#### 4. CONCLUSION

A simple multi-criteria evaluation of nuclear option is done. Different impacts are divided in "measurable" (intern and extern costs) and "non-measurable" (public attitude and investor's risk) impacts. Non-measurable impacts are weighted and expressed in terms of measurable costs. In that way a simple amalgamation of results and easy comparison is possible. A long-term evaluation is also done and the results show that NPP competitiveness will increase in the future.

Improvements of method can be done by taking into consideration more possible impacts and more different options and of course better judged impacts. The change of methodology itself is also possible.

#### REFERENCES

- [1] B.F. Hobbs, P. Meier: Energy Decisions and the Environment: A Guide to the use of Multicriteria Methods, Kluwer Academic Publishers, 2000.
- [2] Ž. Tomšić et al: Economic instruments of environmental protection and climate change mitigation in the liberalized electricity market conditions (in Croatian), study made for Croatian Electric Utility (HEP), FER, Zagreb, 2001.

**BOJAN FRANČ**

[bojan.franc@fer.hr](mailto:bojan.franc@fer.hr)

**University of Zagreb Faculty of Electrical Engineering  
and Computing**

**SILVIA PILIŠKIĆ**

[silvia.piliskic@hops.hr](mailto:silvia.piliskic@hops.hr)

**Croatian Transmission System Operator Ltd.**

**IVO UGLEŠIĆ**

[ivo.uglesic@fer.hr](mailto:ivo.uglesic@fer.hr)

## LIGHTNING DATA UTILIZATION IN POWER SYSTEM CONTROL

### SUMMARY

Lightning location systems (LLS) provide data on lightning activity such as lightning type, GPS location, exact time of the lightning stroke, lightning current amplitude, measurement error, etc. The proper application of LLS data using customized software support can be a powerful decision-making tool in the control, maintenance and development of power systems. The utilization of lightning data in power systems requires a customized software support with specific functionalities. Software functionalities include real time lightning activity visualization with alarm function; analysis, reports and historical lightning activity visualization; spatial correlation between lightning data and alarm zones around geographically represented power system's objects (power lines, power facilities, etc.); calculation of lightning statistics; generation of wide area lightning density maps, generation of high resolution lightning density maps inspecting alarm zones around the power lines; real time correlation between lightning activity and the power system protection equipment (distant protection relays), gathered through the SCADA system. In this paper, emphasis will be given to the application in correlation between faults and outages in the power network and lightning strokes. Today, many power companies monitor data related to circuit breaker operation or re-closing using various equipment. Such equipment allows online monitoring of circuit breakers and alarm statuses of equipment in substations.

**Key words:** circuit breaker operation, correlation, lightning location system, line faults, power system control

## 1 INTRODUCTION

Today, applications of lightning location systems (LLS) are well known in different industries and organizations such as insurance companies, air control, meteorological services, fire departments, military installations, telecommunication networks, network of broadcasting transmitters, oil and gas networks, dealers and distributors of explosives, petrochemical industry, etc.

The electricity companies and electrified railways became a customer of LLS relatively late and only after LLS were sufficient mature. In beginning LLS had numerous weaknesses, e.g. the inability to discern cloud to ground from inter cloud flashes, low detection efficiency, inaccuracies in determination of lightning location, detection of small stroke amplitudes, the inability to detect subsequent strokes, etc. All this prevented use of LLS in design control and management of overhead lines. In recent times the mentioned weaknesses are largely eliminated. Today, the modern LLS are increasingly used by power and distribution operators. Application in transmission and distribution networks and systems is mostly encountered in one or more of the following areas:

- a) in correlation of outages and faults in network with lightning strokes;
- b) in establishing, managing and monitoring of electric power system;
- c) in giving a warning of coming lightning front;
- d) in choosing the route of overhead lines and ways to protect them from lightning, [1-5].

In this paper, emphasis will be given on the application in area described as a) and b).

LLS data can be correlated with data of faults and outages in power network, which may contribute to power quality. Today, many electricity companies are following data related to circuit breaker operation or re-closing using various equipment for registration. Such equipment allows online monitoring of circuit breaker and alarm status of equipment in the substations. Comparison with LLS data shows that not all fault and outages during a thunderstorm are caused by lightning. A certain number of outages could be caused by intense winds during a thunderstorm causing two-phase or one-phase short circuit. The optimum method for determining the real number of circuit breaker tripping and re-closing, caused by lightning, is correlation of fault time and position from relay protection devices



1. Time and date of lightning stroke (UTC);
2. GPS coordinates (2D);
3. Lightning current amplitude (0.1 kA resolution);
4. Lightning type (cloud-ground, inter-cloud);
5. Height (for inter-cloud lightning);
6. 2D statistical locating error (50% probability) [8].

Table I. Turbine regulation model parameters

GPS	TIMESTAMP	TYPE	HEIGHT	AMPLITUDE	ERROR
15.8932 45.7170	29.4.2009 18:57:05.595	CG	-	-15 kA	43 m
15.8920 45.7036	29.4.2009 19:07:32.771	CG	-	-5.2 kA	56 m
15.8508 45.7407	29.4.2009 18:50:47.143	CG	-	72.2 kA	51 m
15.8214 45.7566	29.4.2009 18:50:47.112	IC	3600 (m)	-5.5 kA	59 m
15.8647 45.7595	29.4.2009 19:07:01.673	IC	4100 (m)	4.7 kA	65 m
15.8117 45.7558	29.4.2009 18:49:09.457	IC	5900 (m)	-10.7 kA	87 m

## 2. UTILIZATION OF LIGHTNING LOCATION SYSTEMS IN POWER SYSTEMS

The utilization of lightning location systems in power systems is primarily enabled by one or more specific tasks:

1. Correlation between power outages and faults with lightning strokes;
2. Power system control and management;
3. Early lightning activity warning system;
4. Power system design (overhead line route planning and line protection).

### 2.1. CORRELATING POWER OUTAGES AND FAULTS WITH LIGHTNING STROKES

Lightning data can be correlated with data relevant to power outages and faults in the power system, which can improve the overall quality of power system monitoring. Modern power system operators monitor circuit breaker (CB) operation using various monitoring systems and acquire data through SCADA or similar data acquisition systems in real time. Circuit breaker operation can be correlated with lightning data, showing the number of CB operations, as well as the number of power outages caused by lightning strokes to the overhead lines [3].

### 2.2. CONTROL AND MANAGEMENT OF POWER SYSTEM

A common lightning location systems utilization concerns control and management of power systems, especially during periods when a dispatching centre is attempting to determine the cause of a circuit breaker operation. Information on a lightning stroke during a CB operation in proximity to an overhead line can be vital in determining the cause. The utilization of real time lightning tracking

enables a skilled operator to determine if a power outage was caused by a permanent fault or a transient fault due to a lightning stroke. Such a tool can be particularly useful in the restoration of regular operation, minimizing outage time and cost.

### **2.3. EARLY WARNING SYSTEM**

System operators and engineers can use real time lightning tracking data to organize and prepare teams in areas where high lightning activity is approaching. Equally important is the ability to confirm the lightning front has completely passed the monitored area. LLS data can be used to issue early warning alarms of incoming lightning activity to repair teams in the field, minimizing risks of accidents caused by lightning strokes. In sum, it is important to know the direction of a lightning front when conducting overhead line repairs or field testing.

### **2.4. POWER SYSTEM DESIGN**

Lightning location systems can provide much more precise lightning density maps than the ones currently being used. Current lightning density maps utilize calculations from empiric factors and data from isokeraunic maps. The accuracy of such methods is limited and subject to factors specific to local regions. Improved results were obtained from networks of short range lightning counters (e.g. CIGRE 10 kHz counters). However, neither of these map types produce the level of accuracy and parameters that LLS lightning density maps can provide. The modern power system network design utilizes lightning density maps to aid in optimal overhead line route selection and the determination of adequate line protection equipment (e.g. line surge arresters, ground wires, etc.). With high resolution lightning density maps, it is possible to minimize the number of lightning strokes on overhead lines by selecting routes with a lower lightning stroke density. For existing overhead lines, critical route sections can be identified, and adequate protection can be selected, thus minimizing both cost and future power outages, as well as maximizing reliability [2].

## **3 INTERCONNECTING WITH OTHER SYSTEMS**

The system for lightning data utilization in power systems requires interconnection with three external data sources. The system implements various communication interfaces, which can easily be upgraded. For lightning data input the system implements a client service to receive lightning data from lightning data processing center. Data are obtained in 10 second intervals. The delay between the exact moment of a lightning stroke and the time the data is processed is less than 60 seconds.

For GIS input, a communication interface is available. GIS data contain geometries (points, lines, polygons) of power system facilities (e.g. overhead lines, substations, power plants, etc.). This enables a real-time interconnection to an external GIS database, making it possible to import and synchronize GIS data directly in case of a change. Where an external GIS database is not available the system utilizes a web based tool for GIS data import and management. GIS data enable the spatial correlation between lightning data and geometries representing power system facilities. It also enables the calculation of the exact distance of a fault location caused by a lightning stroke to the nearest substation (Figure 2). This information can be correlated with data from the distant relay protection.



Figure 2. Spatial correlation of lightning stroke with overhead line alarm zones

For the input of data referring to failures in the power system (e.g. power outages, automatic reclosures, circuit breaker operation, distant relay protection operation, etc.) in real time, the system specifies communication interfaces specific to individual needs and conditions. Data from remote systems (protection relays, station computers, etc.) obtained through SCADA can be fetched by implementing clients for DAIS Alarms & Events or OPC server. By specifying which protection equipment and which signal types are to be correlated with lightning strokes, it is possible to determinate events caused by lightning strokes in near real time and present the information to dispatchers accordingly (Figure 3).

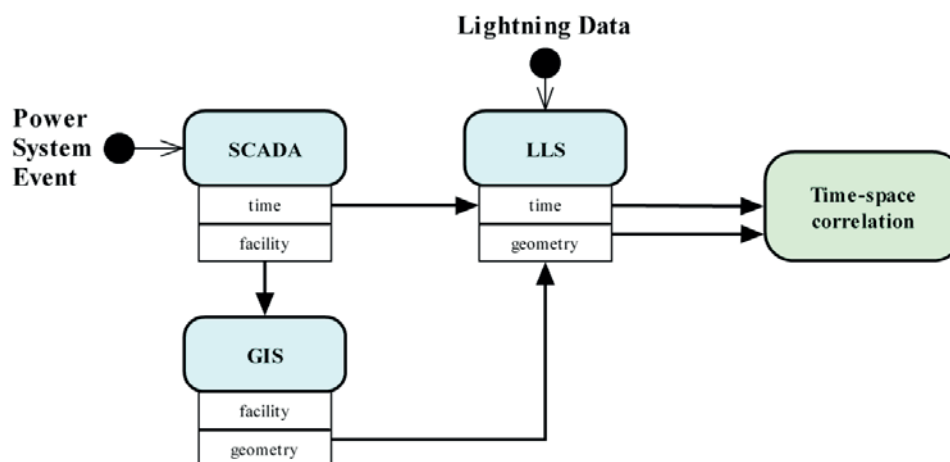


Figure 3. Time-space correlation schema

## 4 LIGHTNING CORRELATED FAULTS – CASE STUDY

### 4.1 Observed Lightning Activity

Two adjacent 110 kV overhead lines have been observed for faults and lightning activity in an area with heightened number of power outages. For calculation of lightning statistics, LLS data for the last three years (2009 – 2011) was available. Although a three-year period is too short to provide a creditable statistic; the obtained data show correspondence with other relevant sources and are sufficient to demonstrate the calculation principles. The LLS measured up to 48 lightning days per year (e.g. the isokeraunic map) for the area surrounding the overhead lines. Figure 4 shows the position of the monitored overhead lines and the isokeraunic map of lightning days for the observed area.

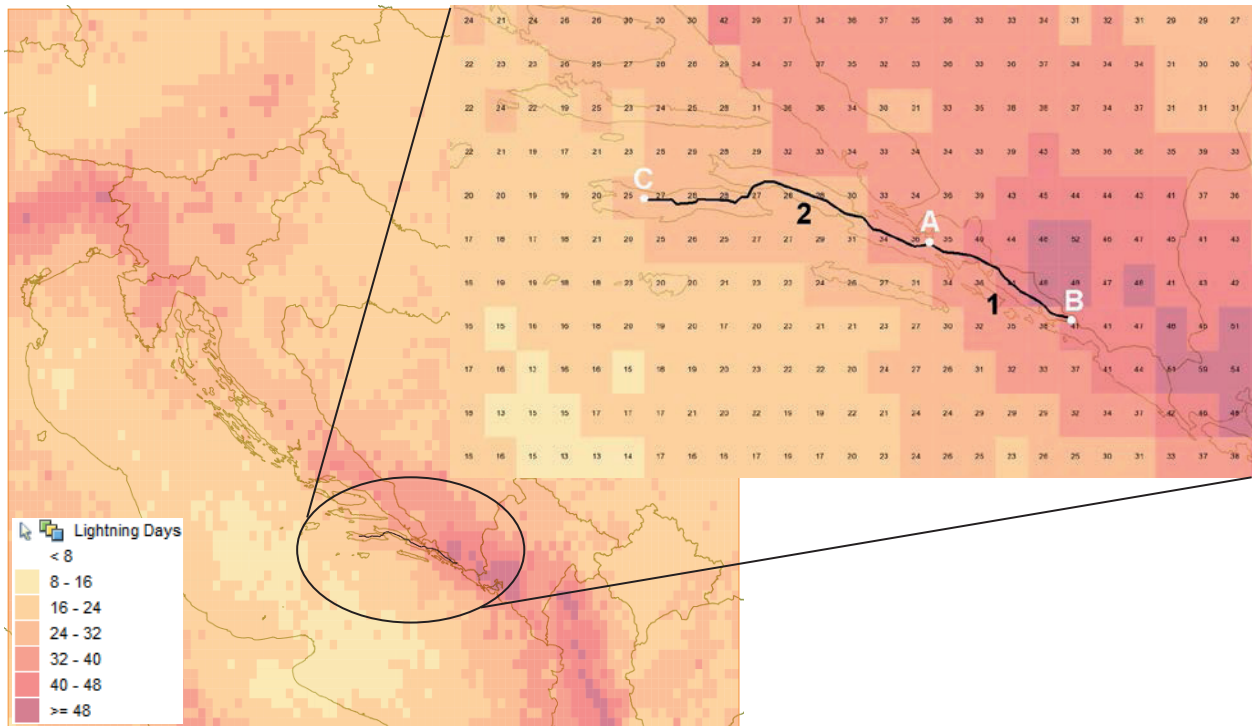


Figure 4. Map displaying isokeraunic map of lightning days (2009-2011) with monitored overhead lines (marked 1 and 2 on the map) and adjacent substation (marked A, B and C)

Lightning statistics for the area surrounding the monitored overhead lines (5720 km<sup>2</sup>) have been calculated for a 3 year period (2009-2011). Analyses show the number of cloud to ground (CG) lightning strokes per month with most of the lightning activity during summer months, Figure 5; CG stroke density (each stroke within a multiple stroke flash is represented individually), Figure 6; CG positive to negative stroke ratio, Figure 7; average and mean CG stroke amplitude, Figure 8 and Figure 9. The winter period is considered to be from November till April and the summer period from May till October. Analyses show much higher lightning activity in summer periods (CG stroke density of 11.01 N/km<sup>2</sup>/year) than in winter periods (2.78 N/km<sup>2</sup>/year) with a total of 6.89 N/km<sup>2</sup>/year for CG lightning strokes.

80% of total CG lightning strokes are detected during summer periods, but higher stroke amplitudes are measured during winter.

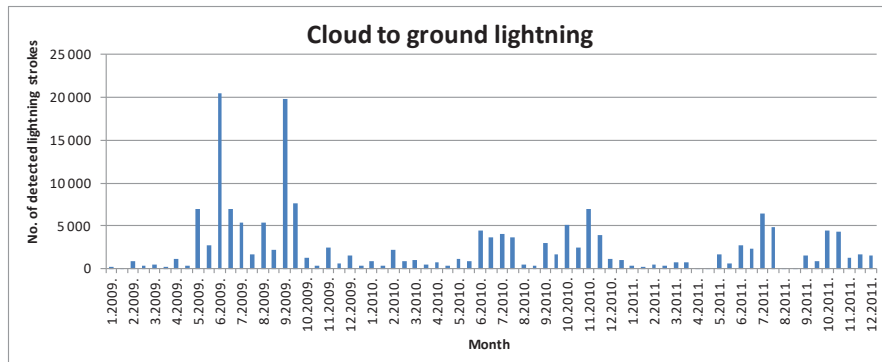


Figure 5. Number of lightning strokes per month

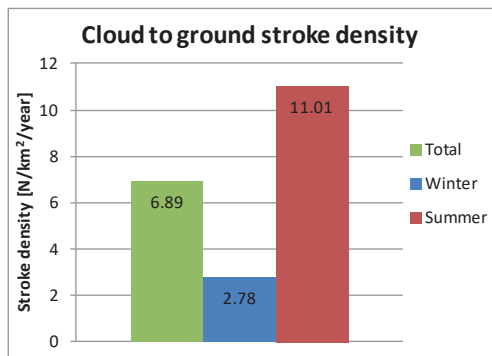


Figure 6. CG stroke density

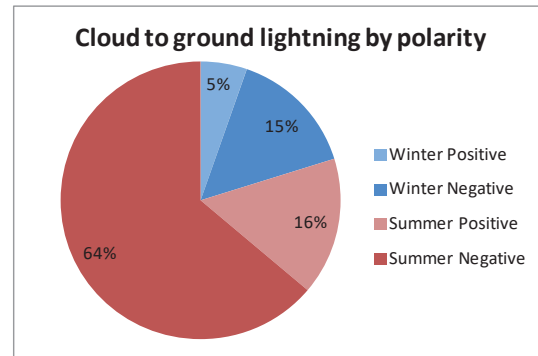


Figure 7. Ratio of CG stroke by polarity for winter and summer periods

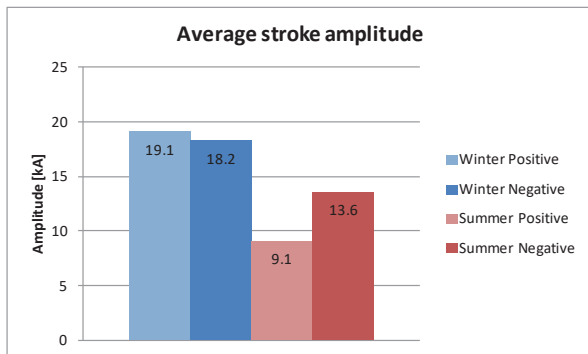


Figure 8. Average value of CG stroke current amplitude

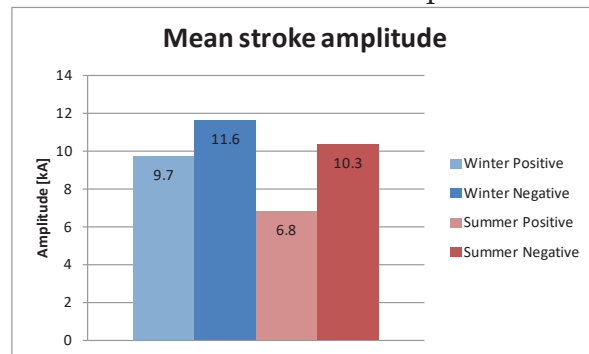


Figure 9. Mean value of CG stroke current amplitude

## 5 RELAY PROTECTION

For the protection of the observed overhead lines distant protection relays of the same type are used. The basic function of the distant protection device is the recognition of the distance to the fault with distance protection measurement. The relay protection device detects the line fault, determines the fault type and initiates an adequate single-pole or three-pole tripping as quickly, as possible. Since both the LLS and the relays are Global Positioning System (GPS) synchronized it is possible

to correlate the data between lightning stroke times and fault detection times. For the purpose of time correlation the relay pick-up time is considered as the fault detection time since the relay is said to ‘pick-up’ when it changes from a de-energized position to an energized position. The relay pick-up is the first action following the point at which a relay has registered an event on the line. Fault determination follows the relay pick-up, after which commands to the circuit breakers may or may not be issued, depending on the duration and type of fault, as well as other parameters.

Laboratory measurements of the relay’s pick-up times were conducted for the relay type used on monitored overhead lines. The testing device was used as the source of the signal for relay device in known time point. Both the testing device and the relay were synchronized by GPS. The results of 21 measurements have shown that the pick-up time of the particular relay varies from 5 ms to 28 ms after the signal generation point (Table II). The average relay pick-up time value, after the signal generation is measured to be 17.05 ms.

Table II. Relay pick-up time delay statistics for 21 measurements

	$\Delta t$ [ms]
Min	5
Max	28
Average	17
Median	17
Max-Min	23

## 6 CORRELATION ON 110 KV TRANSMISSION LINES

Correlation between lightning data and relay protection has been conducted on 110 kV transmission lines which is described in the following cases:

### Case 1)

One of the observed events on a 110 kV overhead line (marked 1 in Figure 4) occurred on 29th July 2011 (Figure 10 and Table III). Distant protection relays in adjacent substations registered pick-ups at 06:35:12.763 and 06:35:12.769 local time. Pickups were registered on a single (top) phase of the overhead line. Commands to circuit breaker were issued and successful automatic reclosures procedures were executed on both sides of the overhead line. The LLS registered a lightning stroke in the overhead line alarm zone with peak amplitude of -18.7 kA at 06:35:12.754 local time. The lightning stroke precedes the registered pick-ups with a time difference of 9 and 15 ms. The fault locator measured the distance to the fault at 20.3 km / 24.1 km from the substations, where the LLS measured 18.4 km / 25.2 km.

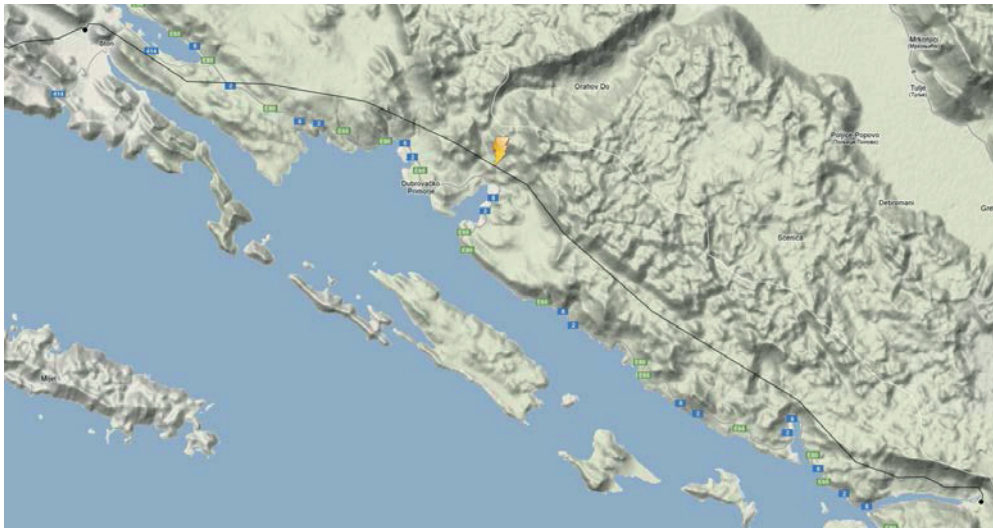


Figure 10. Lightning stroke causing line tripping

Table III Correlated data

Event date	29.07.2011.
Lightning time	06:35:12.754
Pickup time	06:35:12.763 / 06:35:12.769
$\Delta t$ to pickup	9 ms / 15 ms
Lightning amplitude	-18.7 kA
Locating error	910 m
Distance to line	113 m
LLS Fault location	18.4 km / 25.2 km
Fault locator	20.3 km / 24.1 km
$\Delta L$ to fault locator	1.9 km / 1.1 km

Results gathered through survey of the given overhead line provided an adequate method for correlation between LLS data and relay protection data. A more comprehensive and detailed survey was conducted on an adjacent overhead line, which is described next.

### Case 2)

The differences between the fault detection times of protection relays (average pick-up time) and the times of each individual lightning stroke recorded by LLS, which had caused the respective faults, were analyzed over a three-year period for the observed 110 kV overhead line (marked 2 in Figure 4). This overhead line passes through a region which has an average isokeraunic value 25-36 thunderstorm days per year, and is thereby exposed to frequent strokes of lightning.

Overhead line data are shown in Table IV. Construction and corresponding dimensions of the suspension tower of observed 110 kV line is depicted in Figure 11. The shield wire protects the line from all lightning strokes of return-stroke current exceeding the critical current, which is the maximal lightning stroke current that could strike the phase conductor beside the shield wire. The critical current is calculated according to the electro-geometric model, for the highest conductor of the

suspension tower Nc7-T, and for different tower heights from ground to the lower arm. For the tower heights from 11.9 m to 23.45 m critical currents vary in range from 12.1 kA to 26.2 kA.

Table IV 110 kV overhead line data

Line	One-circuit
Tower	Steel-frame
Line length - $\ell$ [km]	78.573
Conductors	240/40 - Al/Steel
Shielding wire	ACS – OPGW
$R_{d1}$ [ $\Omega$ /km]	0.118
$X_{d1}$ [ $\Omega$ /km]	0.414
$R_{01}$ [ $\Omega$ /km]	0.349
$X_{01}$ [ $\Omega$ /km]	1.108

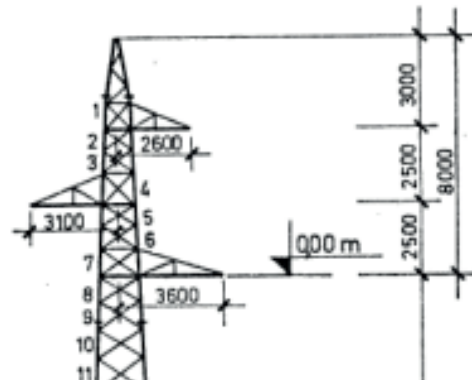


Figure 11 Suspension tower Nc7-T

During the observed three-year period 82 events were registered during which relay protection devices were activated.

From the correlation procedure were excluded those events for which the data about the exact time of the fault detection were not available, as well as the events for which LLS did not indicate any lightning activity.

Hence, the correlation was conducted for 59 events assumed to be caused by atmospheric discharges. The time difference of a maximum of 1 second between the fault detection time of relay protection devices and the time of a lightning stroke recorded by LLS has been determined as the basic precondition for the time correlation.

Figure 12 illustrates an example of the time correlation procedure by using the LLS. According to relay protection device data the fault which has occurred on 2nd June 2009 at the pick-up time of 14:29:34.521 caused the tripping of the line and its outage for 2 minutes. The fault occurred at a distance of 67.5 km according to the data of the fault locator function of the relay protection device of the respective overhead line. The LLS registered one lightning stroke which matches given criteria and which was possible to correlate with the observed relay protection fault detection. The correlated lightning stroke is of cloud-ground (CG) discharge type, stroke current amplitude of -23.3 kA, with a discharge occurrence time 14:29:34.490 and a distance of 67.429 km on the respective overhead line, with a location error of 57 m. Upon further analysis the time difference between the fault detection of the relay protection device and the lightning stroke recorded by LLS is 30 ms and the difference between the relay protection device fault location and the lightning strike location is 88 m, which is 0.1% of the total length of the observed overhead line.

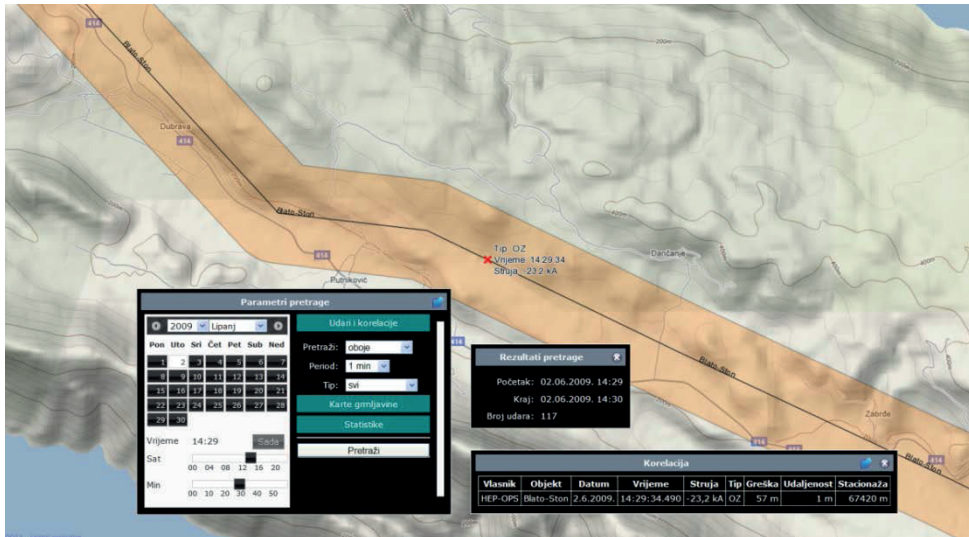


Figure 12 Time correlation between a lightning stroke and the relay pick-up

The same correlation procedure has been conducted for all of the 59 faults registered by a relay protection device on the observed overhead lines with the assumption that they had been caused by atmospheric discharges. Six of the analyzed faults did not match the given criteria of the time difference of a maximum of 1 second between the fault detection time of the relay protection device and the time of the lightning stroke recorded by LLS although there were lightning strokes in the vicinity to the observed overhead lines and in the time period close to the fault detection time.

53 of the analyzed events matched the given criteria of the time difference and the time correlation between the lightning strokes and the protection device fault detection. The time differences between the lightning strokes recorded by LLS and the relay pick-up time for the 53 correlated and analyzed events (transmission line faults) are shown in Figure 13.

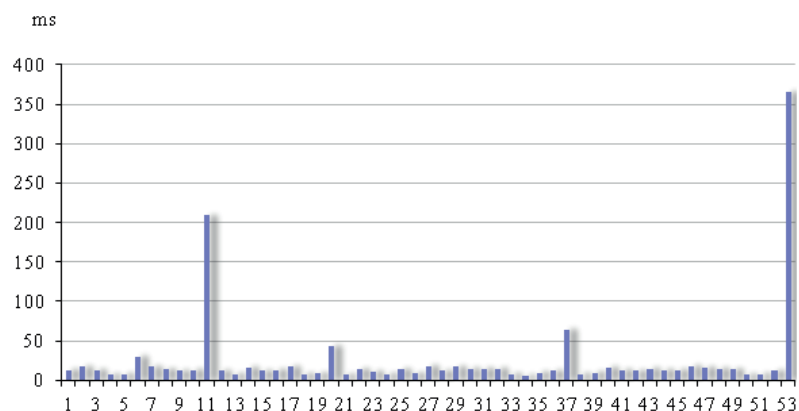


Figure 13 Correlated time differences between lightning strokes and relay pick-ups for 53 events

Figure 14 illustrates that the time differences vary between 6 ms up to 366 ms. Only three values are higher than 50 ms. The median time difference is 13 ms. The distribution of the correlated events according to time differences in the range

of 1-100 ms is illustrated in Figure 14. Figure 15 depicts more precise the time differences up to 30 ms. It can be seen that most of the correlated events have a time difference between 10 ms and 20 ms (Figure 14), with 48 of the 53 correlated events (91%) with time difference up to 18 ms. Results correspond to laboratory measurements of the relay's pick-up times discussed earlier.

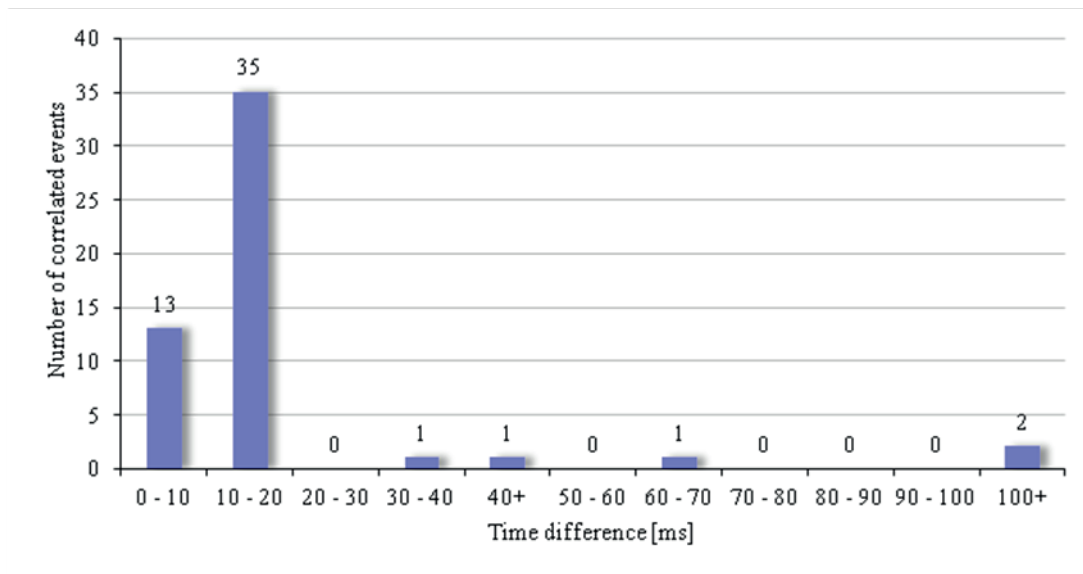


Figure 14 The distribution of correlated events according to time differences between the time of the lightning strokes and the relay protection device pick-up time

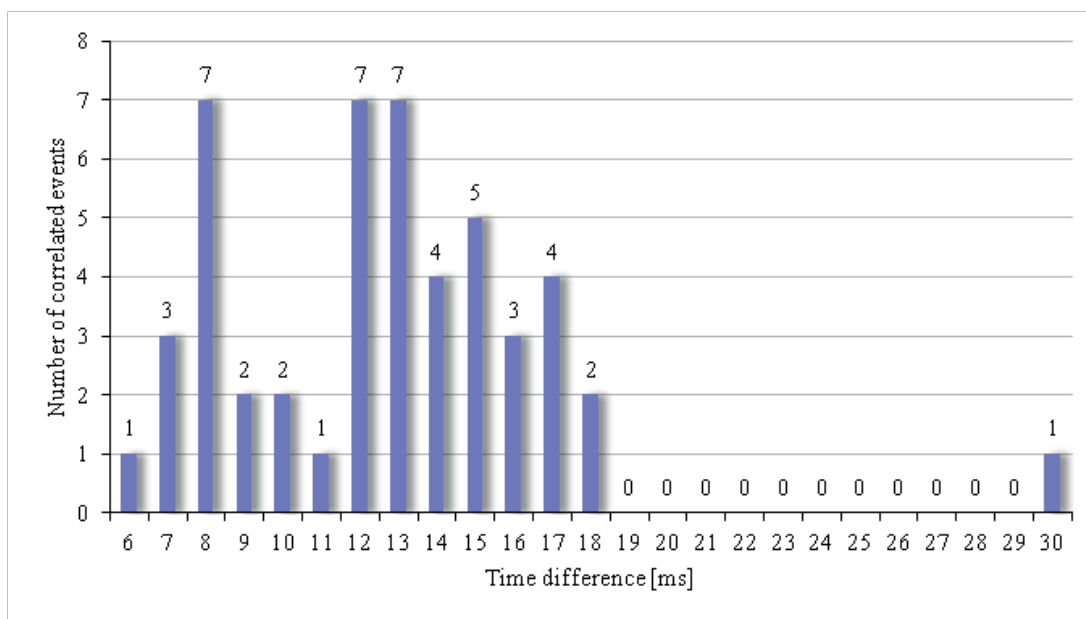


Figure 15 The distribution of correlated events according to the time differences between the lightning strokes and relay protection device pick-up time

For 37 of the events for which the time correlation has been determined and the protection relay data of fault location were available, the difference between the lightning stroke locations determined by LLS and fault locations determined by the relay protection has been analyzed. The results of spatial correlation have revealed

the difference between the lightning stroke locations determined by LLS and the fault locations determined by the relays varies from 0.01% to 10.2% of total overhead line length, where the difference is between 1% and 2% for most of the correlated events, Figure 16. The average difference between the lightning stroke locations determined by LLS and fault locations determined by the relay protection device is 1.37% of total overhead line length.

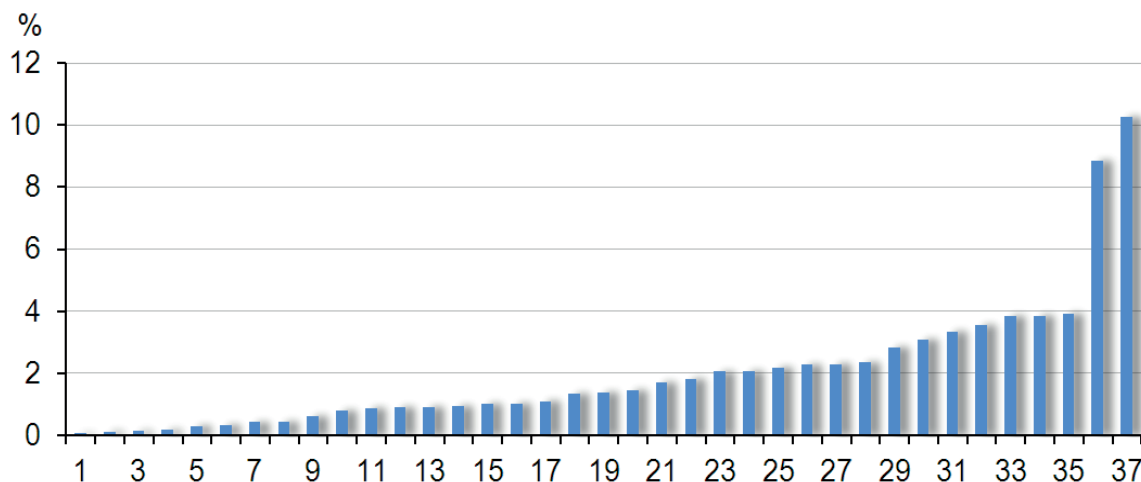


Figure 16 Differences between the lightning strokes locations determined by LLS and fault locations determined by the protection device

The analyses of the differences between the lightning stroke locations determined by LLS and fault locations determined by the relay protection device has been conducted under certain restrictive circumstances. The results of the analyses are influenced by the error of both the relay protection device fault location function and the LLS.

The accuracy of the fault location function of the relay protection device is affected by several factors. For example, the errors in current and voltage transformers which directly affect the distance estimation, uncertainties of the line constants, effects of untransposed transmission lines or influence of changing network configuration.

The observed overhead lines and the respective sensors of LLS are located in the coastal area. Since the sensors measure the magnetic flux directly as function of time the results of a lightning stroke location are influenced by the different conductivity (of land and sea) and, therefore, different field propagation effects [6].

Nevertheless, the results of the analyses of the differences between the lightning stroke locations determined by LLS and fault locations determined by the relay protection device can additionally prove the correlation between faults registered by the relay protection device of the overhead lines and lightning strokes detected by the LLS. Moreover, it could be concluded that the lightning stroke location determined by LLS could be used as information about the fault location on the overhead line, especially when the fault location function of the relay protection device is not available.

## 7 CORRELATION ON 35 KV DISTRIBUTION LINE

A similar procedure could be applied for correlation between outages and lightning strokes of medium voltage distribution lines. Table V shows a print of a station computer monitoring events on a 35 kV distribution line.

The outage of the 35 kV line was on 30th April 2011 in 17:53:16.647. The LLS registered a lightning stroke which matches the given time criteria of 1 second. The correlated lightning stroke was of cloud-ground (CG) discharge type, with stroke current amplitude of 117.2 kA, at 17:53:16.626 local time. The outage of another 35 kV line was on 24th July 2011 in 20:09:20.395. The LLS registered two lightning strokes which match given time criteria of 1 second. The correlated lightning strokes were of cloud-ground (CG) discharge type. The stroke current amplitude of -21.7 kA and -9.1 kA, with discharge occurrence time 20:09:20.174 and 20:09:20.188 respectively.

Table V Station computer event list

Alarm List					
	Date	Time	Signal Group	Signal	Signal Value
1	30.4.2011.	17:53:16.647	35kV line 7SJ632	Switch off	Start
2	30.4.2011.	17:53:16.647	35kV line 7SJ632	I >> Swich Off	Start
3	30.4.2011.	17:53:16.661	Voltage 0.4kV, 50Hz	Outage	Start

## 8 CONCLUSION

Real time lightning tracking can be an effective asset in the management of spatially distributed systems exposed to atmospheric conditions. Such systems represent a powerful tool in the design, protection and control of power systems. Their application can also be found in numerous other systems, including telecommunication, radio and television networks, pipelines, insurance companies, meteorological services, fire fighting agencies, etc.

Nowadays LLs are widely used by many transmission and distribution operators. By utilizing custom software tools and analysing lightning data, correlation with relay protection can be conducted. Correlating relay protection data of faults in the power system with lightning data, useful information for identifying and locating the fault cause can be obtained. Utilizing GPS synchronization in relay protection and LLSs a high degree of success in time correlation is achieved. Lightning strike locations determined by the LLS, correlated and identified as cause of line faults, match with fault locator data within satisfactory tolerance.

The time correlation between line faults and lightning strikes revealed that the protection relays detect faults on the protected transmission line generally with time difference up to 28 ms after a lightning strike, which corresponds to the laboratory measurement results of the relay's pickup time.

The spatial correlation between the faults on the transmission line and the lightning strikes indicate that the median value of differences between the fault location and the lightning strike location is 1,37 percent of total transmission line length of the observed line. This result is obtained by several factors that affect the accuracy of the fault locator, as well as the LLS.

It has been indicated that the time correlation can provide information on the fault cause and the lightning data can serve as information on the fault location.

Results confirm the efficiency of correlating protection relay data with LLS data for the purpose of identifying fault cause. This new information contributes to minimizing the time for identifying outage cause and conducting repairs, which refers on improving power quality.

## 9 REFERENCES

- [1] Diendorfer G., Shulz W., "Ground flash density and lightning exposure of power transmission lines", Power Tech Conference Proceedings, IEEE, Bologna, 2003.
- [2] Kosmač J., Djurica V., "Use of high resolution flash density maps in evaluation of lightning exposure of the transmission lines", INTERNATIONAL CIGRÉ SYMPOSIUM, Zagreb, Croatia, April 18-21, 2007.
- [3] Kosmač J., Djurica V., Babuder M., "Automatic fault Localization Based on Lightning Information", Power Engineering Society General Meeting, IEEE, 2006.
- [4] Bernstein R., Samm R., Cummins K., Pyle R., Tuel J., "Lightning detection network averts damage and speeds restoration", IEEE Computer Applications in Power, April 1996.
- [5] Cummins K. L., Krider E. P., Malone M.D., "The U.S. national lightning detection network and applications of cloud-to-cloud lightning by electric power utilities", IEEE transactions on electromagnetic compatibility, Vol. 40, No. 4., November, 1998.
- [6] H. D. Betz, U. Schumann, P. Laroche, Lightning: "Principles, instruments and applications, review of modern lightning research", Chapter 5: "LINET – an international VLF/LF lightning detection network in Europe", Springer Science, Business Media B.V., 2009.
- [7] B. Franc, M. Šturlan, I. Uglešić, I. Goran Kuliš: Software Support for a Lightning Location System in Croatia, 16. Conference HrOUG 2011, Rovinj, Croatia, 18. – 22. October 2011, written in Croatian
- [8] I. Uglešić, V. Milardić, B. Franc, B. Filipović-Grčić, J. Horvat: Establishment of a new lightning location system in Croatia, Study Committee C4 on System Technical Performance, A Colloquium on: Lightning and Power Systems – Technical Papers, Kuala Lumpur, Malaysia, 2010

**ŽELJKO TOMŠIĆ**

[zeljko.tomsic@fer.hr](mailto:zeljko.tomsic@fer.hr)

**University of Zagreb Faculty of Electrical Engineering  
and Computing**

**GORAN ČAČIĆ**

[goran.cacic@undp.hr](mailto:goran.cacic@undp.hr)

**United Nations Development Programme – Energy  
Efficiency Project in Croatia, Zagreb, Croatia**

**IVAN GAŠIĆ**

[ivan.gasic@fer.hr](mailto:ivan.gasic@fer.hr)

## **ENERGY MANAGEMENT IN THE PUBLIC BUILDING SECTOR – ISGE/ISEMIC MODEL**

### **SUMMARY**

This paper introduces Intelligent Information System for Monitoring and Verification of Energy Management in Cities (ISEMIC) web application that connects processes of gathering data on buildings and their energy and water consumption, monitors consumption indicators, detects any anomalies or irregularities in time, sets energy efficiency targets and reports energy and water consumption savings. ISEMIC enables use of smart meters within an energy management for the first time in the region, along with an analytical part which enables intelligent estimation of energy consumption based on multiple criteria. In the public sector are enormous potential for energy and water savings and thus a large area for ISEMIC web application implementation. ISEMIC web application is developed in July, 2011. Purchase of smart metering equipment and establishment of smart metering infrastructure on institutions of project partners responsible for ISEMIC web application development is in conduction after which a full pilot run will be started. The potential impact of this project is very large and it would be a great example how significant savings can be achieved by systematic energy monitoring and management provided by the use of ISEMIC web application.

**Key words:** Energy management, public buildings, energy consumption, smart meters, intelligent estimation.

# 1 INTRODUCTION

The role of cities is getting more complex due to growth of population, impact on climate change and the need to increase energy security. To meet these requirements, transformation of cities must be initiated in all resource management activities and critical infrastructures, beginning with improving the energy efficiency of public buildings. The role of energy management in achieving sustainable development of cities in the future is great.

Systematic energy management (SEM) in the cities is centred on alteration of human behaviour, changes in the existing organizational structures and application of technical measures to improve energy efficiency is a key prerequisite for the development of the skills and gain of the knowledge required for utilizing the existing potentials of enhancing energy efficiency and sustainable development in the cities. Fully establishment of SEM assumes maximizing the potential of achieving energy efficiency improvements in order to transfer the knowledge through the continuous process of energy management in cities to citizens, which would initiate the process of changing their perspective and behaviour.

The introduction of the SEM is nowadays unthinkable without the use of modern information systems and technologies and introducing advanced IT systems is the first logical step toward applying the concept of “smart cities”. The ultimate goal of introducing the “smart city” concept is achievement of environmentally friendly, efficient and sustainable urban infrastructure that will provide to citizens all necessary services in an economically and environmentally friendly way and additionally the life quality in the cities.

Today, in energy analysis and statistics is common practice of conducting analysis of energy consumption trends at the national level which are then adjusted to the level of individual cities. But in most cases aggregated approach to the analysis of energy data doesn't give us good insight into the appropriateness and effectiveness of selected energy policies on the national level, nor on the local level. If we want to dispose with reliable information about the actual effects of implementation of selected policies at the local level, or if we want to get insight whether they should be corrected and adapted it is necessary to introduce regular monitoring of implementation and evaluation of the effects of conducted energy policies at the local level. The realization of this approach is possible only with the application of methodologies for continuous collection of key data in short and

regular intervals at the local level in order to specific effects can be identified and achievements of the implementation of policies can be reduced to the level of each individual city.

## 2 ISEMIC WEB APPLICATION DEVELOPMENT

In the residential and service sector, information on energy and water consumption is commonly only provided on a monthly basis. Frequently the recipient of the information has no benchmark to assist in determining whether consumption levels are normal or excessive. There are two gaps or barriers which need to be addressed. First, there is a need for a system that provides higher-quality, more detailed information on a more frequent basis. Second, the system should have the capacity to analyze the information received and act on the parameters available to correct possible malfunctions. To overcome these issues, an integrated information system is required, enabling both entries of manual readouts (and accompanied by appropriate education of the staff in the building where energy and water is consumed) and reception of data from intelligent metering systems that capture real-time data.

The Energy Management Information System (EMIS) is software developed in Croatia to help in implementation of energy management programs in public buildings, but it is implemented without any significant analytical engine for data analysis, as accent is put on creating a network of people regularly monitoring and manually entering consumption data in EMIS via the web. Also, there is no smart meter input capability in the system. These two missing features were the focal point of ISEMIC development. ISEMIC upgrades and improves the existing EMIS platform with new functionality for continuous collection, storage and analysis of data on energy consumption of buildings owned by a city, county or ministry. ISEMIC further implements a newly developed methodology for past energy consumption data analysis using regression analysis, least square method, best-fit lines, scatter trending, as well as setting and cascading targets using correlation analysis and risk analysis using probability distribution for planning improvement measures (Figure 1).

Alpha version of ISEMIC web application is developed and installed on server in July, 2011; it can be accessed by following the link: <http://161.53.66.25:8080/IsemicIntro/>.

## 3 ISEMIC WEB APPLICATION DESCRIPTION

Due to ISEMIC web application complexity and large extent of its possibilities only short description will be given in this chapter.

### 3.1 ISEMIC web application architecture

ISEMIC architecture has three levels (Figure 2):

- Web browser on the client side as user interface tool;

- Apache Tomcat as servlet container;
- Oracle database as data storage

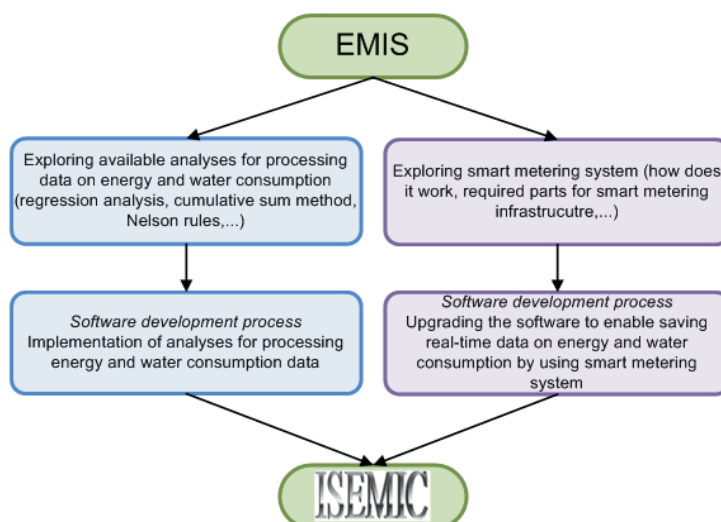


Figure 1. Upgrading EMIS to ISEMIC

Users connect to the application via http protocol (https for user identification). They are obliged to enter their username and password which aren't related to the database credentials.

### 3.2 Users and user roles in ISEMIC web application

Five different user roles are provided in ISEMIC; the system is designed in a way that can support an unlimited number of roles, but these five mentioned roles are preconfigured:

- System administrator (SA),
- Energy administrator (EA),
- Energy manager (EM),
- User (U) and
- Guest (G).

One user can have different roles on different objects.

SA can perform absolutely all operations in ISEMIC, but his main function is administration of whole application, from database backup to monitoring entered documents and photos.

Main function of EA is creating new lower roles (EM, U and G) and objects. He can edit and delete the information about roles and objects. Usually there is one or two person(s) on city, county or ministry level with this role. EA sets goals and limits of energy consumption and has the ability of deleting (false) entered bills. He also deals with data analysis, printing reports and graphs, remote reading monitoring, etc.

EM is a role whose primary function is oversight on certain part of the building. It can be a person in charge for energy, as well as the person in particular agency that requires data for specific data analysis.

U is a role primarily responsible for entering daily and weekly consumption readings. He also monitors remotely entered consumption data; enters monthly bills has the ability to change the wrong input, but not deleting entire bill. He can also edit object general, construction and energy characteristics.

G can only monitor the consumption of certain building(s) for which he is in charge and print reports and graphs on that building(s) or compare them.

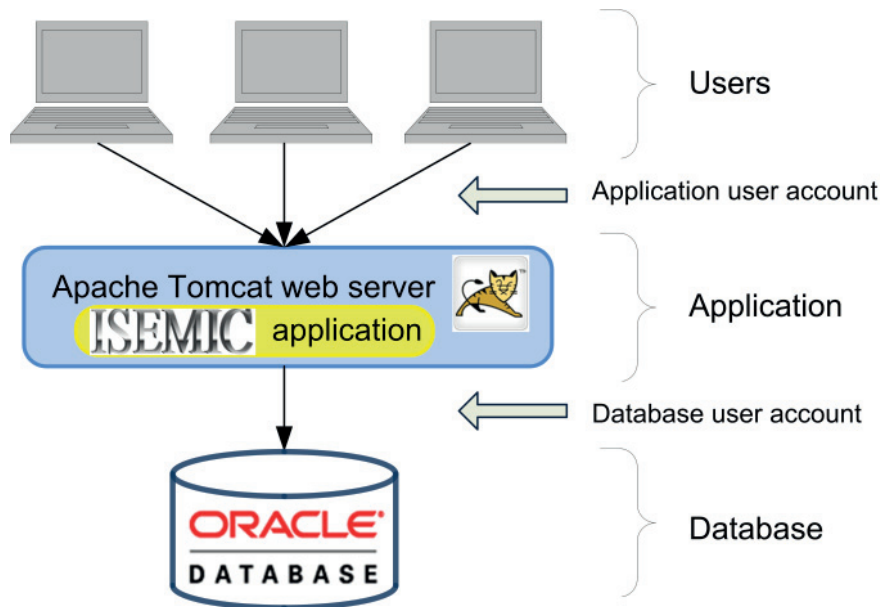


Figure 2. ISEMIC web application architecture

### 3.3 ISEMIC web application structure

Below, application structure for SA user role will be explained because it has embedded all possible functionalities developed in this project. Other user roles don't have their corresponding functionalities; they have reduced SA permissions. How much it is reduced depends on exact user role (EA, EM, U or G). ISEMIC application outline is shown on Figure 3.

ISEMIC web application main menu bar consists of seven main application modules on the left side (Figure 3): *Home*, *Security*, *Objects management*, *Reports and graphs*, *GeoAdministration*, *EnergoAdministration* and *Design*. Each application has its own menu bar – ribbon divided on working groups (which includes function buttons). Each function button has its own working cards ribbon and by click on desired working card its corresponding workspace is opened (Figure 3). In the right corner of the main menu bar are information about status and activities: *Alarms* (indicates the number of alarm messages), *Msg* (indicates the number of

unread messages), *User* (user name of the logged in user), *Edit* (by mouse click on the label, a window for changing password and e-mail address is opened), *About program* (by mouse click on the label, a window with basic information about the parties contributed to the software development) and *Logout* (click to terminate the work in the application and logout).

### 3.4 Data analysis in ISEMIC web application

Data analysis is the main advantage of ISEMIC web application. Manual inputs, as well as data entry through smart meters must pass the check procedures for the value and time consistency to be saved in the ISEMIC. Regression analysis is most often used for past energy and water consumption data analysis. It shows how a dependent variable – energy consumption – is related to the independent one – for example temperature, by providing an equation that allows estimating energy consumption for the given temperature. The relationship between independent and dependent variable in most cases is in linear form which means that the relationship between the points in the graph can be approximated by a straight line and expressed by a linear equation. The resulting line will go through the center of data scatter and therefore is called best-fit line. It has a particular property – sum of the vertical distances of data points from the best-fit line is equal to zero. The correlation coefficient indicates how well a best-fit line explains variations in the value of dependent variable.

Within ISEMIC, cumulative sum (CUSUM) technique is used to track achieved savings.

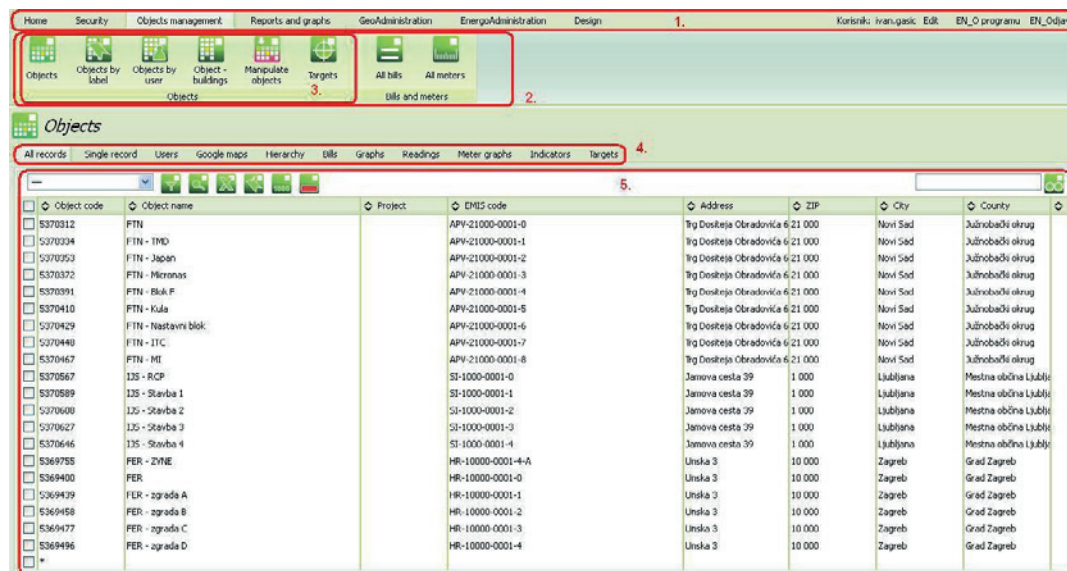


Figure 3. ISEMIC web application outline

1. Main menu bar
2. Menu bar – ribbon
3. Working groups (includes function buttons)
4. Working cards ribbon
5. Workspace

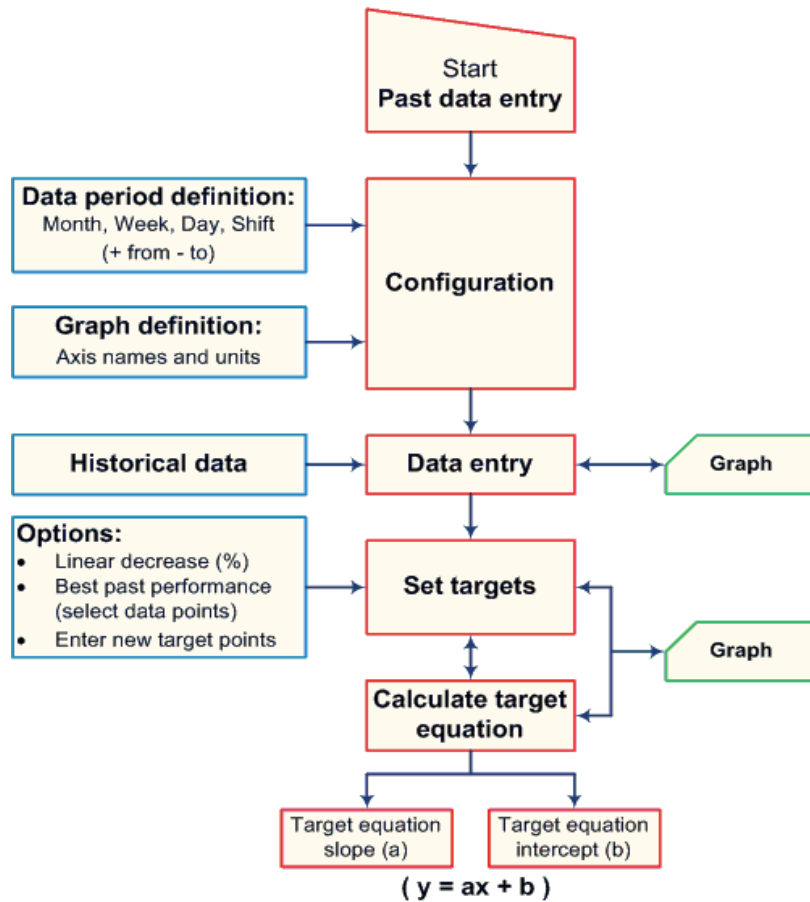


Figure 4. Procedure of setting energy efficiency targets

ISEMIC has the ability to review entered consumption and its monitoring according to the method called Nelson rules.

### 3.5 Setting energy efficiency targets in ISEMIC web application

The procedure of setting energy efficiency targets and their display on the graph is shown in flowchart on Figure 4. Goals can be set as:

- a linear reduction (percentage);
- a new line based on selected points of best efficiency or
- a new line formed on newly defined basis points.

As the result ISEMIC generates new target line equation.

## 4 CURRENT RESULTS OF ISEMIC WEB APPLICATION IMPLEMENTATION

Energy and water consumption data of building complex belonging to Faculty of Electrical Engineering and Computing (FEEC) are entered from bills during period from 2007 – 2010 into the ISEMIC and some of the obtained graphs are presented below.

The first graph (Figure 5) shows the share of each energent in total cost with tax for each year. Next three graphs (Figures 6,7 and 8) show electricity, heat and water total consumption of whole complex of FEEC for each year. It is also possible to view total cost with tax, monthly consumption and monthly cost with tax for each energy sources.

Last graph (Figure 9) shows monthly CO<sub>2</sub> emission during period from 2007 – 2010 caused by electricity consumption. It is also possible to view monthly CO<sub>2</sub> emissions caused by consumption of other energy sources.

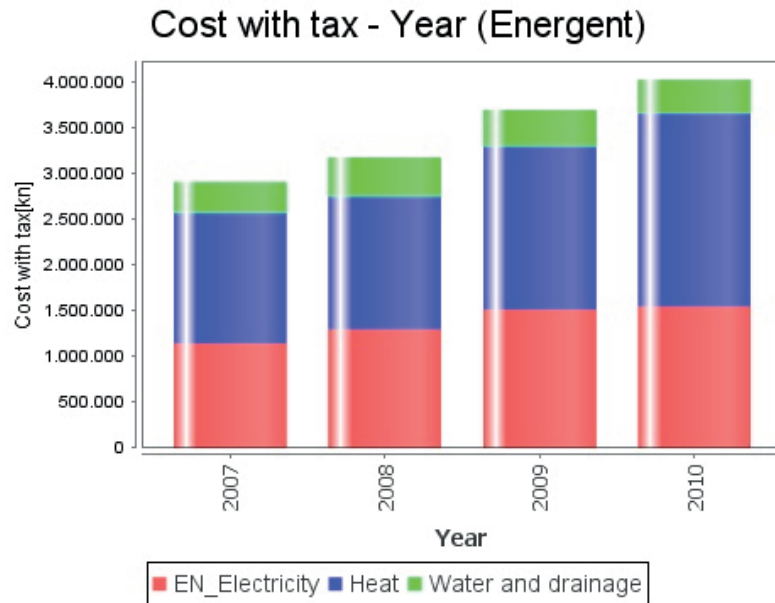


Figure 5. Share of each energy source in total cost with tax

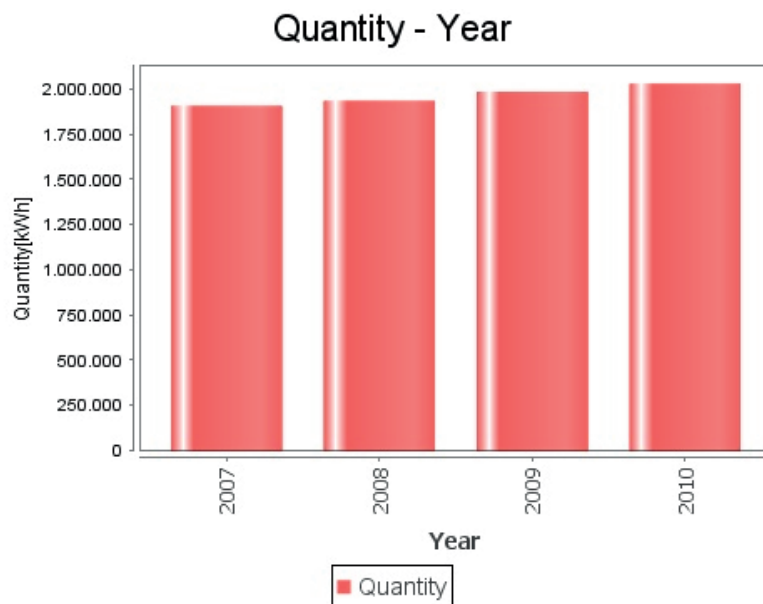


Figure 6. Electricity consumption for each year

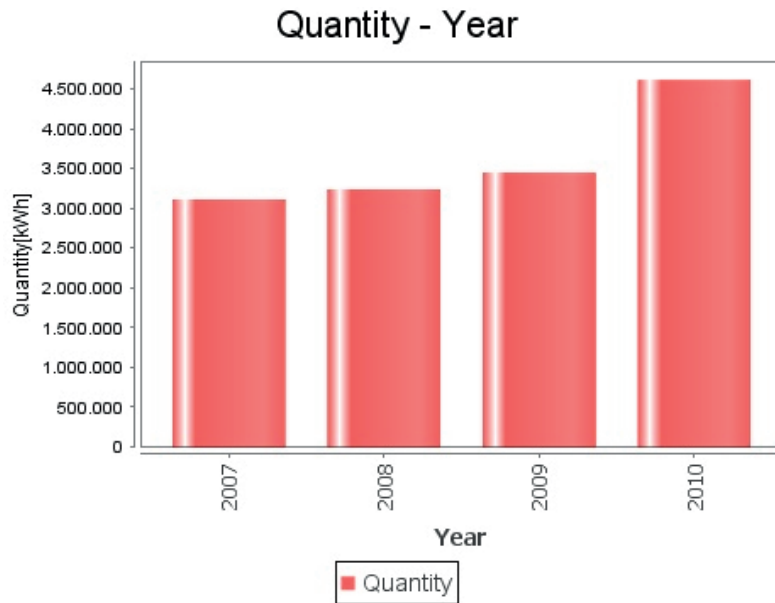


Figure 7. Heat consumption for each year

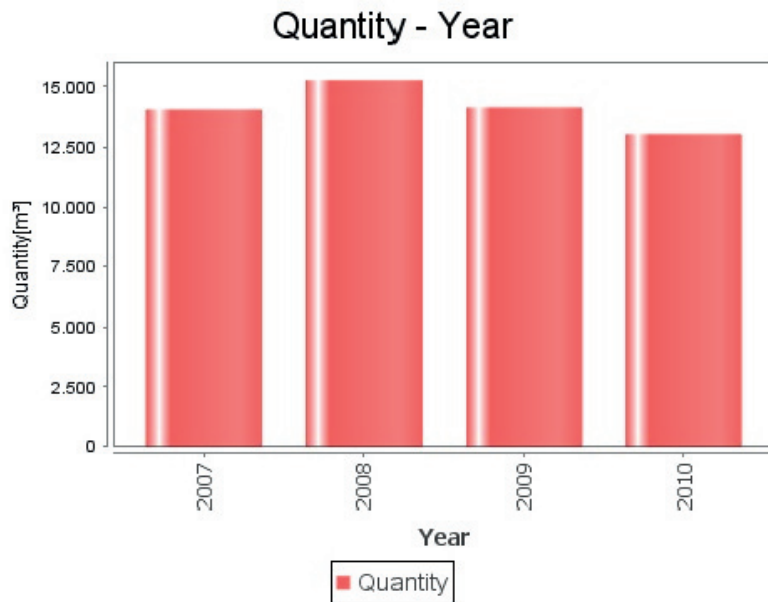


Figure 8. Water consumption for each year

Purchase of smart metering equipment and smart metering infrastructure is in conduction after which more grained energy and water consumption data will be available.

Real time metering of electricity consumption on a daily basis of whole complex of FEEC is currently established and connected with the ISEMIC. Next two figures (Figures 10 and 11) show daily electricity consumption for whole complex of FEEC in January 2011 and 2012. Red points represent total daily consumption during higher tariff, while blue points represent during lower tariff. It

is expected real time consumption metering of other energents (heat and water) of whole complex of FEEC will be established in near future, as well as real time metering of energy and water consumption of individual buildings.

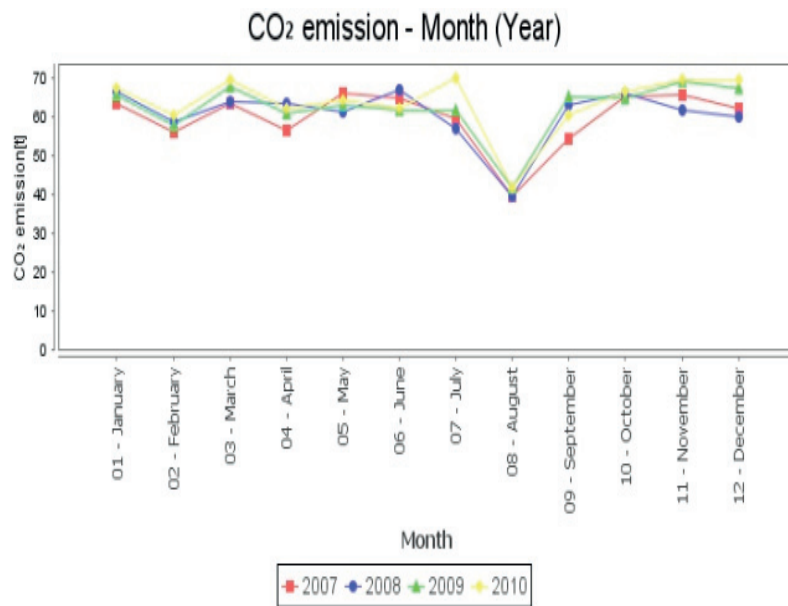


Figure 9. Monthly CO<sub>2</sub> emissions caused by electricity consumption

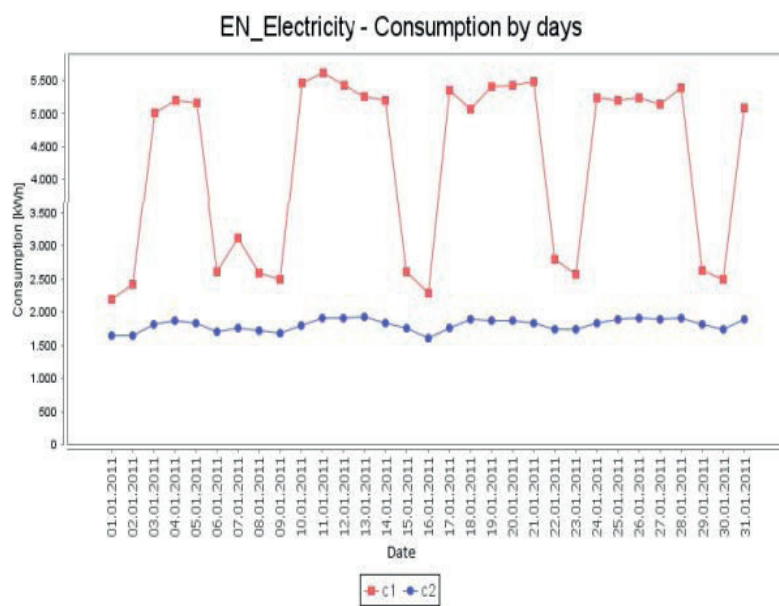


Figure 10. Daily electricity consumption for January 2011

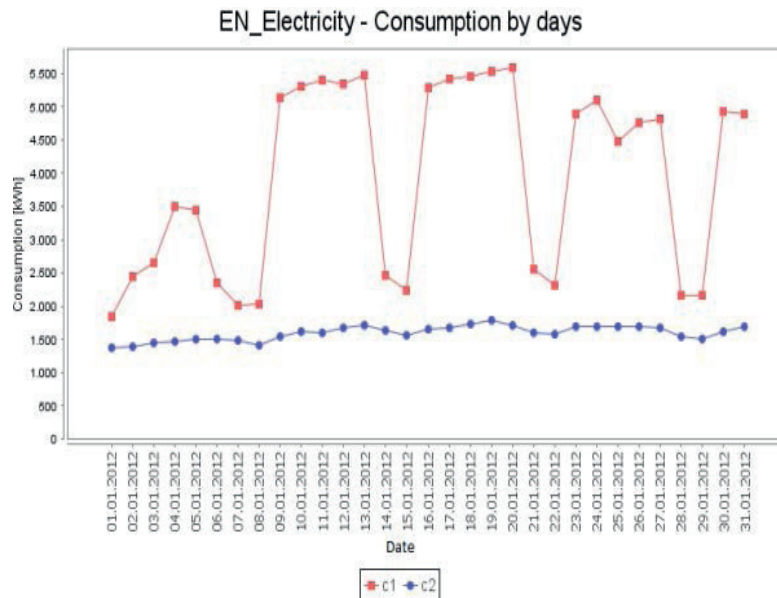


Figure 11. Daily electricity consumption for January 2012

## 5 INNOVATIVE ASPECTS

ISEMIC web application can become very important tool for energy management in public buildings. It will enable local and national authorities to lead by example and have a tool to help in proving positive effects of increasing energy efficiency and installation of smart meters.

ISEMIC creates added value in the following ways of presenting new, ready-to-use concepts:

- Interconnectivity with smart meters subsequent to creation of data bridges, which enables consumption monitoring on a daily basis or more frequently;
- Use of ICT for energy management in buildings as a service rather than a product (only an internet connection is needed);
- Use of algorithms that support expert knowledge and decision makers by discovering patterns of energy usage to identify waste, to find opportunities for change and to set targets for improvements;
- A streamlined, robust system of determining baselines of consumption using regression analysis on past consumption data, defining consumption targets and verification of savings using the CUSUM technique;
- System of accounting for exceptions on outlier values of energy consumption, which are commented by the technical person in the building as well as the city energy manager;
- Monitoring for changes in energy performance to evaluate the effect of improvements that have been made, to check whether consumption targets are being met and to provide evidence of progress towards improved energy savings.

## 6 CONCLUSION

It is expected that ISEMIC will improve energy efficiency in buildings, raise building users' awareness of energy consumption and utilize measurements from smart

meters. Examples from praxis show that introducing an energy consumption monitoring system raises employee awareness on energy expenditure, which leads to 5% of energy and water savings without any additional investments in energy efficiency measures. After full ISEMIC implementation and implementation of some simple energy efficiency measures it is expected that energy and water savings will reach at least 10% of current consumption expenses [5]. It would be a great example how significant savings can be achieved by systematic energy monitoring and management provided by the use of ISEMIC. After successful project finish it is expected that city, county or ministry will show higher interest to connect public buildings in their ownership with the ISEMIC web application and start systematic energy monitoring and management. Connection of private buildings with ISEMIC is expected in further future; with development of remote data reading systems and supporting IT infrastructure ISEMIC will have an important role in development of the concept of „smart cities“.

## 7 REFERENCES

- [1] UNDP (group of authors), Functional specification of ISEMIC web application, 2010
- [2] UNDP (group of authors), Technical specification of ISEMIC web application, 2011
- [3] Goran Čačić, “Poboljšanje efikasnosti korištenja energije i održivosti gradova uvođenjem sustavnog gospodarenja energijom”, 2011
- [4] Goran Čačić, Zoran Morvaj, “Improving efficiency of energy use in cities – towards sustainability through managing energy and changing behavior”, 12. EURA Conference, Madrid, 2009
- [5] J.C.P. Kester, M.J. Gonzalez Burgos, J. Parsons, “Smart metering guide”, Energy research Centre of the Netherlands, 2010

**DAVOR GRGIĆ      SINIŠA ŠADEK      VESNA BENČIK**

davor.grgic@fer.hr      sinisa.sadek@fer.hr      vesna.bencik@fer.hr

**University of Zagreb Faculty of Electrical Engineering  
and Computing**

**DAMIR KONJAREK**

damir.konjarek@enconet.hr

**Enconet d.o.o.**

## **DECAY HEAT CALCULATION FOR SPENT FUEL POOL APPLICATION**

### **SUMMARY**

The automatic procedure was developed for fuel assembly decay heat calculation based on PARCS 3D burnup calculation for fuel cycle depletion, and ORIGEN 2.1 calculation during both depletion and fuel cooling. Using appropriate pre-processor and post-processor codes it is possible to calculate fuel assembly decay heat loads for all fuel assemblies discharged from reactor. Simple graphical application is then used to distribute fuel assemblies within fuel pool and to calculate any fuel assembly, SFP rack, or whole pool heat load at arbitrary time. The application can be used for overview of fuel assembly burnups, cooling times or decay heats. Based on given date it is possible to calculate whole pool heat load and time to boiling or time to assembly uncover using simple mass and energy balances. Calculated heat loads can be input to more detailed thermal-hydraulics calculations of spent fuel pool. The demonstration calculation was performed for NPP Krsko spent fuel pool.

**Key words:** burnup calculation, decay heat, ORIGEN, PARCS, spent fuel pool

## 1. INTRODUCTION

It was always important to have fast and accurate decay heat prediction, both in the core and in Spent Fuel Pool (SFP), but after accident in NPP Fukushima that is even more important. Calculation procedures are used based on existing well known computer codes, developed pre and post processors and some simple additional heat balance modules to calculate decay heat in reactor, or in SFP, both for selected assemblies of whole inventory. For decay heat calculation it is possible to use detailed ORIGEN 2.1 [1], [2] based calculation or fast calculation based on implementation of ANS Decay Heat Standard [3]. Calculated heat sources can be used for fast checking of core of SFP heat-up or as input in more complicated thermal hydraulics calculations.

## 2. ORIGEN 2.1 CALCULATION

ORIGEN 2.1 is old well known code able to calculate radioactive inventory and decay heat of nuclear fuel for selected depletion scheme and for prepared cross section and decay libraries. It is possible to use its newer versions distributed as part of SCALE package, but old version is easier to use, faster, and it is still able to give reliable results for scoping purposes. Most of the heat input in SFP is coming from last discharged spent fuel and it is more important to have accurate calculation for last depletion cycle. It is especially important if we have, due to some reason, to stop the plant and discharge the fuel to spent fuel pool. The same is always true for decay heat produced within reactor core during shutdown period.

In order to provide accurate burnup information needed for ORIGEN 2.1 calculations on fuel assembly bases, we used 3D multi cycle depletion capability from PARCS code [4]. As result of an additional postprocessing of PARCS calculation 2D distribution of fuel assembly burnups are produced for each internal PARCS depletion step. Using developed ORIGEN preprocessing code that and other information are used to prepare ORIGEN input for depletion of each fuel assembly in the core or in the spent fuel pool. As part of preprocessing time vector with decay time points is prepared and converted to ORIGEN DEC statements. It is possible to select calculation for any available fuel assembly or for all available of assemblies.

The scheme is valid not just for last depletion cycle, but for any past cycle for which necessary data are prepared. In Figure 1 burnup distributions are shown for cycle burnups 150 MWd/tU and 19500 MWd/tU, for NEK Cycle 26 [5]. Corresponding burnup increment to neighbouring cycle burnup point used in PARCS depletion is shown in Figure 2. Equation (1) is then used by preprocessor to calculate Fuel Assembly (FA) power needed for ORIGEN IRP commands. The formula is based on information on FA burnup increment, FA high metal mass and time spent for that depletion step. ORIGEN postprocessor is then used to retrieve decay heat data for input time points.

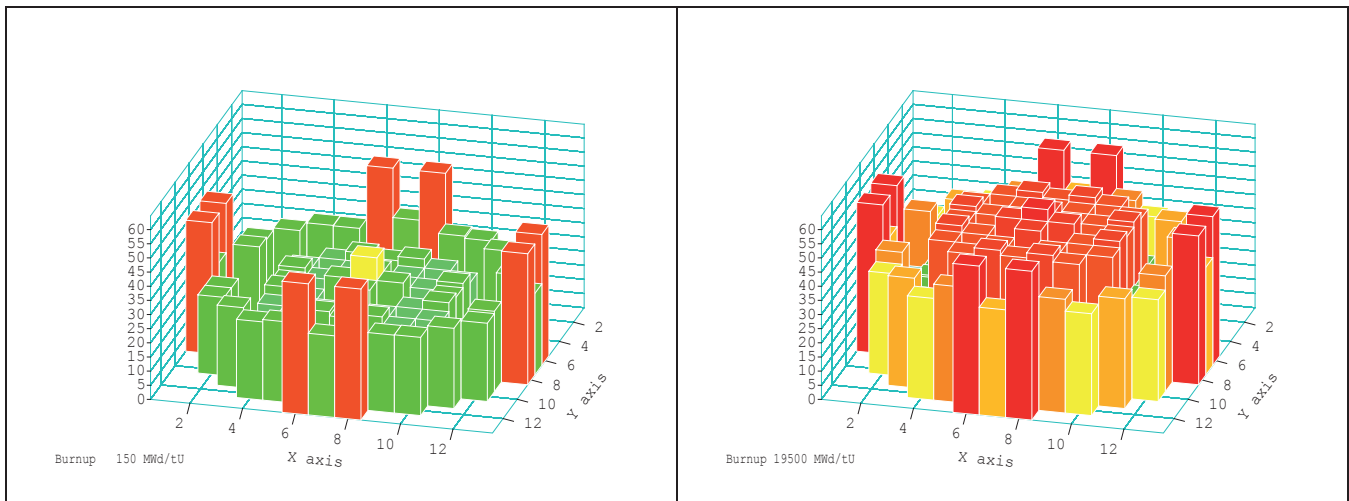


Figure 1. Cycle 26 distribution of FAs burnup, cycle burnup 150 MW/tU and 19500 MWd/tU

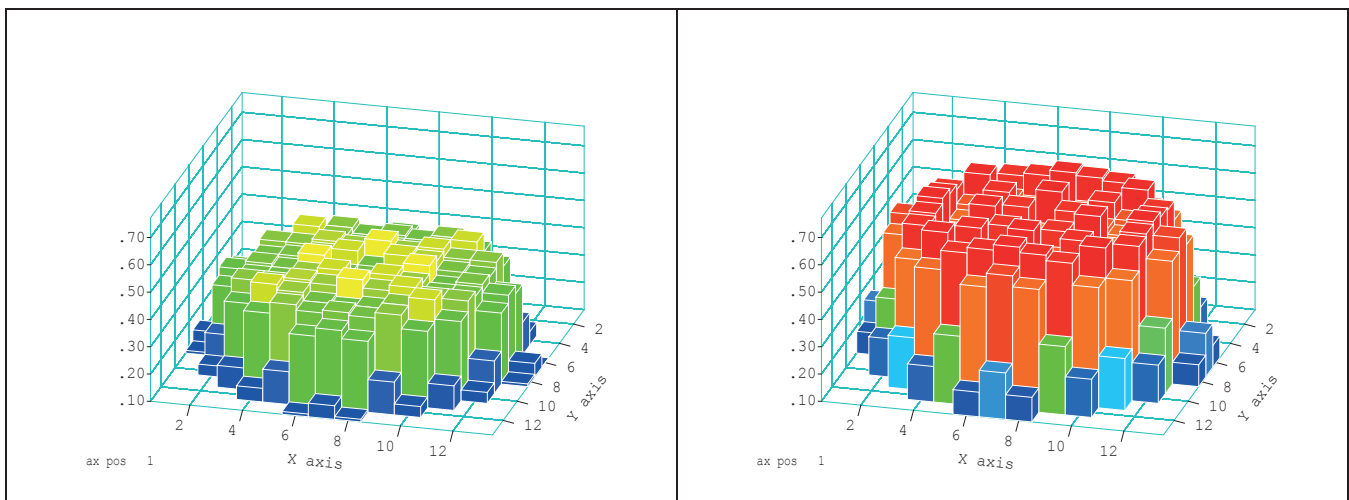


Figure 2. Increments in FAs burnup to get cycle burnup of 500 MW/tU and 20000 MWd/tU

ORIGEN simulation were performed for NEK Cycle 26, decay periods up to 3 hours, up to 100 hours, up to 30 days and up to 365 days. First time period is usual

for core safety analyses, second is minimum cooling time before moving fuel from core to SFP, third is period usually analysed from RG 1.27 point of view (Ultimate Heat Sink (UHS) analysis), and fourth is time scale important for long term calculation of fuel in SFP. The results for 3 hours, 100 hours, and 365 days are shown in Figure 3 to Figure 5. Decay heat due to fission product (FP), actinides (ACT), activation products (AP), and total decay heat power are given.

$$P_{sf,n} = \frac{\Delta burnup_{i,n} \left[ \frac{MWd}{MTIHM} \right] \cdot m_{u,i} [MTIHM]}{t_n [d]} = \text{_____} [MW] \quad (1)$$

The plant specific calculation was performed for whole core inventory (121 FAs), on assembly by assembly basis. Approximate number of ORIGEN input lines is 10000 (that is why input preprocessor is necessary). The calculation can be performed for current cycle too (based on available PARCS results). It can be performed for current burnup (defined in preprocessor input), and can be used if unanticipated plant shutdown is experienced or if removal of the fuel to SFP is needed.

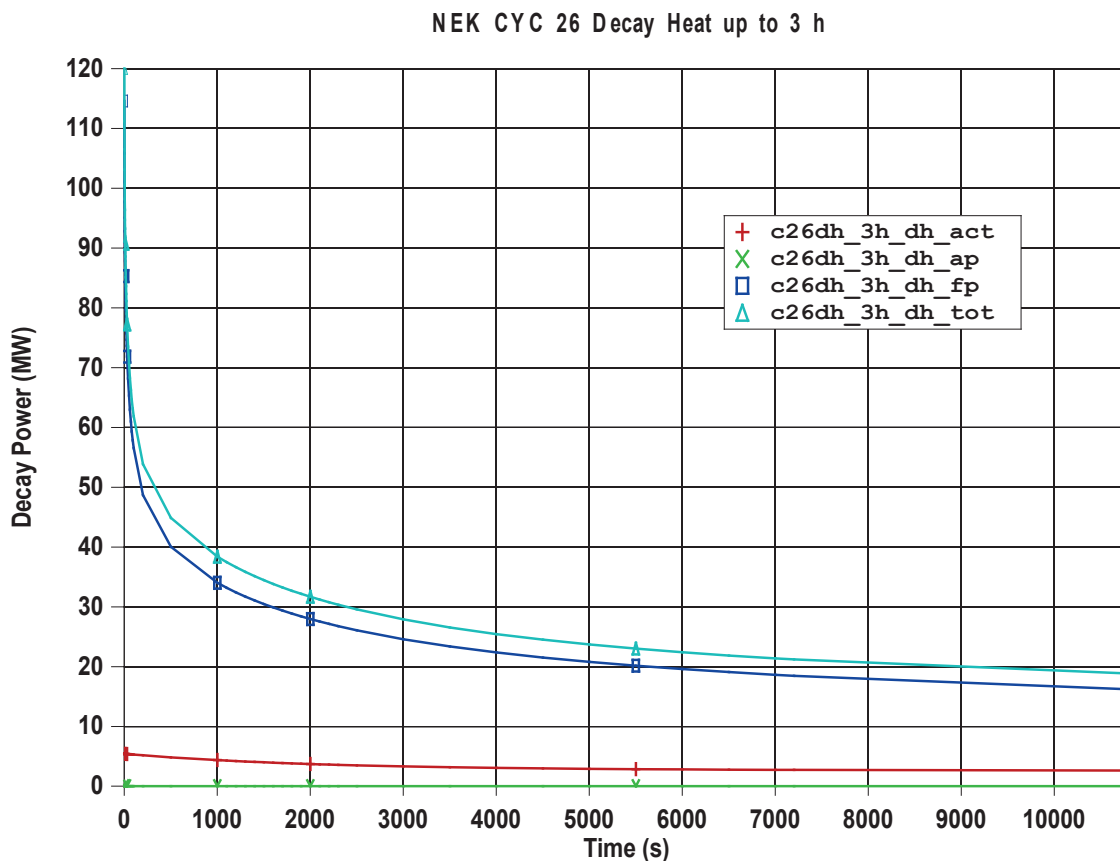


Figure 3. ORIGEN 2.1 calculated decay heat for cycle 26, up to 3h after shutdown

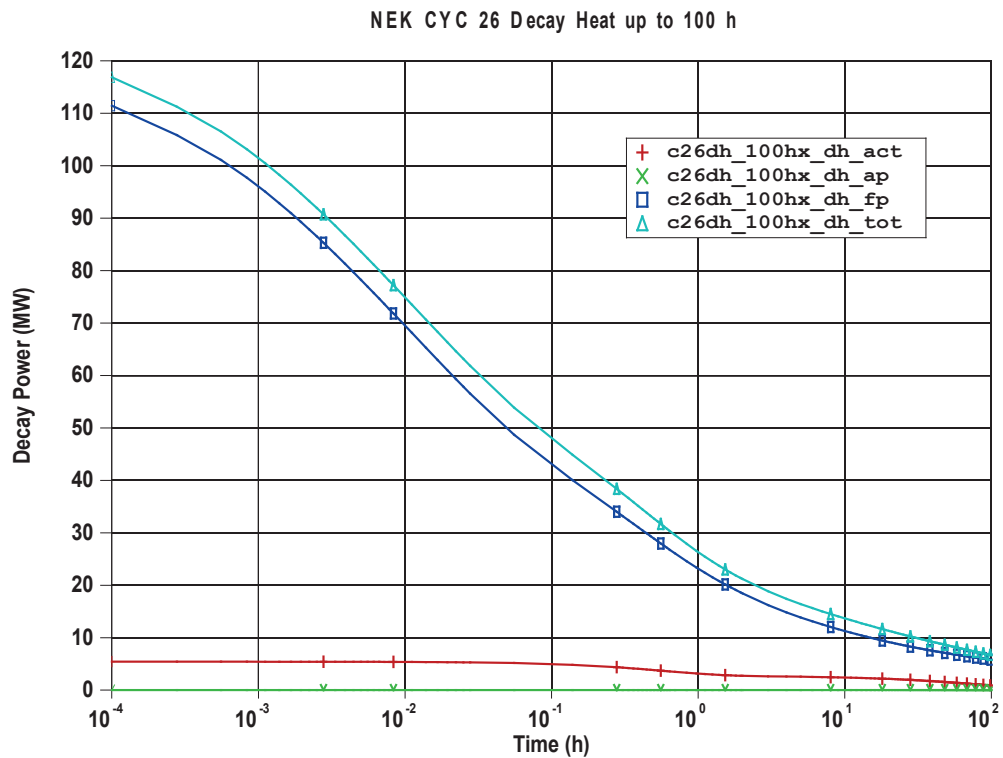


Figure 4. ORIGEN 2.1 calculated decay heat for cycle 26, up to 100h after shutdown

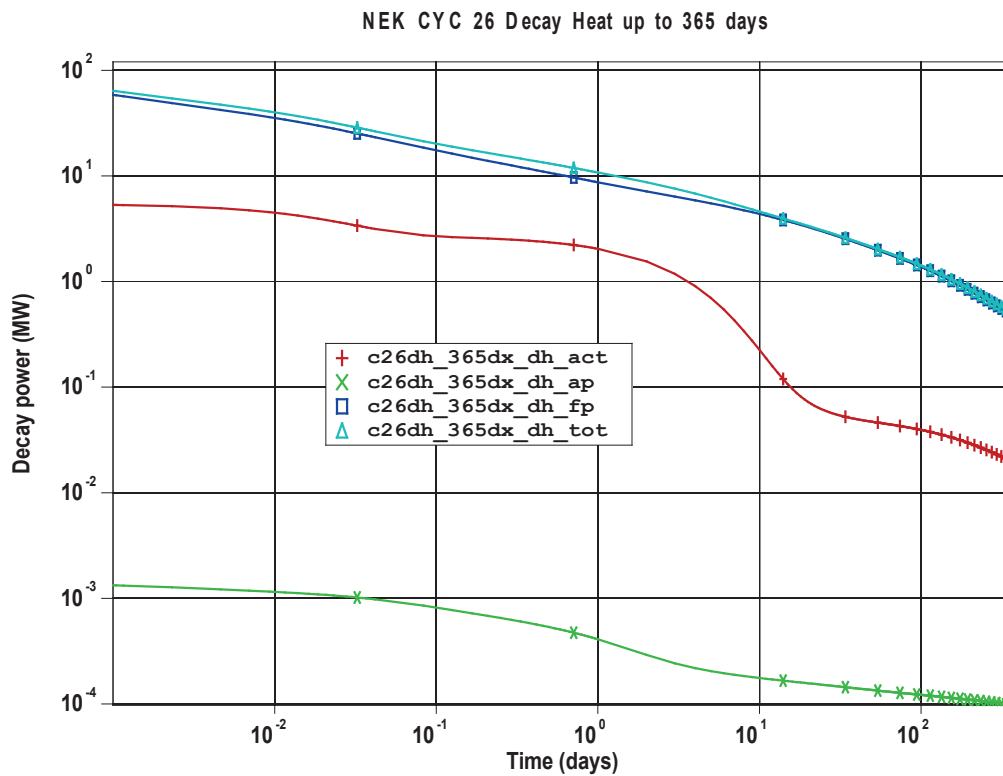


Figure 5. ORIGEN 2.1 calculated decay heat for cycle 26, up to 365 days after shutdown

### 3. SPENT FUEL POOL APPLICATION

Number of fuel assemblies in spent fuel pool is usually larger than current core loading and often approximate calculation is enough to check for time to boiling or time to fuel uncover or simple spent FAs statistics. Approximate number of spent FAs in NEK SFP is around 1200. In order to speed-up calculation process, detailed ORIGEN calculation can be replaced with fast decay heat calculation based on ANS Decay heat Standard. The decay heat calculation is part of graphical user application capable to provide simple FAs data base and manipulation (can be used during refueling). The same type of input data is used for both types of decay heat calculation.

#### 3.1 ANS Standard Decay Heat Calculation

The reactor decay heat can be calculated using the ANSI/ANS-5.1-2005 standard [5], and small computer routine based on it. The calculation takes into account the time reactor core spent at power in operation before shutdown, and take into account  $2\sigma$  uncertainties for decay heat power obtained after fission of 4 isotopes. For period of the interest for the calculation, conservative fixed uncertainty of 2% (one  $\sigma$ ) was used. It is assumed that calorimetric uncertainty is 2% and that nominal power is 1994 MW (provided in input). Two uncertainties were combined as statistically independent to obtain overall uncertainty of 4,47%, used in the calculation.

The simple f90 module f90 is used in the process of decay heat calculation. The code uses Tables 9 to 12 from the standard ANSI/ANS-5.1 in the calculation of decay heat after fission of following isotopes: U-235, Pu-239, U-238, Pu-241.  $\alpha_i$  and  $\lambda_i$  values from the tables as well as provided formulas (2) for calculation of energy release in MeV per fission were implemented in Fortran 90 programming language.

$$F(t, T) = \sum_{i=1}^{23} \frac{\alpha_i}{\lambda_i} \exp(-\lambda_i t) [1 - \exp(-\lambda_i T)] \quad (MeV / fission) \quad (2)$$

T is time spent at power, and t is time from initial fission till time when decay heat is needed. Both times are in seconds.

Practical implementation of above formula for decay heat power of isotope i at time t(s) after final shutdown, for operation lasting Tn seconds at power Pn (out of npow power intervals) is given in (3).

$$P'_{di}(t, T_n) = \frac{P_{in}}{Q_i} \cdot \left\{ \sum_{j=1}^{23} \frac{\alpha_{ji}}{\lambda_{ji}} \exp(-\lambda_{ji} (t + \sum_{n=1}^{npow} T_n)) [1 - \exp(-\lambda_{ji} T_n)] \right\} \quad (3)$$

Index i is used to label i-th isotope undergoing fission, n is for n-th power interval (counting from the interval when reactor was first at power), index j is used for internal summation of exponential terms for isotope i. Pin means power coming from isotope i in power interval n, and Qi means fission gain of isotope i.

The sample results for decay heat power (infinite operation time and plant specific operation time), for decay power and total released energy, are given in Figure 6 and Figure 7. The calculation was performed to provide required decay heat during verification of UHS capacity.

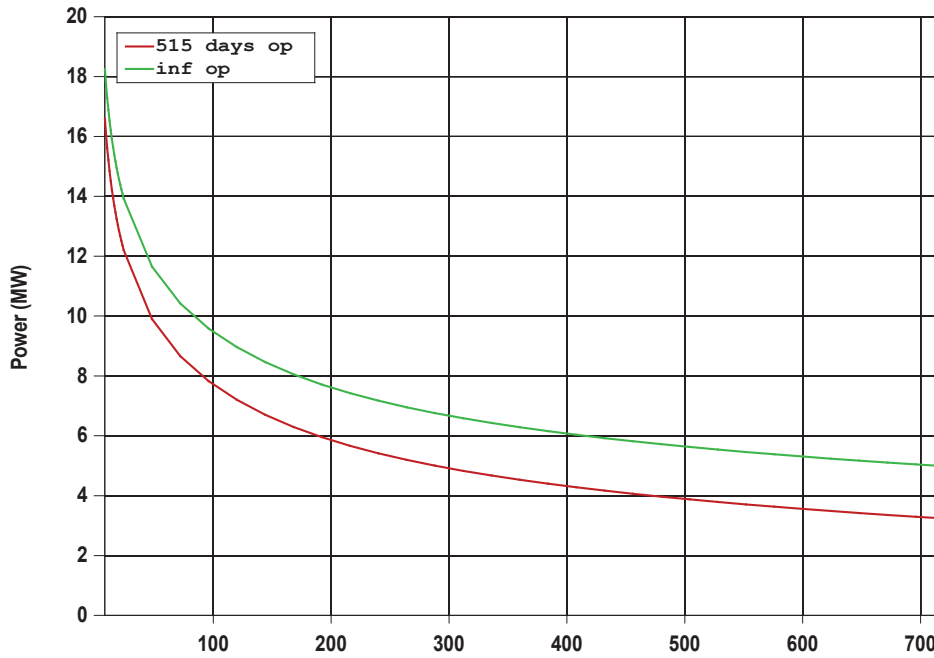


Figure 6. Power vs. time (h) for 30 days after shutdown calculated, ANS Std based routine

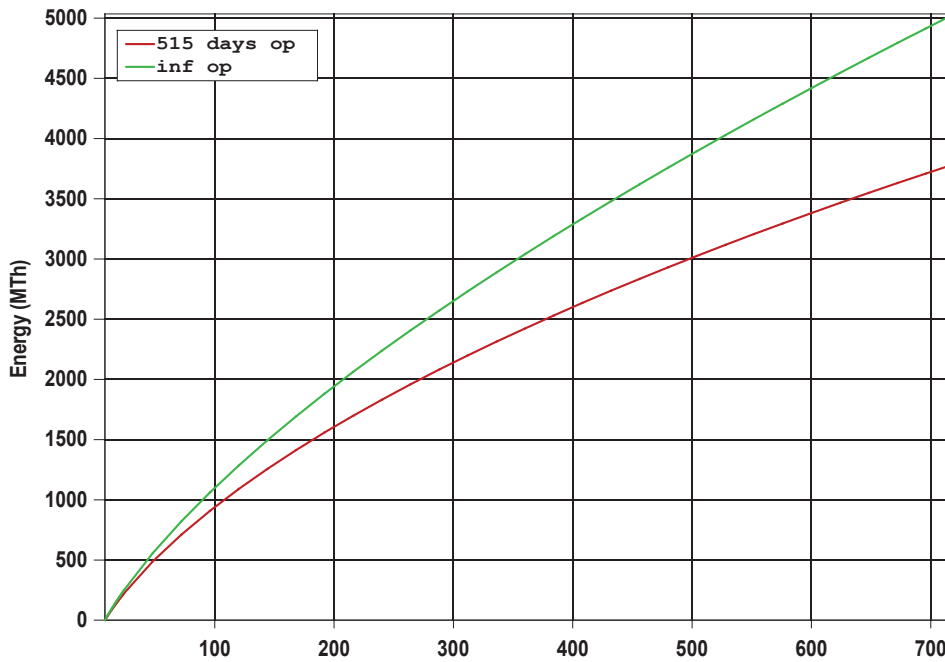


Figure 7. Energy vs. time (h) for 30 days after shutdown calculated, ANS Std based routine

### 3.2 SFP Graphical Interface

Decay heat power module is part of graphical application used to support different thermal hydraulics calculations of spent fuel pool. The application is able provide graphical representation of current position of spent FAs in SFP (Figure 8), based on USAr data [7], and associated data (time spent in pool for each FA (Figure 9), FA burnup (Figure 10), and FA decay heat power (Figure 11)), for any selected point in time. Decay heat can be obtained for any FA, any group of FA (e.g. rack), or whole pool. It is possible to provide time points and to get decay heat power versus time to be used in other codes or just to see time dependent decay heat in pool during depletion cycle (Figure 12) or during refueling.

The application has simple thermal hydraulic module capable to perform simple calculations of pool water heatup, time to boiling and time to fuel uncover for different initial scenarios (configuration of the pool, initial amount of water, presence of leakage and similar) [8]. Time to boiling dependence for different initial amounts of water and for increasing decay heat is shown in Figure 13. Calculated elevation of water in pool versus time for different scenarios is shown in Figure 14. It should be mentioned that used calculation is simple energy balance type of calculation and can be used as scoping calculation or as a preparation for more detailed calculations of the pool.

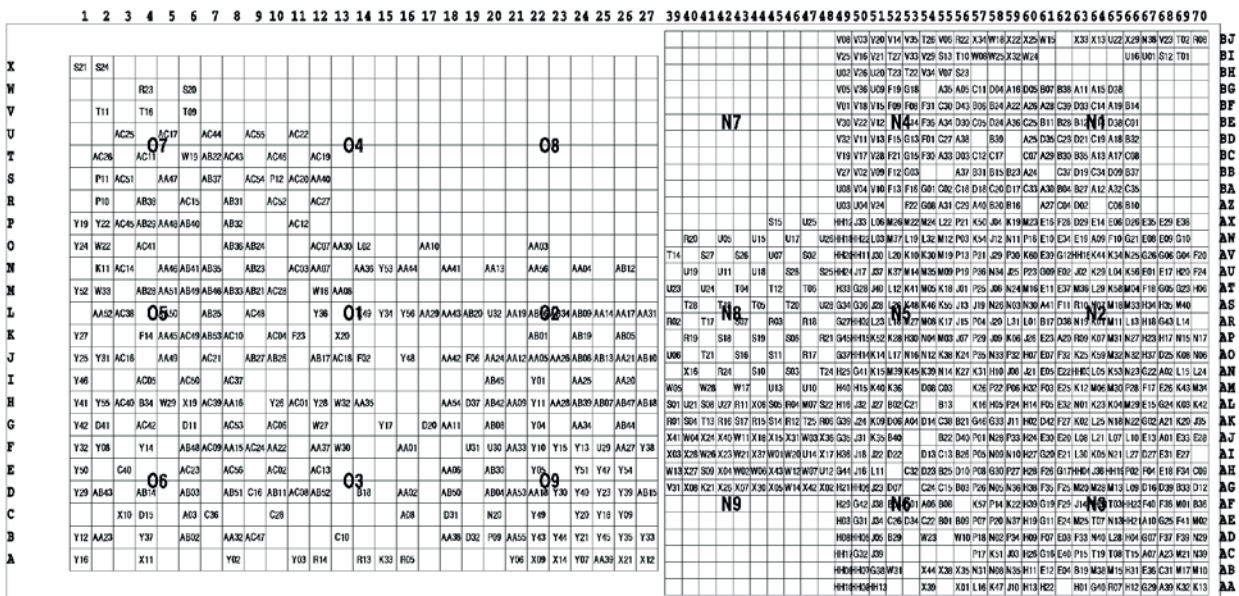


Figure 8. Layout of NEK SFP

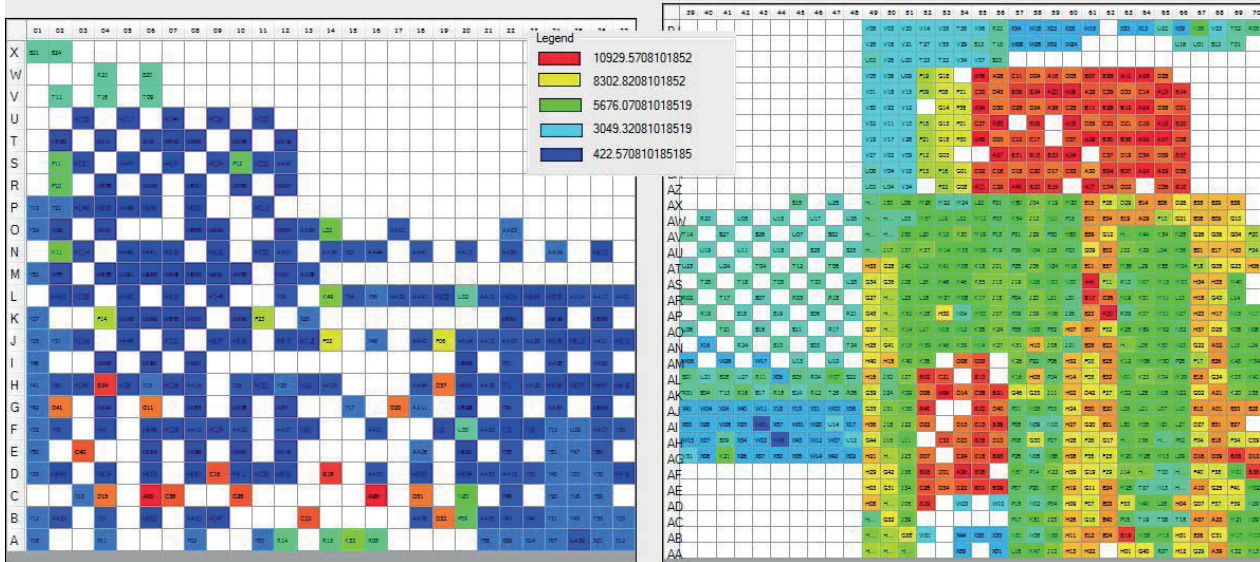


Figure 9. Time spent in pool (days) for different FAs (June 2013)

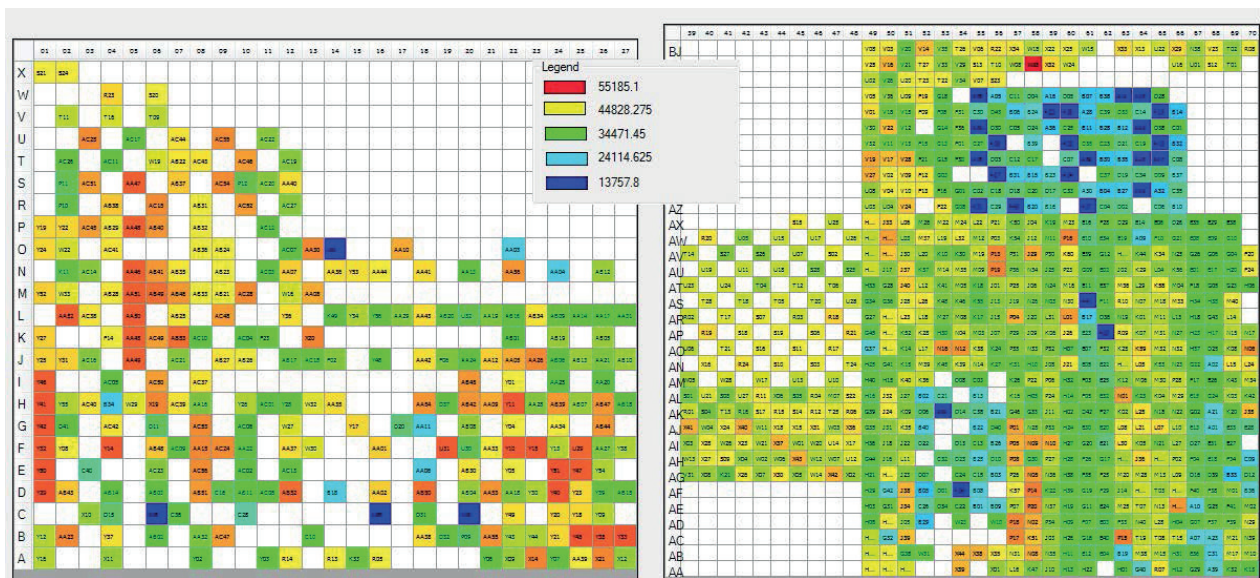


Figure 10. Burnup (MWd/tU) for FAs in SFP (June 2013)

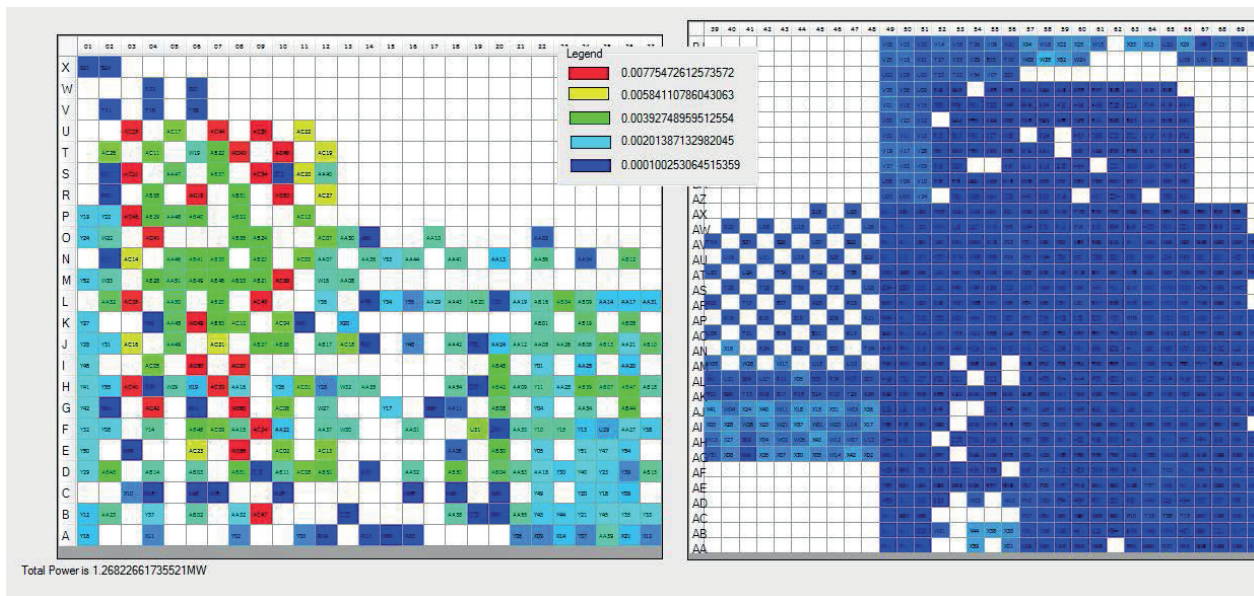


Figure 11. Decay heat (MW) for FAs in SFP (June 2013)

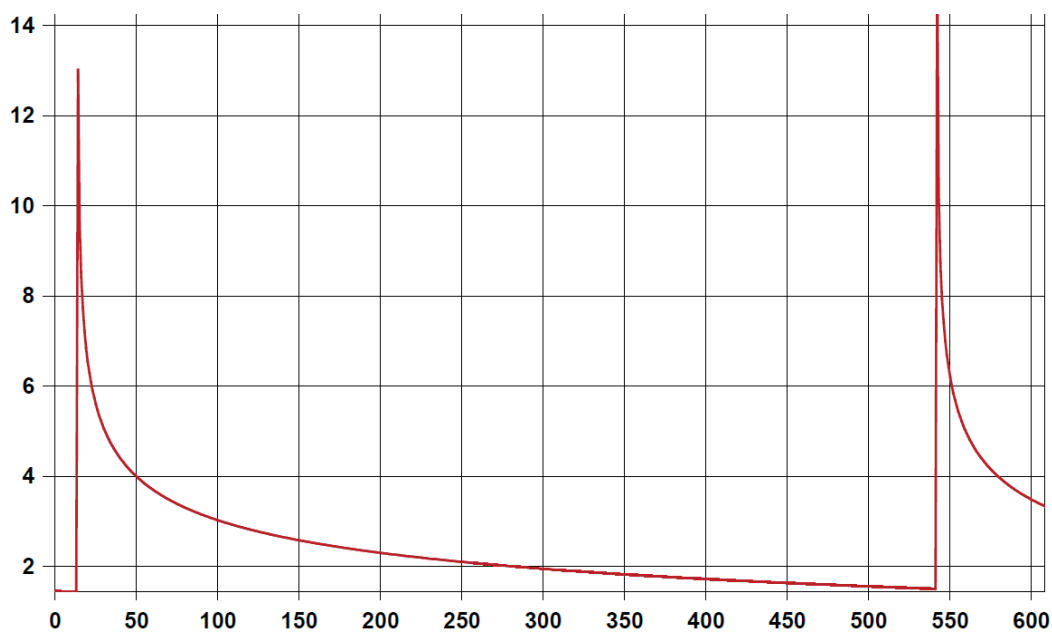


Figure 12. Total decay heat (MW) vs. Time (days) in SFP for two successive refuelings

NEK SFP

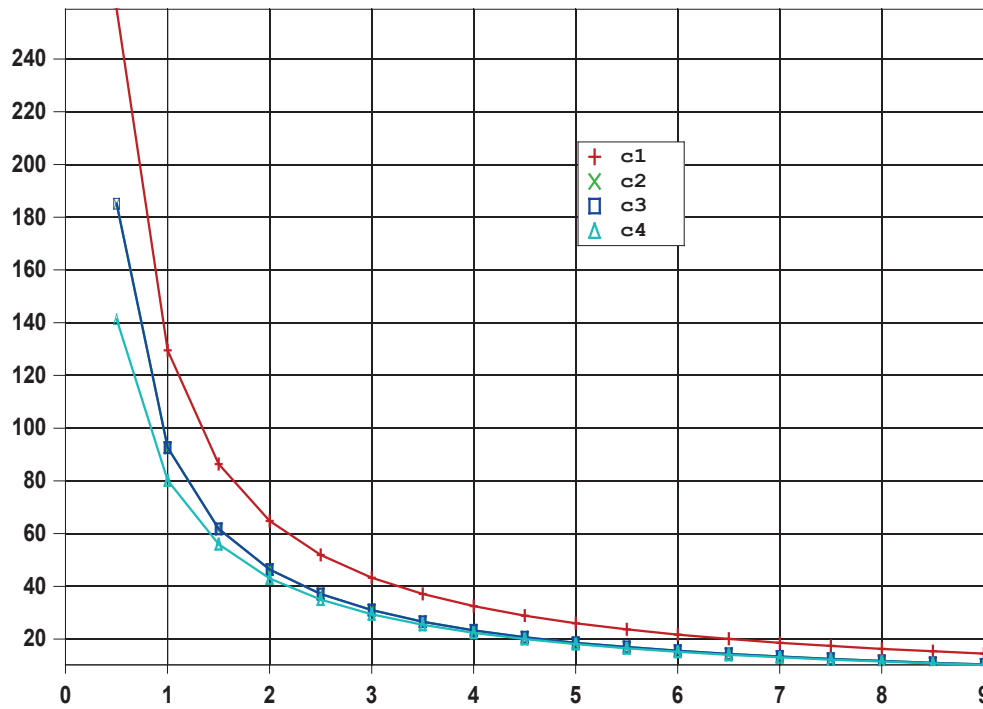


Figure 13. Time to boiling (h) vs. Decay heat (MW) for different scenarios

NEK SFP

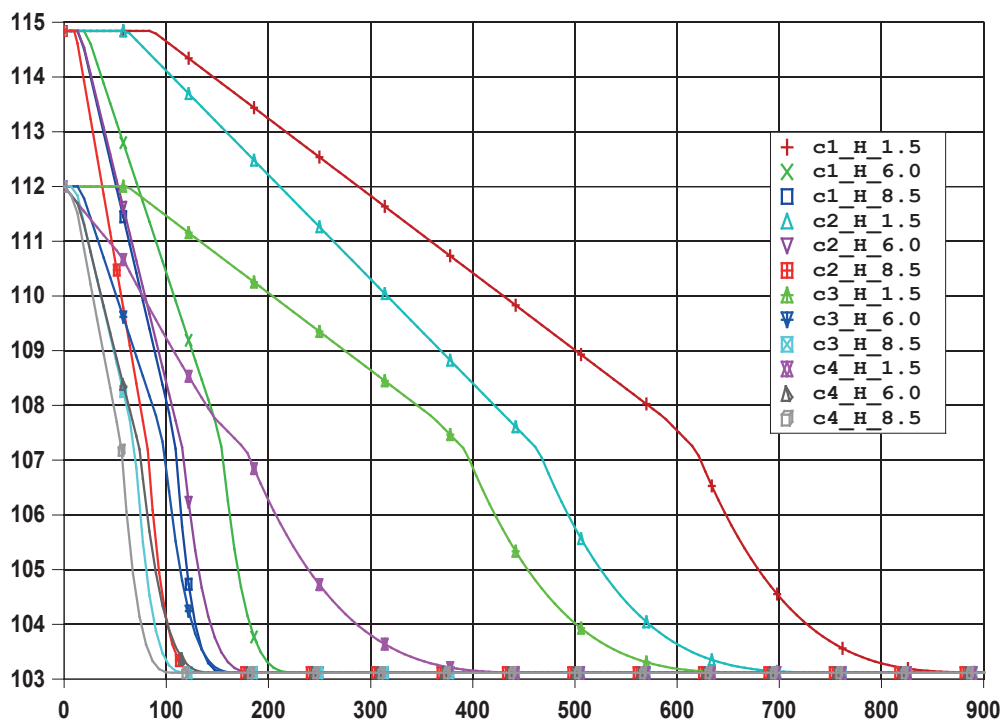


Figure 14. Elevation of water in pool (m) vs. time (h) for different scenarios and different level of decay heat (MW)

## 4. CONCLUSION

PARCS 3D burnup calculation can be used as effective means of providing power for ORIGEN depletion steps for plant specific decay heat calculation of fuel assembly basis. The developed procedure uses mix of well known codes and auxiliary routines to provide pre and post processing. FA burnups can be used to calculate plant specific decay heat for core or SFP. Due to amount of data needed for multi cycles calculation automatic pre-processor for ORIGEN input preparation (FA based depletion) is needed.

In addition to ORIGEN calculation fast module is available for both core and SFP decay heat calculation based on ANS standard decay heat calculation. In case of SFP it is part of graphical user application capable to trace position, time spent in pool, acquired burnup and current generated decay heat in each fuel assembly. The application is useful to predict total or per FA decay heat for other thermal hydraulics calculation in core or SFP. Simple calculation procedure is able to calculate water heatup for obtained time dependent decay heat or to calculate time to boiling and water level.

## 5. REFERENCES

- [1] A.G. Croff, "A User's Manual For The ORIGEN2 Computer Code", ORNL/TM-7175 (CCC-371), Oak Ridge National Laboratory, July 1980.
- [2] A.G. Croff, "ORIGEN2: A Versatile Computer Code For Calculating The Nuclide Compositions And Characteristics of Nuclear Materials", Nuclear Technology, 62, 335-352, September 1983.
- [3] Decay Heat Power in Light Water Reactors, ANSI/ANS-5.1-2005.
- [4] US NRC, PARCS v2.6, US NRC Core Neutronics Simulator, Draft, November 2004.
- [5] The Nuclear Design and Core Management of the Krsko Nuclear Power Plant, Cycle 26, WCAP-17597-P rev. 0, May 2012.
- [6] Regulatory Guide 1.27, Rev. 2 – Ultimate Heat Sink for Nuclear Power Plants, 1976.
- [7] NEK USAR, Rev. 20.
- [8] A.S. Benjamin et al., "Spent Fuel Heatup Following Loss Of Water During Storage", NUREG/CR-0649, SAND77-1371, 1979.

**MILJENKO BREZOVEC**

[miljenko.brezovec@hep.hr](mailto:miljenko.brezovec@hep.hr)

**HEP Generation Ltd**

**IGOR KUZLE      MATEJ KRPAN**

[igor.kuzle@fer.hr](mailto:igor.kuzle@fer.hr)      [matej.krpan@fer.hr](mailto:matej.krpan@fer.hr)

**University of Zagreb Faculty of Electrical Engineering  
and Computing**

## **DETAILED MATHEMATICAL AND SIMULATION MODEL OF A SYNCHRONOUS GENERATOR**

### **SUMMARY**

Synchronous generator theory has been known since the beginning of its use, but the modelling and analysis of synchronous generators is still very existent in the present-day. Modern digital computers enable development of detailed simulation models, thus individual power system elements, including synchronous generators, are represented by the highest degree order models in power system simulation software packages. In this paper, first, a detailed mathematical model of a synchronous generator is described. Then, a simulation model of a synchronous generator developed based on the presented mathematical model. Finally, a transient stability after a short-circuit is simulated using real generator parameters.

**Key words:** block-diagram model, mathematical model, synchronous generator, short-circuit, transient stability

## 1. INTRODUCTION

In electric power system (EPS) simulation software packages today, individual elements can be represented by the models of the highest order of accuracy. By the virtue of state-of-the-art digital computers, in many cases it is not necessary to use simplified and reduced order models based on numerous assumptions anymore. In spite of this, using the most detailed mathematical models does not guarantee the quality and credibility of calculation results. The cause of unsatisfactory results is usually the lack of sufficiently accurate values of parameters on which a certain model is based on. Generally, the more detailed the mathematical model is, the more parameters it requires to be known. As many data for power system calculations (e.g. transient stability, short-circuit, power flow, etc.) are usually hard to obtain, it is clear that it isn't always the best solution to use the most detailed mathematical models. Equipment manufacturers usually provide data about the most of needed parameters, e.g. of synchronous generators, but there are a lot of older generators in the operation today for which it is difficult to determine even the most basic parameters such as synchronous reactance or exciter forced voltage.

Different power system calculations have very different purposes so the demands on accuracy are different as well—from tuning of the protection relays or automatic regulators to analysis of assumed operational scenarios. The issue of detailed modelling, primarily of generators and turbines, and their control systems is especially accentuated in stability calculations. Detailed nonlinear models of generators are described in [1-4]. The most popular is simplified linearized third order model, used by Demello and Concordia [5]. This model is further developed in [6] for small-signal stability analysis. Automatic voltage regulator (AVR) with voltage control loop essentially changes the synchronous generator dynamics. In [7], extended state-space model including the effects of excitation system and generator amortisseurs is used. In this paper the influence of excitation system is not considered and focus is only on generator model. The impact of generator modelling complexity is the subject of many transient stability studies, such as [8-11].

When modelling the synchronous generator, the rest of the EPS is usually replaced with an infinite bus. When researching stability of a generator working in a multi-machine system where the total power is a lot larger than the power of the individual generator (along with a strong grid), only the impact of a short-circuit close to the generator terminals is analysed. As the length of a transient is relatively short (2 s do 5 s), physical properties of the analysed machine have the prevailing impact on the properties of machine swing response.

## 2. SYNCHRONOUS GENERATOR MODEL

Although the theory of synchronous generator has been known since the beginning of its application, the research of modelling and analysis of synchronous generators is still very much ongoing. Mathematical description of electromechanical systems operation such as synchronous generator generally leads to a system of differential equations which is regularly nonlinear due to the multiplication of state variables. With the increase of computing power, the capabilities for modelling and analysis are increased as well. This has resulted in a large number of models that differ depending on the type of research they are intended for and on the degree of desired accuracy.

There are different approaches when developing a mathematical model and the corresponding simulation model of a synchronous generator. The most common approach is based on general two-reaction theory upon which a three-phase winding of a generator is substituted by one equivalent, fictitious two-phase winding projected onto the direct ( $d$ ) and quadrature ( $q$ ) rotor axis. The field winding is represented as a  $d$ -axis winding and the reaction of damper winding caused by the eddy currents in the cylindrical rotor is substituted by fictitious windings in  $d$ -axis and  $q$ -axis.

### 3. PARK'S TRANSFORMATION

Mathematical description of a synchronous generator can be significantly simplified with proper variable transformation. One of the possible stator variables (currents, voltages, fluxes) transformation is known as Park's or  $d$ - $q$  transformation. The number of variables after a transformation generally remains the same and in general case, substitution with new variables should be observed as a completely mathematical operation, thus no physical interpretation of fictitious is necessary. In this case, according to [1], the applied transformation can be physically interpreted because the new variables are obtained by projecting the real variables onto the three axes (direct, quadrature and stationary):

$$\mathbf{i}_{0dq} = \mathbf{P} \mathbf{i}_{abc} \quad (1)$$

$$\mathbf{i}_{0dq} = \begin{bmatrix} i_0 \\ i_d \\ i_q \end{bmatrix} \quad \mathbf{i}_{abc} = \begin{bmatrix} i_a \\ i_b \\ i_c \end{bmatrix} \quad (2)$$

$$\mathbf{P} = \sqrt{\frac{2}{3}} \begin{bmatrix} \frac{1}{\sqrt{2}} & \frac{1}{\sqrt{2}} & \frac{1}{\sqrt{2}} \\ \cos \vartheta & \cos\left(\vartheta - \frac{2\pi}{3}\right) & \cos\left(\vartheta + \frac{2\pi}{3}\right) \\ \sin \vartheta & \sin\left(\vartheta - \frac{2\pi}{3}\right) & \sin\left(\vartheta + \frac{2\pi}{3}\right) \end{bmatrix} \quad (3)$$

Current  $i_d$  can be imagined as a current through a fictitious winding which rotates with the same speed as rotor windings and has such position that its axis always aligns with the field winding axis. The magnitude of current in this fictitious winding will be such that it will induce a magnetomotive force in the  $d$ -axis equal to the sum of magnetomotive forces in real phase windings. The current  $i_q$  can be imagined in the same way, but the difference is that the axis of the fictitious winding aligns with the neutral axis of the rotor. Current  $i_0$  is identical to the zero-sequence current component and it exists only when the sum of phase currents is different than zero. Zero-sequence is not considered in the generator analysis so the two-reaction representation is simplified which facilitates the setting of generator equations.

Park's transformation is unique, thus an inverse transformation  $\mathbf{P}^{-1}$  exists as well, defined as:

$$\mathbf{i}_{abc} = \mathbf{P}^{-1} \mathbf{i}_{0dq} \quad (4)$$

$$\mathbf{P}^{-1} = \sqrt{\frac{2}{3}} \begin{bmatrix} \frac{1}{\sqrt{2}} & \cos \vartheta & \sin \vartheta \\ \frac{1}{\sqrt{2}} \cos\left(\vartheta - \frac{2\pi}{3}\right) & \sin\left(\vartheta - \frac{2\pi}{3}\right) \\ \frac{1}{\sqrt{2}} \cos\left(\vartheta + \frac{2\pi}{3}\right) & \sin\left(\vartheta + \frac{2\pi}{3}\right) \end{bmatrix} \quad (5)$$

Coefficient  $\sqrt{\frac{2}{3}}$  is chosen such that  $\mathbf{P}^{-1} = \mathbf{P}'$  which means Park's transformation is orthogonal.

#### 4. VOLTAGE EQUATIONS

Figure 1 shows rotor and stator windings of a three-phase synchronous generator. The considered synchronous generator has three stator windings ( $a$ ,  $b$ ,  $c$ ), a field winding ( $F$ ) and two fictitious windings, one in  $d$ -axis ( $D$ ) and one in  $q$ -axis ( $Q$ ) which substitute the reaction of damper windings or dampening caused by eddy currents in a cylindrical rotor. These six windings are magnetically linked, and flux linkages are a function of the rotor position.

Voltage equations for these six linked circuits can be written in a matrix form:

$$\begin{bmatrix} v_a \\ v_b \\ v_c \\ -v_F \\ -v_D=0 \\ -v_Q=0 \end{bmatrix} = \begin{bmatrix} r & 0 & 0 & & & \\ 0 & r & 0 & & & \\ 0 & 0 & r & & & \\ & & & r_F & 0 & 0 \\ \mathbf{0} & & & 0 & r_D & 0 \\ & & & 0 & 0 & r_Q \end{bmatrix} \begin{bmatrix} i_a \\ i_b \\ i_c \\ i_F \\ i_D \\ i_Q \end{bmatrix} - \begin{bmatrix} \dot{\psi}_a \\ \dot{\psi}_b \\ \dot{\psi}_c \\ \dot{\psi}_F \\ \dot{\psi}_D \\ \dot{\psi}_Q \end{bmatrix} + \begin{bmatrix} \mathbf{v}_n \\ \mathbf{0} \end{bmatrix} \quad (6)$$

where

$$\mathbf{v}_n = -r_n \begin{bmatrix} 1 & 1 & 1 \\ 1 & 1 & 1 \\ 1 & 1 & 1 \end{bmatrix} \begin{bmatrix} i_a \\ i_b \\ i_c \end{bmatrix} - L_n \begin{bmatrix} 1 & 1 & 1 \\ 1 & 1 & 1 \\ 1 & 1 & 1 \end{bmatrix} \begin{bmatrix} \dot{i}_a \\ \dot{i}_b \\ \dot{i}_c \end{bmatrix} \quad (7)$$

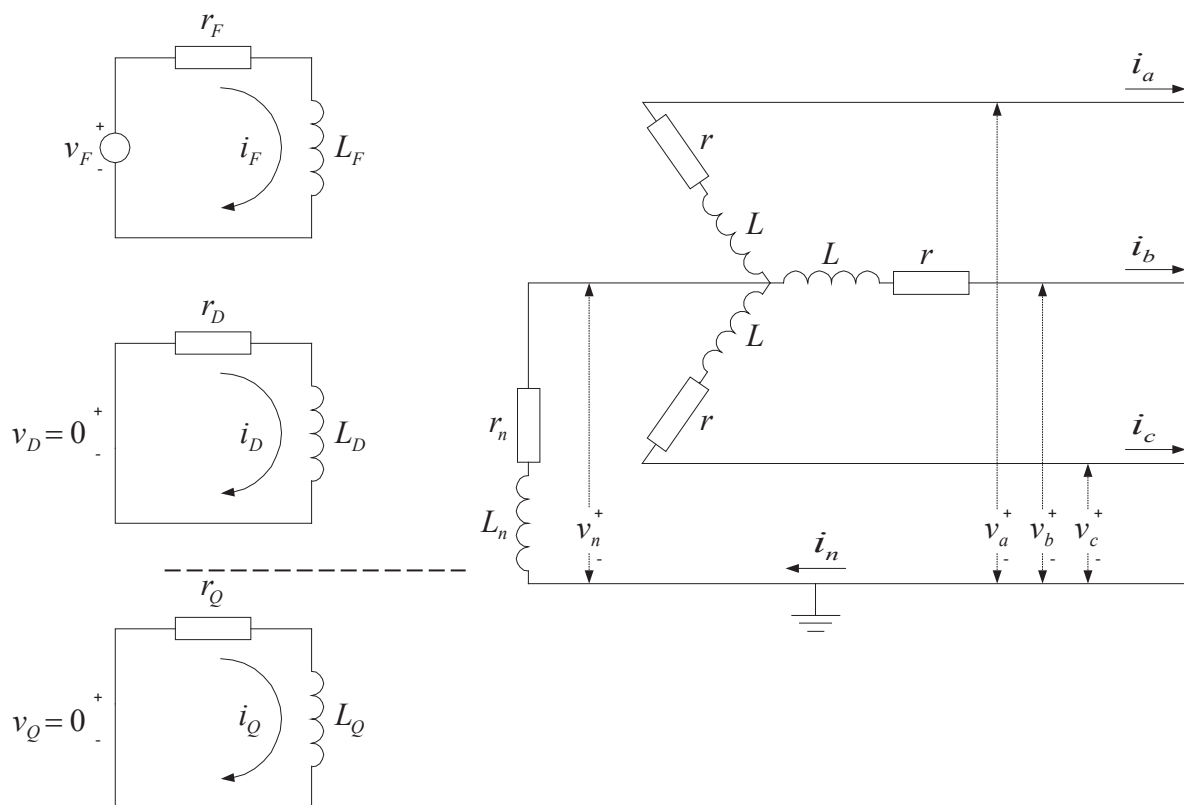


Figure 1. Synchronous generator windings

By applying Park's transformation, (6) becomes

$$\begin{bmatrix} v_0 \\ v_d \\ v_q \\ -v_F \\ 0 \\ 0 \end{bmatrix} = - \begin{bmatrix} r & 0 & 0 & | & 0 & 0 & 0 \\ 0 & r & 0 & | & 0 & 0 & 0 \\ 0 & 0 & r & | & 0 & 0 & 0 \\ \hline 0 & 0 & 0 & | & r_F & 0 & 0 \\ 0 & 0 & 0 & | & 0 & r_D & 0 \\ 0 & 0 & 0 & | & 0 & 0 & r_Q \end{bmatrix} \begin{bmatrix} i_0 \\ i_d \\ i_q \\ i_F \\ i_D \\ i_Q \end{bmatrix} - \begin{bmatrix} \dot{\psi}_0 \\ \dot{\psi}_d \\ \dot{\psi}_q \\ \dot{\psi}_F \\ \dot{\psi}_D \\ \dot{\psi}_Q \end{bmatrix} + \begin{bmatrix} 0 \\ -\omega\psi_q \\ \omega\psi_d \\ 0 \\ 0 \\ 0 \end{bmatrix} \quad (8)$$

By substituting for flux linkages

$$\begin{bmatrix} \psi_0 \\ \psi_d \\ \psi_q \\ \psi_F \\ \psi_D \\ \psi_Q \end{bmatrix} = \begin{bmatrix} L_0 & 0 & 0 & | & 0 & 0 & 0 \\ 0 & L_d & 0 & | & kM_F & kM_D & 0 \\ 0 & 0 & L_q & | & 0 & 0 & kM_Q \\ \hline 0 & kM_F & 0 & | & L_F & M_R & 0 \\ 0 & kM_D & 0 & | & M_R & L_D & 0 \\ 0 & 0 & kM_Q & | & 0 & 0 & L_Q \end{bmatrix} \begin{bmatrix} i_0 \\ i_d \\ i_q \\ i_F \\ i_D \\ i_Q \end{bmatrix} \quad (9)$$

(8) becomes:

$$\begin{bmatrix} v_0 \\ v_d \\ v_q \\ -v_F \\ 0 \\ 0 \end{bmatrix} = - \begin{bmatrix} r+3r_n & 0 & 0 & | & 0 & 0 & 0 \\ 0 & r & \omega L_q & | & 0 & 0 & k\omega M_Q \\ 0 & -\omega L_d & r & | & -k\omega M_F & -k\omega M_D & 0 \\ \hline 0 & 0 & 0 & | & r_F & 0 & 0 \\ 0 & 0 & 0 & | & 0 & r_D & 0 \\ 0 & 0 & 0 & | & 0 & 0 & r_Q \end{bmatrix} \begin{bmatrix} i_0 \\ i_d \\ i_q \\ i_F \\ i_D \\ i_Q \end{bmatrix} - \begin{bmatrix} L_0+3L_n & 0 & 0 & | & 0 & 0 & 0 \\ 0 & L_d & 0 & | & kM_F & kM_D & 0 \\ 0 & 0 & L_q & | & 0 & 0 & kM_Q \\ \hline 0 & kM_F & 0 & | & L_F & M_R & 0 \\ 0 & kM_D & 0 & | & M_R & L_D & 0 \\ 0 & 0 & kM_Q & | & 0 & 0 & L_Q \end{bmatrix} \begin{bmatrix} \dot{i}_0 \\ \dot{i}_d \\ \dot{i}_q \\ \dot{i}_F \\ \dot{i}_D \\ \dot{i}_Q \end{bmatrix} \quad (10)$$

As only balanced three-phase systems are usually analysed, the zero-sequence equations are usually omitted. By row-switching in order to group  $d$ -axis variables together and  $q$ -axis variables together, voltage equations (10) become

$$\begin{bmatrix} v_d \\ -v_F \\ 0 \\ \dots \\ v_q \\ 0 \end{bmatrix} = - \begin{bmatrix} r & 0 & 0 & \omega L_q & \omega kM_Q \\ 0 & r_F & 0 & 0 & 0 \\ 0 & 0 & r_D & 0 & 0 \\ \dots & \dots & \dots & \dots & \dots \\ -\omega L_d & -\omega kM_F & -\omega kM_D & r & 0 \\ 0 & 0 & 0 & 0 & r_Q \end{bmatrix} \begin{bmatrix} i_d \\ i_F \\ i_D \\ \dots \\ i_q \\ i_Q \end{bmatrix}$$

$$- \begin{bmatrix} L_d & kM_F & kM_D & 0 & 0 \\ kM_F & L_F & M_R & 0 & 0 \\ kM_D & M_R & L_D & 0 & 0 \\ \dots & \dots & \dots & \dots & \dots \\ 0 & 0 & 0 & L_q & kM_Q \\ 0 & 0 & 0 & kM_Q & L_Q \end{bmatrix} \begin{bmatrix} \dot{i}_d \\ \dot{i}_F \\ \dot{i}_D \\ \dots \\ \dot{i}_q \\ \dot{i}_Q \end{bmatrix} \quad (11)$$

## 5. ROTOR SWING EQUATION

Rotor swing equation is usually written in the following form:

$$J \frac{d\omega_m}{dt} = M_m - M_e \quad (12)$$

where  $J$  is the moment of inertia ( $\text{kg}\cdot\text{m}^2$ ),  $\omega_m$  is the mechanical angular velocity (rad/s),  $M_m$  is the mechanical torque (Nm),  $M_e$  the electrical torque (Nm). Difference between mechanical and electrical torque is called an accelerating torque. Equation (12) can be written in terms of power instead of torque:

$$J \frac{d\omega_m}{dt} \omega_m = P_m - P_e \quad (13)$$

Electrical angular velocity is usually used instead of mechanical angular velocity. The relation between mechanical and electrical velocity is given by

$$\omega = p\omega_m \quad (14)$$

where  $p$  is the number of pole pairs. It can be shown [1] that by substituting mechanical angular velocity with electrical angular velocity and by introducing per-unit values instead of real values, (12) becomes

$$\frac{2H}{\omega_R} \frac{d\omega}{dt} = M_m - M_e \quad (15)$$

where  $H$  is an inertia constant (MWS/MVA),  $\omega_R$  is the rated electrical speed (rad/s),  $\omega$  is the electrical angular velocity (rad/s), while mechanical and electrical torque are in per-unit (p.u.). With the assumption that angular velocity  $\omega$  is approximately

constant, the accelerating power is numerically approximately equal to the accelerating torque (p.u.). Thus, the swing equation can be written as

$$\frac{2H}{\omega_R} \frac{d\omega}{dt} \cong P_m - P \quad (16)$$

Rated speed  $\omega_R$  is equal to

$$\omega_R = 2\pi f_R \quad (17)$$

where  $f_R$  is the nominal frequency (Hz), thus (16) can be written as

$$\frac{d\omega}{dt} = \frac{\pi f_R}{H} (P_m - P_e) \quad (18)$$

The generator swing equation is written in the form of (18). In the case of small disturbances the swing equation could be written as transfer function

$$\frac{\Delta\omega}{\Delta m_m - \Delta m_e} = \frac{1}{2Hs} \quad (19)$$

where  $s$  is the Laplace operator [12].

## 6. ELECTRICAL POWER AND ELECTRICAL TORQUE

Power at the three-phase synchronous generator's terminals is generally calculated as

$$P_e = v_a i_a + v_b i_b + v_c i_c = \mathbf{v}_{abc}^t \mathbf{i}_{abc} \quad (20)$$

By applying Park's transformation on currents and voltages in (20), while keeping in mind that the transformation is orthogonal, the expression for generator power expressed in terms of new voltage and current variables is given as

$$P_e = v_d i_d + v_q i_q + v_0 i_0 \quad (21)$$

As only balanced three-phase systems are usually observed, the expression (21) simplifies to

$$P_e = v_d i_d + v_q i_q \quad (22)$$

By substituting expressions for  $v_d$  and  $v_q$  from voltage equations the power equation becomes

$$P_e = (i_d \dot{\psi}_d + i_q \dot{\psi}_q) + (i_q \psi_d - i_d \psi_q) \omega - r(i_d^2 + i_q^2) \quad (23)$$

From this, by using certain assumptions, the simplified expression for an electric torque of a synchronous generators is obtained

$$M_e = i_q \psi_d - i_d \psi_q \quad (24)$$

which is usually used when modelling a synchronous machine.

## 7. EQUIVALENT CIRCUIT OF A SYNCHRONOUS GENERATOR

By expanding equation (9) for flux linkages, it can be shown that flux linkages of mutual inductances can be written as:

$$\psi_{AD} = i_d(L_d - l_d) + kM_F i_F + kM_D i_D = L_{AD}(i_d + i_F + i_D) \quad (25)$$

$$\psi_{AQ} = i_q(L_q - l_q) + kM_Q i_Q = L_{AQ}(i_q + i_Q) \quad (26)$$

where  $L_{AD}$  and  $L_{AQ}$  are magnetizing inductances of windings in d and q axes.

$$L_{AD} \cong L_D - l_D = L_F - l_F = L_d - l_d = kM_F = kM_D = M_R \quad (27)$$

$$L_{AQ} \cong L_Q - l_Q = L_q - l_q = kM_Q \quad (28)$$

Expressions (25) and (26) for flux linkages of mutual inductances can be represented by current injection in the magnetizing branch, Figure 2. In order to obtain a complete equivalent circuit, it is necessary to consider voltage equations. From (8), for  $d$ -axis windings, the following expressions are obtained:

$$v_d = -r i_d - l \dot{i}_d - L_{AD}(\dot{i}_d + \dot{i}_F + \dot{i}_D) - \omega \psi_q \quad (29)$$

$$-v_F = -r_F i_F - l_F \dot{i}_F - L_{AD}(\dot{i}_d + \dot{i}_F + \dot{i}_D) \quad (30)$$

$$v_D = -r_D i_D - l_D \dot{i}_D - L_{AD}(\dot{i}_d + \dot{i}_F + \dot{i}_D) = 0 \quad (31)$$

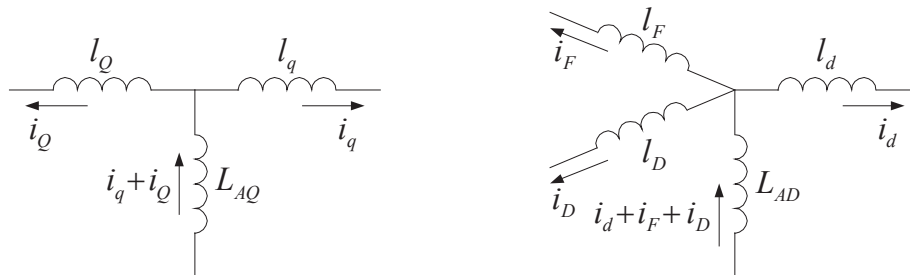


Figure 2. Flux linkages inductances of a synchronous generator

These voltage equations are represented by an equivalent circuit shown in Figure 3. The three circuits ( $d$ ,  $F$  and  $D$ ) in the  $d$ -axis are connected by the mutual inductance  $L_{AD}$  through which a sum of currents  $i_d$ ,  $i_F$  and  $i_D$  is flowing. A voltage source  $\omega \psi_q$  is included in the  $d$ -axis stator winding circuit.

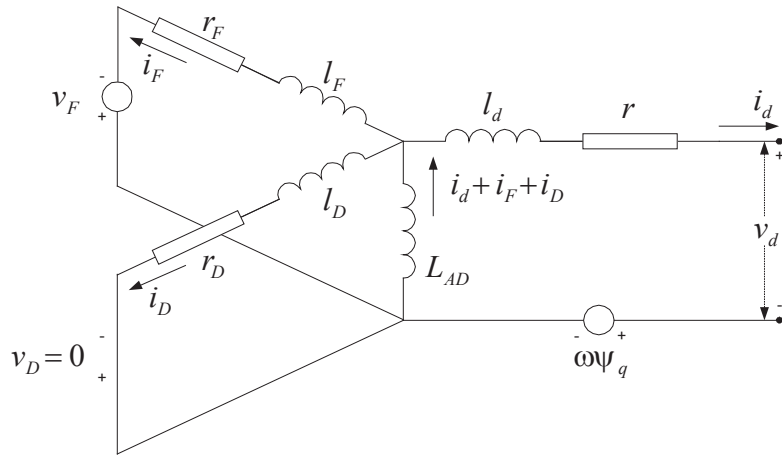


Figure 3. Equivalent circuit of  $d$ -axis

Voltage equations for  $q$ -axis windings are as follows:

$$v_q = -r i_q - l \dot{i}_q - L_{AQ}(\dot{i}_q + \dot{i}_Q) + \omega \psi_d \quad (32)$$

$$v_Q = -r_Q i_Q - l_Q \dot{i}_Q - L_{AQ}(\dot{i}_q + \dot{i}_Q) = 0 \quad (33)$$

and from these equations, the equivalent circuit of  $q$ -axis is constructed shown in Figure 4. Just like in  $d$ -axis, the sum of currents also flows through the magnetizing branch and a voltage source  $\omega \psi_d$  exists in the  $q$ -axis winding circuit.

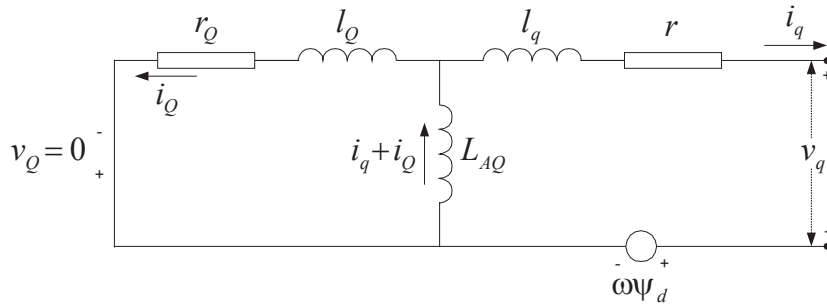


Figure 4. Equivalent circuit of  $q$ -axis

## 8. FLUX LINKAGES STATE SPACE MODEL OF A GENERATOR

It can be shown that the following relations between currents and flux linkages result from (9):

$d$ -axis:

$$i_d = \frac{1}{l_d}(\psi_d - \psi_{AD}) \quad (34)$$

$$i_F = \frac{1}{l_F} (\psi_F - \psi_{AD}) \quad (35)$$

$$i_D = \frac{1}{l_D} (\psi_D - \psi_{AD}) \quad (36)$$

where

$$\psi_{AD} = \frac{L_{MD}}{l_d} \psi_d + \frac{L_{MD}}{l_F} \psi_F + \frac{L_{MD}}{l_D} \psi_D \quad (37)$$

with equivalent  $d$ -axis inductance defined as:

$$\frac{1}{L_{MD}} = \frac{1}{L_{AD}} + \frac{1}{l_d} + \frac{1}{l_F} + \frac{1}{l_D} \quad (38)$$

$q$ -axis:

$$i_q = \frac{1}{l_d} (\psi_q - \psi_{AQ}) \quad (39)$$

$$i_Q = \frac{1}{l_Q} (\psi_Q - \psi_{AQ}) \quad (40)$$

where

$$\psi_{AQ} = \frac{L_{MQ}}{l_q} \psi_q + \frac{L_{MQ}}{l_Q} \psi_Q \quad (41)$$

with equivalent  $q$ -axis inductance defined as

$$\frac{1}{L_{MQ}} = \frac{1}{L_{AQ}} + \frac{1}{l_q} + \frac{1}{l_Q} \quad (42)$$

The expressions for flux linkages result from voltage equations (6):

$d$ -axis:

$$\dot{\psi}_d = -\frac{r}{l_d} \psi_d + \frac{r}{l_d} \psi_{AD} - \omega \psi_q - v_d \quad (43)$$

$$\dot{\psi}_F = -\frac{r_F}{l_F} \psi_F + \frac{r_F}{l_F} \psi_{AD} + v_F \quad (44)$$

$$\dot{\psi}_D = -\frac{r_D}{l_D} \psi_D + \frac{r_D}{l_D} \psi_{AD} \quad (45)$$

$q$ -axis:

$$\dot{\psi}_q = -\frac{r}{l_q}\psi_q + \frac{r}{l_q}\psi_{AQ} + \omega\psi_d - v_q \quad (46)$$

$$\dot{\psi}_Q = -\frac{r_Q}{l_Q}\psi_Q + \frac{r_Q}{l_Q}\psi_{AQ} \quad (47)$$

## 9. LOAD EQUATIONS

Equations (11), (15) and (24) represent a detailed model of a synchronous machine where the currents are state variables. With the assumption that  $v_F$  and  $M_m$  are known, the aforementioned system of equations does not completely describe the synchronous generator as long as the unknown variables  $v_d$  and  $v_q$  are not expressed in terms of state variables  $i_d$  and  $i_q$ . The prerequisite for this is known conditions at the machine's terminals, i.e. the load at the infinite bus must be taken into account as well as the value of impedance between the generator and the grid.

There are different ways to represent the load: constant impedance, constant power, constant current or any of the possible combinations of these three. For generator modelling, the load representation that will define relations between voltages, currents and angular velocity (load angle) obtained by solving the load flow is required. To simplify the generator model analysis, the rest of the electric power system is replaced by an infinite bus, thus the system influence is reduced to an impedance, and magnitude and angle of the voltage phasor at the infinite bus.

For a generator connected to an infinite bus via step-up transformer and a transmission line of equivalent resistance  $R_e$  and inductance  $L_e$ , the terminal voltage of the generator is calculated as

$$\begin{bmatrix} v_a \\ v_b \\ v_c \end{bmatrix} = \begin{bmatrix} v_{\infty a} \\ v_{\infty b} \\ v_{\infty c} \end{bmatrix} + R_e \begin{bmatrix} i_a \\ i_b \\ i_c \end{bmatrix} + L_e \begin{bmatrix} \dot{i}_a \\ \dot{i}_b \\ \dot{i}_c \end{bmatrix} \quad (48)$$

The infinite bus voltage is a balanced three-phase voltage

$$\mathbf{v}_{\infty abc} = \sqrt{2} V_{\infty} \begin{bmatrix} \cos(\omega_R t + \alpha) \\ \cos(\omega_R t + \alpha - 2\pi/3) \\ \cos(\omega_R t + \alpha + 2\pi/3) \end{bmatrix} \quad (49)$$

where  $V_{\infty}$  is the RMS value of the grid voltage.

It can be shown that by using Park's transformation and (50)

$$\mathcal{G} = \omega_R t + \delta + \pi/2 \quad (50)$$

expression (49) becomes

$$\mathbf{v}_{\infty 0dq} = \mathbf{P} \mathbf{v}_{\infty abc} = \sqrt{3} V_{\infty} \begin{bmatrix} 0 \\ -\sin(\delta - \alpha) \\ \cos(\delta - \alpha) \end{bmatrix} \quad (51)$$

thus, the expression (48) in  $0dq$  system is as follows:

$$\mathbf{v}_{0dq} = V_{\infty} \sqrt{3} \begin{bmatrix} 0 \\ -\sin(\delta - \alpha) \\ \cos(\delta - \alpha) \end{bmatrix} + R_e \mathbf{i}_{0dq} + L_e \dot{\mathbf{i}}_{0dq} - \omega L_e \begin{bmatrix} 0 \\ -i_q \\ i_d \end{bmatrix} \quad (52)$$

## 10. BLOCK DIAGRAM OF A SYNCHRONOUS GENERATOR

To develop a corresponding block element based simulation model from a certain mathematical model, the mathematical model must be represented by a block diagram. Detailed nonlinear model of a synchronous generator in a block form is shown in figures 5 through 8.

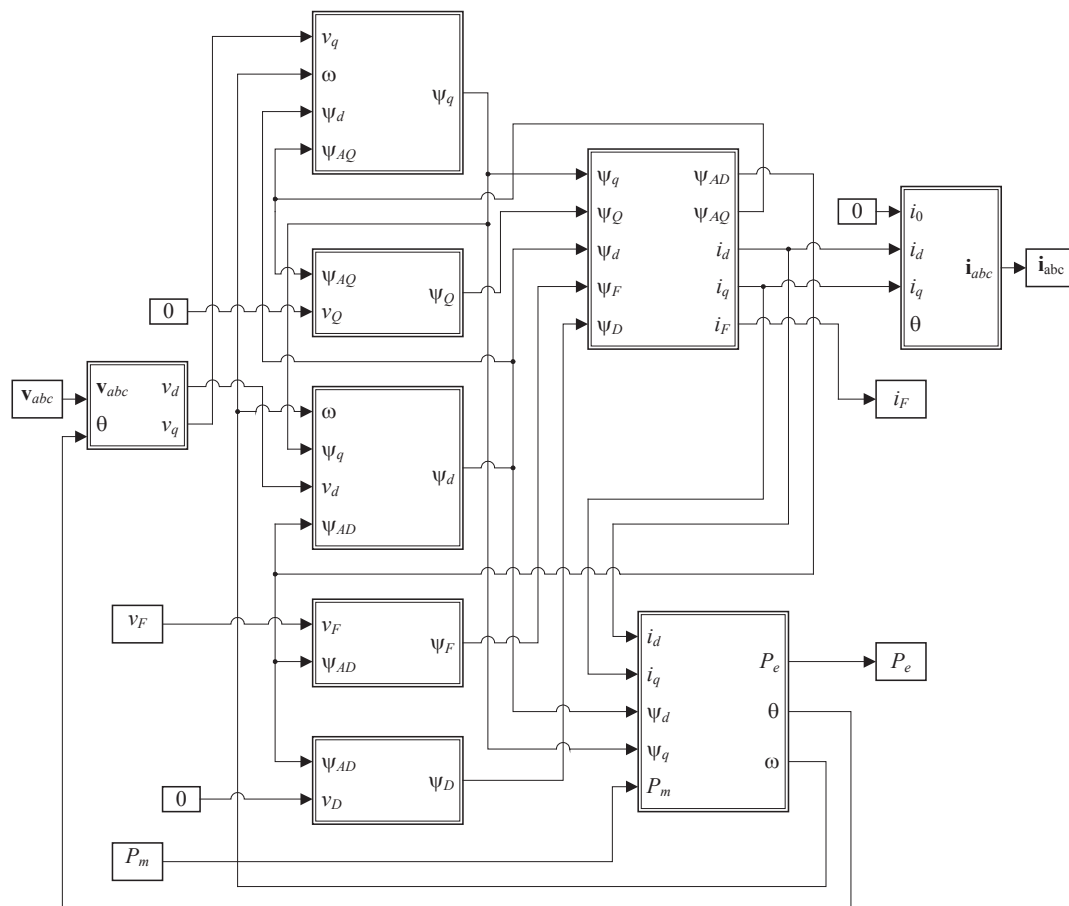


Figure 5. Complete generator system block diagram

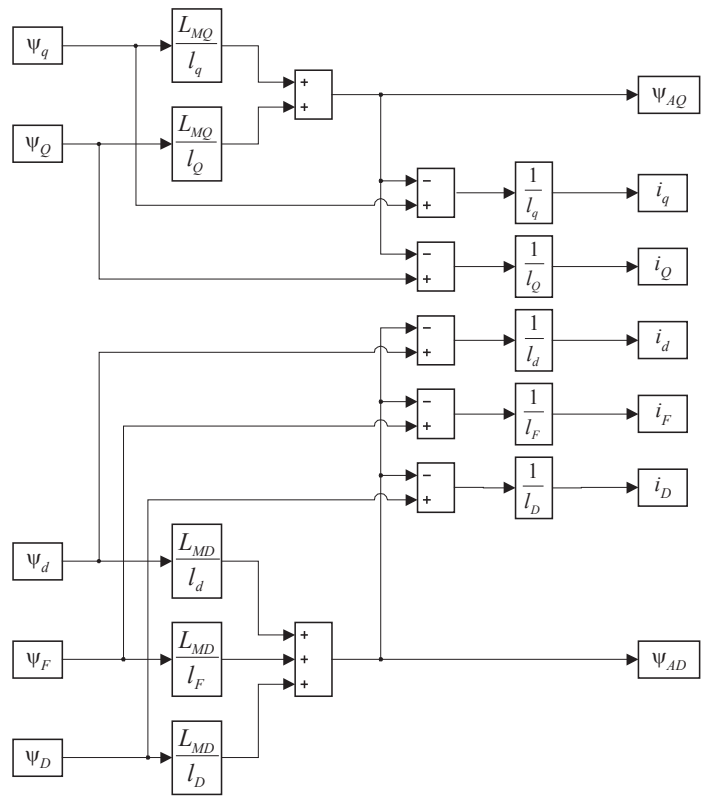


Figure 6. Calculation of currents and flux linkages of mutual inductances

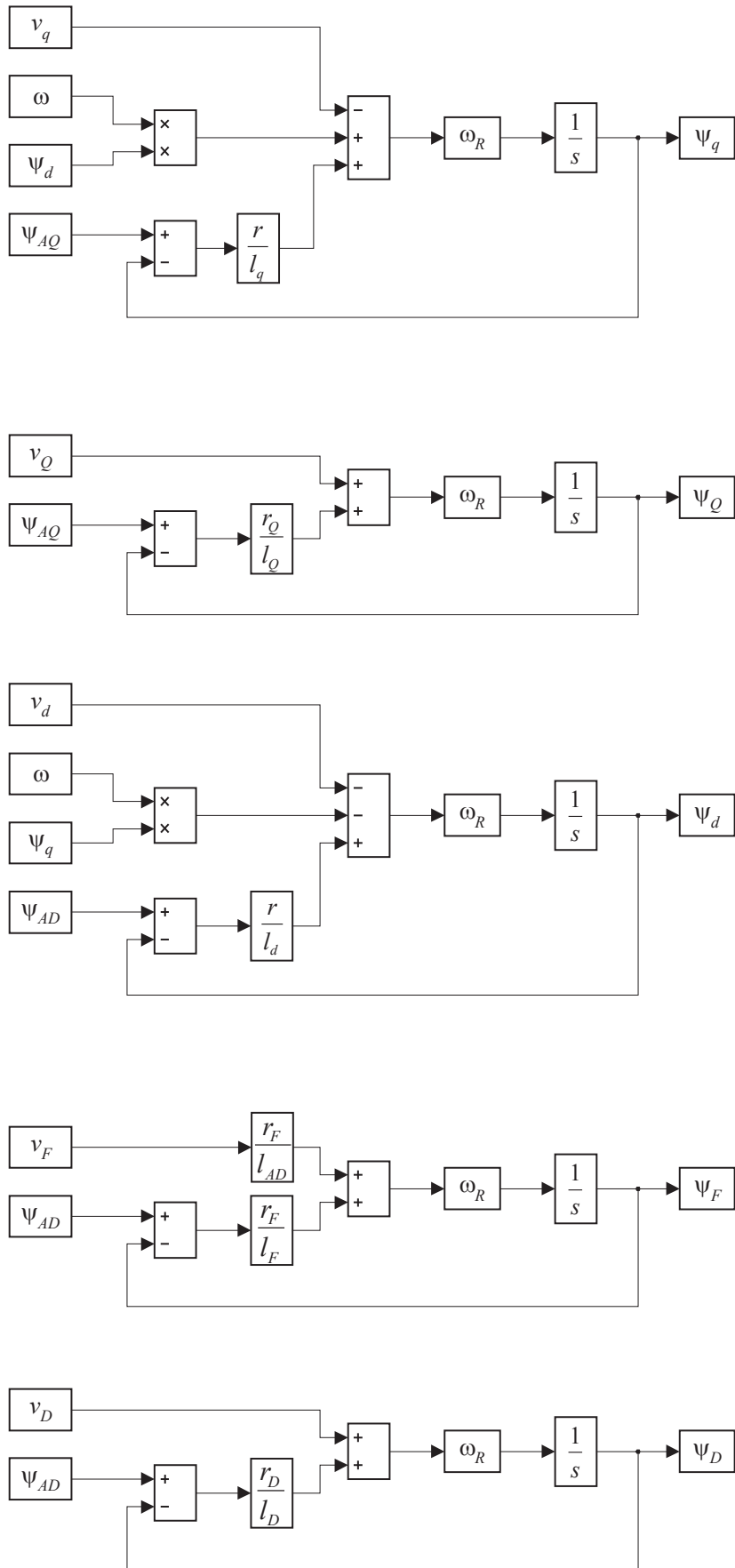


Figure 7. Calculation of flux linkages

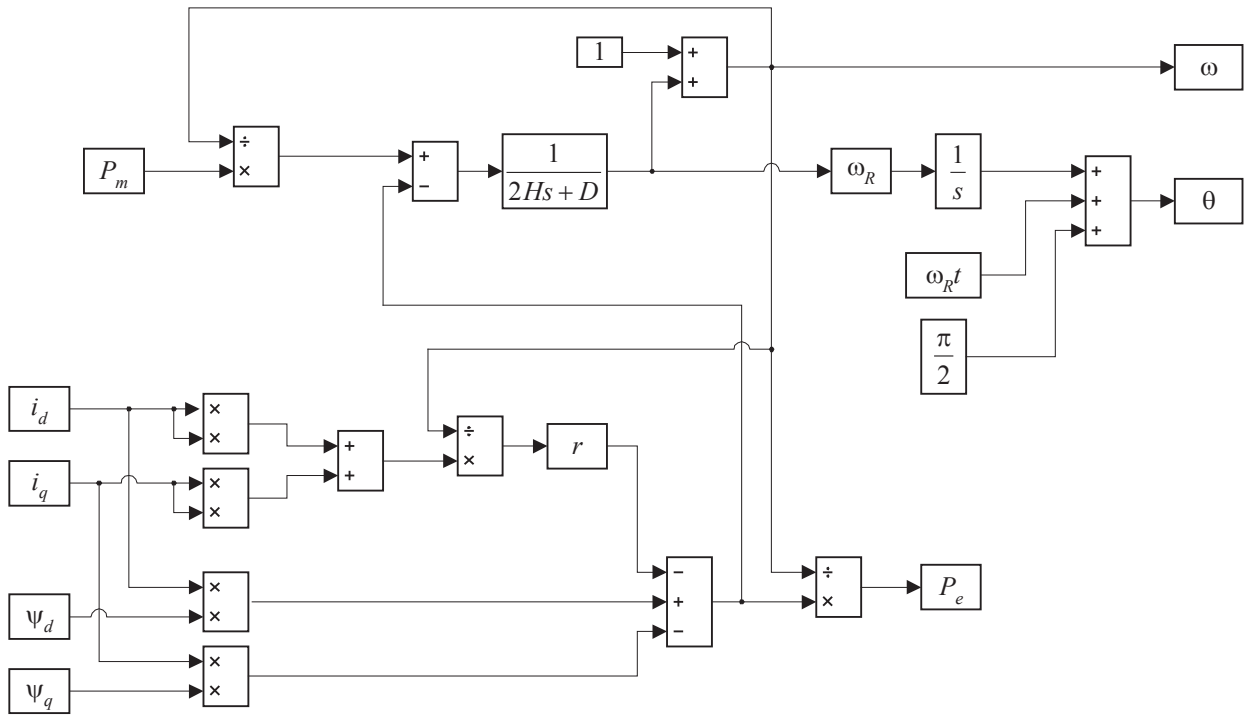


Figure 8. Mechanical part of the generator and electric power calculation

## 11. SYNCHRONOUS GENERATOR PARAMETERS

Data acquisition necessary for calculations and parameter determination is an important step in the modelling process. Sometimes, acquiring even the most basic generator and corresponding control systems data can present a huge obstacle, especially when dealing with older machines that are still in operation. Thus, generator models with standard parameters are often used, i.e. reactances and time constants identified for the equivalent circuits in the  $d$  and  $q$  axis which are given by most generator manufacturers. Standard parameters are being used for the detailed generator model presented in this paper.

## 12. Standard generator parameters

During a disturbance in the rotor circuits, certain currents are induced under the terms of which some of them diminish more quickly than the others. Thus, the following generator parameters differ:

- subtransient – determine the quickly diminishing components,
- transient – determine the slowly diminishing components,
- synchronous – determine the constant (steady) components

Standard generator parameters are reactances as seen from generator terminals associated with fundamental frequency during steady-state, transient

and subtransient states along with corresponding time constants that determine the currents and voltages falloff gradient.

Besides reactances and time constants as standard generator parameters, it is also necessary to know the inertia constant  $H$  which determines the dynamic behaviour of the turbine-generator. The value of the inertia constant (MWs/MVA) can be determined using (53)

$$H = \frac{1}{2} \frac{J \omega_m^2}{S_n} \quad (53)$$

where  $J$  is the moment of inertia of the turbine-generator ( $t \cdot m^2$ ),  $\omega_m$  the (nominal) mechanical speed of the shaft (rad/s),  $S_n$  the volt-ampere base of the turbine-generator, usually the nominal apparent power (kVA). Moment of inertia describes the influence of the total rotating mass of the turbine-generator consisting of rotating mass of the turbine and rotating mass of the generator, while the contribution of the water mass must also be considered when dealing with hydroelectric turbines.

### 13. DETERMINING THE MODEL PARAMETERS FROM STANDARD GENERATOR PARAMETERS

Calculation of rotor mutual inductances is done according to the equivalent circuits (Figure 3 for  $d$ -axis, Figure 4 for  $q$ -axis) and by utilizing (27) and (28).

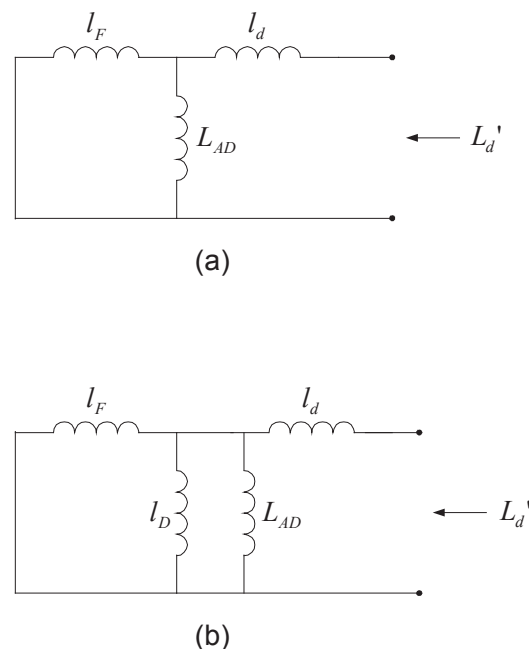


Figure 9. Equivalent circuit for  $d$ -axis inductance: (a) transient, (b) subtransient

$d$ -axis transient inductance according to Figure 9a is given by

$$L_d' = l_d + \frac{L_{AD}l_F}{L_{AD} + l_F} \quad (54)$$

from which the field winding leakage inductance can be expressed as

$$l_F = L_{AD} \frac{L_d' - l_d}{L_d - L_d'} \quad (55)$$

Similarly, according to Figure 9b,  $d$ -axis subtransient inductance is given by

$$L_d'' = l_d + \frac{1}{1/L_{AD} + 1/l_D + 1/l_F} \quad (56)$$

from which the  $d$ -axis damper winding leakage inductance can be expressed as

$$l_D = L_{AD}l_F \frac{L_d'' - l_d}{L_{AD}l_F - L_F(L_d'' - l_d)} \quad (57)$$

Finally,  $d$ -axis damper windings inductance and field winding inductance are given by

$$L_D = L_{AD} + l_D \quad (58)$$

$$L_F = L_{AD} + l_F \quad (59)$$

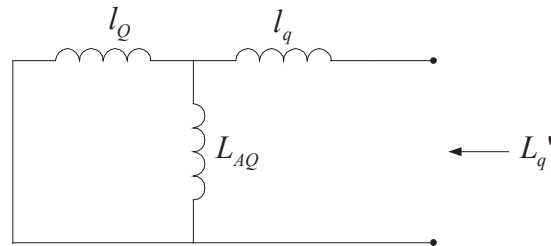


Figure 10. Equivalent circuit for  $q$ -axis subtransient inductance

Analogously for the  $q$ -axis, from Figure 10 follows:

$$L_q'' = l_q + \frac{L_{AQ}l_Q}{L_{AQ} + l_Q} \quad (60)$$

From which the  $q$ -axis damper winding leakage inductance is expressed as

$$l_Q = L_{AQ} \frac{L_q'' - l_q}{L_q - L_q''} \quad (61)$$

and then the  $q$ -axis damper winding inductance is given by

$$L_Q = L_{AQ} + l_Q \quad (62)$$

It can be shown that the field winding resistance and the damper windings resistance can be determined from aforementioned reactances by using the following expressions:

$$r_F = \frac{l_F + L_{AD}}{\omega_R T_{d0}'} \quad (63)$$

$$r_D = \frac{l_D + L_d' - l_q}{\omega_R T_{d0}''} \quad (64)$$

$$r_Q = \frac{l_Q + L_{AQ}}{\omega_R T_{q0}''} \quad (65)$$

where the time constants are in (s).

Time constants of short-circuited windings are given by

$$T_d'' = T_{d0}'' \frac{L_d''}{L_d'} \quad (66)$$

$$T_d' = T_{d0}' \frac{L_d'}{L_d} \quad (67)$$

$$T_q'' = T_{q0}'' \frac{L_q''}{L_q} \quad (68)$$

where subscript 0 denotes open circuit time constants.

## 14. SYNCHRONOUS GENERATOR PARAMETERS

Synchronous generator model described in chapter 2 represents a system of time dependent differential equations. In steady-state, differential equations disappear because all magnitudes are constant. Stability analysis of some system generally begins from a steady state of that system. Then, a disturbance is applied and dynamic behavior is then observed.

Phasor diagrams are usually used to display steady-state relations as shown in Figure 11. Figure 11 displays the phasor diagram for the developed generator model connected to an infinite bus through impedance  $R_e + jX_e$ .

Steady state can be defined in multiple ways. The most common way is defined by conditions at the generator terminals—voltage, active and reactive power. In this case, the power factor is calculated as

$$\cos \varphi = \frac{P}{\sqrt{P^2 + Q^2}} \quad (69)$$

where  $P$  and  $Q$  are initial active and reactive power, respectively.

To calculate  $d$ -axis and  $q$ -axis components of currents and voltages of the generator and of the grid voltage, angles  $\delta$ ,  $\beta$  and  $\varphi$  (see Figure 11) have to be known.  $\delta$  and  $\beta$  are determined from the phasor diagram and  $\varphi$  is determined from the power factor.

First, generator current is calculated:

$$I = \frac{P}{V \cos \varphi} \quad (70)$$

Then, active and reactive component of generator current are calculated:

$$I_r = I \cos \varphi \quad I_x = -I \sin \varphi \quad (71)$$

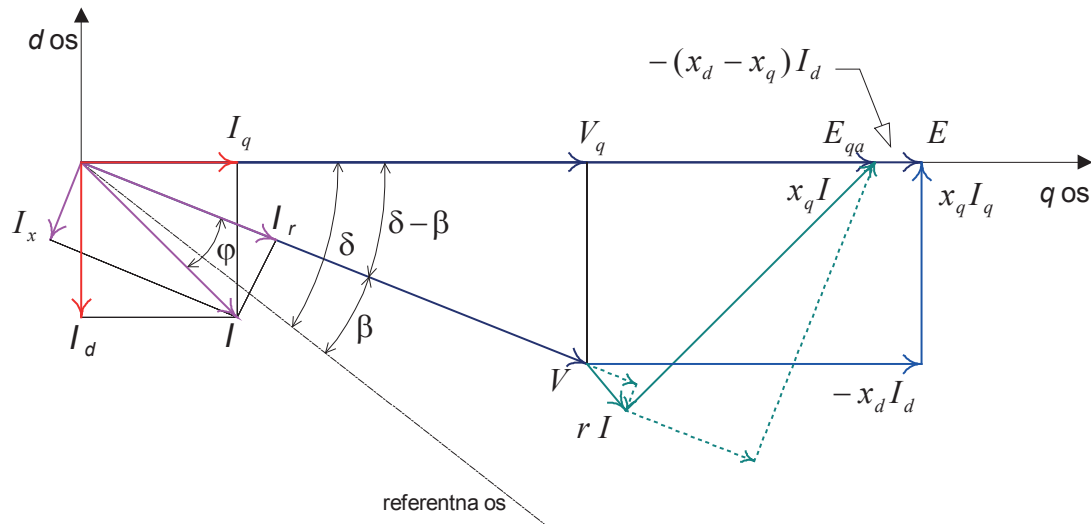


Figure 11. Generator phasor diagram

Angle between  $q$ -axis and terminal voltage vector is calculated by

$$\delta - \beta = \arctan \frac{x_q I_r + r I_x}{V + r I_r - x_q I_x} \quad (72)$$

$d$ -axis and  $q$ -axis components of generator currents and terminal voltage:

$$I_d = -I \sin(\delta - \beta + \varphi) \quad I_q = I \cos(\delta - \beta + \varphi) \quad (73)$$

$$V_d = -V \sin(\delta - \beta) \quad V_q = V \cos(\delta - \beta) \quad (74)$$

Induced EMF and excitation current:

$$E = V_q + rI_q - x_d I_d \quad (75)$$

$$I_F = \frac{E}{L_{AD}} \quad (76)$$

Flux linkages:

$$\psi_d = L_d I_d + L_{AD} I_F \quad (77)$$

$$\psi_F = L_{AD} I_d + L_F I_F \quad (78)$$

$$\psi_D = (I_d + I_F) L_{AD} \quad (79)$$

$$\psi_q = L_q I_q \quad (80)$$

$$\psi_Q = L_{AQ} I_q \quad (81)$$

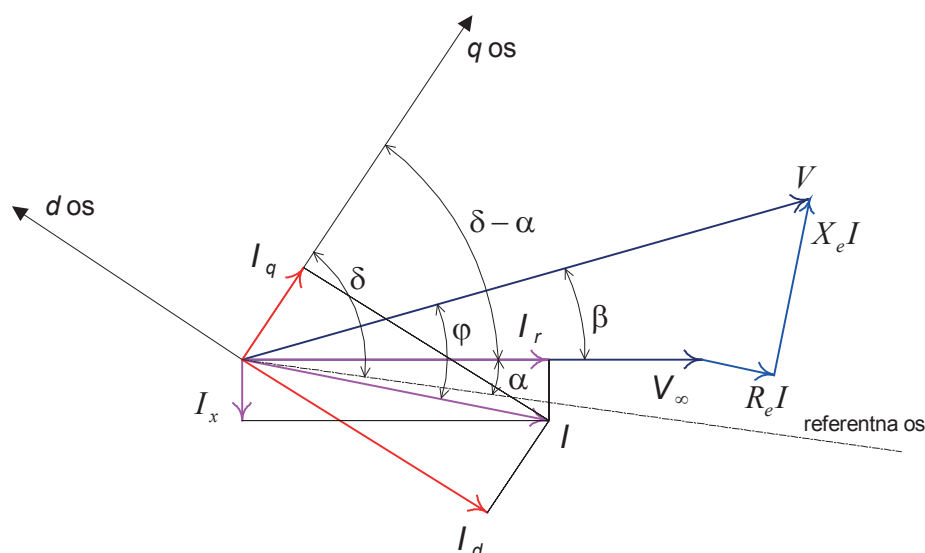


Figure 12. Phasor diagram of generator terminal voltage and grid voltage

Grid voltage vector equation:

$$\bar{V}_\infty = \bar{V} - \bar{Z}_e \bar{I} \quad (82)$$

According to Figure 12, (82) can be expressed as follows:

$$V_\infty \angle (\alpha - \beta) = V - Z_e I (\cos(-\varphi) + j \sin(-\varphi)) \quad (83)$$

From (83), grid voltage  $V_\infty$  and angle difference  $\alpha - \beta$  can be determined. Load angle (angle between grid voltage vector and  $q$ -axis) is determined from:

$$\delta - \alpha = (\delta - \beta) - (\alpha - \beta) \quad (84)$$

## 15. SIMULATION RESULTS

Time-domain simulations have been conducted using the synchronous generator model developed in this paper. Parameters from a real hydroelectric power unit in HPP Dubrava (42 MVA) are used in the simulations. Parameters are shown in Table I.

Table I: Generator parameters of HPP Dubrava

$d$ -axis synchronous reactance	$x_d$ (p.u.)	1.346
$q$ -axis synchronous reactance	$x_q$ (p.u.)	0.940
$d$ -axis transient reactance	$x_{d'}$ (p.u.)	0.446
$d$ -axis subtransient reactance	$x_{d''}$ (p.u.)	0.330
$q$ -axis subtransient reactance	$x_{q''}$ (p.u.)	0.370
Stator leakage reactance	$x_l$ (p.u.)	0.243
$d$ -axis open-circuit transient time constant	$T_{d0'}$ (s)	1.660
$d$ -axis open-circuit subtransient time constant	$T_{d0''}$ (s)	0.118
$q$ -axis open-circuit subtransient time constant	$T_{q0''}$ (s)	0.035
Stator resistance	$r$ (p.u.)	0.006
Inertia constant	$H$ (s)	1.2

Three-phase short-circuit fault at the infinite bus has been simulated as a typical example for different initial conditions.

Current and voltages responses in figure 13 are simulation results for following initial conditions:

generator active power  $P = 0,75$  (p.u.)

generator reactive power  $Q = 0,25$  (p.u.)

generator terminal voltage  $V = 1$  (p.u.) .

Simulations have been also made for different fault durations.

Figure 14 show load angle responses for fault durations of 0.1 s and for fault durations equal to and larger than critical clearing time which is 0.165 s for given scenario.

Model is verified comparing simulated and measured values. Responses of HPP Dubrava generator A on three-phase short circuit in the neighbouring grid (HPP Varaždin) are shown in Figure 15. Simulated and measured responses agree

very well, and small differences are probably caused by model parameters which could be calibrated.

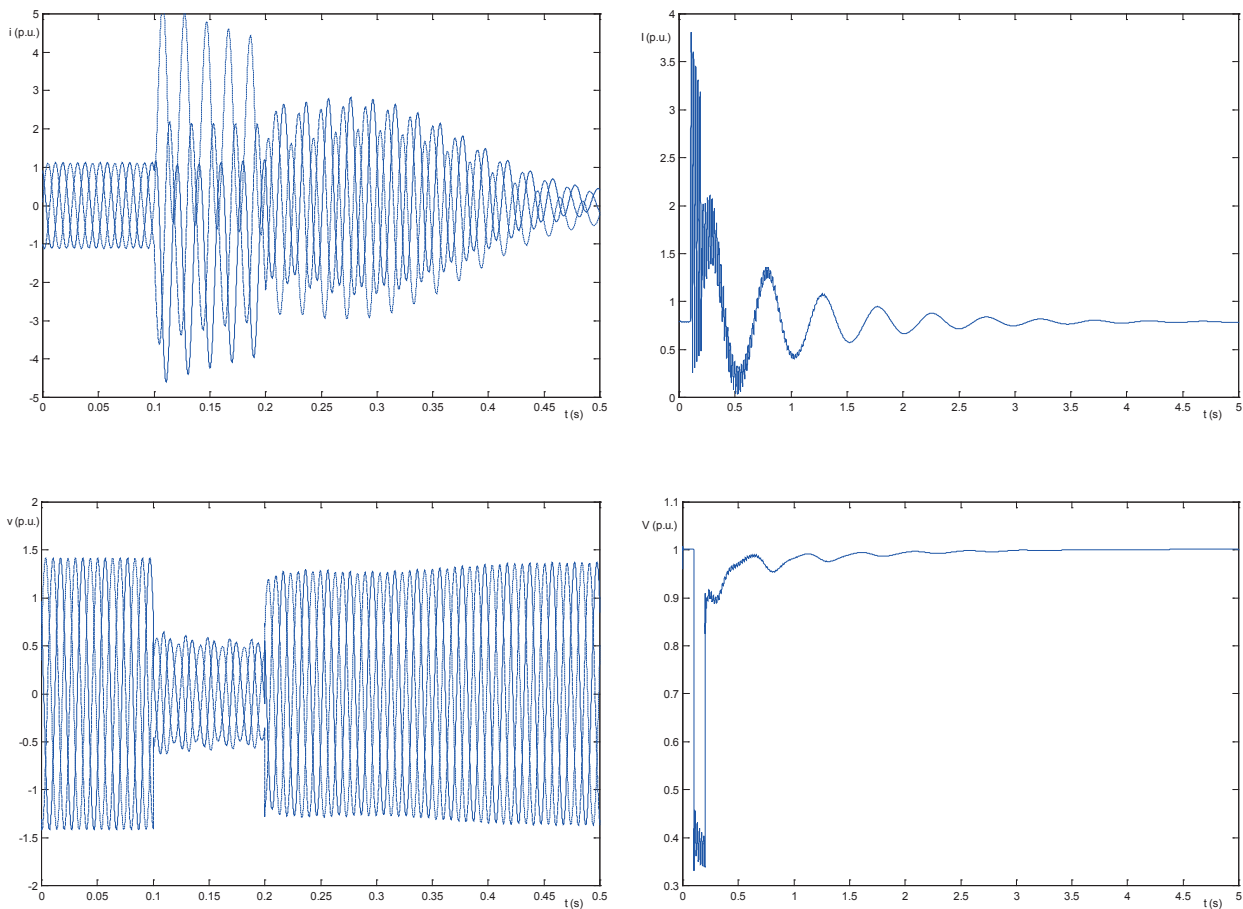


Figure 13. Simulated results – currents and voltages responses (the short-circuit is applied at 0.1 s and removed at 0.2 s)

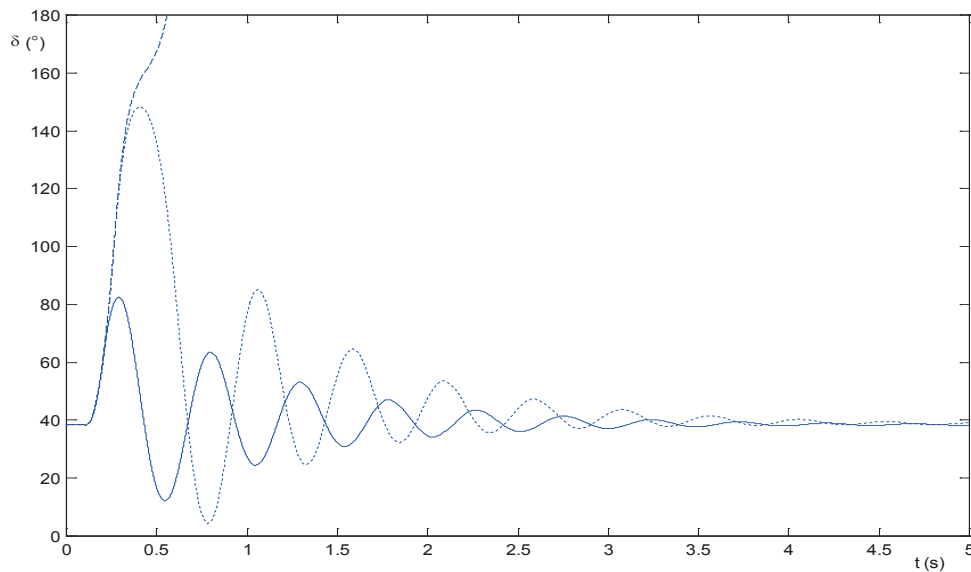


Figure 14. Load angle response for different fault duration (0.1, 0.165 and 0.17 s)

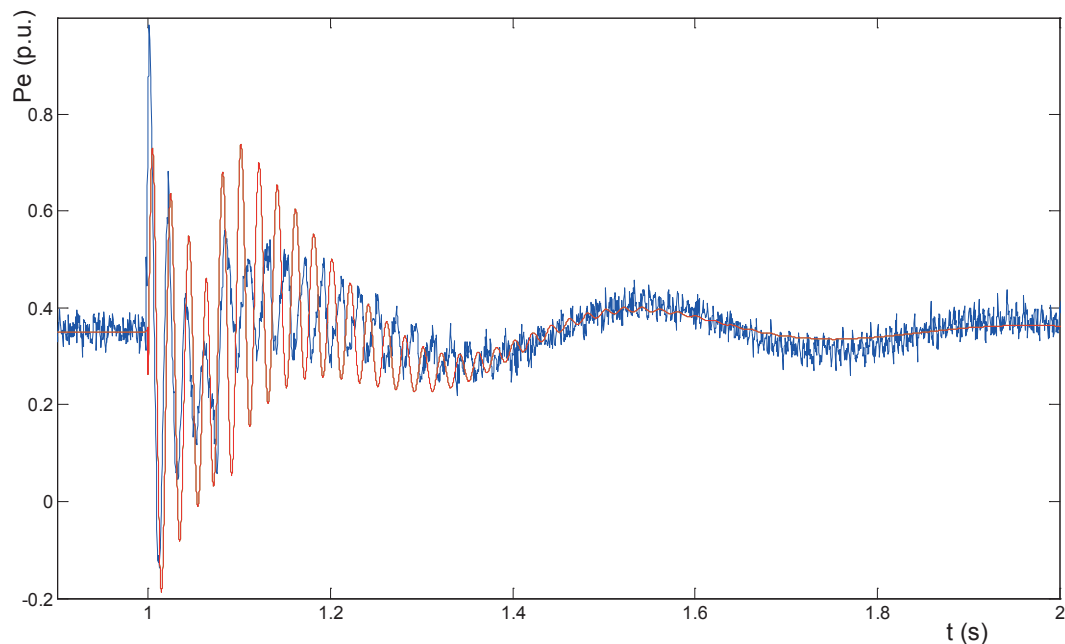


Figure 15. Simulated and measured responses comparison (the short-circuit is applied at 1 s and removed at 1.1 s)

## 16. CONCLUSION

Thanks to the modern digital simulation systems even the most complex mathematical models can be translated into adequate simulation models. Therefore, high-order models that provide the highest degree of accuracy (with respect to the existing theory) are used more and more for power system elements modelling instead of low-order simplified models for simulating power system operation. The presented mathematical and simulation model of a synchronous generator allows the analysis of all electrical and mechanical units during faults and in different time scales. As an example, in this paper, the generator response to a three-phase short-circuit fault at the infinite bus (most commonly used type of short-circuit fault in stability analysis) have been shown. With minor adjustments, other types of faults can be simulated as well. The change of initial conditions and parameters is simple so different responses can be simulated and compared in order to analyze the impact of different initial conditions and parameters on the dynamic response of a generator. The block diagram model can be easily integrated with other models (foremost, the excitation and voltage control system and turbine with turbine governor systems).

Because of very high accuracy, the described model is used in Power System Laboratory at the Department of Energy and Power Systems, Faculty of Electrical Engineering and Computing, University of Zagreb to compare computer simulations with recorded dynamics of the generator after some switching operations [13].

## 17. ACKNOWLEDGEMENT

This work was supported by the Croatian Science Foundation under project "FENISG – Flexible Energy Nodes In Low Carbon Smart Grid" (grant no. IP-2013-11-7766).

## 18. NOMENCLATURE

$E$	internal EMF induced by excitation current
$f_R$	nominal frequency (Hz)
$H$	inertia constant (s)
$i_a i_b i_c$	generator armature current - phases $a, b, c$
$i_0 i_d i_q$	generator current - $0, d, q$ system
$i_F i_D i_Q$	field winding current, $d$ and $q$ axis damper winding current
$I$	generator RMS current
$I_r I_x$	active and reactive component of generator current
$I_d I_q$	$d$ and $q$ axis generator current
$I_F$	excitation current
$J$	moment of inertia ( $\text{kg}\cdot\text{m}^2$ )
$k$	mutual inductance coefficient
$L_0 L_d L_q$	stator winding inductance - $0, d, q$ system
$L_F L_D L_Q$	field winding inductance, $d$ and $q$ axis damper winding inductance
$L_n$	generator neutral point grounding inductance
$L_d' L_q'$	$d$ and $q$ axis transient inductance
$L_q''$	$q$ -axis subtransient inductance
$l_d l_q$	stator winding leakage inductance – $d, q$ components
$l_F l_D l_Q$	field winding leakage inductance, $d$ and $q$ axis damper winding leakage inductance
$L_{AD} L_{AQ}$	$d$ and $q$ axis winding magnetizing inductance
$L_{MD} L_{MQ}$	$d$ and $q$ axis equivalent inductances
$L_e$	equivalent inductance between the generator and the infinite bus
$M_F M_D M_Q$	armature winding and field winding mutual inductance, $d$ and $q$ axis damper winding mutual inductance
$M_R$	field winding and $d$ -axis damper circuit mutual inductance

$M_e$	electrical torque
$M_m$	mechanical torque
$p$	number of pole pairs
$P_e$	electrical power
$P_m$	mechanical power
$P$	(initial) generator active power
$Q$	(initial) generator reactive power
$r$	armature winding resistance
$r_F r_D r_Q$	field winding resistance, $d$ and $q$ axis damper winding resistance
$r_n$	generator neutral point grounding resistance
$R_e$	equivalent resistance between the generator and the infinite bus
$S_n$	generator nominal apparent power (kVA)
$t$	time (s)
$T_{d0}' T_{q0}'$	$d$ and $q$ axis open-circuit transient time constant (s)
$T_{d0}''$	$d$ -axis open-circuit subtransient time constant (s)
$T_d' T_q'$	$d$ and $q$ axis short-circuit transient time constant (s)
$T_d''$	$d$ -axis short-circuit subtransient time constant (s)
$v_a v_b v_c$	generator terminal voltage - phases $a, b, c$
$v_0 v_d v_q$	generator terminal voltage – 0, $d, q$ system
$v_F v_D v_Q$	field winding voltage, $d$ and $q$ axis damper winding voltage
$v_n$	generator neutral point voltage
$v_{\infty a} v_{\infty b} v_{\infty c}$	infinite bus voltage - phases $a, b, c$
$V_{\infty}$	infinite bus RMS voltage
$V$	generator RMS voltage
$V_d V_q$	$d$ and $q$ axis generator voltage
$x_d x_q$	$d$ and $q$ axis synchronous reactance
$X_e$	equivalent reactance between the generator and the infinite bus
$Z_e$	equivalent impedance between the generator and the infinite bus
$\alpha$	infinite bus voltage phase shift (rad)
$\beta$	infinite bus voltage and generator voltage phase shift (rad)
$\delta$	$q$ -axis phase shift with respect to the reference axis; load angle (rad)
$\varphi$	Phase shift between generator voltage and generator current (rad)
$\psi_a \psi_b \psi_c$	stator winding flux linkages - phases $a, b, c$

$\psi_0$ $\psi_d$ $\psi_q$	stator winding flux linkages - 0, $d$ , $q$ system
$\psi_F$ $\psi_D$ $\psi_Q$	field winding flux linkage, $d$ and $q$ axis damper winding flux linkage
$\psi_{AD}$ $\psi_{AQ}$	$d$ and $q$ axis mutual inductance flux linkages
$\mathcal{G}$	instantaneous generator voltage angle (rad)
$\omega$	angular frequency (rad/s)
$\omega_m$	mechanical angular frequency (rad/s)
$\omega_R$	nominal (synchronous) angular frequency (rad/s)

All magnitudes for which no units have been specified are expressed in per-unit unless specified otherwise in the text.

## 19. REFERENCES

- [1] J. Machowski, J.W. Bialek and J.R. Bumby, Power system dynamics: stability and control, John Wiley & Sons, 2008.
- [2] P.M. Anderson, A.A. Fouad, Power System Control and Stability, IEEE Press, 1993.
- [3] P.M. Anderson, Analysis of Faulted Power Systems, IEEE Power Systems Engineering Series, 1995.
- [4] Z. Sirotić, Z. Maljković, Sinkroni strojevi, Element, Zagreb, 1996.
- [5] F.P. DeMello, C. Concordia, Concepts of Synchronous Machine Stability as Affected by Excitation Control, IEEE Transactions on Power Apparatus and Systems, Vol. PAS-88, No. 4, April 1969, pp. 316-329
- [6] P. Kundur, Power System Stability and Control, McGraw-Hill, 1995
- [7] M. Brezovec, B. Brkljac, I. Kuzle, Influence of Operating Conditions on Hydrounit Power Oscillations, IEEE EuroCon 2013, Zagreb, Croatia, 1-4 July, 2013, pp. 1453-1459
- [8] IEEE Committee Report, Current Usage and Suggested Practices in Power System Stability Simulations for Synchronous Machines, IEEE Transactions on Energy Conversion, Vol. 1, No. 1, March 1986, pp. 77-93
- [9] S. Babić, Utjecaj načina modeliranja generatora na rezultate proračuna prijelazne stabilnosti elektroenergetskog sistema, Energija, No. 5, 1991, pp. 155-164
- [10] C.C. Young, Equipment and System Modeling for Large-scale Stability Studies, IEEE Transactions on Power Apparatus and Systems, Vol. PAS-91, No. 3, 1972, pp. 99-109

- [11] I. Kamwa, Experience with Computer-Aided Graphical Analysis of Sudden-Short-Circuit Oscillograms of Large Synchronous Machines, IEEE Transactions on Energy Conversion, Vol. 10, No. 3, September 1995, pp. 407-414
- [12] M. Brezovec, I. Kuzle and T. Tomiša, Nonlinear Digital Simulation Model of Hydroelectric Power Unit With Kaplan Turbine, IEEE Transactions on Energy Conversion, Vol. 21, No. 1, March 2006, pp. 235-241
- [13] I. Kuzle, J. Havelka, H. Pandžić and T. Capuder, Hands-On Laboratory Course for Future Power System Experts, IEEE Transactions on Power Systems, Vol. 29, No. 4, July 2014, pp. 1963-1971

**JOSIP KAJIĆ, HRVOJE PIRIĆ, FILIP RENDULIĆ, MARIN CERJAN**

[josip.kajic@hep.hr](mailto:josip.kajic@hep.hr), [hrvoje.piric@hep.hr](mailto:hrvoje.piric@hep.hr), [filip.rendulic@hep.hr](mailto:filip.rendulic@hep.hr),  
[marin.cerjan@hep.hr](mailto:marin.cerjan@hep.hr)

**HEP Trade Ltd, Ulica Grada Vukovara 37, 10 000 Zagreb**

**MARKO DELIMAR**

[marko.delimar@fer.hr](mailto:marko.delimar@fer.hr)

**University of Zagreb, Faculty of Electrical Engineering and Computing**

## SUMMARY

This paper presents electricity power generation capacities in South East Europe (SEE). Due to a high share of hydro power generation, hydrology has a major influence on energy balance and power markets in SEE. Power markets are facing the impact of a rising number of renewable energy generation facilities. This paper describes influences of energy availability on power markets and energy generation within three hydrological scenarios (dry, normal and wet scenario). Short-term electricity prices are analyzed in terms of production and consumption on three major power exchanges in Romania, Hungary and Slovenia. Findings demonstrate influences of weather conditions on power markets in SEE through energy production, security of supply and risks facing power producers.

**Key words:** hydro power generation, SEE power market, hydrological scenarios

## 1. INTRODUCTION

Power system planning sector has always been a great challenge due to the complexity of the power system and its most important characteristics; simultaneity of production and consumption. Considering the time horizon, there are three types of planning: long-term, medium-term and short-term planning. There is no explicit definition of the time interval for each of the planning type. In general, long-term planning deals with strategic guidelines of the county energy policy. Medium-term planning defines guidelines of the energy policy in the near future up to 5 years which are needed to provide finances for the implementation of projects and changes in the electricity market. Short-term planning refers to time horizon up to a month. Generally, short-term planning determines the future demand for electricity and plans how to secure it, taking into account criteria of safety and feasibility.

Load forecasting is the oldest problem in the power sector, very popular in professional and scientific community. Nowadays, load forecasting methods and models ensure the forecast error below 3% [2]. The second part of the planning process relates to production planning and purchase or sale of electricity. The costs of production are made of fixed and variable costs. Fixed costs are related to financing and operation of power plants while the variable costs are related to the cost of fuel. Share of fixed and variable costs for various types of power plants are shown in Figure 1.

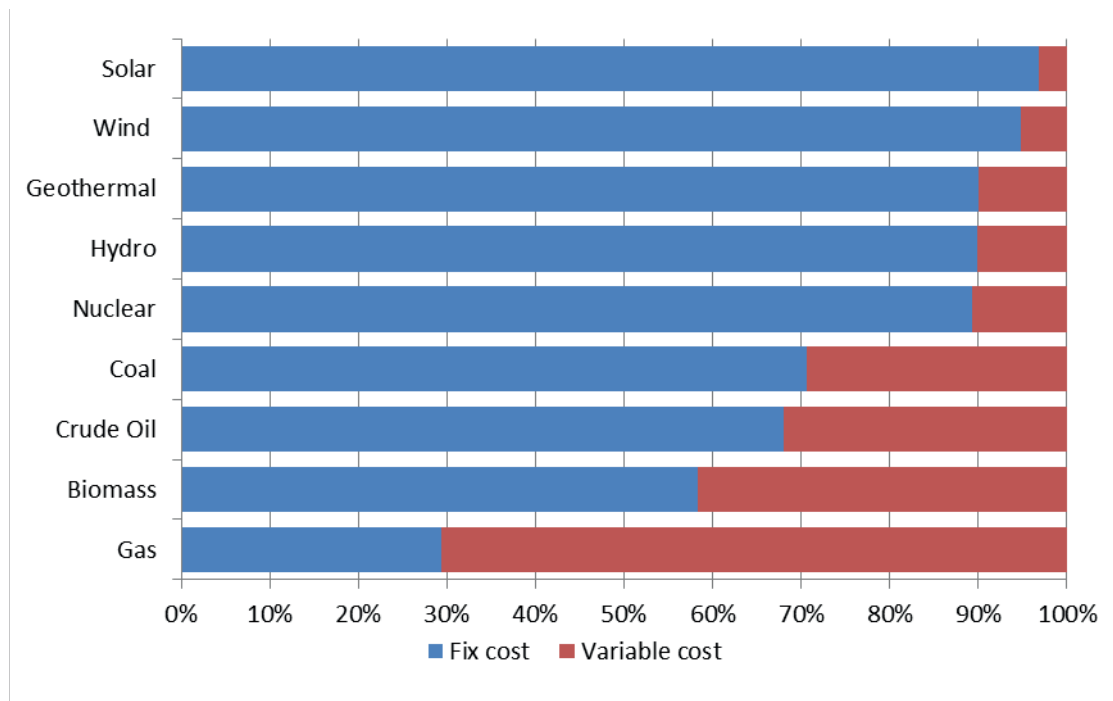


Figure 1. Share of fixed and variable costs in electricity production by technology

Optimization of the production portfolio for energy companies needs to meet several criteria: maximum safety, availability and profitability. Criteria refer to the security of supply for electricity consumers, maximum availability of production facilities and maximizing revenue in market conditions. Disregarding the rules can lead to adverse social and economic consequences that may cause serious economic damage. The production is planned according to the so-called merit order list (MOL). It represents the distribution of power plants by variable cost for production of an additional MWh. Example of MOL is shown in Figure 2.

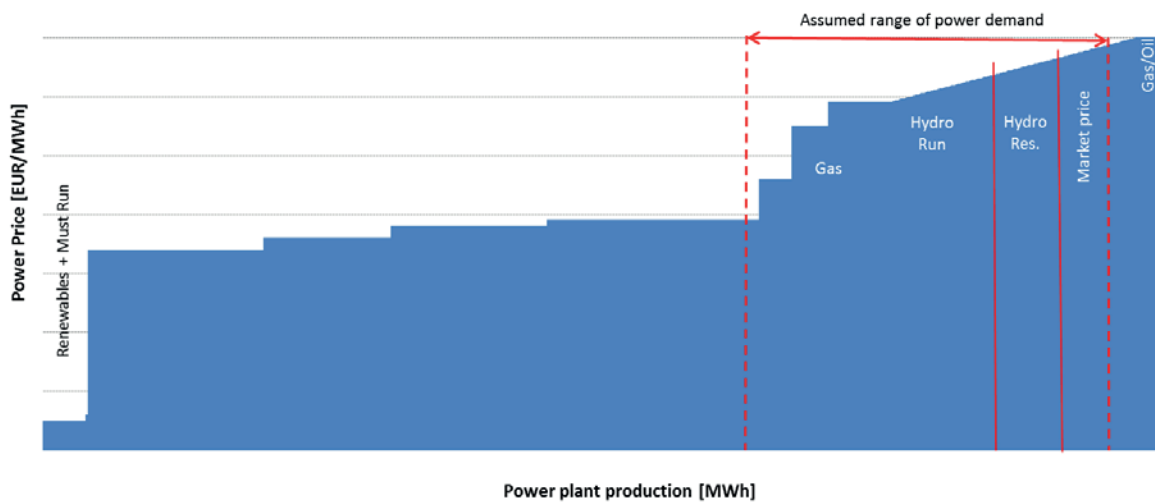


Figure 2. Merit order list for a power system

For power plants on the MOL, the general rule is that the electricity should be imported if the market price is lower than the production cost of additional MWh. It is used for economic optimization of the power plant schedule (considering the above mentioned criteria). Another problem is how to valorize production for hydro power plants (HPP). There are two categories, run-of-river and storage HPP. Run-of-river power plants must produce energy depending on water inflows due to inability to store water. The value of this energy can be evaluated by the current market price. Unlike run-of-river power plants, storage HPP can produce energy at the time of arrival of water inflows and sell it at the current market price or store water in reservoirs and produce energy at another point in time when the market price is estimated to be higher. One way of valorizing the price of energy produced from HPP is presented in paper [1].

However, all criteria in portfolio management don't have equal importance; there are parts of production that are not included in the economic criterion. Those parts are called must run units (MR). They include power plants that must remain in operation for the safety reasons. Power plants (that generate electricity for maintaining the stability of the transmission network) or a combined heat and power plant (CCGT) (which supplies a large population with heat while producing electricity as a derivative throughout the cycle) are included in the MR. Run-of-river HPPs can be added in MR since their exclusion from the production process can

lead to unwanted overflow. Renewable energy sources (RES) are also MR because they belong to protected category of environmentally acceptable energy production and have an advantage over other energy sources.

Liberalization and restructuring of the electricity market introduced additional variables to production planning. Competition has brought in new opportunities in the power sector in terms of flexibility and possibilities for a more efficient planning, introducing increasingly complex market mechanisms such as cross-border capacities trading as well as volatile production from renewable energy sources. The primary focus of this paper will be the management of electricity produced in different market scenarios. The analysis will be performed on the data for South Eastern Europe (SEE), characterized by a large share of HPP with seasonal production characteristics. The actual data will show cases of extreme market deviations accompanied by descriptions of the conditions under which they occur. The first two chapters describe the power characteristics of the SEE. Afterwards, different hydrological scenarios will be analysed as well as their impact on price movements in power markets. Analysis will show the risks that occur in the SEE power sector.

## 2. ENERGY CHARACTERISTICS OF SEE REGION

The SEE Region consists of the following countries: Slovenia, Hungary, Croatia, Bosnia and Herzegovina, Serbia, Bulgaria, Romania, Macedonia, Albania, Montenegro, Kosovo and Greece. Some of those, formed by a disintegration of larger countries, have power systems developed for energy needs of their former countries. Today, these countries are independent facing the consequences of their historical development. GDP per capita ranges from 3.800 USD to 24.500 USD. GDP has fallen compared to 2011 for all countries in the region [9]. Development of new projects in those countries has been further reduced by the economic crisis as well as the socio-economic situation and the economic decline, which caused a further reduction in foreign investment due to financial instability and indebtedness. The economic structure of the countries in the region is shown in Figure 3. There is equal ratio between high, medium and low developed countries.

Figure 4 shows the monthly load dynamics in the region during the 2012 and the average daily load. Total load of the region in a year amounted to about 227 TWh [12]. Annual load ranges from 1,9 TWh in Montenegro to 53,8 TWh in Romania. Load value is highest in winter, a little lower in summer and lowest in spring and autumn. Changes in load during the year depend on weather conditions, temperature and the length of day. During the last decade, summer consumption increased, which can be explained by low prices of cooling systems, and partly by tourism, as some countries have sea access. The exceptionality of the load in 2012 was in February. Extremely low temperatures have resulted in a deviation from normal load values, i.e. in load reduction compared to January. The impact of such "anomaly" will be analyzed in detail in later chapters.

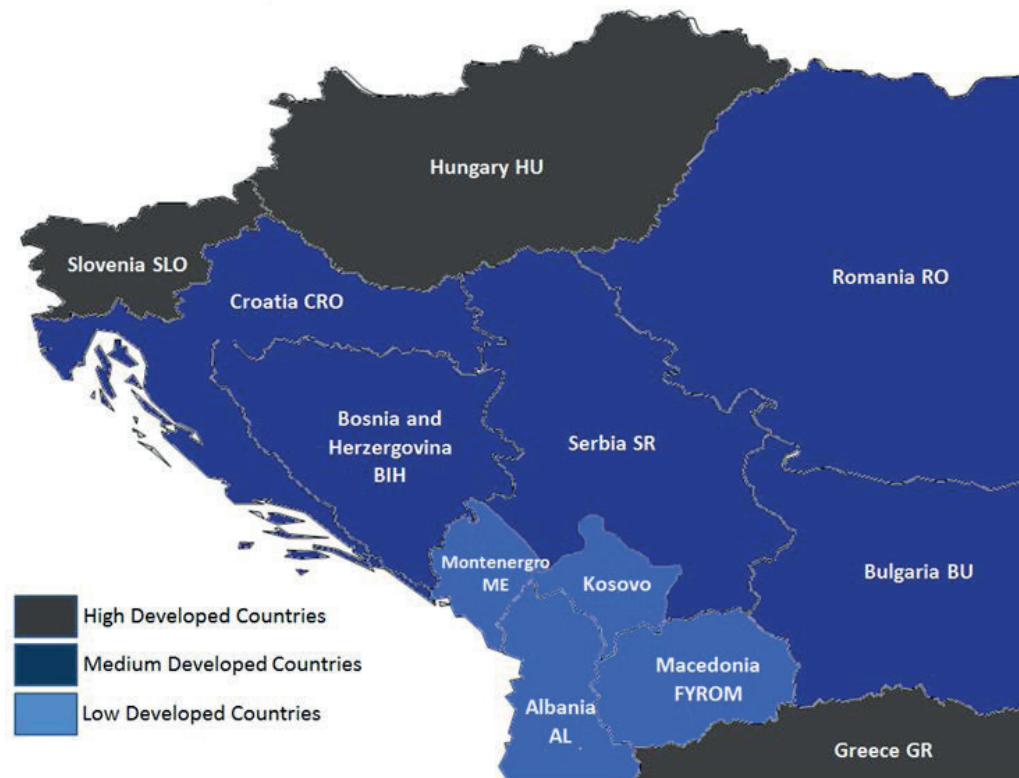


Figure 3. Economic characteristics of the countries in the SEE region

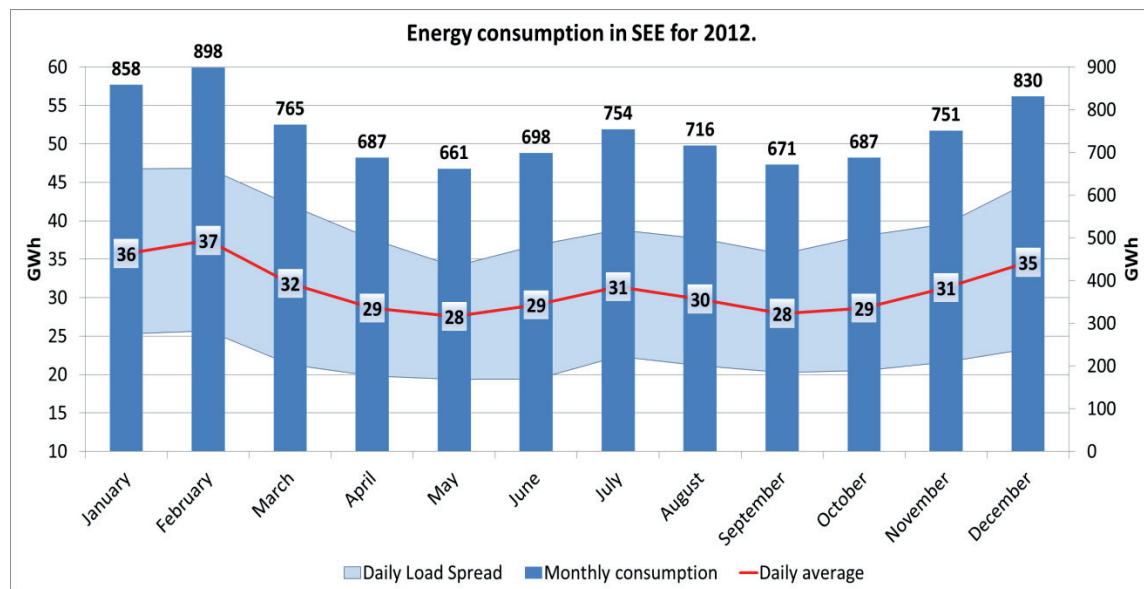


Figure 4. Load dynamics in the SEE region - 2012

Maximum hourly demand of 47 GWh/h in the region in 2012 was on February 2nd (19th hour). Minimum hourly load of 19 GWh/h was recorded on May 1st (6th hour). Those are the days with maximum (984 GWh) and minimum (571 GWh) regional daily loads in the year. During the winter, the peak load is usually achieved earlier (19th hour), and in the summer, the peak load occurs during later hours (22th hour) because of a longer day.

The average load curve is the mean hourly value of load in the 2012. Table 1 shows the minimum and maximum values of the average load curve by countries.

Table I. Load parameters in SEE for 2012.

Load (MWh/h)	RO	GRE	SER	HU	BUG	CRO	BIH	SLO	MK	MNE
Min daily load	5.122	4.490	3.415	3.406	3.382	1.377	1.043	1.061	751	339
Max daily load	6.865	6.906	5.279	4.881	4.881	2.315	1.652	1.579	1.100	516
Ration max/min	134%	154%	155%	143%	144%	168%	158%	149%	146%	152%

Also, the percentage difference is shown between the maximum and minimum load value (percentage describes load growth during the day compared to the night). Smaller increase is desirable, because high differences between a nightly minimum and a daily maximum can cause problems for the power system management. For example, in Croatia, for a nightly load of 1.300 MWh/h, it's necessary to have an additional average production of 1.000 MWh/h, of which a large part of power plants would have to work only a few hours a day. This kind of load curve would be covered by import. Romania is in the most favourable situation since it does not need to activate a lot of peak power plants and is in a better position to plan the power system production.

Table II. Share of installed power capacity in SEE for 2012.

Country	HPP (%)	NPP (%)	TPP (%)	RES (%)	Sum (MW)
Romania	33%	7%	49%	11%	17.750
Greece	22%	0%	66%	12%	16.499
Bulgaria	23%	16%	52%	9%	12.167
Hungary	1%	23%	71%	5%	8.775
Serbia	35%	0%	65%	0%	8.179
Croatia	48%	8%	39%	5%	4.267
BiH	52%	0%	48%	0%	3.700
Slovenia	46%	9%	43%	2%	3.656
Albania	91%	0%	6%	3%	1.570
Macedonia	41%	0%	57%	2%	1.409
Montenegro	75%	0%	24%	1%	882
SEE	30%	8%	55%	7%	78.855

Table 2 shows the installed power capacity (according to data collected from all available sources: power system operators, market operators, owners of power plants) in the region. Total installed capacity is 78,86 GW, of which a share of nuclear power plants (NPP) is 8%, thermal power plants (TPP) 55%, hydro power plants (HPP) 30%, with annually more installed capacities that use renewable energy sources (RES) which 2012 had a share of 7%. The highest share of renewable energy sources is installed in Greece (12%), the smallest in Serbia and BIH. NPP plants are installed in 5 of the 11 countries. Variety of installed power sources is essential for any power system. Albania is a country that is almost entirely dependent on the hydrological situation and has 91% of its installed capacities in HPP, Montenegro 75% and around 50% in Croatia, BIH and Slovenia. These countries are hydro dependent and in case of dry periods they have to import electricity. TPP share is the largest in Hungary, 71% of total installed capacity, 66% in Greece and 65% in Serbia while about 50% TPP is used in BIH, Bulgaria, Romania and Macedonia.

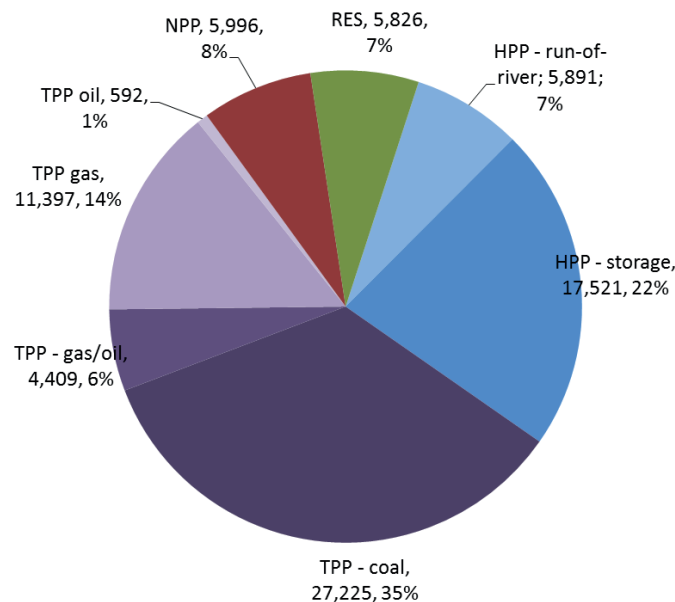


Figure 5. Installed production capacities in the SEE region 2012

From installed TPP, 62% are coal-fired, 26% gas-fired while the other TPPs use crude oil (older TPPs) and TPP that are either gas or oil-fired (can run on both fuels and are older and usually less effective). Coal can be declared as the most important energy source, because coal-fired TPPs amount to 35% of the total installed capacity in the region. Of installed HPPs, a quarter of them are run-of-river, while others are HPPs with storage.

Engaging the production of electricity from a specific source depends on its technical and financial characteristics. NPPs and coal-fired TPPs have low variable costs and thus are technically designed as baseload power plants. Gas-fired TPPs have higher variable costs, but due to their flexibility and fast start-up time they are used for the regulation of power a system. RES are the most variable sources of electricity because they depend entirely on the weather. HPPs, whose share of

installed capacity is approximately 30%, also depend on the weather, but because of the seasonality of hydrological phenomena their production can be stochastically predicted and in that way are maneuverable. Given the large share of HPPs and RES in the region, it can be concluded that the region is exposed to a high risk of extreme weather conditions (drought/extremely high precipitation level).

When the country cannot produce sufficient electricity to meet demand, it is necessary to import it. Usually, electricity is traded bilaterally or through power exchanges. Trading may be a few hours up to several years in advance. Countries that can't meet the demand by their own production usually conclude an annual contract. Any surplus or shortage of energy is traded on daily, weekly or monthly bases. With development of the electricity market in the region, the amount of energy traded on power exchanges is constantly growing and bilateral trade is decreasing. There are three power exchanges in the SEE region: OPCOM (Romania), Southpool (Slovenia) and HUPX (Hungary). Volume traded on OPCOM in 2012 averaged to 1.120 MWh/h (total: 10,7 TWh), on Southpool 500 MWh/h (total: 4,4 TWh) and on HUPX 720 MWh/h (total: 7,2 TWh). In summary, traded volumes on power exchanges represent 10% of the total load in the region. At the end of 2012 HUPX expanded (by Hungary) in Slovakia and the Czech Republic ("Market coupling"), leading to an increase in trading volume, which at the beginning of 2013 amounted to more than 1.000 MWh/h. By developing power exchanges, a further increase in trading volume is expected. Earlier, the SP connected to the Italian market resulting in the increase of the trading volume above 720 MWh/h. Before market coupling, trading volume on Southpool and HUPX was lower by 50%. Increased market liquidity resulted in more market participants turning to power exchanges since volatility of electricity prices is lower with increase in traded volumes.

For importing or exporting electricity into and out of the country it is necessary to ensure cross-border transfer capacity (CBTC). It is common for transmission system operators to have auctions for allocating CBTC on yearly, monthly and daily basis. Capacity auctions are called explicit auctions. As noted, power exchanges don't have to be related to a particular country and, in market coupling CBTC is already included in the price of electricity (implicit auction). Lately, auction platforms have been joining at explicit auctions. One example is the CAO ("Central Allocation Office") – currently organizes CBTC auctions for Slovenia, Hungary and Croatia (among many other countries in Europe). It is expected that in the future the CAO (or similar platforms) will organize auctions for even more countries instead of all operators independently running auctions. This allows a simpler and a more transparent trading. The main entrances to the region are borders of Austria with Hungary and Slovenia. These borders are particularly interesting since trade volumes range between 25.000 – 35.000 MWh/h on the German power exchange EEX, and the situation on that power exchange affects the prices on the power exchanges in the SEE region.

### 3. ELECTRICITY PRODUCTION IN SEE REGION

Energy position of the SEE region over the last five years is shown in Figure 6, which endorses the aforementioned quantitative risk associated with the HPP production. In overall, 2012 was an extreme year, which means that it alternated periods of extreme drought and above-average precipitation as well as periods of extreme temperatures.

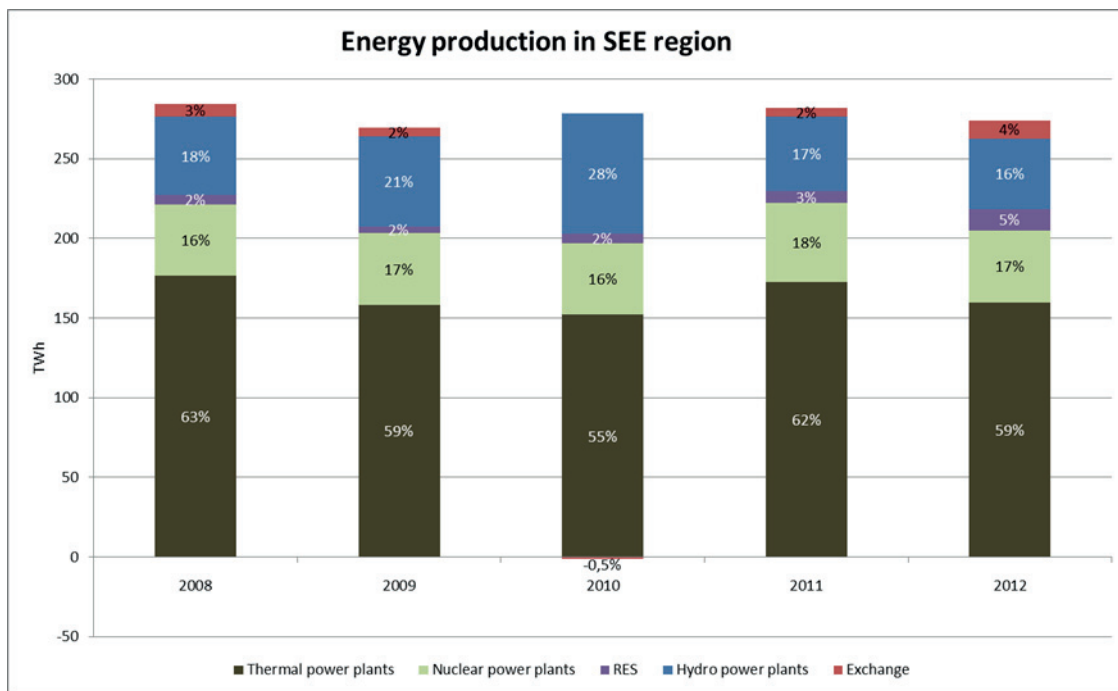


Figure 6. Production in the SEE region 2008 to 2012.

HPP production had significant variations (lowest production in the last 5 years was recorded in 2012). On the other hand, 2010 was a record year for HPP production and the region exported electricity. That year was followed by the unfavorable hydrological period (2011) which extended early 2012. For comparison, the production of HPPs in 2012 was up to 4 TWh lower on a monthly basis than the production in 2010. As a result, the increase in imports occurred in the region at a total of 5% (the largest volume of imports in the last 5 years).

HPP production in the region in the first quarter of 2012 was the lowest for that period in the last 15 years [10]. Although hydrologically just a little weaker than the 2011, another unfavorable circumstance was an unusual cold in early 2012 (February 2012 temperatures were below  $-25^{\circ}\text{C}$ ). This period recorded a high production of TPPs, which on a monthly basis amounted to 16 TWh, representing about 63% of a total share in covering the load diagram. In February, production of storage HPPs increased due to an increase in market prices. Because the import is

limited by CBTC, all available sources of electricity were used to cover an extremely high load. Some countries in the region were forced to put their TPPs with lower efficiency into operation, in order to cover their electricity needs. Adding import to that amount, it turns out that 69% of the load curve was covered with TPP production and imports.

The HPP production covered only 16% of the total load. Throughout the spring, run-of-river HPPs increased their production, but because of the maintenance of TPPs and NPPs, imports continued to cover a large part of the load in the whole region. After extremely cold winter and poor hydrology, came a period of extreme heat (temperatures over 40°C). During this period, the HPP production is low and countries again turn to import and production from expensive TPPs, which together reached 64% of the total load. As the year went by, the hydrological conditions improved and the total load was lower than previous years. The region was able to recover and even achieve above-average HPP production (last 5 years). Increased hydrology caused a decline in imports, especially in November. Last quarter was marked by the highest production from RES, primarily from wind power plants (30% of annual production).

Production by sources (GWh) for the region in 2012 is given in Table 3. Share of coal TPPs reached 45%. Other TPPs have participated with 13%, NPPs with 17% and HPPs with 16% also participated in covering the load diagram, while the RES have participated with the 5%.

Table III. Production in the SEE region by sources

TPP				HPP		RES			NPP	Exchange
159.766				44.016		11.489			45.297	11.571
Coal	Gas	Oil	Gas/oil	Storage	Run of river	Wind	Biomass	Solar		
122.617	29.955	385	6.809	22.798	21.219	8.091	1.977	1.421		
45%	11%	0%	2%	8%	8%	3%	1%	1%	17%	4%

As mentioned in the previous chapter, the share of HPPs is 30% of the total installed generating capacity in the region, which is explained by the fact that the whole region has a great hydropower potential. Large rivers combined with natural and artificial lakes make this region very suitable for the construction of HPPs. Five countries have the largest share of installed capacity in HPPs. Figure 7 shows the dependence on energy production from HPPs over the last five years and how the influence of hydrology reflects on energy import into the region. It is obvious that 2008, 2009 and 2011 were years with the average hydrology with fluctuations through various periods. Import to the region had a share from 1,9 to 3% in covering the total load of the region. To understand this dependence, it's necessary to while the total exchange was negative, which means that consider years with very wet and very dry hydrology. Production of HPP plants in the region in 2010 totalled to 75,51 TWh the region exported electricity [11]. Just two years later, production was as much as 30 TWh lower, thus automatically making countries in the region importers of electricity.

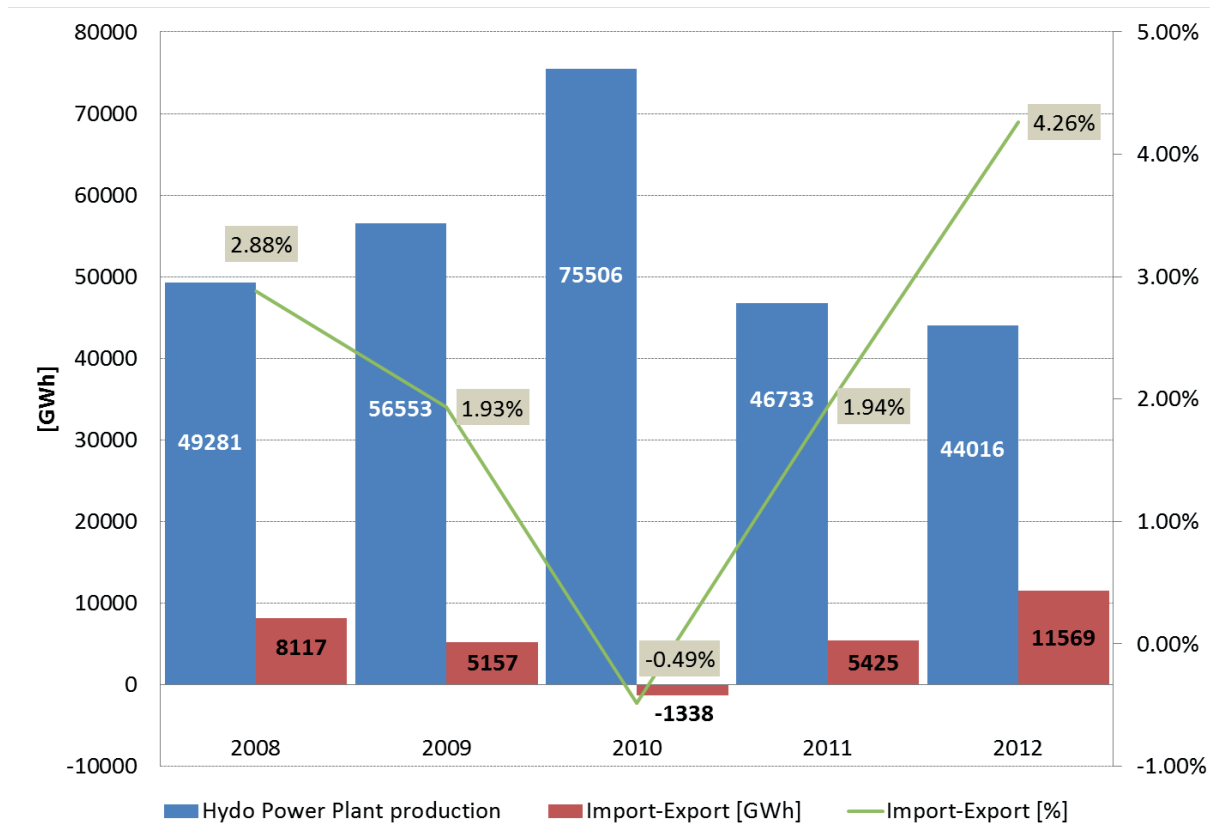


Figure 7. Dependence on hydropower production

Good hydrological conditions in 2010 had the biggest impact in Bulgaria, BIH, Romania and Albania as these countries ended the year as exporters of electricity, while Slovenia, Montenegro and Serbia were very close to becoming one. Two years later the situation in the region turned upside down. Despite the long drought through 2011 and 2012, the only countries that were net exporters at the end of year were Bulgaria and BIH. It is interesting to note that Albania, a country which production capacity is 91% in HPPs, in 2010 had a total export of 730 GWh, and a year later imported 3.167 GWh. Even Hungary, a country whose HPPs account for only 1% of total production capacity, failed to become an exporter of electricity, regardless of the 71% share in TPPs, due to problems such as the cost of fuel, maintenance, outages, load etc.

Share of import in the region's total electricity consumption in 2012 was 4,25%. This percentage averaged to about 5% in the first nine months, but as already mentioned, extreme hydrological conditions in the last quarter greatly reduced this percentage. The largest import was in February (6,3 %), and the lowest in November (1,6 %) of the total load curve.

On hourly basis, in 2012 the region imported 61,6% of the time, and exported 38,4% of the time. If we observe only the installed power, all countries except Macedonia (no data for Kosovo) had enough of their own generation capacity installed to cover peak loads in 2012. However, unavailability of generating units (failures, maintenance) and the need capacity margins in the power system must be taken

into account in production process. Serbia would need 93% of installed capacity to cover peak load, Albania 82%, Montenegro 80%, and Croatia 75% [12]. Most countries in the region were dependent on import due to unfavorable conditions. Some countries have achieved a record of their peak loads. For example, in Croatia the maximum peak load amounted to 3.193 MWh/h. For comparison, in 2013 the maximum peak load in the same period amounted to 2.813 MWh/h, which is a big difference on an hourly basis. Among the countries in the region, only Bulgaria was independent from import throughout the year. Bosnia and Herzegovina was also an exporter at the end of the year, thanks to its HPP production, which totalled to more than 1 TWh in the last quarter of the year. Other countries that were exporters in certain months were Serbia, Slovenia, Romania and Croatia (if NPP Krško does not count as import since its 50% is owned by Croatia and located in Slovenia), while net importers were Macedonia, Greece and Hungary.

#### 4. SIMULATION

Considering the structure of the installed HPPs in the region, it is important to notice how their production affects the market trends in the region. Weather conditions that affect the HPP production are stochastic and are very hard to predict. Based on available data for the past 17 years [10], Figure 8 shows the distribution of HPP production. It is interesting to note in Figure 8, that there are two ranges of production which cover about 82% of the production value (54-65 TWh) which means that the average annual production may only exceed the mean value about 18%.

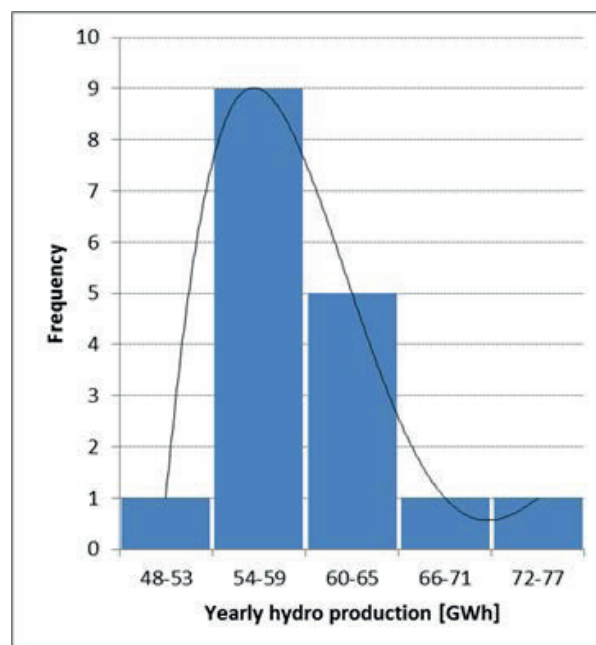


Figure 8. Distribution of HPP production

Hydrology in the region is seasonal, which is shown in Figure 9. (statistics for the past 17 years [10]). The range is higher in the first and fourth quarter of the year (production depends mostly on precipitation), and the middle of the year depends more on the snow from the mountains melting and the use of reservoirs. Average HPP production in 2012 was 13% lower than the mean value. Especially critical was the first quarter in which the lowest production in the last 17 years was recorded.

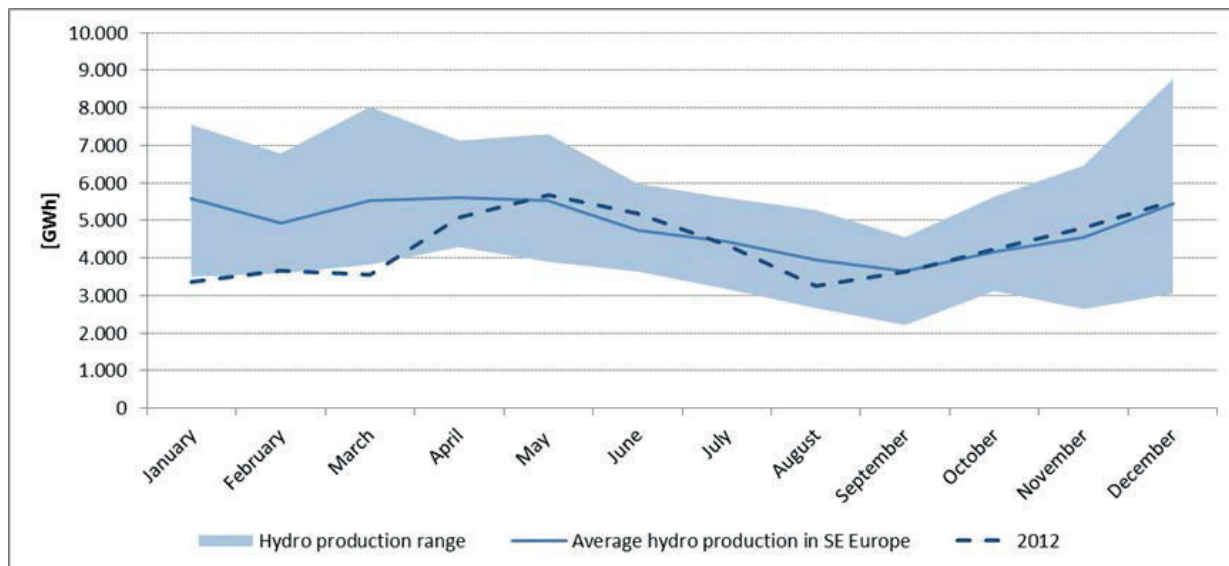


Figure 9. The range of monthly HPP production in the SEE region

Considering this fact, simulations of market price trends depending on the variable costs of TPPs and HPP production are shown below. To confirm the hypothesis about the high influence of hydrology on price movements in the region, the 2012 data will be used.

To prove the impact HPP production on the electricity price on the market, a fundamental analysis is made, which is based on the merit order list (MOL) with average production price for available power plants in the region. When creating the MOL and calculating the cost of production from individual power plants, some of the assumptions shown in Table 4 are taken into account. Fuel prices are taken according to data from [13], assuming that the fuel purchased is 70% from long-term contract and 30% from short-term contract, so that the prices have been assumed as a weighted percentage of forward and spot contracts.

Table IV. Assumed characteristics of TPP and fuel prices

Fuel	Power Plant Efficiency	Fuel Caloric Value	Fuel price
Coal	(35-41)%	24.800 kJ/kg	(85-120) USD/t
Gas	(41-59)%	33.338 kJ/m <sup>3</sup>	(28-34) EUR/MWh
Crude Oil	(25-35)%	39.774 kJ/kg	(100-116) USD/bbl

Figure 10. shows the achieved balance by countries in the region for 2012. The most volatile parameter was import, which in February was equal to the maximum possible value, while at the end of the year fell down to 4 times lower value

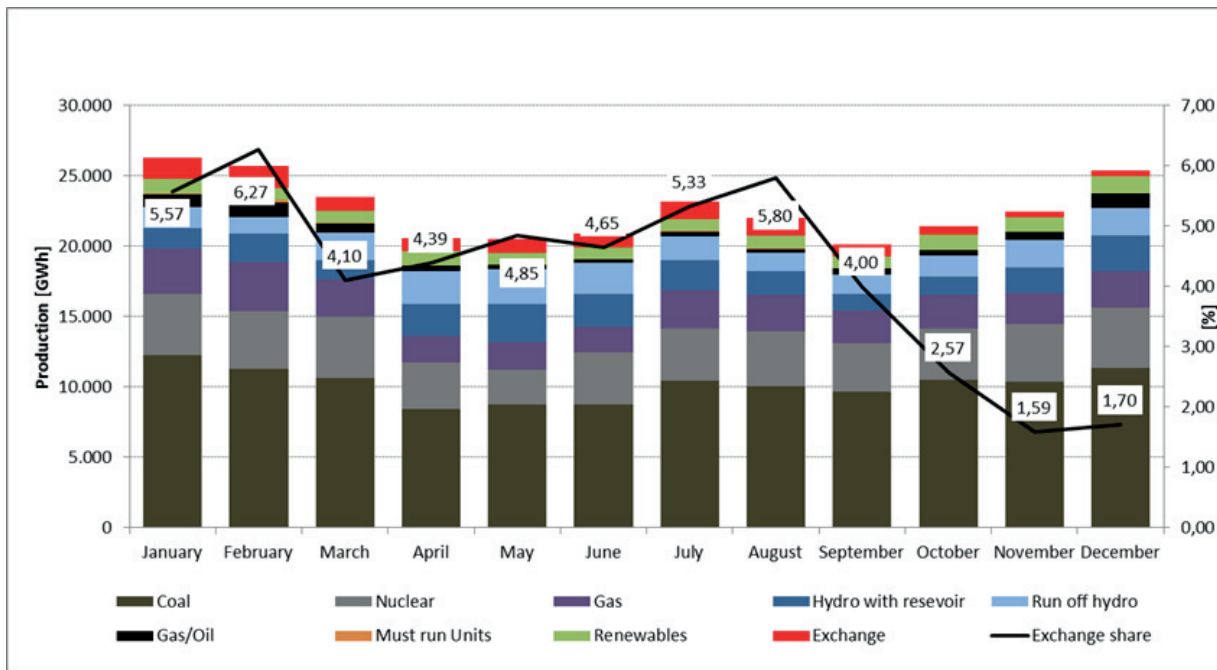


Figure 10 Energy balance - SEE region 2012

Import has a limit (like each energy source), while HPP production depends on water inflows and use of the reservoirs. Correlation between HPP production and share of import is shown in Figure 11.

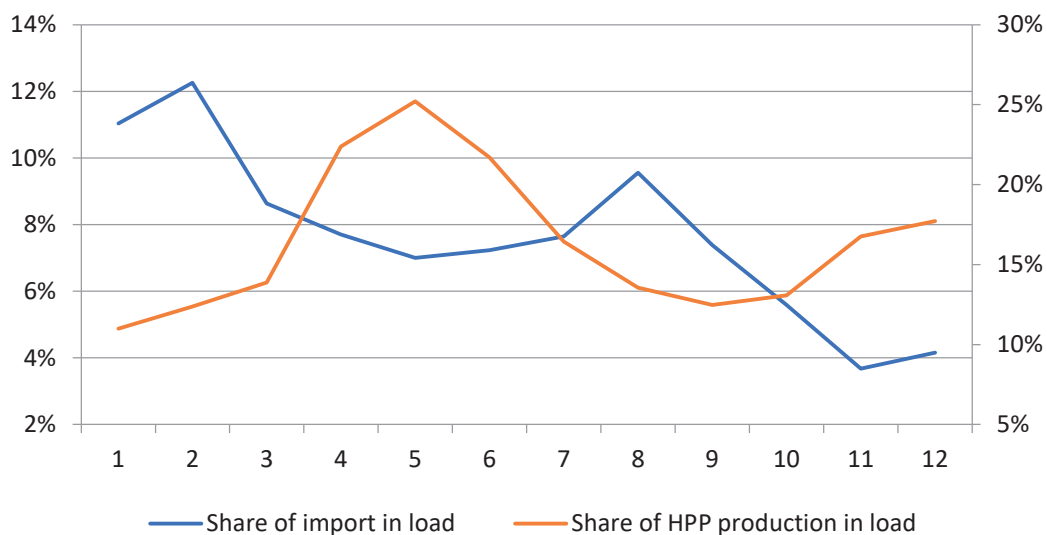


Figure 11. Correlation of share of HPP production and import volumes

HPP production ranges from 2.500 GWh to 5.000 GWh per month. As mentioned in previous chapters, reduced HPP production directly affects the increase in imports and vice versa. Regarding prices, market position of the SEE region depends heavily on the production of HPPs (as well as the load). Market players are well aware of the situation in the power systems of the region and they try to take advantage of their position. For example, if it is evident that the HPP production is (or will be) below the average, it is expected that the market will react (maybe more than it really should), and market players will try to make a higher profit. February and November will be specifically analyzed (February as a month of a very high load and low hydrology and November as the month of a lower load and high hydrology).

Two selected months have been observed because they were completely opposite (hydrologically). All mentioned conditions have had great impact on the electricity price on the market (caused by changes in price of producing additional MWh). Marginal cost of production (MOL) for February 2012 is shown in Figure 12.

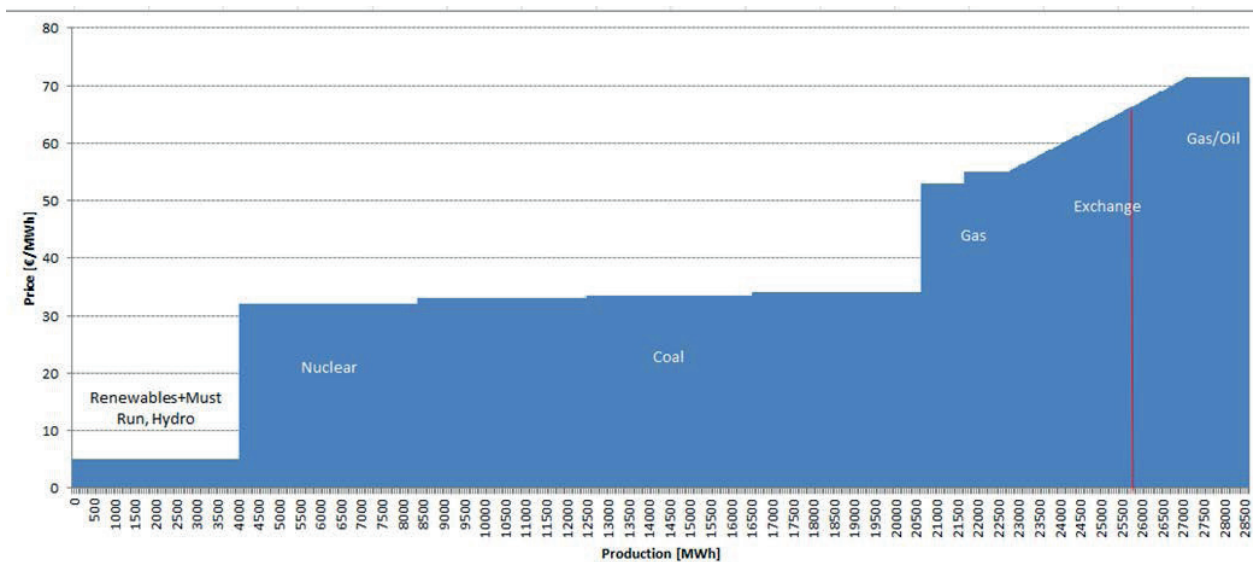


Figure 12. MOL for the SEE region - February 2012

MR power plants for February are renewable energy sources, run-of-river HPPs and CCGTs. NPPs are the cheapest ones and therefore are used as baseload power plants (98% of installed capacities in operation). Coal-fired TPPs have a slightly higher price of production and 80% of maximum possible capacities were in operation. From other TPPs, only inefficient and the most expensive ones weren't in operation. Gas-fired TPPs are considerably more expensive than coal-fired TPPs (depending on the efficiency of the plant and the price of fuel). One part of gas-fired TPPs were in the must run category, while the other part was in operation because the price of production was similar to the market price. The gap between the cost of production of gas-fired TPPs and the price of producing additional MWh (mostly gas and crude oil-fired TPPs) is filled with import at a corresponding price.

Regions dependence on import caused price movements: an increase in the CBTC price (import in the region) and the price on the power exchanges. The red vertical line in Figure 12 indicates the total load of the SEE region in February. The level of load directly affects electricity price. Higher load means that red line goes more to the right on the MOL. As a result, price determined with MOL is higher (possibly affecting market price). In addition to these reasons, unfavorable situation in the region suggests the same situation in the rest of Europe. Energy (outside the SEE region) is practically produced from expensive sources and therefore the import has to be more expensive. Cost of additional MWh was around 70 EUR.

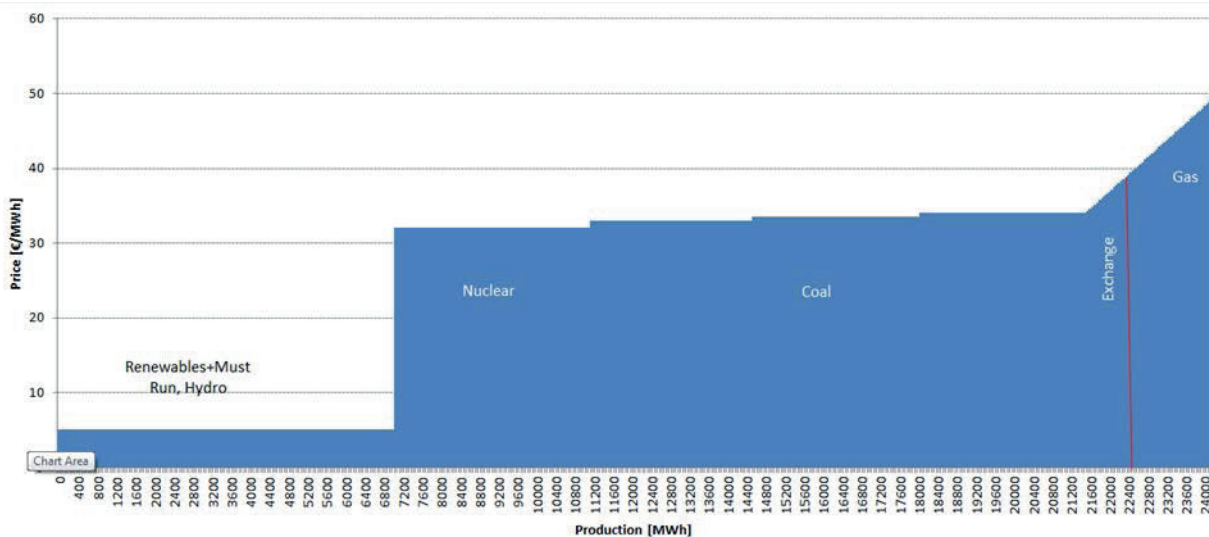


Figure 13. MOL for the SEE region - November 2012

In November, total load was 13% lower than in February (below average for that month) [12]. The same power plants as in February were used as MR. Production of run-of-river HPPs increased by 65% (storage HPPs produced 9% less), while the total HPPs produced 20% more energy. The assumption is that all reservoirs were filling up as they entered the rain season almost empty. The plan was to fill reservoirs to a certain limit and have that energy available later on. Expensive power plants were not in operation (reduction of gas-fired TPP production by 38% and gas/oil-fired TPPs by 40% compared to February). As a result there was a change in the market - the region could meet its energy demand (changes which market players were well aware of). Also, favourable hydrology in the region indicates that in other parts of Europe the situation is also improving which could affect the price as well (as in February). The result is a reduction in imports to 1,6% of total load, and a very large reduction in the price on the market (to less than 40 EUR/MWh).

Determination of the price with different graphical and computational methods led to the following results shown in Figure 14. The red curve represents the weighted price of three power exchanges in the region and a blue line represents calculated price of the merit order list. The price of electricity import practically depends on the possibility to cover the load in the SEE region, which is directly related to the HPP production.

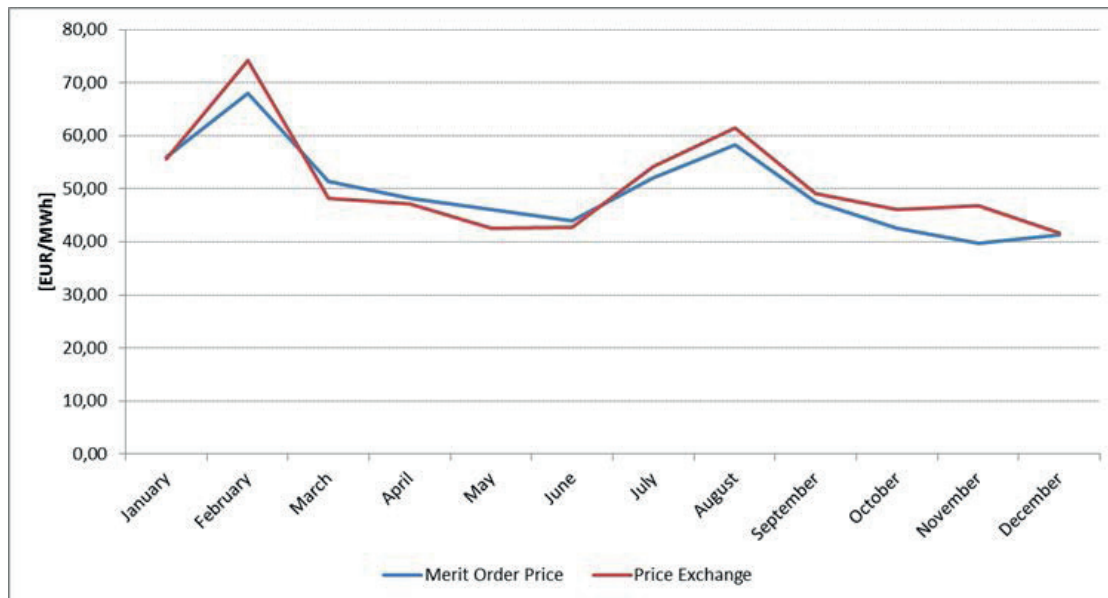


Figure 14. Correlation of market and MOL price

## 5. CONCLUSION

This paper shows that although energy balance in the SEE region depends on global energy trends and market prices in the rest of Europe, hydro production has major impact on energy balance of the SEE region. The SEE region has necessary installed production capacities to cover the load from various power sources, but part of the power plants are old and with low efficiency. These factors directly influence the high price of energy production for the SEE region. The price of producing an additional MWh which is related to the market price can be determined with the merit order list. The arrangement of power plants depends on their production availability and the power system requirements. This paper has shown that good hydrological periods result in increases hydro production in the SEE region, reducing the electricity prices on energy markets. On the other hand, dry periods mean lower share of hydro production, which results in increased imports and prices on energy markets.

The solution to short-term planning can be found in further development of the electricity market, by increasing the amount of trading volume on the power exchange. Additional products like long-term contracts with and without physical delivery and options could reduce the existing risks. Combination of different contract types could decrease the exposure to statistically hardly predictable circumstances caused by weather conditions. With a rising share of renewable energy sources, the SEE region will become even more exposed to risk of weather dependent power plant production. Regional energy exchange might be one of the solutions for incoming challenges.

## 6. ACKNOWLEDGEMENT

This work was presented on the 8th International Conference on Deregulated Electricity Market Issues in South-Eastern Europe - DEMSEE 2013 - in Cavtat, Croatia on 24-25 September 2013.

## 7. REFERENCES

- [1] Cerjan, M.; Marcic, D.; Delimar, M.; Short term power system planning with water and energy trade value optimization, 8th International Conference on the European Energy Market (EEM 2011), 269-274, 2011
- [2] Heiko Hahn, Silja Meyer-Nieberg, Stefan Pickl; Electrical load forecasting methods: Tools for decision making, European Journal of Operational Research 199 (902-9 07), 2009
- [3] Bajs D.; Majstrovic G.; Existing SEE Transmission System and Development, Power & Energy Society General Meeting, 2009. PES '09. IEEE, 1-7, 26-30 July 2009, Calgary, AB
- [4] Hammons, T.J.; Configuring the power system and regional power system developments in Southeast Europe, Universities Power Engineering Conference, 2004. UPEC 2004. 39th International (Volume:3), 1319-1326 vol. 2, 8 September 2004, Bristol, UK
- [5] Koritanov, V.S.; Veselka, T.D.; Modeling the Regional Electricity Network in Southeast Europe; Power Engineering Society General Meeting, 2003, IEEE (Volume:1), 399-404, 13-17 July 2003
- [6] Mijailović, S.; Review of electricity supply and demand in South East Europe; Power Engineering Society General Meeting, 2003, IEEE (Volume:1), 13-17 July 2003
- [7] Grbešić M., Goić, R.; Estimation of Variable Costs for Thermal Power Plants and Security of Power System Operation, VI savjetovanje Bosanskohercegovačkog komiteta CIGRE, 28.9. – 02.10., 2003, Neum
- [8] Goić, R., Lovrić, M., Žodan, M.; Sensitivity and risk analysis of power system annual variable cost achievement, 5. savjetovanje HK CIGRE, 04-08 November, 2011, Cavtat
- [9] [www.imf.org](http://www.imf.org), 05/21/2013
- [10] <https://www.entsoe.eu/data/data-portal/production> , 21/02/2013
- [11] <https://www.entsoe.eu/data/data-portal/exchange> , 21/02/2013
- [12] <https://www.entsoe.eu/data/data-portal/consumption>, 21/02/2013
- [13] [www.pointcarbon.com](http://www.pointcarbon.com), 18/03/2013

IVAN RAJŠL      SLAVKO KRAJCAR      PERICA ILAK

[ivan.rajšl@fer.hr](mailto:ivan.rajšl@fer.hr)      [slavko.krajcar@fer.hr](mailto:slavko.krajcar@fer.hr)      [perica.ilak@fer.hr](mailto:perica.ilak@fer.hr)

University of Zagreb Faculty of Electrical Engineering  
and Computing

## RISK-AVERSE APPROACH FOR ASSESSMENT OF INVESTMENT IN A RUN-OF-THE-RIVER POWER PLANTS WHILE CONSIDERING REDUCED WATER AVAILABILITY

### SUMMARY

Investment in the facility for harnessing a stream of water is usually characterized by long payback period. Hence investment choice not only needs to be optimal, but it also needs to be robust enough to cope with uncertainties which occur during payback period. In this research, a family of flow duration curves is created to model stochastic nature of water availability. The risk-constrained approach for assessment of investments in cascaded hydropower plants is proposed in a form of a mixed-integer linear programming. Proposed approach will manage a risk of large financial losses induced by these uncertainties. The project of run-of-river power plants on the Sava river stretch (Croatia) from border with Slovenia to the city of Sisak is analyzed.

**Keywords:** Assessment of investment, Small hydropower plant, Mixed-integer linear programming, Conditional value-at-risk, Sava river, Croatia

# 1 NOMENCLATURE

$c(\cdot)$	Specific investment cost function (€/kW).
$E(i, t)$	Electricity produced for energy market by plant $i$ in period $t$ (MWh).
$F_\alpha$	Special function used for risk shaping of CVaR (€).
$H_{max}(i)$	Maximal possible head of a pondage $i$ (m).
$H_r(i)$	Rated head of a plant $i$ (m).
$H(i, t)$	Head of pondage $i$ in period $t$ (m).
$I$	Set of indices of the reservoirs/plants,
$I=\{\text{'Podsused' , 'Prečko' , 'Zagreb1' , 'Zagreb2' , 'Zagreb3' , 'Zagreb4'}\}$	$i \in I$ .
$I_{>10MW}$	Subset of plants with capacity above 10 MW, $I_{>10MW} \subset I$ .
$I_{\leq 10MW}$	Subset of plants with a capacity of 10 MW and under, $I_{\leq 10MW} \subset I$ .
$i_x$	Inflation index.
$Inv(t)$	Investment cost of a cascade in period $t$ (€).
$n$	Capacity factor.
$\min CVaR(k)$	$k^{th}$ profit tolerance, an i.e. parameter used for risk exposure reduction in risk shaping procedure (€).
$NPV(\omega)$	Net present value of scenario $\omega$ (€).
$om(\cdot)$	Specific operating and maintenance cost function (%).
$O\&M(t)$	Operating and maintenance cost of a cascade in period $t$ (€).
$P_{max}(i)$	Capacity of plant $i$ (MW).
$p(\omega)$	Probability of price scenario $\omega$ .
$Q_{min}(i)$	Minimum water discharge of plant $i$ (m <sup>3</sup> /s).
$Q_{max}(i)$	Maximum water discharge of plant $i$ (m <sup>3</sup> /s).
$Q_{res}(i)$	Residual flow of plant $i$ (m <sup>3</sup> /s).
$q(i, t)$	Total water discharge of plant $i$ in time step $t$ (m <sup>3</sup> /s).
$R(t)$	Revenue of a cascade in time period $t$ (€).
$r$	Discount rate.
$T$	Set of indices of the steps of the optimization period, $T=\{1, 2, \dots, T_{max}\}$ , $t \in T, T_{max} \in \{20, 25, 30\}$ .
$U_i$	Set of upstream reservoirs of plant $i$ .
$V_{min}(i)$	Minimal possible utilizable volume of a plant $i$ (m <sup>3</sup> ).
$V_{max}(i)$	Maximal possible utilizable volume of a plant $i$ (m <sup>3</sup> ).
$V(i, t)$	Utilizable volume of a plant $i$ in time interval $t$ (m <sup>3</sup> ).
$W(i, t)$	Forecasted natural water inflow of the reservoir $i$ in time step $t$ (m <sup>3</sup> ).
$weight(t)$	Distribution of investment cost along $y$ time intervals, $t \in y \subset T$ .
$X(i, t)$	Water content of the reservoir $i$ in time step $t$ (m <sup>3</sup> ).
$X_{avg}(i, t)$	Average water content of the reservoir $i$ in time step $t$ (m <sup>3</sup> ).
$X_{max}(i)$	Maximal content of the reservoir $i$ (m <sup>3</sup> ).
$X_{min}(i)$	Minimal content of the reservoir $i$ (m <sup>3</sup> ).
$X(i, 0)$	Initial water content of the reservoir $i$ (m <sup>3</sup> ).
$X(i, T_{max})$	Final water content of the reservoir $i$ (m <sup>3</sup> ).
$Y$	Number of hours in one year, 8760 (h).
$\pi_{fit}(t)$	Feed-in-tariff in time step $t$ (€/MWh).

$\pi_e(t)$	Forecasted price of electricity in time step $t$ (€/MWh).
Greek	
$\alpha$	Percentile used for the CVaR where $1-\alpha$ defines the worst events (%).
$\rho_v(blok)$	Slope of the block $blok$ of the utilizable volume function ( $m^3/m^3/s$ ).
$\rho_j(i)$	Slope of the performance curve $j$ of plant $i$ ( $MWh/m^3$ ).
$\zeta$	The decision variable which defines the Value at Risk (€).
$\eta$	Variable used for obtainment of the CVaR (€).
$\Omega$	Set of indices representing future states of knowledge, it is a set of scenarios that can occur, $\Omega = \{1, 2, \dots, \Omega_{\max}\}$ , $\omega \in \Omega$ , $\Omega_{\max} \in \mathbb{N}$ .

## 2 INTRODUCTION

Careful planning is a necessity if a goal is a profitable hydropower project. Careful planning assumes precise modelling and simulation which is especially needed when long payback period is assumed, which is the case for the hydropower projects. For that reason, the risk-constrained approach for assessment of investment in run-of-the-river power plants is presented while considering reduced water availability. The methodology will manage the risk of large financial losses. There are many risks induced by many other influences, and this approach can be adapted to them as well, but for formulation clearness, here, only the risk of financial losses induced by declining water availability is considered. Also, only direct benefit of investment is considered, such as selling electricity on the wholesale market. Indirect benefits of improved water management are not considered here such as flood prevention, reduced water stress, and e.g. [1]. The objective of this work is to maximize the net present value from selling electricity on the wholesale market. It is a continuation of the work done in the [2] which is significantly improved here by implementing the family of the flow duration curves (FDC) which represents water availability scenarios, and conditional value-at-risk (CVaR) a risk measure used for risk management. The generated scenarios combined with the risk-constraining approach results in a robust investment plan. The reconnaissance level of detail is warranted, and some basic requirements when considering investing in hydropower plants will be discussed. The usage of the FDC for the economic evaluation of hydropower plants (HPP) is well documented [3], [4] and [5]. The procedure when conducting a hydrologic study is to establish how much water is available to divert through the turbine and at which hydraulic head. Here, the line potential is observed which denotes the theoretical potential of streams and rivers which could be harnessed through a continuous chain of imaginary run-of-river plants as depicted in Fig. 1.

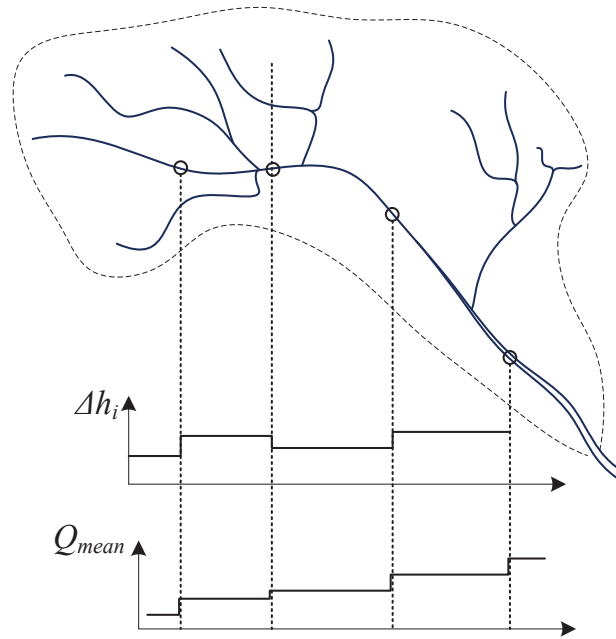


Figure 1. The line potential is a function of a mean annual flow and the head difference  $\Delta h_i$  of a reach

The hydro potential is obtained by subdividing a stream or river into reaches along which discharge and longitudinal slope are approximately uniform as illustrated in Fig. 1 and is defined by mean annual discharge and the elevation difference between the beginning and the end of a reach [6]. Additional information on financial aspect of hydropower systems can be found in [7] and technical aspects of small-scale HPP projects in [8]. Approaches how to evaluate potential location for HPP is given in [9], and more detailed insight is given in [10]. Therefore, in section III problem description and mathematical formulation of the model is given, in IV the case study is given of the potential investment in a cascaded run-of-the-river HPPs on the Sava river in Croatia.

### 3 PROBLEM DESCRIPTION AND FORMULATION

#### 3.1 Flow-Duration Curve

When river line potential is established, the utilizable potential of each river reach is calculated. The utilizable potential is a function of utilizable volume of water and generating unit performance curve. The utilizable (usable) volume,  $V$ , is defined by FDC as illustrated in Fig. 2.

When extremely high flows,  $Q_{ext}$ , occur, then tail water rises so high that the net power head is so small for the power plant to function. Unless there is an available storage to regulate flows to more favorable discharge rates, or a sluice to

divert extreme flows from the main riverbed, then HPP will be inoperable in extremely high flows. The residual flow,  $Q_{res}$ , and HPP minimum turbine discharge  $Q_{min}$  are taken into account to evaluate utilizable volume correctly. The water availability scenarios are modeled with the four FDCs depicted in Fig. 3.

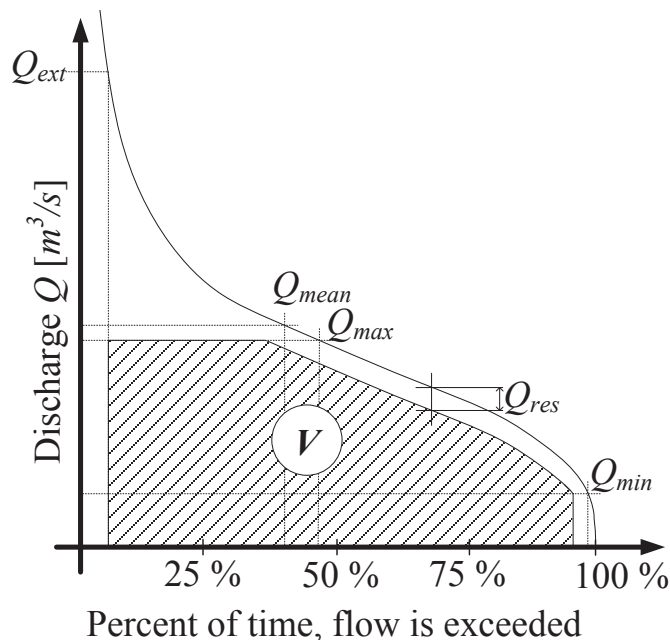


Figure 2. Generic FDC, the dashed area is usable volume  $V$  and is always less than ideally possible volume due to the turbine characteristics.

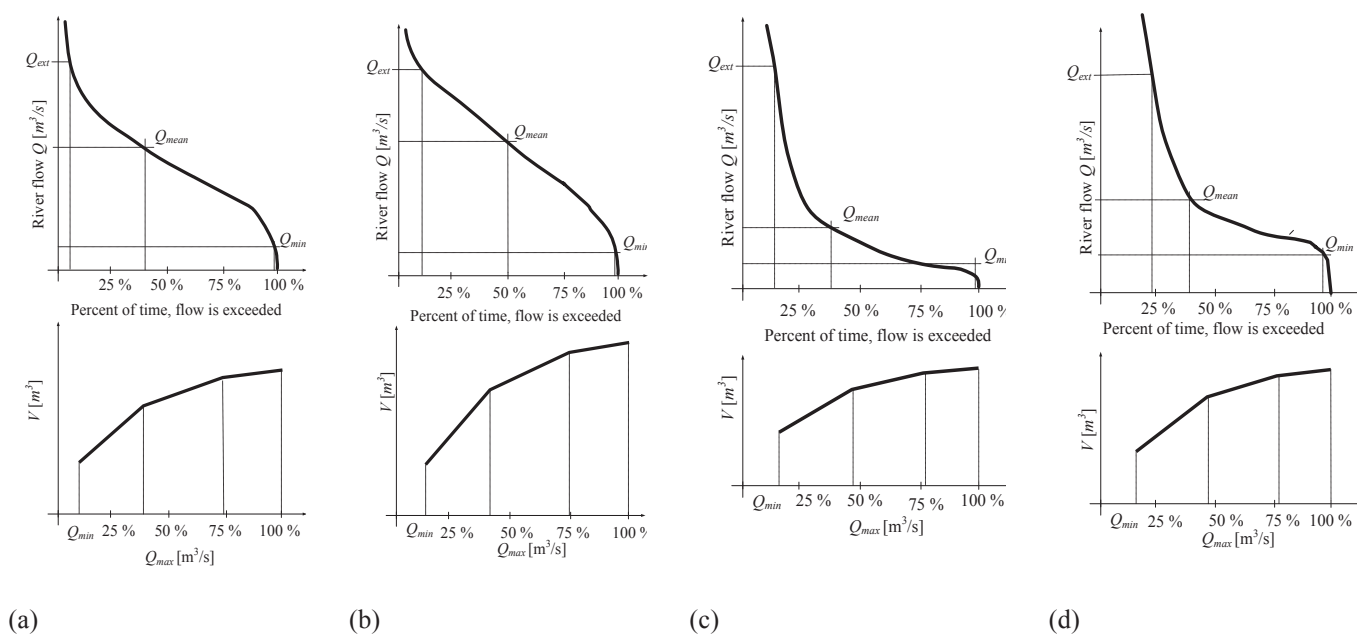


Figure 3. Four FDCs and associated usable volume for (a) average water availability, (b) high water availability and (c) low water availability are generated according to (d) normal distribution of mean flow

## 4 HEAD

A design head is defined as the head at which the turbine will operate at the best efficiency. Usually, a planner from the power studies determines the head at which best efficiency is desired then provides this value to the hydraulic machinery specialist to select an appropriate turbine design. Also, usually it is desirable to obtain the best efficiency in the head range where the project will operate most of the time, the design head is commonly specified at or near the average head. Additionally, for run-of-river projects, design head can be determined from a head-duration curve by identifying the midpoint of the head range where the project is generating power (Fig. 4). The design head usually is based on the yearly operation. Also, it could be based on operation in the peak demand months when dependable capacity is significant. Contrary, the pondage projects, which operate primarily for peaking, a design head is usually based on the weighted average head (weighted by the amount of electricity produced at each head). The rated head is defined as the head where rated power is obtained with turbine wicket gates fully opened. Thus, it is the minimum head at which rated output can be obtained. The selection of rated head is a compromise based on cost and efficiency. Therefore, a net head versus discharge curve (Fig. 5a) is developed which shows the tail water and forebay elevation dependence with discharge (Fig. 5b). Here the head computation is directly implemented in the performance curve (1).

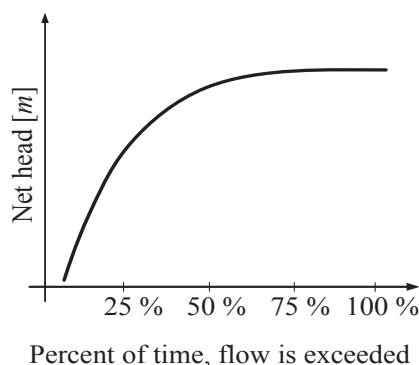


Figure 4. Typical head-duration curve (HDC)

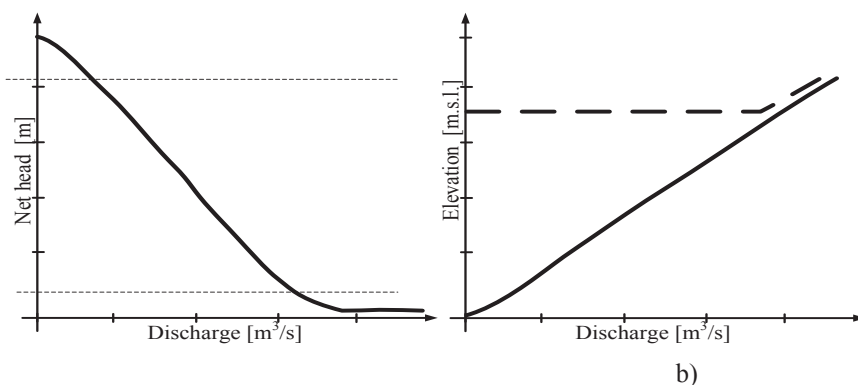


Figure 5. The depiction of a: a) head-discharge curve, b) pool elevation (dashed) and tail water elevation curve (solid). Net head is the forebay elevation minus the tailwater elevation minus the trashratch and penstock head losses.

Using FDC and head discharge curve, head duration curve (HDC) can be constructed (Fig. 4). The FDC and HDC methods are limited to small hydro projects, particular run-of-river projects. To obtain a reasonable estimate of the annual power production performance curves of turbine-generator units are used (Fig. 6). The performance curves account for efficiency characteristics and operating range limitations consistent with the turbine type likely to be installed. More on performance curves in [8].

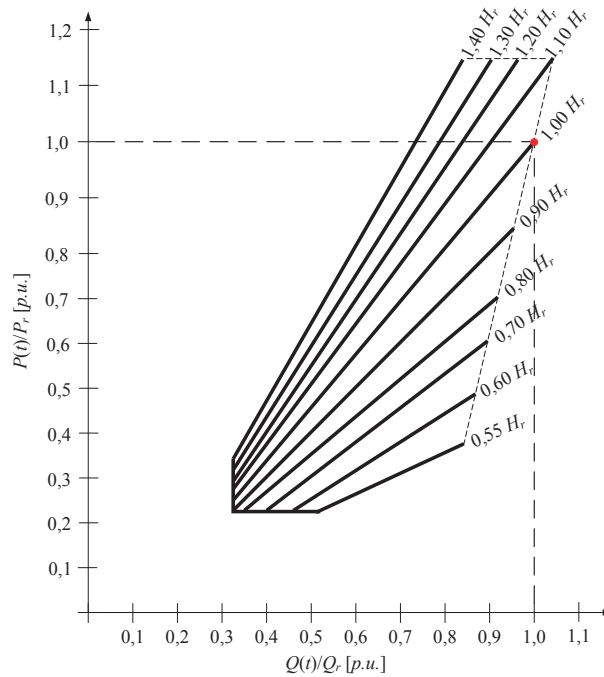


Figure 6. Variable pitch propeller without wicket gates

In this paper performance curves (Figure 6) have been modeled through a piecewise linear formulation of Hill chart [11]. Figure 6 shows linear performance curves with its associated slope  $\rho$  which is defined by HPP conversion capabilities (MW/m<sup>3</sup>). The Cavitation and vibration problems limit turbines to a minimum discharge of 30 to 50 percent of rated discharge Energy production performance curve (7).

To assure that best choice of rated head  $H_r$ , rated turbine discharge  $Q_{max}$  and number of units  $N$  is selected, all combinations of scenarios  $H_r$ ,  $Q_{max}$  and  $N$  should be calculated, a procedure for determining optimal rated flow, number of units, and a head is shown in Fig. 8 of [2]. The general procedure is to calculate and compare energy produced of turbines having a higher and a lower rated flow. Following establishment of the rated flow it needs to be checked if power is being lost because turbine discharge is consistently below lower boundaries, then HPP maximal capacity  $P_{max}$  is lowered, and more units are added. If energy production  $E(i, t)$  increase is substantial, cost of the alternatives may be determined from the HPP specific investment cost function (Fig. 7) and O&M specific costs function (Fig. 8). Also, the first selection of the number of turbines needs to be compared with the lesser number of units. The rated head of the turbine can be further refined by

optimization in a similar manner. The annual power production is computed for higher and lower heads with the same capacity rating. The rated head yielding the highest annual output should be used. The greater the chosen value of the maximal turbine discharge, the smaller proportion the year that the system will be operating at full power, i.e., it will have a lower capacity factor  $n$  [2].

To calculate annual energy production it is necessary to calculate annual utilizable volume  $V$  correctly. To do that  $V$  needs to be expressed as a function of HPP maximum water discharge  $Q_{max}$  as explained in Eq. (11)-(15) in [2]. Essential characteristic of used function is its concave nature necessary to ensure convexity in optimization problems and to assure strong duality.

## 5 REVENUES AND EXPENSES

The largest share of investment cost for large hydropower plant is typically taken up by civil works for the construction of the hydropower plant (such as a dam, tunnels, canal and construction of powerhouse, etc.). Electrical and mechanical equipment usually contributes less to the cost. However, for hydropower projects where the installed capacity is less than 5 MW, the costs of electro-mechanical equipment may dominate total cost due to a high specific cost of small-scale equipment [7]. The specific cost of investment in HPP is depicted in Fig. 7 and is a piecewise linear function. HPP usually require little maintenance, and operation costs will be low. When in cascade along a river, centralized control can reduce O&M costs to low levels. In this study O&M specific costs are depicted on Fig. 8 according to [7].

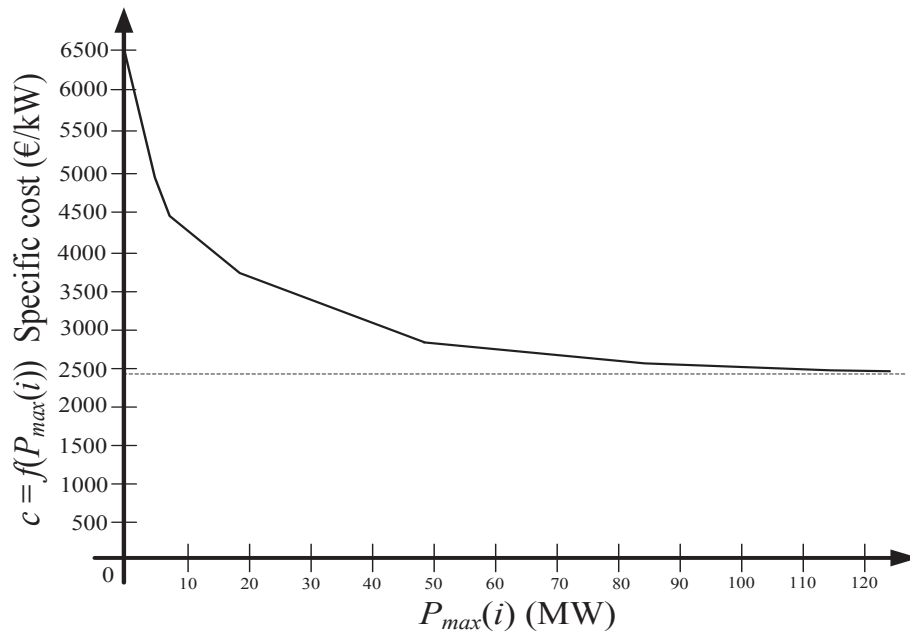


Figure 7. The specific investment cost of an HPP as a function of installed capacity.

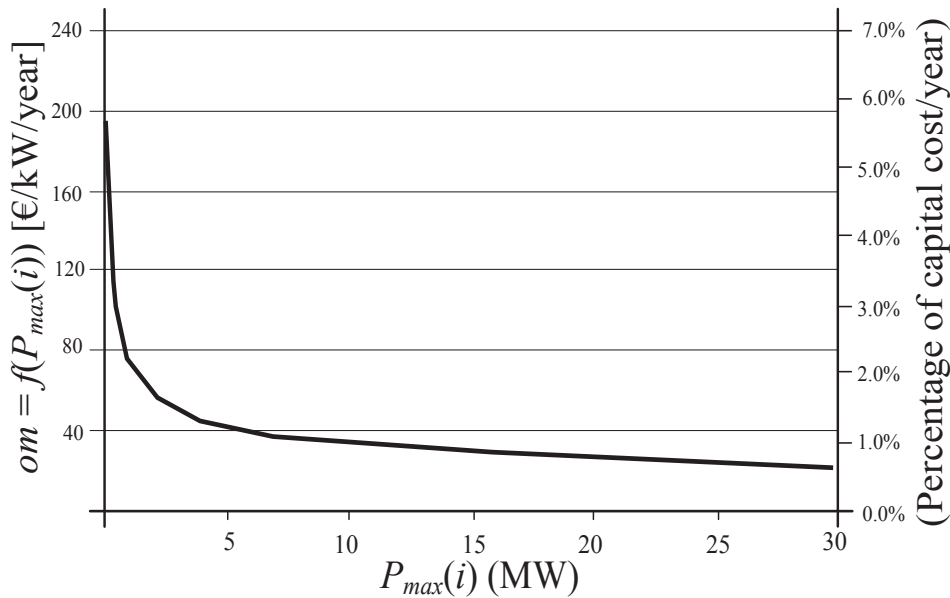


Figure 8. Specific O&M costs as a function of installed capacity.

## 6 OBJECTIVE FUNCTION

Maximize the net present value (NPV) of the project:

$$NPV = \sum_{t=y+1}^{t=T} \frac{(1+i_x)^t (R(t) - O\&M(t))}{(1+r)^t} - \sum_{t=1}^{t=y} \frac{(1+i_x)^t Inv(t)}{(1+r)^t} \#(1)$$

Expression (1) assumes that the project will be developed in  $y$  years (time intervals). At the end of  $y^{\text{th}}$  year the whole development is finished and paid. The electricity revenues and O&M costs are made effective at the end of each year and begin at the end of the  $y^{\text{th}}$  year [10]. All variables and parameters are defined in the nomenclature.

Revenue part of (13):

$$R(t) = \pi_e(t) \cdot \sum_{i \in I_{>10MW}} E(i, t) + \pi_{fit} \cdot \sum_{i \in I_{\leq 10MW}} E(i, t) \quad \forall i \in I, \forall t \in T \#(2)$$

where the first part of (2) denotes revenues from wholesale electricity market and the second part, revenues of eligible units (under 10 MW) from feed-in-tariff (FIT).

Operating and maintenance part:

$$OM(t) = \frac{\sum_{i \in I} om(P_{max}(i))}{100} \cdot \sum_{t=1}^{t=y} \frac{(1+i)^t Inv(t)}{(1+r)^t} \quad \forall i \in I, \forall t \in T \quad \#(3)$$

Investment cost:

$$Inv(t) = weight(t) \cdot \sum_{i \in I} c(P_{max}(i)) \cdot P_{max}(i) \quad \forall i \in I, \forall t \in T \quad \#(4)$$

The (5) defines how investment cost is distributed over  $y$  years.

$$\sum_{t=1}^y weight(t) = 1 \quad \#(5)$$

## 7 RISK MEASURE

An easy way to incorporate risk into linear model is to use CVaR [12] as a measure of risk. The  $\alpha$ -CVaR in Fig. 9 is an average profit in worst  $1-\alpha$  (i.e., 15%) scenarios and  $\alpha$ -VaR is minimal profit which company can expect in rest  $\alpha$  (i.e. 85%) scenarios.

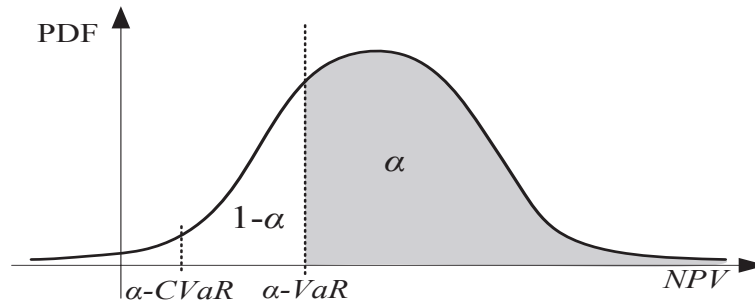


Figure 9. Hypothetical PDF of an NPV.

In the next section  $\alpha$ -VaR and  $\alpha$ -CVaR are formulated using the profit probability distribution function (PDF) as depicted in Fig. 9. Both  $\alpha$ -VaR and  $\alpha$ -CVaR can be calculated by solving a simple optimization problem of a convex type in one dimension. For this purpose, the function (6) is formulated.

$$F_{\alpha}(Variables, \zeta) = \zeta - \frac{1}{1-\alpha} \sum_{\omega=1}^{\Omega_{max}} p(\omega) \cdot [\zeta - NPV(\omega)]^+ \quad (6)$$

where  $[\zeta - NPV(\omega)]^+ = \max\{0, \zeta - NPV(\omega)\}$ , and  $\omega$  denotes one water availability scenario, i.e., one FDC as depicted in Fig. 3 for which the NPV is calculated.

When maximizing (6) over all variables defined in model, (8) and (9) are obtained.

$$\max_{(Variables, \zeta) \in \mathbb{R}^{No. of var} \times \mathbb{R}} F_{\alpha}(Variables, \zeta) \quad (7)$$

$$\alpha - CVaR = F_{\alpha}(Variables^*, \zeta^*) \quad (8)$$

$$\alpha - VaR = \zeta^* \quad (9)$$

where *Variables* denotes all variables defined in nomenclature.  $\zeta$  is shown separately only to point out its importance. In (7)-(9) risk measure is expressed as a daily value which manages risk occurred during a whole day. Since this model already has defined an objective function, special function is thus brought in the optimization problem in the form of a constraint (10).

$$F_{\alpha}(Variables, \zeta) \geq minCVaR \quad \#10$$

When implementing constraint (10), risk is “shaped” using profit tolerance *minCVaR*. When set of profit tolerances *minCVaR(k)*,  $\forall k \in N$  is introduced in optimization model and requirement (11) is valid, then  $\alpha$ -CVaR can be heuristically obtained using algorithm described in Fig. 10.

$$minCVaR(k - 1) < minCVaR(k) < minCVaR(k + 1) \quad \#(11)$$

Linear formulation of CVaR as implemented is shown in (12)-(14).

$$\eta(\omega) \geq 0 \quad \forall \omega \in \Omega \quad (12)$$

$$\eta(\omega) \geq NPV(\omega) - \zeta \quad \forall \omega \in \Omega \quad (13)$$

$$\zeta - \frac{1}{1 - \alpha} \sum_{\omega=1}^{\Omega_{max}} p(\omega) \cdot \eta(\omega) \geq minCVaR(k) \quad (14)$$

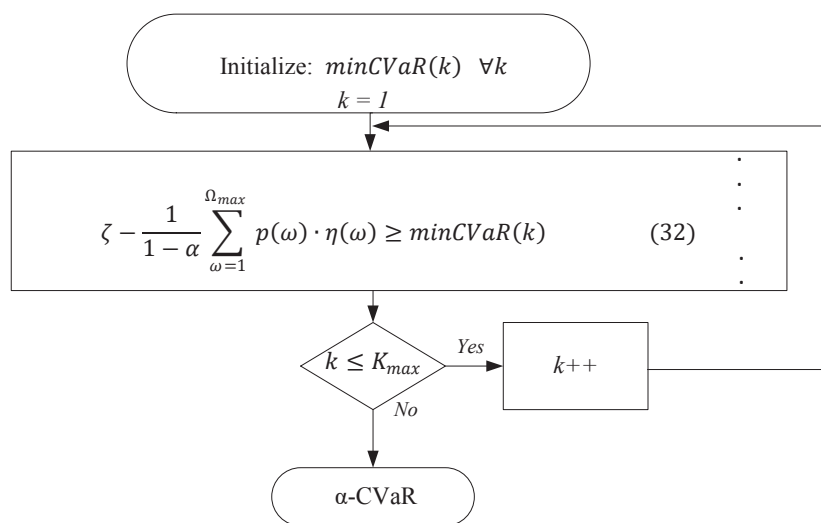


Figure 11. Simple heuristic algorithm for obtaining  $\alpha$ -CVaR

Model is defined as a mixed-integer linear program using indexed assignments [13]. The presented results were obtained on 3.4 GHz based processor with 8 GB RAM using CPLEX under General Algebraic Modeling System (GAMS).

## 8 RESULTS AND DISCUSSION

Virtual hydropower system (HPS) Sava (Croatia) is modelled as illustrated in Fig. 9. The observed six river reaches consists of six pondages, six run-of-river HPP and a sluice. Tributary line potential is not considered.

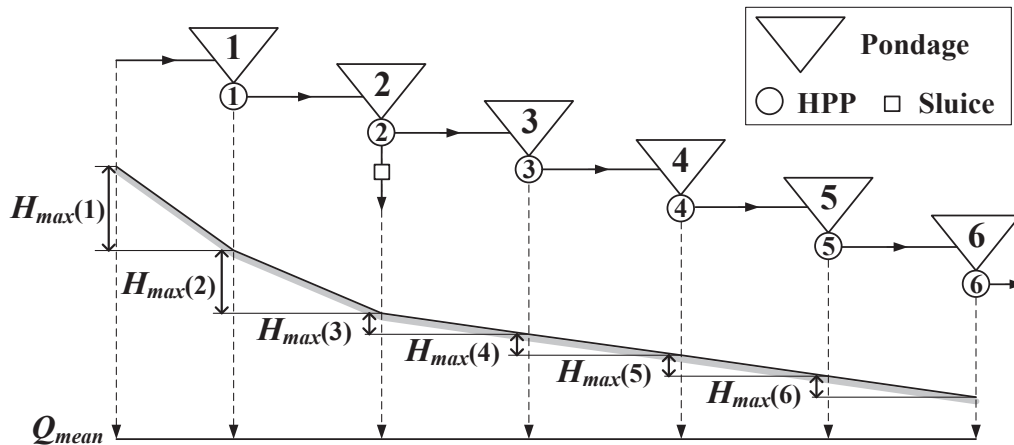


Figure 11. Heuristic algorithm for assessment of investment in cascaded run-of-river HPPs.

Because of computational efficiency, it should be noted that time periods of 1 year are considered. Since there is a sluice in pondage 2, extreme water flows will not reduce utilizable volume by extreme tail water rise. The conventional propeller and very low head (VLH) Kaplan turbines are considered which are operated at power outputs with flows from 40 to 100 percent of rated flow  $Q_{max}(i)$ . Performance curves (Figure 6) and pondage (Figure 11) parameters are shown in Table 1.

Table I HPP performance curves and associated pondage parameters

HPP	$\rho_1$	$X_{min}$	$X_{max}$	$H_{max}$
1	2,207E-5	3E6	4.078E6	9
2	1,839 E-5	4.6E6	6.75E6	7,5
3	9,197E-6	1.2E6	1.903E6	3,75
4	9,197E-6	1.2E6	1.9406E6	3,75
5	9,197E-6	0.4E6	0.7875E6	3,75
6	9,197E-6	1.7E6	2.718E6	3,75

Since there is no significant tributary in observed river reaches, one FDC is constructed and is assigned to all six river reaches for each scenario. The four FDC

based on daily flows of periods from time intervals: 1997 to 1987, 1988 to 1993, 1988 to 1998 and 1994 to 1999 are used. Resulting FDCs are linearized and are depicted in Figure 12. For confidentiality reasons only the averaged data of four FDC will be shown in the paper, therefore: Mean annual discharge  $Q_{mean}$  for each river reach is 320 m<sup>3</sup>/s. Residual water flow  $Q_{res}$  is 20 m<sup>3</sup>/s. Maximal flow  $Q_{ext}$  of each river reach is 800 m<sup>3</sup>/s. Electric energy price  $\pi_e$  is 43.6 €/MWh and is an average price of base load power at EPEX Spot (EEX, 2012) for 2003 to 2012 period. Feed-in-tariff  $\pi_{fit}$  is set at 56 €/MWh. Discount rate  $r$  is 8.2 %. Inflation index  $i$  is 2%, a number of investment years  $y$  is 1 and utilizable volume function slopes  $\rho_1$  and  $\rho_2$  are 0.8616 and 0.3618 respectively (Fig. 12). The number of units is set to  $N(i) = 1$  for all plants. Stabilizing head  $H(i, t)$  of each river reach is one of the major concerns in this study where maximal possible head  $H_{max}(i)$  is predetermined by geographical and urbanization constraints, thus rated head  $H_r(i)$  won't be optimized. Results are obtained for the period  $T_{max} = 30$  years with scenario matrix.

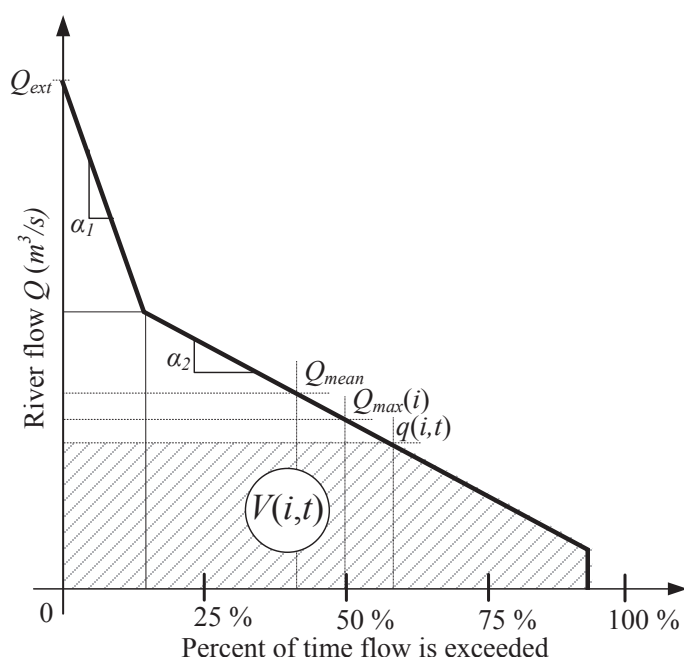


Figure 12. Linearized FDC less residual flow and extreme flows

Table II Averaged Results of Four Scenarios With and Without CVaR

	Without	With
$Q_{max}/Q_{mean}$	<b>0,75</b>	<b>0,70</b>
$n$	<b>0,8616</b>	<b>0,82</b>
$NPV$ (mil. €)	<b>16,1</b>	<b>13,5</b>
$IRR$ (%)	<b>8,7891</b>	<b>7,532</b>
$W$ (GWh)	<b>461,22</b>	<b>403,3</b>
$I$ (mil. €)	<b>259</b>	<b>239</b>
$P_{max}(1)$ (MW)	<b>17,879</b>	<b>17,455</b>
$P_{max}(2)$ (MW)	<b>14,899</b>	<b>14,321</b>
$P_{max}(3)$ (MW)	<b>7,45</b>	<b>7,12</b>

	Without	With
$P_{max}(4)$ (MW)	<b>7,45</b>	<b>7,12</b>
$P_{max}(5)$ (MW)	<b>7,45</b>	<b>7,12</b>
$P_{max}(6)$ (MW)	<b>7,45</b>	<b>7,12</b>

## 9 CONCLUSION

Simulation showed favorable NPV and IRR which means that the HPS Sava project is economically sound. Additional simulations should be conducted for wide range of possible future scenarios. Additionally, adjusting model to desired accuracy and detail will result in computational intensive simulation and will provide valuable data on run-of-river cascade long-term schedule.

## 10 REFERENCES

- [1] L. H. Knutsen and R. Holand, "Investment Strategy for Small Hydropower Generation Plants in Norway," 2010.
- [2] P. Ilak and S. Krajcar, "Assessment of Investment in Small Hydropower Plants ," *Energy and Environment Research*, vol. 3, no. 2, pp. 33-45, July 2013.
- [3] G. H. Hickox and G.O. Wessenauer, "Application of duration curves to hydroelectric studies," *Transactions of ASCE*, vol. 98, no. 1276-1308, 1933.
- [4] J. K. Searcy, *Flow-duration curves: Manual of Hydrology: Part 2. Low-Flow Techniques*, UNITED STATES DEPARTMENT OF THE INTERIOR, Ed. WASHINGTON , USA: UNITED STATES GOVERNMENT PRINTING OFFICE, WASHINGTON : 1959, 1959.
- [5] C. C. Warnick, *Hydropower engineering*. Moscow, Idaho: Englewood Cliffs, NJ : Prentice-Hall, ©1984., 1984.
- [6] H. W. Weiss and A. O. Faeh, "Methods for evaluating hydro potential," in *Hydrology in Mountainous Regions. I - Hydrological Measurements; the Water O/cte* (Proceedings of two Lausanne Symposia, August 1990). IAHS Publ. no. 193,1990. , Lausanne, Switzerland, 1990.
- [7] "Hydropower Renewable energy Technologies: Cost Analysis Series, vol. 1," IRENA, 2012.
- [8] "U.S. Army corps of enginners. Feasibility Studies for Small Scale Hydropower Additions: Hydrologic Studies Volume III.," USACE, 1979.
- [9] " A cross-section, Small Hydroelectric plants. West Virginia University, FS-13.," WVU, 1978.
- [10] "Layman's Guidebook on how Develop a Small Hydro Site.," ESHA, 2004.

- [11] X. Guan, A. Svoboda, and C. A. Li, "Scheduling hydro power systems with restricted operating zones and discharge ramping constraints. ," in *IEEE Trans. Power Syst.*, 1999, pp. 14, 126-131.
- [12] R. T. Rockafellar and S. Uryasev, *Conditional Value-at-Risk for General Loss Distributions*. Seattle, WA: University of Washington, Department of Mathematics, 2001.
- [13] R. Rosenthal. (2012, January ) GAMS-A User's Guide; GAMS Development Corporation: Washington, DC, USA. [Online]. <http://www.gams.com/dd/docs/bigdocs/GAMSUsersGuide.pdf>

**SINIŠA ŠADEK**

sinisa.sadek@fer.hr

**DAVOR GRGIĆ**

davor.grgic@fer.hr

**University of Zagreb Faculty of Electrical Engineering  
and Computing**

## **NPP KRŠKO CONTAINMENT MODELLING WITH THE ASTEC CODE**

### **SUMMARY**

ASTEC is an integral computer code jointly developed by *Institut de Radioprotection et de Sûreté Nucléaire* (IRSN, France) and *Gesellschaft für Anlagen- und Reaktorsicherheit* (GRS, Germany) to assess nuclear power plant behaviour during a severe accident (SA). The ASTEC code was used to model and to simulate NPP behaviour during a postulated station blackout accident in the NPP Krško. The accident analysis was focused on containment behaviour; however the complete integral NPP analysis was carried out in order to provide correct boundary conditions for the containment calculation. During the accident, the containment integrity was challenged by release of reactor system coolant through degraded coolant pump seals, molten corium concrete interaction and direct containment heating mechanisms. Impact of those processes on relevant containment parameters, such as compartments pressures and temperatures, is going to be discussed in the paper.

**Key words:** ASTEC, core melt, direct containment heating, molten corium concrete interaction, PWR

## 1. INTRODUCTION

Release of radioactive material into the environment is a major concern during a hypothetical severe accident. A last barrier for a radioactive release in a pressurized water reactor (PWR) nuclear power plant (NPP) is the containment, a reinforced concrete structure which encloses main components of the primary cooling circuit. Since the containment has a large interior volume, it cannot withstand a significant pressure difference between the inner and the outer surfaces. Failure of a reactor pressure vessel (RPV) and discharge of a core melt may challenge the containment integrity.

A station blackout accident combined with a small LOCA following degradation of reactor coolant pump (RCP) seals was chosen as a reference severe accident (SA) event. The loss of coolant from the reactor cooling system (RCS) and unavailability of safety injection (SI) systems will lead to core uncover, heat-up and, finally, degradation and melting. Formation of an in-core molten pool and its slumping to the RPV lower head may cause failure of the RPV bottom wall due to increased thermal and mechanical stresses. The released corium accumulates at the concrete bottom of the reactor cavity. Molten corium concrete interaction (MCCI), which begins after the corium hits the cavity bottom, is accompanied with release of hydrogen and carbon monoxide which are flammable and explosive gases. Inert gas CO<sub>2</sub> is also produced and, although it does not represent an explosion hazard, its rather high production rate will be the main contribution factor to the containment pressure increase. Beside the MCCI, another phenomenon called direct containment heating (DCH) will be responsible for the containment pressurization and heat-up. In the case of the DCH, molten debris is dispersed in the containment atmosphere where the decay heat of the melt is transferred to containment structures and walls, and also to air and steam. With increase of the amount of the corium discharged during the DCH, the effects of the MCCI will be less severe; however accumulation of gases in the containment can lead to substantial pressure increase rate. Containment integrity, thus, can be more seriously challenged during the DCH than the MCCI.

The ASTEC code version ASTEC-V2.0-rev3p1 was used in the calculations. The ASTEC is a modular computer code consisting of 13 coupled modules that model different SA phenomena. For the purpose of presented analyses eight modules were used: CESAR, ICARE, CPA, MEDICIS, RUPUICUV, CORIUM, COVI and SYSINT. The CESAR module computes two-phase thermal hydraulics (TH) in the primary and secondary circuits. Modelling is based on a 1D, two-fluid, five-equation approach. One incondensable gas (hydrogen) is available. The ICARE module models in-vessel core degradation and vessel rupture [1]. The thermal hydraulics in the core is based on a 1D swollen water level approach completed by a 2D gas modelling. The corium behaviour in the lower plenum is based on a 0D modelling of corium layers (oxide, metallic and debris layers) with a 2D meshing of the RPV lower head. The molten corium concrete interaction is simulated by the MEDICIS module [2]. Direct containment heating generated by discharge of corium after the vessel rupture is modelled by the RUPUICUV module [3] and the behaviour of corium droplets transported by high pressure melt ejection into the containment atmosphere and the sump by the CORIUM module [4]. Inside the

containment the CPA module is responsible for the thermal hydraulic and aerosols behaviour calculation and the COVI module for the hydrogen build-up (a simple model assuming a virtual combustion, i.e. an adiabatic total combustion without any feedback on the CPA thermal hydraulics). For the H<sub>2</sub> and CO combustion analysis in the containment, a more detailed model (the so-called CPA-FRONT) exists in the ASTEC-V2 but it was not used here. The SYSINT module manages all engineered safety features such as spray actuation, the safety injection system, accumulator injection, pump operation, etc.

Other five modules are ELSA, SOPHAEROS, ISODOP, IODE and DOSE. The ELSA module takes care of fission products and structural material release from the core, while their transport in the RCS is modelled by the SOPHAEROS module. The ISODOP module calculates the fission products and actinide isotope decay, the IODE module the iodine chemistry and the DOSE module, dose rates in different containment compartments.

## 2. MATHEMATICAL MODEL OF THE NUCLEAR POWER PLANT

The NPP Krško mathematical model includes detailed models of primary and secondary systems, Figure 1, and the containment, Figure 2. The reactor coolant system, steam generators (SG), steam lines, feedwater and auxiliary feedwater (AFW) pipes are modelled as a set of thermal hydraulic volumes connected by junctions, to which heat structures were attached to simulate heat losses to the environment. The ICARE module is used to model the reactor core and the CESAR module to model all other plant systems: primary and secondary circuit pipings, the pressurizer and the steam generators. Heat losses from the primary system to the containment are modelled with the substructure HEAT from the CONNECTION structure.

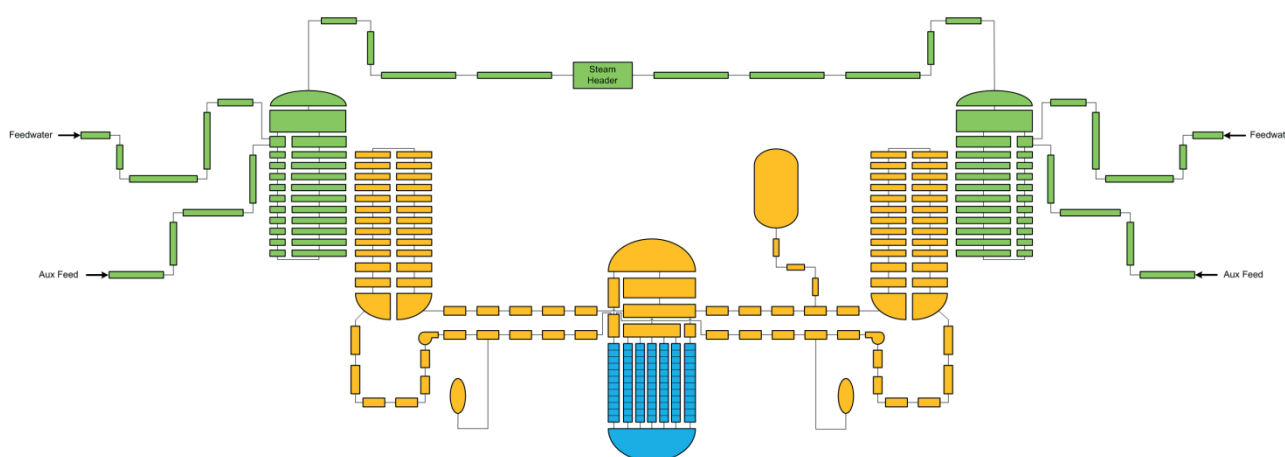


Figure 1. Primary and secondary systems nodalization for the ASTEC calculation

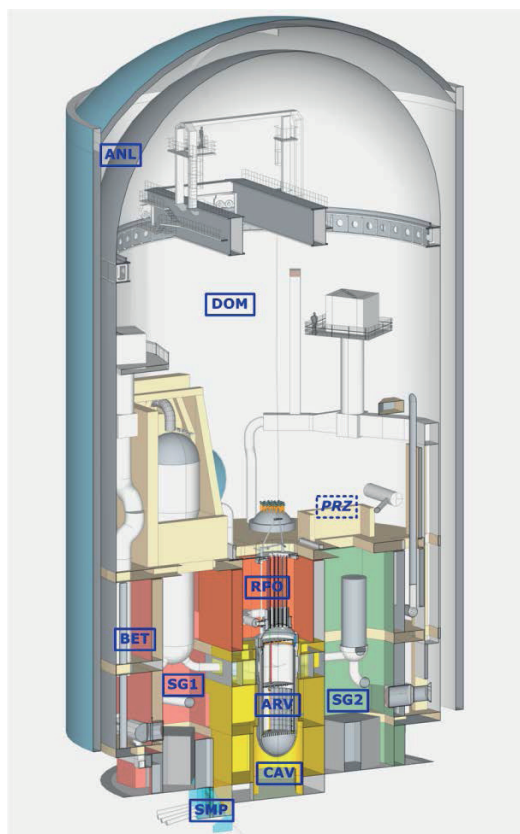


Figure 2. Containment 3D nodalization sketch for the ASTEC calculation

The containment building is represented with 10 control volumes:

1. DOM (containment dome) – cylindrical/spherical air space above the reactor pool, steam generators and pressurizer compartments,
2. ANL (annulus) – air space between the steel liner and the containment building,
3. SG1 (steam generator 1 compartment) – air space in the SG1 compartment that contains components SG1 and RCP1,
4. SG2 (steam generator 2 compartment) – air space in the SG2 compartment that contains components SG2 and RCP2,
5. PRZ (pressurizer compartment) – air space in the compartment that contains pressurizer and primary system safety and relief valves,
6. BET (between) – lower compartment below the containment dome placed between SG1, SG2 and PRZ compartments excluding the reactor pool and the reactor pressure vessel area,
7. RPO (reactor pool) – air space above the reactor vessel filled with water during the shutdown, otherwise empty,
8. ARV (around reactor vessel) – air space between the reactor vessel and the primary shield walls,
9. CAV (reactor cavity) – air space below the reactor vessel including the instrumentation tunnel,
10. SMP (containment sump) – the lowest control volume below the SG1 compartment that contains the recirculation sump.

An additional control volume with a large volume and fixed temperature (35 °C) is used to represent the environment. This volume is necessary for the code to calculate heat losses from the containment building. Heat transfer coefficient from the outside containment wall to the environment is calculated by the code.

The control volumes are connected with 23 junctions. That number of junctions is larger than required just to connect simply the volumes. More than one opening is used between the same volumes if they are located at different elevations to promote internal thermal mixing flow, what can be important for long term containment transients. For example, there are three connections between the BET volume and SG1 and SG2 compartments, respectively, at floor levels. There are also more than one connection between the DOM volume and volumes SG1, SG2 and PRZ. Pressurizer and steam generator compartments are open and the junction areas between those compartments and the dome are large, between 6 m<sup>2</sup> and 35 m<sup>2</sup>. Other connections, such as between ARV and SG1 and SG2 compartments which are through cold and hot leg openings in the primary shield wall are smaller; their values were taken to be 1 m<sup>2</sup>. Connection between the sump and the cavity is based on cross section area of 4 inch pipe. The largest connection area is between the reactor pool and the dome, 108 m<sup>2</sup>. The sump and the cavity are connected to the SG1 compartment and the BET volume, respectively. The reactor sump is below the SG1 compartment with the connection area being 4.5 m<sup>2</sup>. The cavity is indirectly connected to the lower containment compartment (BET) through the water tight door. Depending on the state of that door, two cavity types might develop, the “wet cavity” and the “dry cavity”, depending on the possibility of water flow from the lower compartment to the cavity. Both cases were analyzed and discussed in the next section.

Heat sinks are represented with 79 heat structures. The steel liner, the containment building wall, internal concrete and steel walls and floors are explicitly modelled. Five heat structures are used to model the steel liner and the containment wall. Internal walls and structures, such as the polar crane and fan coolers, are represented with 66 heat structures. Floors at three different elevations are represented with three heat structures. The last five heat structures represent the bottom concrete floor. The heat transfer coefficients for convective heat exchange between TH volumes and structures are calculated internally by the code. Total convective heat transfer areas are as follows:

1. Steel liner – 5950 m<sup>2</sup>
2. Containment building concrete wall – 6940 m<sup>2</sup>
3. Internal walls and structures
  - a. Concrete – 2940 m<sup>2</sup>
  - b. Steel (stainless and carbon steel) – 31150 m<sup>2</sup>
4. Floors (concrete) – 1560 m<sup>2</sup>
5. Bottom concrete floor (foundation) – 510 m<sup>2</sup>

### 3. RESULTS OF THE CALCULATION

#### 3.1 Accident Description

The analyzed transient was a station blackout which included the loss of both off-site and on-site AC power. The only systems available were passive safety systems: accumulators and the turbine driven AFW system. The high-pressure and the low-pressure safety injection pumps were disabled. Containment safety systems, fan coolers and sprays, were also inoperable. Following the loss of AC power, RCP seals will overheat due to non-existent cooling normally provided by the charging pumps, a break will be formed and coolant will be released from the reactor cooling system to the containment.

Reactor coolant pumps and the feedwater pumps were tripped at 0 s. At the same time the break at both RCPs was opened. Shortly afterwards, the reactor and the turbine were tripped due to the low cold leg coolant flow. Power-operated pressurizer and steam generator relief valves were disabled, as well as pressurizer heaters. Safety valves were operable, but only SG valves were actuated, since due to the LOCA conditions, primary system pressure decreased from the beginning of the transient and, thus, no overpressure on the pressurizer safety valves occurred that would lead to their opening.

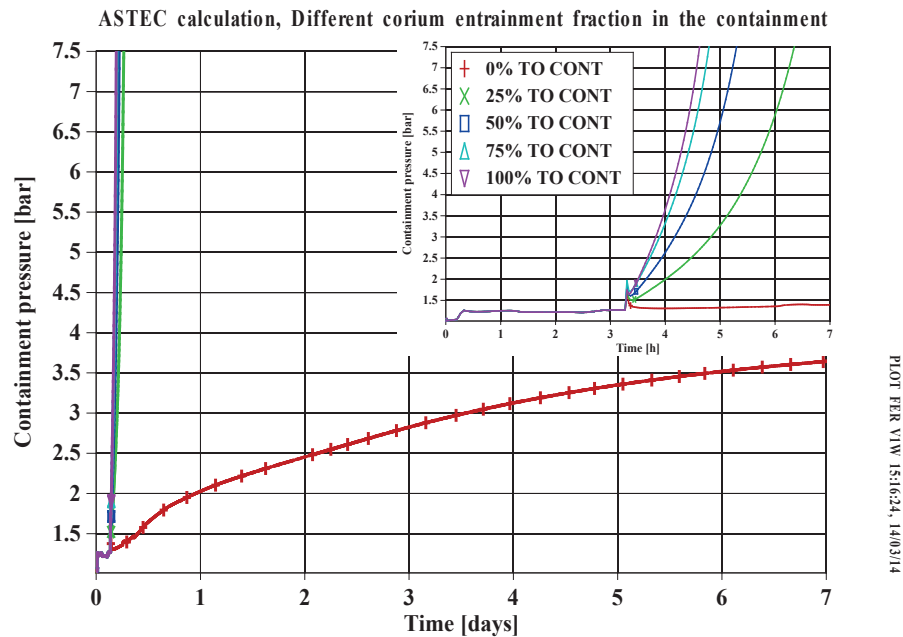
Five cases were analyzed depending on the fraction of entrained corium reaching the containment atmosphere after the breach of the reactor vessel. The fraction was varied in the increments of 25%, from 0% to 100%. Dispersed corium debris would heat up the air and the structures on which it adheres making it an extra heat source in the containment, along with the mass and energy release from the primary system.

Additionally, results of the “wet cavity” and the “dry cavity” calculations were compared. The cavity is separated from the containment by the water tight door. The door is closed during the normal NPP operation and only after its failure, caused by the pressure build-up during the MCCI, water could enter the cavity. The “wet cavity” model assumed no door was present from the start of the accident maximizing water inflow to the cavity and providing enhanced cooling of the corium. In the “dry cavity” model there was no connection between the cavity and the annular space surrounding it. However, some water accumulated in the cavity because of the condensation of steam released from the primary system, but its quantity was negligible.

#### 3.2 Containment Behaviour

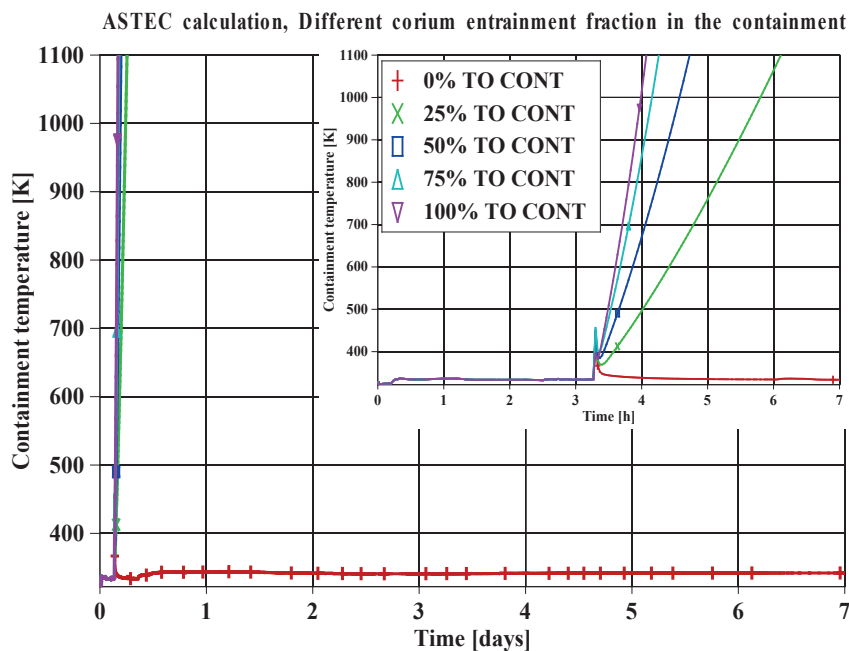
Containment pressures are shown in Figure 3 and containment temperatures in Figure 4. After the opening of the breaks and release of the primary coolant, the pressure will increase to 120 kPa and remain more or less constant during the next three hours. In the meantime, the reactor core will overheat and melt due to the absence of the active safety injection systems. Relocation of the molten material to

the RPV lower head will cause the heat-up and breach of the reactor vessel, and release of the corium into the containment cavity.



PLOT PER VIEW 15:16:24, 14/03/14

Figure 3. Containment pressure for different corium entrainment fractions



PLOT PER VIEW 16:00:35, 14/03/14

Figure 4. Containment temperature for different corium entrainment fractions

Discharge of the molten corium is followed by the blow-down of primary circuit gases. If the blow-down is significant enough; the primary pressure at the time of the vessel failure is around 5 MPa; it may cause entrainment of the corium debris by the hot gases flowing from the cavity to the other compartments of the containment. Dispersal of the corium as finely particulate droplets may potentially result in a rapid heating and pressurization (direct containment heating). Only a

fraction of the corium will reach the containment depending on the user's input. Five cases were analyzed with the fractions being set to 0%, 25%, 50%, 75% and 100%. When no DCH was taken into account, a steady pressure increase was calculated with the containment temperature being almost constant at 70 °C. The pressure rise was attributed to accumulation of incondensable gases released during the process of the molten corium concrete interaction. Decay heat of the fission products inside the corium was efficiently removed by conduction through the containment floor and by convection into the environment.

Corium entrainment led to fast temperature and pressure increase. In less than three hour time, for the case with the minimum fraction of dispersed corium, the containment pressure reached 7.5 bar, the value for which the containment failure probability is 50% according to the NPP Krško containment fragility curve. Heat transfer coefficient from corium droplets to the atmosphere was 500 W/m<sup>2</sup>K as recommended by the ASTEC development team and the heat transfer was enhanced by assuming a rapid thermal equilibrium between the droplets in the containment atmosphere which is a default option in the code [3].

In the case with no corium discharge in the containment, as already mentioned, the temperature was constant, but the pressure rose from 1.2 bar to 3.6 bar. The main reason was production of carbon dioxide during the MCCI process. Figure 5 shows partial pressures of gases in the containment. A direct influence of the CO<sub>2</sub> partial pressure on the total containment pressure can be observed. Immediately, after the MCCI started, hydrogen and carbon monoxide were produced as a result of oxidation of metals contained in the corium. Their accumulation and oxidation heat release were the reasons for the pressure and temperature increase in the first 11 hours. After all metals had oxidized, only CO<sub>2</sub> was produced afterwards. There was no abruptly pressure rise because no hydrogen or CO ignition was calculated to occur.

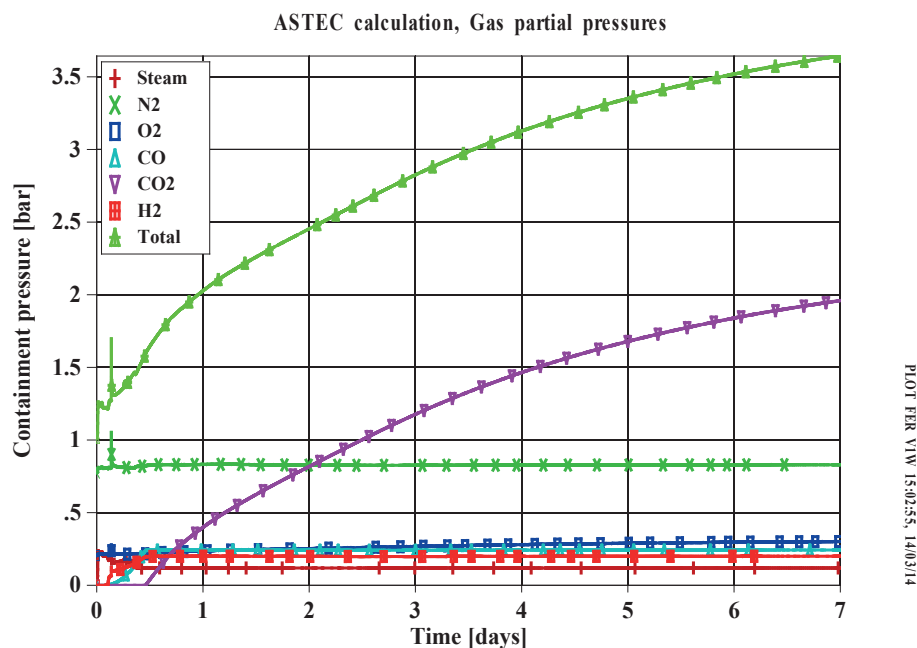
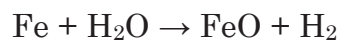
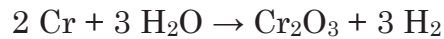
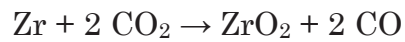


Figure 5. Gas partial pressures in the containment

Hydrogen, CO and CO<sub>2</sub> are products of the concrete decomposition by the molten corium. At temperatures 600–900 °C calcium carbonate is decomposed into calcium oxide and carbon dioxide [5]:



The reaction is endothermic, thus CaCO<sub>3</sub> absorbs energy of the radioactive decay of the fission products in the melt. The released CO<sub>2</sub> and steam produced by evaporation of water from the concrete will be used for the metals oxidation:



Oxidation of zirconium and chromium are exothermic reactions, while iron oxidation is an endothermic reaction [5]. The code assumes that all CO<sub>2</sub> is going to be spent on metals oxidation, so as long as there are free metal atoms, hydrogen and CO are released in the containment, but no CO<sub>2</sub>. Afterwards, calcium carbonate decomposition will be the only reaction associated with release of incondensable gases (CO<sub>2</sub>). This becomes apparent when gas masses are compared (Figure 6). Up to 11 hours of the transient, metals oxidation process generated H<sub>2</sub> and CO, while the mass of CO<sub>2</sub> was 0 kg. Metals consumption after 11 hours marked the start of CO<sub>2</sub> release and termination of H<sub>2</sub> and CO generation.

The final amount of gases produced during the accident is shown in Table I. Since CO<sub>2</sub> starts to be generated later in the accident, its mass is different than 0 kg only in the case with no corium entrainment. Hydrogen and CO masses depend on the calculation time and mass of reacted corium. The case with 100% corium entrainment fraction results with the lowest amount of hydrogen and carbon monoxide. The latter is only 0.2 kg because for CO to be produced, there has to be CO<sub>2</sub> available which is, on the other hand, mainly produced by the concrete dissolution. Assuming complete corium dispersal out of the reactor cavity, the temperature necessary for CaCO<sub>3</sub> decomposition will not be achieved and, thus, no CO<sub>2</sub> will be released. The amount of hydrogen is 8 kg higher than the mass generated during the oxidation of the reactor core in the in-vessel phase of the accident (206.6 kg). That additional hydrogen was mainly produced during the oxidation reaction of corium debris scattered throughout the containment with the steam already present in the containment atmosphere. In short, as the fraction of entrained corium increases, the MCCI process becomes less important and CO and CO<sub>2</sub> production decreases. Positive consequence of that is not only the pressure reduction but also the fact that CO is an explosive gas. Hydrogen is still being generated, but now, beside the MCCI, also during the oxidation of metals in the corium particles. That reaction is less significant than the corium oxidation in the reactor cavity due to a smaller amount of accumulated heat. The shortcoming of the

corium entrainment is the process of direct containment heating which results in a much faster containment pressurization.

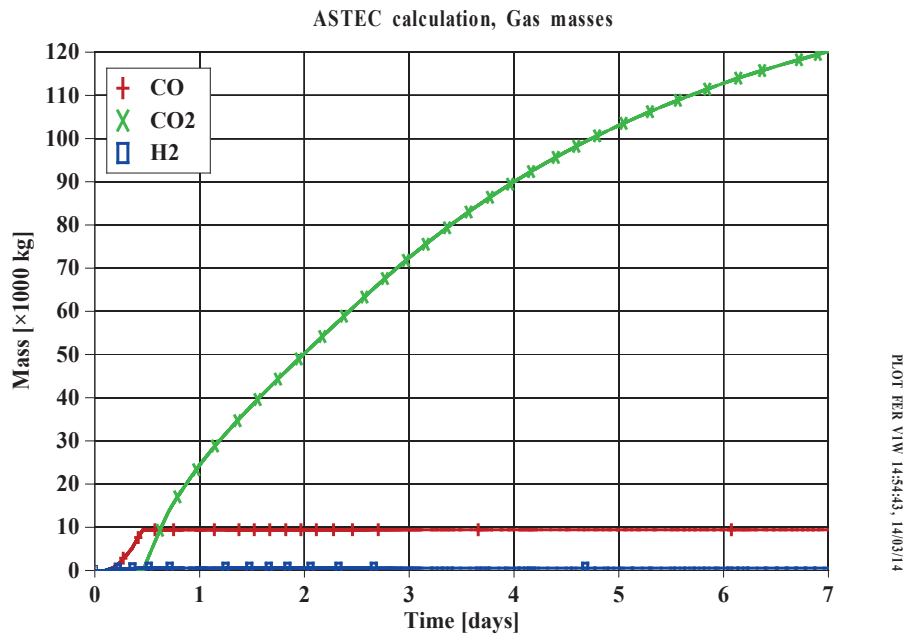


Figure 6. Mass of incondensable gases in the containment

Table I. Final amount of incondensable gases

Case	Hydrogen [kg]	Carbon monoxide [kg]	Carbon dioxide [kg]
0%	555.3	9392	120122
25%	321.2	1801	0
50%	272.7	230.1	0
75%	267.9	72.7	0
100%	214.7	0.2	0

The molten corium concrete interaction will erode the concrete as shown in a sketch on Figure 7. The MCCI is preceded by the processes of corium slumping from the vessel into the cavity and the primary circuit gases blow-down which both lasted for few seconds after the RPV failure. During the slumping there was no corium fragmentation in the water present in the cavity. In the ASTEC ex-vessel modules there is no simulation of the fragmentation process. The corium jet fragmentation can at present time only be accounted for in the ICARE lower head modelling. Therefore, without the DCH that could transport corium fragments outside the cavity domain, the MCCI simulation in the ASTEC is in that case starting with the corium composition and arrangement strictly as it is when entering the cavity from the vessel during the slumping process. At the end of the slumping phase, the corium is assumed to be located on the containment bottom, completely filling the cavity floor. The spreading area is relatively large (38.2 m<sup>2</sup>), so the initial corium thickness is less than 10 cm. Nevertheless, its potential for

concrete dissolution is large enough to cause severe damage of the containment floor.

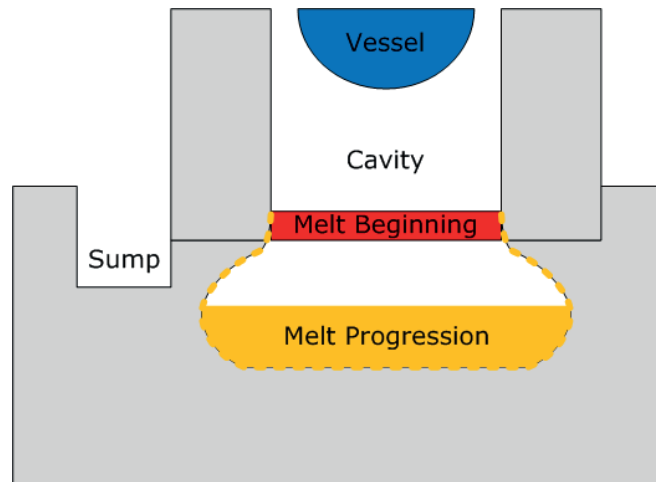


Figure 7. Cavity erosion during the MCCI

Figure 8 shows initial and final cavity temperature profiles, indicating concrete degradation during the MCCI. Maximum radial and vertical erosion depths are shown in Figure 9, while the mass of eroded concrete is shown in Figure 10. Concrete erosion is a progressive process that could not be mitigated due to continuous production of decay heat inside the melt. Hence, the mass of molten corium released from the vessel was 23.75 tons and the mass of dissolved concrete after seven days of molten corium concrete interaction reached 500 tons with the tendency to increase further. The cavity erosion was modelled to be two dimensional. The amount of liquefied concrete was calculated based on the data of the latent heat of fusion, corium-concrete phase diagrams and the concrete composition [2]. The former two data-sets and appropriate correlations are incorporated in the code package. The concrete composition was entered in the input file. Bali correlation was used to compute the heat transfer coefficient between the corium and the concrete [6].

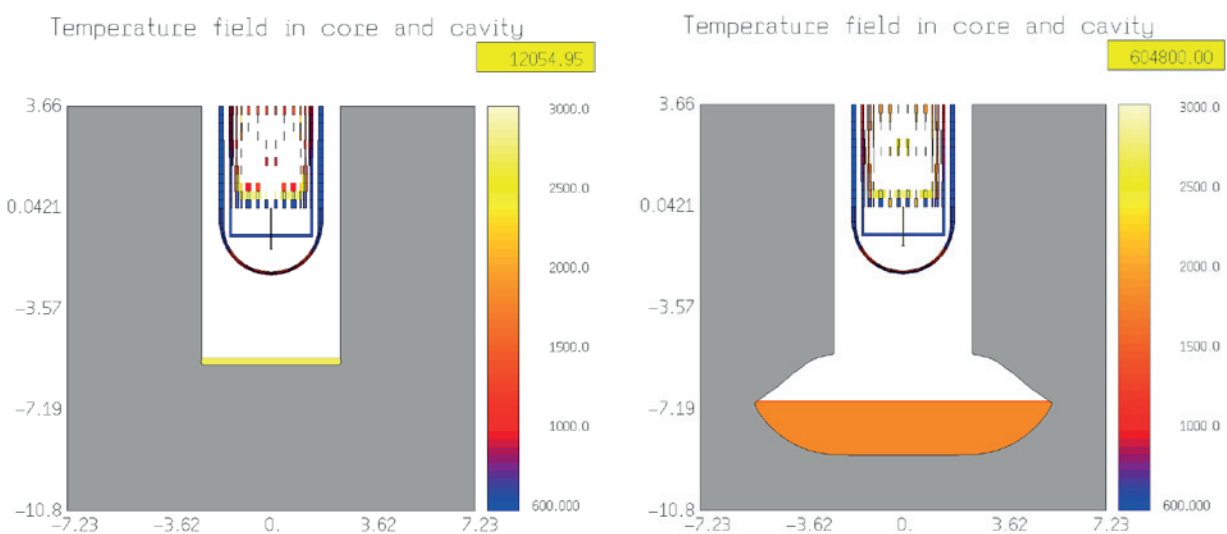


Figure 8. Initial and final cavity temperature profiles as calculated by ASTEC

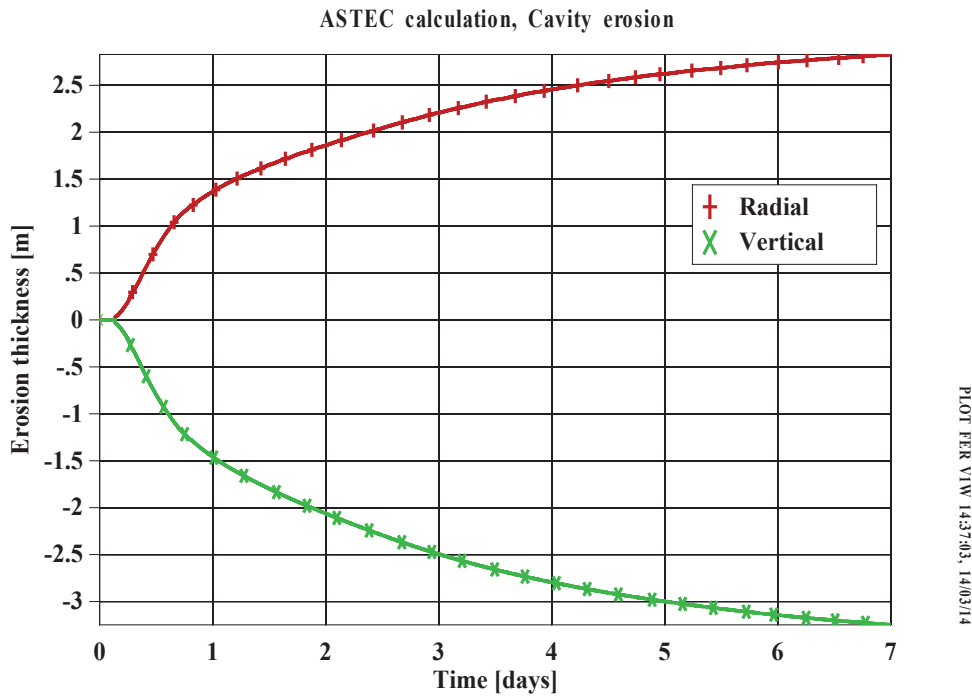


Figure 9. Cavity erosion depths in radial and vertical directions

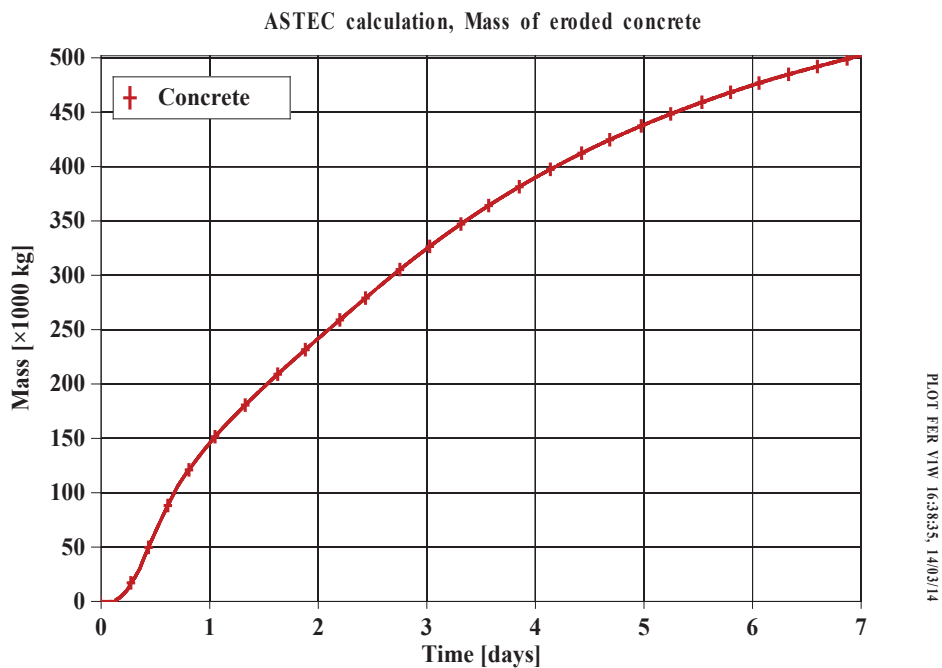


Figure 10. Mass of eroded concrete

### 3.3 Influence of Cavity Flooding

Previous calculations were performed with the water already present in the cavity before the melt was released out of the reactor vessel. Water entered the cavity compartment through the narrow space between the lower compartment and the cavity areas. Normally, that connection does not exist because the space is

closed with the water tight door preventing the leakage. The door could only be breached by the over-pressurization during, for example, the process of MCCI. A calculation with no cavity flooding was performed and its results were compared with the “wet cavity” analysis results, Figure 11 and Figure 12.

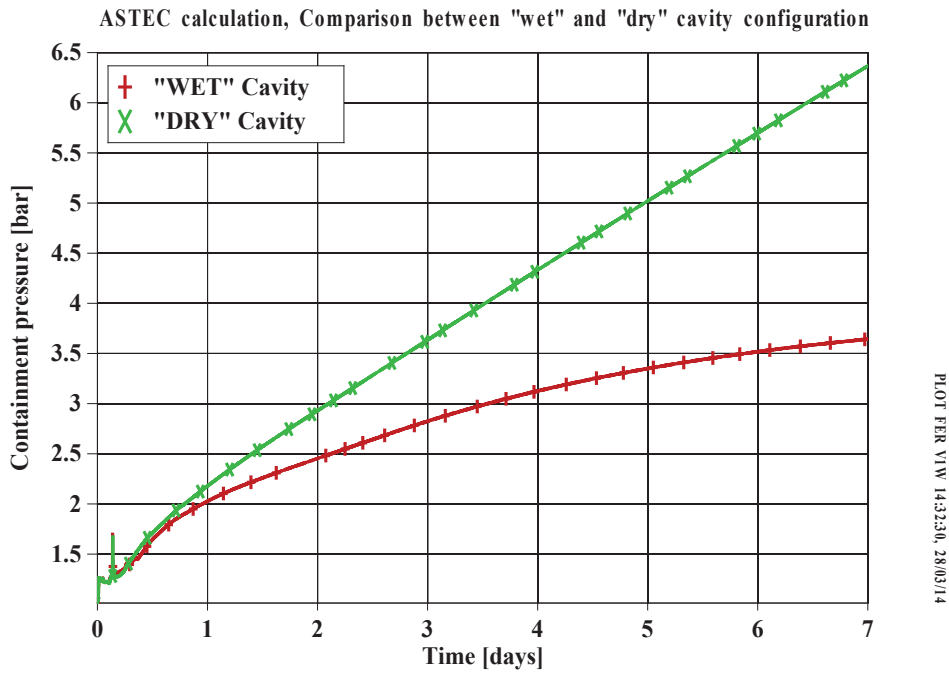


Figure 11. Containment pressure for the cases with and without the water present in the cavity

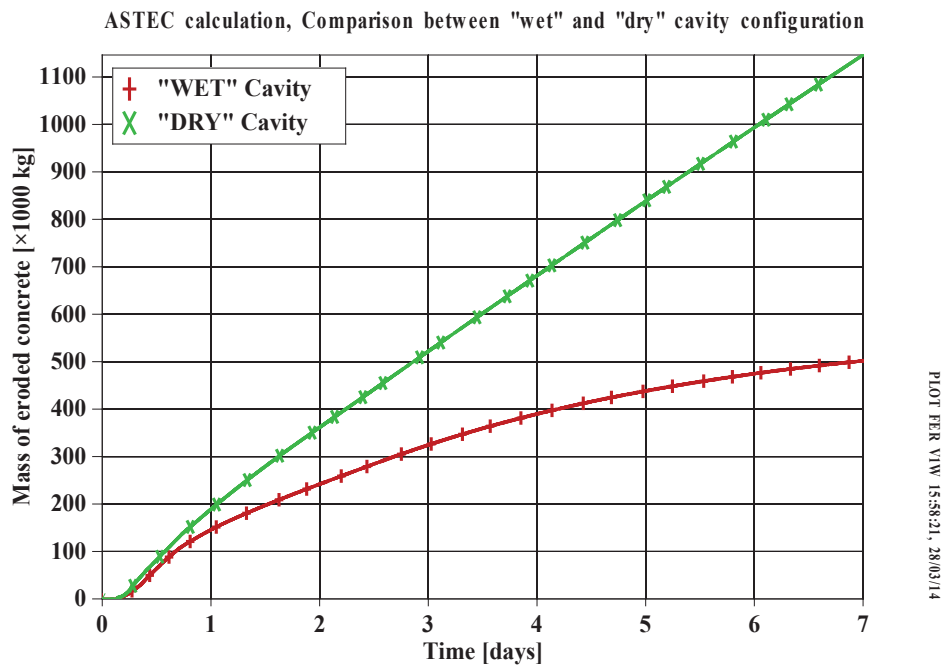


Figure 12. Mass of eroded concrete for the cases with and without the water present in the cavity

A dry cavity at the time of corium discharge from the RPV in the containment influenced latter containment behaviour. The pressure increased faster than in the case with the flooded cavity because more carbon dioxide was released during the MCCI. The molten corium concrete interaction was more intensive; more concrete was dissolved and larger quantities of H<sub>2</sub>, CO and CO<sub>2</sub> were released.

The impact of the dry cavity was not as important as the DCH regarding the containment integrity. The rate of pressure rise was more than ten times higher for the DCH than for the MCCI mechanisms. The DCH was accompanied with a fast temperature increase caused by the containment atmosphere heat-up. The heat transfer from the dispersed corium to the air and steam forced the pressure to increase with the same rate as the temperature. On the other hand, there was no significant temperature increase during the MCCI. The process of concrete erosion is mainly endothermic [5] except for the initial period of metal oxidation. Decay heat inside the corium was removed by conduction through the containment foundation, while on the top of the molten material, formation of a crust altered the heat transfer to the surrounding air.

#### 4. CONCLUSION

PWR containment behaviour during a hypothetical severe accident was analyzed with the ASTEC code. The sequence included release of the coolant from the primary system and discharge of corium after the breach of the reactor pressure vessel. The containment was modelled with ten control volumes representing real compartments such as steam generator, pressurizer, sump and cavity compartments. The largest volume was the containment dome above the elevation of the uppermost floor slab.

Containment integrity depends on the inside pressure and temperature. The initial release of steam only slightly affected the pressure. Main reasons for the containment heat-up and pressurization were the molten corium concrete interaction and the direct containment heating. During the MCCI molten corium dissolves the concrete and incondensable gases hydrogen, carbon monoxide and carbon dioxide are released. Primarily, CO<sub>2</sub> is responsible for the pressure rise because of its large quantity. Temperature increased by 10 °C shortly after the start of the concrete erosion due to oxidation of metals in the corium but afterwards it did not change a lot because concrete decomposition is an endothermic process. The MCCI is an undesirable severe accident event for the reason of producing flammable and explosive gases H<sub>2</sub> and CO. No hydrogen or CO deflagration was calculated to occur.

Molten debris dispersion in the containment atmosphere (DCH) led to rapid heat-up and pressurization. Decay heat in the melt was transferred to containment structures and walls, and also to air and steam which, due to low heat capacity, experienced fast temperature rise. The containment pressure reached the threshold value for the rupture three hours after the release of the corium in the containment.

In the case with no DCH, the containment pressure was less than the limiting pressure for more than a week, thus, providing important time window to undertake mitigating actions.

## ACKNOWLEDGMENTS

The authors would like to express their gratitude to the IRSN for providing the ASTEC code and to the NPP Krško for providing the plant data.

## REFERENCES

- [1] P. Chatelard, N. Chikhi, L. Cloarec, O. Coindreau, P. Drai, F. Fichot, B. Ghosh, G. Guillard, "ASTEC V2 Code: ICARE Physical Modelling", ASTEC-V2/DOC/09-04, DPAM-SEMCA-2009-148, Revision 0, 2009.
- [2] F. Duval, M. Cranga, "ASTEC V2 MEDICIS MCCI Module: Theoretical Manual", DPAM/SEMIC 2008-102, Revision 1, 2008.
- [3] M. Cranga, P. Giordano, R. Passalacqua, C. Caroli, L. Walle, "ASTEC V1.3: RUPUICUV Module: Ex-vessel Corium Discharge and Corium Entrainment to Containment", ASTEC-V1/DOC/03-19, Revision 1, 2003.
- [4] C. Seropian, F. Jacq, L. Walle, "Description of the CORIUM Module of the ASTEC Code", ASTEC-V1/DOC/04-11, Revision 0, 2004.
- [5] Z.P. Bažant, M.F. Kaplan, "Concrete at High Temperatures: Material Properties and Mathematical Models", Longman (Addison-Wesley), monograph and reference volume, 412 + xii pp., London, 1996.
- [6] J.M. Bonnet, "Thermal Hydraulic Phenomena in Corium Pools for Ex-vessel Situations: The Bali Experiment", In Proceedings of the 8<sup>th</sup> International Conference on Nuclear Engineering 2000, ICONE-8, number ICONE-8177, Baltimore, Maryland, USA, 2000.

ŽELJKO TOMŠIĆ

[zeljko.tomsic@fer.hr](mailto:zeljko.tomsic@fer.hr)

University of Zagreb Faculty of Electrical Engineering and Computing  
Department of Energy and Power Systems

## FROM MARKET UNCERTAINTY TO POLICY UNCERTAINTY FOR INVESTMENT IN POWER GENERATION: REAL OPTIONS FOR NPP ON ELECTRICITY MARKET

### SUMMARY

In the electricity sector, market participants must make decisions about capacity choice in a situation of radical uncertainty about future market conditions. Sector is characterized by non-storability and periodic and stochastic demand fluctuations. Capacity determination is a decision for the long term, whereas production is adjusted in the short run. Paper looks on the main contributions in investment planning under uncertainty, in particular in the electricity market for capital intensive investments like NPP. The relationship between market and non-market factors (recent UK policy example) in determining investment signals in competitive electricity markets was analysed. Paper analyse the ability of competitive electricity markets to deliver the desired quantity and type of generation capacity and also investigates the variety of market imperfections operating in electricity generation and their impact on long-term dynamics for generation capacity. Paper analyses how price formation influences investment signals. Number of factors (including market power, wholesale price volatility, lack of liquidity in the wholesale and financial market, policy and regulatory risks etc.) contribute to polluting the price signal and generating sub-optimal behaviour.

**Key words:** power generation, nuclear power plant, electricity market, market uncertainty, investments, generation capacity

# 1 INTRODUCTION

The recent high volatility in fuel markets, combined with environmental regulation policies, has introduced major uncertainties into the planning of generation capacity expansion. These uncertainties make generators' decisions to invest in new capacities more difficult.

Volatile fuel prices, concerns about the security of energy supplies, and global climate change are coinciding to strengthen the case for building new nuclear power generation capacity.

There is an emerging consensus that there is no obvious “silver bullet” for addressing the global energy and climate challenge - the solution will be comprised of a variety of technologies on both the supply and demand side of the energy system. In addition to energy efficiency and low-carbon renewable options, two technologies that could do much of the heavy lifting in the future are carbon capture and storage (CCS) and nuclear power (NP). However, the views on NP and its potential role in meeting the projected large absolute increase in global energy demand, while mitigating the risks of serious climate disruption, are highly divergent. Part of the continuing controversy is due to the large risks and uncertainties underlying the cost elements of NP and electricity market price. These risks and uncertainties are reflected in the wide range of cost estimates. The cost overruns and schedule delays of Finland's new Olkiluoto plant and French Flamanville, are rekindling old fears about NP being far too complex and costly, and raising new questions about the viability of new nuclear plants, especially in deregulated electricity markets. Indeed, the costs of nuclear power stations (and large coal-fired power stations, particularly those with carbon capture and storage) remain uncertain. On the other hand, the fact that countries seem keen to build nuclear power stations suggests that their relative cost compared to low-carbon alternatives still seems attractive to at least some potential investors.

Proponents argue that in relation to the objectives of electricity supply security, resource efficiency, and mitigating the threat of climate change, NP performs very well. NP represents a well-established technology for generating electricity that produces no carbon or other climate-relevant emissions; NP is amenable to significant scaling-up and thus can provide large amounts of power; and NPPs use a natural resource (uranium) with advanced technologies, it could provide enough fuel to meet the world's electricity needs for several centuries. Sceptics claim that NP is costly and technically complex. It involves the use of highly toxic materials that must be kept secure from attack or theft. Moreover, a viable technology for the permanent disposal or reprocessing of spent nuclear fuel has not yet been fully demonstrated. Finally, even in a carbon-constrained world, NP may be less economically attractive than a host of decentralized energy efficiency and distributed generation technologies.

## **2 INVESTMENT AT ELECTRICITY MARKET**

In several industries, market participants must make decisions about capacity choice in a situation of radical uncertainty about future market conditions and decide on the level of output to be produced after the state of nature has unravelled. These industries are normally characterised by non-storability and periodic and stochastic demand fluctuations. In these cases capacity determination is a decision for the long term, whereas production is adjusted in the short run.

In the electricity sector, generation must take place just in time, and ought to ensure second by second supply demand balance, but capacities need to be installed well in advance, at times when companies face considerable demand and cost uncertainty when choosing their capacity. For electricity markets it is moreover well-known that demand fluctuates systematically over each day, month or year. It is natural to expect that companies try to anticipate those patterns when they make their investment decisions. Electricity generation is generally considered the typical example of an activity that is most effectively carried out by establishing a competitive market.

But also investment in new power is essential for a well-functioning electricity market. Still, today decisions pertaining to investment in new capacity are surrounded by considerable uncertainties about the future economics of the projects. One reason is that in a deregulated market private investors typically have to bear a greater portion of the investment risk compared to a monopoly utility in a regulated market. This favours flexible investment alternatives with short-lead times and low capital requirements. Moreover, energy and climate policy – with feed-in tariffs for RES or green certificate system and the European emission trading systems for CO<sub>2</sub> (EU ETS) - may add to investment uncertainties. Delayed and uncertain permitting processes also increase investors' risks.

## **3 SECURITY OF SUPPLY ON ELECTRICITY MARKETS**

Security of electric power supply become recently very important issue in energy policies but the adaptation of command and control rules that entailed a certain level of security of supply in the monopolistic context to a state of competition has not been trivial. It has represented the transition from a monopolistic organisation to a competitive one. This normally means an increase

(rather than reduction) in the level of complexity in the market structure and regulation.

Matters related to security of supply can be defined in many different ways, and the term Security of Supply can mean different things in different countries and in a variety of contexts. It also includes a number of different concepts.

Security of supply incorporates the sufficiency of supply sources and/or production capacity to meet peak demand at a reasonable cost (*Supply Adequacy*). It also includes the availability of flexible and reliable import, transmission and production capacity to deliver energy when and where it is required (*Reliability*). Finally, security of supply also takes into consideration the ability of the system to mitigate the risk of one or more sources of supply becoming restricted or very expensive (*Diversity*).

The definitions that are used in the sector for issues related to Reliability and Security of supply [1].

- Supply Adequacy is a measure of the capacity of the power system to serve the aggregate electric power and energy requirements of the customers within the quality standards (voltage limits and ratings) of the system and taking into consideration planned and unplanned outages of the system components.
- Reliability of the system means in general, the ability to deliver at each point in time and at each location of the network, within a specified safety standard, the amount of power desired.
- Security of supply covers a wide range of measures of power system ability to withstand sudden disturbances (such as electric short circuits or unanticipated losses of system components). Security of power supply is a complex concept that involves a number of actions necessary to guarantee system integrity. It includes supply adequacy, reliability and diversity.

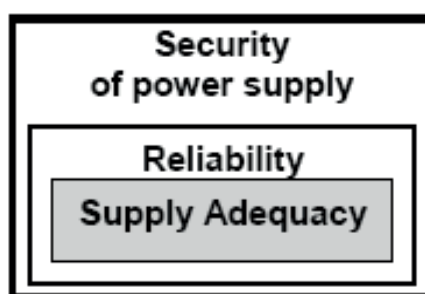


Figure 1 Security of power supply, Reliability, Supply Adequacy [2]

### 3.1 Supply adequacy issues in electricity markets

Investment decision under uncertainty in energy markets has attracted significant attention in recent years, and policy makers in many countries are debating whether competitive wholesale electricity markets are providing appropriate incentives to stimulate adequate investment in new generation

capacity. Looking at the evidence deriving from different markets shows that organised wholesale markets are currently failing to support investment in generation capacity, mainly because of the inefficiency of price signals during peak hours.

One idea to solve this problem is Capacity payments that maybe will be able to restore efficient investment incentives. Some recent policy contributions highlight that policy intervention may have a significant effect on the quantity (and type) of additional capacity installed.

Non-storability and the periodic fluctuation of demand and supply have a major impact on the economic behaviour of markets presenting these characteristics.

In the last century, the electricity supply has been designed mainly in two variants:

- A vertically integrated public monopoly; or
- Different local monopolies for the distribution-retailing phase for small customers and a national company in the production-transportation phase, integrated by a long-term contractual relationship.

The opening up of the network system imposes a new organisational style based on competition between producers. According to this new model there are phases in which competition is possible, and others characterised by monopolies. The distribution and transportation networks are considered natural monopolies, thus controlled by a regulating body that has to ensure access to every company, whereas the production and the selling (wholesale and retail) are free activities based on competition. With the liberalisation process of the electricity market, regulated monopolists have been transformed into competing companies.

Competitive wholesale markets for electricity and energy often fail to provide adequate net revenues to attract investment in generation to meet reliability criteria. In addition, it is also argued that short-term price volatility is more extreme and frequent than in other commodity markets, because storage for electricity is too costly for commercial application.

Lastly, another factor that is considered crucial when evaluating the adequacy of new capacity investment is the possibility, for the policy makers, to change market rules and market institutions.

Impacts to investment decision can be market based and policy based risk factors.

Impacts of *typical market based factors* to electricity investment are:

- i) large variations in demand over the year;
- ii) the need to balance physically the supply and demand and supply at every point of the network;
- iii) non-storability of electric power;

- iv) inability to control power flows to most individual consumers;
- v) limited use of real time pricing by retail consumers;
- vi) necessity to rely on non-price mechanism (blackouts) to ration imbalances, because markets cannot clear quickly enough to do so.

In this context in order to make sure that an economic signal (price of the electric power and ancillary services) reaches the market it should exist mechanism which is able to make consumers' preferences explicit to suppliers.

*Policy based risk factors* are those related to the various forms that policy intervention may take in energy markets in order to minimise the effects of the specific features of the energy market on consumers. It is possible to distinguish between “ordinary” market uncertainties and uncertainties that are induced by policies. Market and other external uncertainties such as fluctuations in fuel prices and reservoir levels can to some degree be perceived as easier to manage than the uncertainties that stem from various policies. However, policy uncertainty either encourages investors to adopt a - wait and see strategy or increases the risk premium they require on their investments. Both can increase costs for consumers by pushing up market prices. At the same time environmental policies may require additional investments to meet tighter standards, or for some capacity to close.

The problem is particularly acute for investments such as nuclear, carbon capture and storage (CCS) and renewables that rely not on a tangible commodity that consumers need (energy), but on markets created by government to reflect benefits to society (carbon reduction). They typically consist in price restrictions, regulatory uncertainty and regulatory intervention.

- *Price restrictions* - A price cap is sometimes required to protect consumers against excessive prices in times of scarcity. This is normally a regulatory intervention with high distorting power when it comes to investment decisions because it is difficult to determine the optimal level of an efficient price cap. As a consequence it is typical to have a long-run average shortage of capacity and too little reliability in most electricity system.
- *Regulatory uncertainty* – Investment risk is significantly affected by regulatory intervention. These factors are considered among the main drivers for inadequate generation capacity. Policies intervention may cause prices in electricity not to raise high enough to support new investments, particularly because regulators will be unwilling to allow prices to spike during periods of system tightness due to concerns surrounding market power.

#### **4 THE IMPACT OF LIBERALIZATION OF MARKETS ON INVESTMENT CHOICES IN NUCLEAR POWER**

Since future investments in nuclear power generation capacity will be made within this new market context, it is interesting to see the impact of this modification on investments choices made by electricity producers. In particular it

is question if electricity generators who will have chosen this production means will continue to prefer large capacity units as they did in the past, to optimize the benefit of the size effect and thus enjoy attractive production costs, or if the uncertainty related to the competitiveness of electricity markets will encourage them to choose smaller units to reduce the risk. In other words, how to choose between the flexibility of the modular investment and the efficiency of the high capacity unit due to increase in economy of scale?

Intuitively, the solution offered by modular power plants would appear to be most suitable for a competitive environment with strong uncertainties about the supply and the price of electricity. Because of the irreversibility of the investment in the high capacity unit, it is optimal for the producer to invest only if the market price of electricity is high enough compared to the cost of electricity. The option of making sequential decisions when several medium sized nuclear modules are used enables the producer to be more aggressive in its investment strategy by initiating the construction of the first unit at a smaller critical price of electricity.

The presence of uncertainties of future returns and costs are amongst the more critical factors affecting the willingness to invest.

In the context of a liberalized market environment, investment in power generation comprises a large and diverse set of risks. These business risks include [3]:

- factors that influence the demand for electricity and impact the supply of capital and labour;
- regulatory controls (economic and non-economic) and political risks that generally affect revenues, costs, and financing conditions;
- price and volume risks in the electricity market;
- fuel price and supply risks; and
- risks arising from the financing of investment.

The presence of uncertainties of future returns and costs are amongst the more critical factors affecting the willingness to invest. There is however little consensus in the economic literature on how and to what extent policy uncertainty connected to carbon pricing specifically (e.g., emissions trading schemes) will affect investment behaviour in the power sector suggests that climate policy will not add any significant uncertainties for electricity investors in the future, and even stimulate firms' investment incentives, at least if the policy is consistent over a longer time period. The main obstacle for investors is instead the fuel price. Thus, it is important to analyse how the implementation of a specific policy affects the behaviour of the investor.

#### **4.1 Market uncertainty and NPP**

The actual competitiveness of NPP must be analysed in a wider perspective. It cannot only rely on the analysis of greenhouse gas emissions; since nuclear is a very complex and expensive technology and many more aspects come into play. The liberalization of electricity markets shows that the fate of nuclear is strongly

affected by energy market structure. The loss of some main favourable conditions (governmental support, certainty of demand, a price regime based on recovering the production cost increase by charging higher prices to consumers, etc.), lead to a drop of the number of nuclear plants built from 1990 to 2005 to only 1.7 nuclear plants per year (mainly in developing countries) compared to 17 nuclear plants per year built in the period 1970-1990. In liberalized electricity markets decisions about energy technologies are driven by the expected returns, taking into account the risks (afforded by the company, rather than by consumers as in a monopoly regime) linked to costs and revenues. Moreover, nuclear energy has to face new competitors such as renewable source technologies, characterized by a lower carbon content, better environmental footprint, increased population acceptance and higher growth rates favoured by cost reduction driven by technological innovation.

## 5 ECONOMIC AND FINANCIAL RISKS OF NUCLEAR POWER

From a strictly economic point of view three main risk factors are must be considered: (a) construction time, (b) investment costs and (c) variability of operating costs. Most of the existing plants have been built under a monopolistic regime, with governmental guarantees and controlled market prices, low capital costs and low investment risk. The investment risk, and the capital cost increased with deregulation of energy markets and were charged to electrical companies, penalizing capital intensive investments projects with long time return on investment and low technological flexibility [4]. Instead, investments in alternative power sources, like combined cycle gas turbine plants and smaller renewable plants have been favoured [5]. In such a context, investments on nuclear sector became uncertain and very variable. Considering a large size nuclear plant (1000-1600 MW), construction costs are up to 10 or 15 times higher than those required for the construction of a natural gas plant (100-700 MW). The projected costs also tend to increase due to the extension of construction time (cost overruns). Finally, costs for nuclear plants decommissioning are estimated as about 25% of the original investment costs. The total costs of a nuclear plant can be split into about 60-75% *fixed* costs (capital repayments, interest allowed, decommissioning costs) and 25-40% *variable* costs (for instance, the cost of uranium and labour). Unlike gas and carbon plants, the share of nuclear fuel cost on total production costs is small.

While the cost of electricity uncertainty factors related to security aspects, licensing, escalation of decommissioning costs, radioactive wastes disposal, might contribute to increase the financial risk perceived from private investors and, consequently, the level of expected return. Rogner and Langlois [6] highlight that the future of nuclear power depends on the competitiveness strategies that industries, supported by technological innovation, will adopt to guarantee the economic and financial sustainability and reduce the safety risks. Such targets require strong political support to the nuclear industry. For instance, the

problems related to waste disposal and safety involves suitable technological solutions and communication, able to achieve social consensus. Therefore, an energy policy which includes the use of nuclear power among its energy sources will have to handle three problems: overcoming the scarcity of public funds, choosing the best nuclear technology available, and finally conducting a cost-benefit analysis to compare nuclear with others renewable sources [7].

In liberalized markets investments are profit motivated, with the choice of technology left to the market. The redistribution of risk among the different stakeholders is likely to make nuclear generation unattractive for an investor, even when its levelized costs are similar to the levelized costs of the dominant technology, for several reasons.

First, investors have a strong preference for a shorter payback period, which makes investments with short lead time more attractive. Nuclear lead times (5 years in the most optimistic scenario given the historical record) are, for engineering and licensing reasons, much longer than CCGT lead times (2 years).

### **5.1 The challenge of financing nuclear power**

With its capital intensity and cautionary experiences of engineering difficulties and regulatory creep during construction, new nuclear build is likely to require a substantial risk premium over competing technologies.

Given all these challenges to new nuclear build, what explains the 2004 decision to build a new nuclear power unit in Finland? The large capital costs of the plant have been financed by very long-term power purchase agreements. Interest in such long-term agreements, which are rare in liberalized markets, has been triggered by the specificities of local industries that have very long investment cycles and are extremely sensitive to the price of electricity. The Finnish electricity company Teollisuuden Voima Oy (TVO) is a cooperative grouping of local utilities and large industrial consumers, which are mainly paper makers with a very long investment cycle (over 40 years). Each shareholder will enjoy electricity at production cost during the life of the plant (60 years), i.e. at a very stable price, in proportion to its share, as well as holding a useful option on the future carbon price.

These long-term power purchase agreements enabled financing at low cost, which substantially improves nuclear economics. The Finnish case is therefore in many ways reminiscent of the institutional environment that made nuclear a competitive technology in the days of regulated monopoly (at least for certain fuel price configurations), through the transfer of investment and operation risks to consumers via contractual arrangements.

The Finnish example reminds us that low discount rates are obtainable in liberalized markets when the risks have been adequately mitigated, in this case by very long-term effectively fixed price power purchase agreements with large, credit-worthy consumers who necessarily (given their involvement in the forest industry) must take a very long-term outlook. It is not impossible to identify such consumers in other liberalized markets, but the dominant assumption is that electricity

consumers are generally uninterested in hedging their risk exposure to electricity price fluctuations.

Vertically integrated companies with both generation and retailing can effectively internalise the risk of wholesale power price volatility without an explicit contract, and are thus well placed to hedge wholesale price risks.

## **5.2 The potential financial benefits of nuclear power**

There are potentially two attributes of nuclear power generation that could make it more appealing to investors. First, nuclear generation costs are insensitive to both gas and carbon prices (as are most renewables). Therefore, rising gas prices and carbon trading or carbon taxes will make nuclear more competitive against CCGTs and coal-fired plants. Second, investing in nuclear can be thought as a hedge against the volatility and risk of gas and carbon prices for a (large) generating company. The uncertainty over the evolution of gas and carbon prices implies that there is an option value associated with being able to choose between nuclear power and other fossil fuel technologies in the future. Moreover, the hedging value of a nuclear power investment to a company is not restricted to the insensitivity of this plant to gas and carbon price risks. For a company already operating some fossil fuel generation plants, investing in a nuclear plant reduces the company's overall exposure to fossil fuel and gas prices.

While most valuation studies of competitive generation technologies take account of different gas and carbon prices through sensitivity analysis, as far as the authors know, there is no published study valuing nuclear as a hedge against uncertain gas and carbon prices from a company perspective. Assessing the economics of a nuclear or CCGT power plant investment from a company perspective requires taking into account the complementarity of the risk-returns profiles of the different technologies that the company operates.

## **6 INVESTMENT IN ELECTRICITY GENERATION - THE UNCERTAIN FINANCIAL AND ECONOMIC FUTURE**

If nuclear power is relevant to future energy needs, several factors must be taken into account. While electric growth in developed countries has been very low over the last decade, there is no assurance that this trend will continue. Even growth that is quite modest by historical standards would mandate new plants. Replacement of aging plants will call for still more new generating capacity.

In addition to the slowdown in electric load growth, power plants also have been cancelled and deferred due to the widely acknowledged deterioration in the financial condition of utilities.

Looking ahead, the prospects for substantial numbers of new central station power plants appear fairly uncertain. The prospects for more nuclear plants appear even more uncertain.

The ratio between electricity growth rates and GDP growth rates has indeed dropped.

Future growth of GDP is a major source of uncertainty, both because income and industrial production are assumed by economists to have major impacts on electricity demand, and because of some deep uncertainties about the future direction of the economy. Even the fairly narrow range of GDP growth rates of 2 to 3 percent that has been assumed by the major electricity demand projections implies a range of electricity demand growth rates of about 2 to 3 percent over the long run if electricity demand follows the income response patterns identified in recent the past.

Future electricity prices and their impacts are a second source of uncertainty about electricity demand growth. This is both because there is disagreement about future change in electricity prices and because there is uncertainty about how electricity demand responds to electricity prices.

There is generally less agreement about the impact of electricity prices on electricity demand than there is about the impact of changes in GDP. Most analysts agree that the short-run response of electricity demand to an increase in electricity prices is very limited.

The combined effect of uncertainty about future electricity and natural gas (and oil) prices and uncertainty about how electricity demand responds to changes in electricity prices is enough to explain a range of uncertainty in electricity demand from very slow growth to quite rapid growth.

Power companies' executives contemplating the construction of long lead time power plants must contend with considerable uncertainty about the probable future growth rates in electricity demand.

In summary - the need for new power plants depends on both the growth rates in electricity demand and on the need for replacement of existing generating capacity.

## **7 NUCLEAR POWER GENERATION: COST-BENEFIT ANALYSIS UNDER UNCERTAINTY**

Few years ago started so called nuclear renaissance that could be attributed to:

- An extremely strong record of global nuclear operations, with no high-profile incidents, for over two decades helped shift the perceptions about the environment and health risks of the nuclear energy.
- There was a fading memory of the Three Mile Island and Chernobyl accidents.
- High volatility in the fossil fuel prices called for an increased diversity in electricity generation, and

- Increased public concern over the greenhouse gas emissions meant that nuclear energy was one of the leading candidates to shoulder the increased future energy demands.

The events in Fukushima however derailed the onset of a nuclear renaissance with the focus back on the safety of NPP. These events are likely to cause major regulatory changes thus further increasing the uncertainties in already uncertain economics of the nuclear industry. It can be argued that the nuclear renaissance began faltering even before the unfolding of events at Fukushima. This was due to the concerns over the large risks and uncertainties underlying the cost elements of nuclear power. These risks and uncertainties were reflected in the wide range of cost estimates for nuclear power plants. The cost overruns and schedule delays of Finland's new Olkiluoto plant and France's Flamenville plant are rekindling old fears about nuclear power being far too complex and costly. This raises new questions about the viability of new nuclear plants, especially in deregulated electricity markets.

Negative wholesale prices have become more common as European countries turn to renewables, particularly Germany with its forced march away from nuclear power, known as the *Energiewende*. Neighbours such as Poland and the Czech Republic complain that power surges from Germany are playing havoc with their grids [8]. Across Europe a strange consequence of subsidised renewables is that some governments now want to pay power companies to maintain the capacity to produce electricity from fossil fuels to ensure that backup power is available. More perversely, Europe is burning more heavily polluting coal at the expense of cleaner and more flexible gas. This is because coal is cheap, the gas market is far from liquid and the carbon-emissions systems broken [8]. Therefore, in the longer term, increasing concerns about the CO<sub>2</sub> emissions added to the need for electricity in bulk without intermittency may imply stronger prospects for nuclear power. The future of nuclear power depends on resolving the issues of safety of operations, safe management of radioactive wastes and measures to prevent proliferation [9]. However, in a deregulated electricity market, the economics of NPPs will also be an important determinant of nuclear energy's role in the future global energy mix.

Current electricity price on Power Exchanges (Figure 2 show recent prices of electricity and CO<sub>2</sub> allowances on EEX and HUPX power exchange and base price for next year) are so low that no new Power plant can be competitive on electricity market and that almost all investment will be in renewable energy sources because of support schemes (feed-in tariffs or Green certificates).

New nuclear generating capacity would give rise to direct costs as well as a range of external costs and benefits. These would call for the valuation of the following:

- environmental benefits - reduced GHG emissions to be gained from adding nuclear rather than coal- or gas-fired generating capacity;
- fuel mix diversification value of nuclear power as a hedge against uncertain fossil fuel and carbon prices;

- costs of radioactive waste disposal;
- risks associated with radioactivity release from all fuel cycle activity;
- risks of proliferation from the nuclear fuel cycle; and
- financial liabilities arising from the back-end activities of the nuclear fuel cycle-e.g., decommissioning and waste management.

It must be stated at the outset that it is difficult to quantify the costs and risks related to nuclear safety and especially to nuclear proliferation. It should also be noted that the original risk analysis of nuclear power might have underestimated the true probability of reactor meltdown. And while modern reactors are claimed to achieve a very low risk of serious accidents, this needs to be assessed as it is dependent on “best practices” in construction and operation.

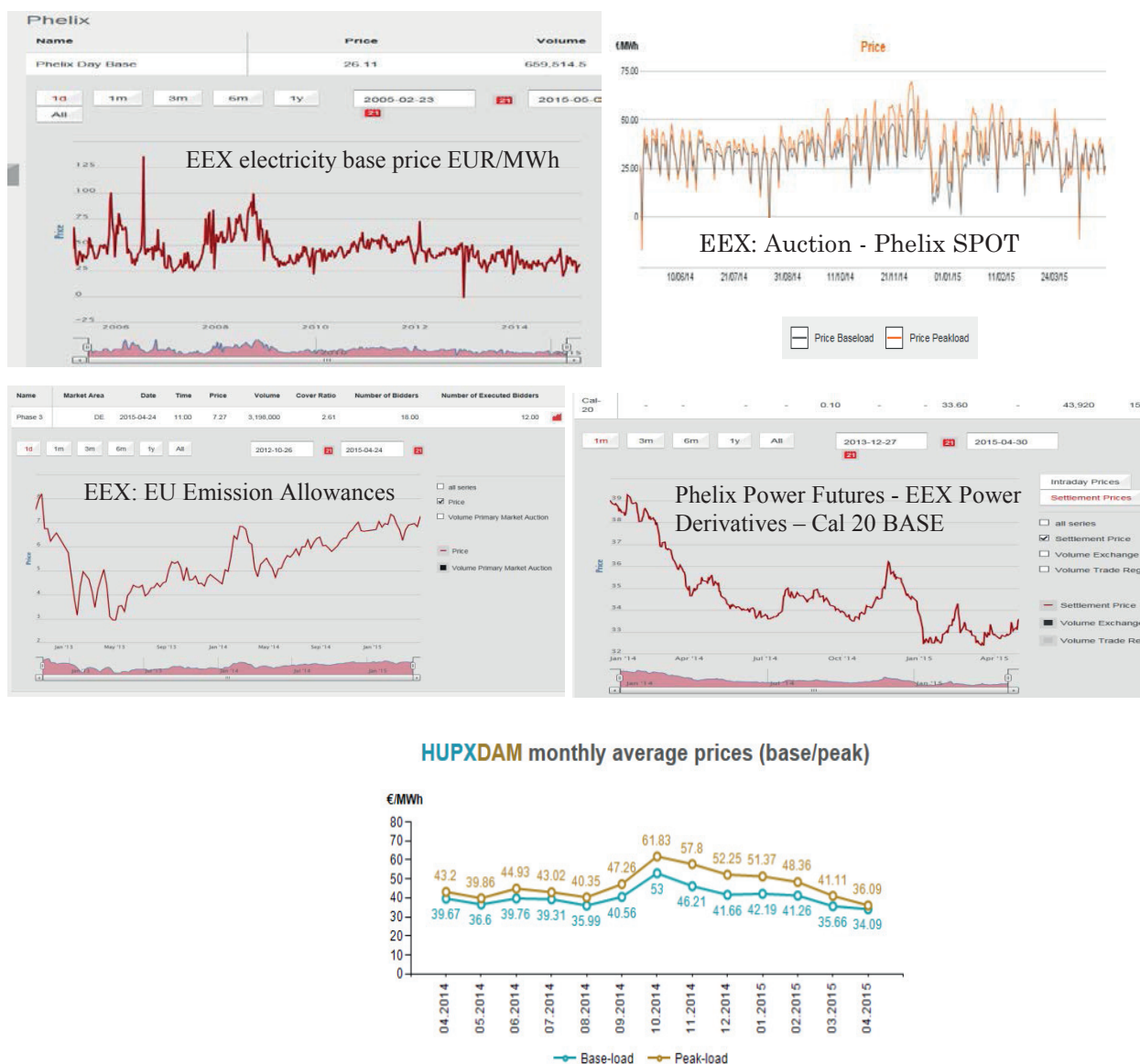


Figure 2 Market prices of electricity and CO<sub>2</sub> on EEX (Phelix) and HUPX

## 8 ALTERNATIVE CONTRACTING AND OWNERSHIP PRACTICES FOR NEW NUCLEAR POWER PLANTS

Innovative financing techniques have been investigated to disentangle the high construction risks from the lower operation risks of new nuclear build. Whether it involves project finance or corporate finance, the financing arrangements of a nuclear power plant are likely to involve refinancing once the plant has started production.

Countries embarking on a nuclear program, as well as countries whose programs have been dormant for extended periods of time, have expressed a number of common challenges that include the availability of the required human resources, securing financing, and managing waste. Some alternative contracting and ownership schemes, such as Build-Own-Operate (“BOO”), Build-Own-Operate-Transfer (“BOOT”) models, and regional ownership approaches might address these common challenges. These structures have been used in non-nuclear power projects and in other industries successfully for decades and although they have been discussed within the nuclear industry community, they have not been used for nuclear power plants until the recent announcement of the Akkuyu project in Turkey.

### 8.1 Overview of classical contractual and ownership structures

Previously, governments have used public sector funds either using tax revenue or electricity tariff subsidies to finance nuclear power. This enabled transfer of the risks and development costs to a regulated customer base. Whether local industry could provide the nuclear technology or whether such technology had to be purchased from abroad, the end result traditionally has been that owner/operator of the NPP was either government owned and/or regulated through the regulated customer base that it serviced.

However, the recent trend shows that globally governments are increasingly looking for investors to finance new infrastructure investments. Prior and current development of NPPs has occurred either through sovereign or corporate-based structures. This development history is one of leadership by public entities in a regulatory environment that enabled transfer of the risks and development costs to a regulated customer base. As markets have liberalized there is now less opportunity to cover development costs through the regulated customer base. Instead, potential NPPs in those regions must be assessed on the strength of the underlying economics of the project within a competitive market structure.

Traditionally, project structures have favoured the presence of a national or regional utility that has served as the owner/operator. This owner/operator, either on the strength of its own balance sheet or through the support of sovereign funds or guarantees, has provided the equity component for these NPPs with debt financing (both commercial lending and Export Credit Agency financing). Such structures imply that a knowledgeable, well-capitalized entity (most likely, a national or regional utility) will serve as the owner/operator as well as develop the

project. In many cases this development is with extra-national assistance for the nuclear technology via Engineering, Procurement, and Construction (EPC) contracts that may include operational assistance as well.

Historically, nuclear power development occurred either (i) as part of a national nuclear power program that has been led by the host government (e.g., France, India, the People’s Republic of China), or (ii) by national or regional utility companies that have been able to recover project costs through a regulated rate base (e.g., the current U.S. nuclear fleet). The following are the three basic NPP financing structures: *Sovereign-based model*, *Corporate-based mode*, *Project-based model*.

Figure 3 shows the relationship between the different models relative to risk, measured by the following parameters that discuss allocation of risk:

- Degree of market unbundling and market liberalization: The project model scores highest against this parameter, with the sovereign and corporate model scoring lower.
- Amount of risk transferability (from public to private sector): The corporate model scores the highest against this parameter, followed by the project model, then the sovereign model.
- Degree of recourse on shareholders: The corporate and sovereign model score the highest against this parameter (note the government being viewed as a shareholder), followed by the project model.

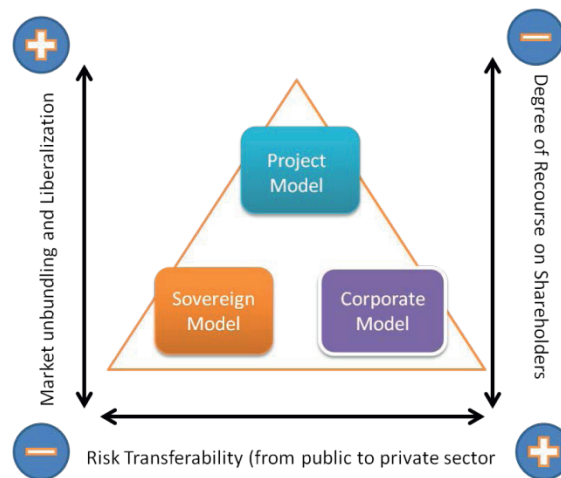


Figure 3 Different Contracting Models and Financing Techniques [10]

## 8.2 Description of the BOO(T) Concept

In a BOO or a BOOT structure (Figure 4), a private or non-private whereby an entity (called the Developer) is granted the right by the public sector or host government to develop, finance, build, own, operate, and maintain a facility for a specified period during which the entity owns the project and retains revenue and associated risk. Under a BOOT, at the end of the period, ownership of the facility is transferred to the host government. BOO and BOOT structures have been used successfully in a variety of infrastructure projects, but the Akkuyu project in

Turkey is the first in the nuclear industry. Under such structures, the Developer is responsible for bringing together project development capabilities, to include: technology; engineering, procurement, and construction; fuel supply; operations; and financing. As such, these types of contractual arrangements are a package deal since all of the project components of developing a nuclear power plant are included. Very simply, the BOO(T) structure places the responsibility for delivering the project on the Developer.

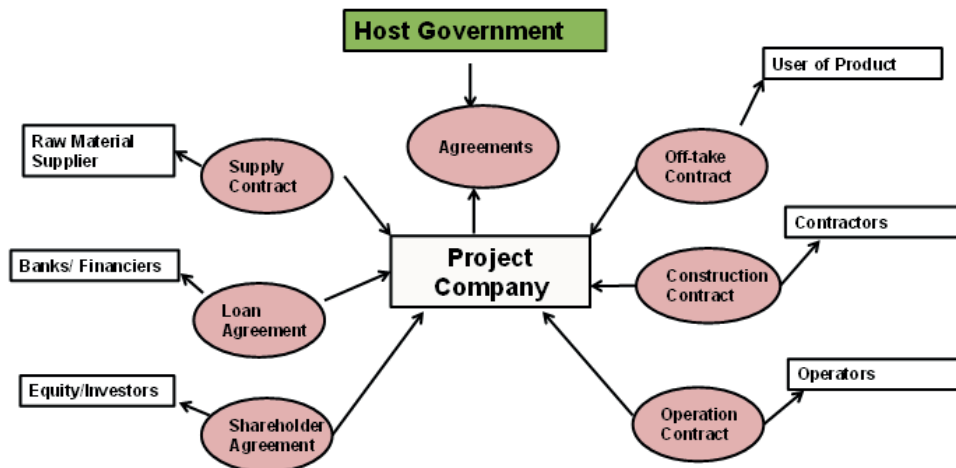


Figure 4 Typical structure for a BOO(T) Project [10]

This is normally achieved by creating a project company, which is a cooperative venture between the private and non-private entity, built on the expertise of each partner, which best meets clearly defined public needs through the appropriate allocation of resources, risks, and rewards. It undertakes the development, financing, construction and operation of a facility.

While Developer concerns will focus, to a large extent, on the linkage between the aggregate costs to develop the project and the sale price of electricity (and the period over which such price might be guaranteed by the host government), the Developer will also look to the many issues in assessing the risks associated with a particular project.

It is important to note that, while a BOO(T) structure could envision a situation whereby the licensed operator could be responsible for both spent fuel and decommissioning, the host government will have to establish the framework under which such tasks are performed.

## 9 CONCLUSIONS

The purpose of this paper was to analyse how increased uncertainty affects investment projects in the power sector with focus on nuclear power plants. Investment timing and technology choice are of principal interest to not only to

policy-makers but also to the various market participants. Due to the non-storage characteristics of electricity, investments are crucial in order to balance supply with future demand expectations and its timing can therefore strongly affect the power price. Furthermore, there exist a limited number of alternative technologies available for power production. Each technology is associated with different cost structures and uncertainties in input price, power price and policy formulations, which together with the irreversibility of the investment affect the investment behaviour.

The nuclear power industry is facing a period of extreme uncertainty. The conclusion that results from review of many studies worldwide is a *uncertain* scenario about the majority of aspects of nuclear energy development. Nuclear development scenarios seem to be associated to higher costs and prices than in the past. Shortages in the nuclear supply chain as well as the indefinite state of spent fuel worldwide could create additional barriers. Significant *uncertainties* are also linked to environmental impacts (uncertain GHG emission estimates, scarce knowledge of the contribution to other impact categories); to financial analysis (nuclear investment in competitive market is penalized compared to renewable sources and gas-fired generation, as it is characterized by high capital costs, long time return on investment and low flexibility; these factors contribute to increase the financial and economic risk for investors) as well as to macroeconomic analysis (it is uncertain the role that nuclear could have in addressing energy security; since gas-fired generation is the major competitor of nuclear in a cost-benefit perspective, the potential benefit of new nuclear is strongly affected by gas prices, carbon prices and nuclear costs).

In particular, when "facts are uncertain, values in dispute, stakes high and decisions urgent", the concept itself of "feasibility" must be converted from "technical and economic feasibility" into a more complex framework, shift from the expert community to an "extended peer community" consisting of all those affected by an impact who are ready to enter into dialogue on it. They bring in alternate points of view, that include local knowledge and expertise not generally accounted for in normal scientific reports.

Now the carbon policy uncertainty has significant impact on power generation investments. At the market level, carbon policy uncertainty incentivizes excess capacity investment in both fossil and renewable technologies, which over long run, given electricity demand is to some degree elastic, can be beneficial for both consumers and generating companies. At the economy wide level sufficient long run policy stringency and certainty is needed in carbon policy to meet near and long term emission reduction targets, with a carbon price of \$100/t for carbon dioxide equivalent emission or more.

Despite recent revived interest in nuclear power, the prospects for merchant nuclear investment in liberalized industries without government support do not seem promising. The reason is relatively simple: quite apart from overcoming any regulatory and public opinion difficulties, the economic risks of nuclear power have

been adversely affected by liberalization. High capital cost, uncertain construction cost, and potential construction and licensing delays are likely to lead private investors to require a substantial risk premium over coal and gas fired power plants to finance at least the first new nuclear units. Recent cost estimates reveal both the large underlying nuclear cost uncertainties and different interpretations of the impact of liberalization on the cost of finance and hence investment choices.

These results imply that there is little private value to merchant generating companies in retaining the nuclear option in risky European electricity markets with gas and carbon prices.

Because difficulties for financing new nuclear power plants new financing models have been developed like BOO/BOOT structure, Contract for difference in UK or "*Mankala*" model in Finland (whereby a limited liability company is run like a zero-profit-making co-operative for the benefit of its shareholders).

In a BOOT structure, a private or non-private entity is granted the right by the public sector to develop, finance, build, own, operate, and maintain a facility for a specified period during which the entity owns the project and retains the revenue and associated risk. The Developer is the entity that takes the responsibility for delivering the project (i.e., commissioning a nuclear power plant). Under a BOOT, at the end of the period, ownership of the facility is transferred to the public sector or host government. BOO is like BOOT, except the original entity owns the project outright and retains the revenue and associated risk in perpetuity [10].

Recently on the opposite the U.K. Government clearly accepts that there is a social or consumer value in '*keeping the nuclear option open*' as this has formed a part of U.K. government policy [12, 13]. The Finnish experience shows that if well-informed electricity-intensive end users with long time horizons are willing to sign long-term contracts, then nuclear new build can be a realistic option in liberalized markets.

Climate change policies can easily distort market signals, insulating renewables generation from market dynamics. This in turn reduces the proportion of the market that is effectively opened to competitive forces. When renewable support policies are undertaken, investments in conventional technologies suffer (especially in capital intensive investment like in nuclear power plant). This produces distorting effects on the generation mix. Policy intervention, rather than market forces, is able to select artificially winners and losers, thus potentially undermining, in the long run, the necessary diversity of the energy mix.

Carbon policy uncertainty has significant impact on power generation investments and that these impacts can be different depending on which level of investment decision making is being considered. At the firm level, carbon policy uncertainty creates path dependency in resources acquisition with the result that new investment decisions depend on the existing power generation assets and how they interact with the carbon policy risk.

At the market level, carbon policy uncertainty incentivizes excess capacity investment in both fossil and renewable technologies, which over long run, given electricity demand is to some degree elastic, can be beneficial for both consumers and generating firms. At the economy wide level, our results show that sufficient long run policy stringency and certainty is needed in carbon policy to meet near and long term emission reduction targets, with a carbon price of \$100/t for carbon dioxide equivalent emission or more.

Currently nuclear power plants present too many financial risks as a result of uncertainties in electricity market, electric demand growth, very high capital costs, operating problems, increasing regulatory requirements, and growing public opposition. However, enough utilities have built and building nuclear reactors within acceptable cost limits, and operated them safely and reliably to demonstrate that the difficulties with this technology are not insurmountable.

## 10 REFERENCES

- [1] UCTE. (2002). UCTE - Power Balance forecast 2002-2004. Brussels: UCTE.
- [2] Alessandro Rubino: Investment in Power generation: From market uncertainty to policy uncertainty. Real Options Approach applied to the UK electricity market, University of Siena
- [3] IEA (International Energy Agency)/NEA (Nuclear Energy Agency), 2010. Projected Costs of Generating Electricity. OECD Publication, Paris
- [4] Romerio F., 2007. Nuclear energy between past and future. An assessment based on the concept of risk. Competition and Regulation in Network Industries. Volume 2, No. 1.
- [5] Zorzoli G. B., 2005. Il mercato elettrico dal monopolio alla concorrenza. Franco Muzzio Editore, Roma.
- [6] Rogner H.,-H., Langlois L., 2000. The economic future of nuclear power in competitive markets. International Atomic Energy Agency (IAEA). Vienna, Austria.
- [7] Linares P., Conchado A., 17 agosto, 2009. The economics of new nuclear power plants in liberalized markets. Università Pontificia Comillas. <http://www.iit.upcomillas.es/pedrol/documents/economicsnuclear.pdf>
- [8] The Economist. When the wind blows. Available at: <http://www.economist.com/news/europe/21585029-hopes-fears-and-worrieseuropes-quest-renewable-energy-when-wind-blows>, 2013.
- [9] E. Commission. The sustainable nuclear energy technology platform. Special Report, 2007.
- [10] Financing of Nuclear Power Plants, IAEA Nuclear Energy Series No. NG – T – 4.2, IAEA, Vienna (2008).
- [11] Ioannis N.Kessides Nuclear power: Understanding the economic risks and uncertainties, Energy Policy 38 (2010) 3849–3864

- [12] UK Department of Energy and Climate Change: Long-term Nuclear Energy Strategy, 2013, available from [www.gov.uk](http://www.gov.uk)
- [13] UK Department of Energy and Climate Change: Electricity Market Reform – Contract for Difference: Contract and Allocation Overview, 2013, London, UK, available from [www.gov.uk/decc](http://www.gov.uk/decc).

VESNA BENČIK   DAVOR GRGIĆ   NIKOLA ČAVLINA   SINIŠA ŠADEK

vesna.bencik@fer.hr   davor.grgic@fer.hr   nikola.cavlina@fer.hr   sinisa.sadek@fer.hr

University of Zagreb Faculty of Electrical Engineering and Computing

## OPTIMIZATION OF OPDT PROTECTION FOR OVERCOOLING ACCIDENTS

### SUMMARY

Overcooling accidents are typically resulting in power increase due to negative moderator feedback. There are more protection set points responsible for terminating power increase. OPDT protection set point is typically protection from exceeding fuel centre line temperature due to reactivity and power increase. It is important to actuate reactor trip signal early enough, but to be able to filter out events where actuation is not necessary. Different concepts of coolant temperature compensation as part of OPDT set point protection were studied for decrease of feedwater temperature accident and for small main steam line breaks from full power for NPP Krško. Computer code RELAP5/mod 3.3 was used in calculation. The influence of different assumptions in accident description as well as nuclear core characteristics were described.

**Key words:** OPDT protection, overcooling accident, RCS temperature measurement, RELAP5, RTD bypass

## 1. INTRODUCTION

The accidents that manifest in the overcooling of the primary side are typically caused by a failure on the secondary side that lead to an increased heat removal in the steam generators. In the presence of the negative moderator reactivity coefficient, the excessive cooling of the primary side leads to an increase of nuclear power. The temperature increase in reactor vessel which is a measure of the core heat power will increase whereas the cold leg temperature decreases due to increased heat removal. The coolant temperature decrease leads also to an increase of coolant density and outsurge from the pressurizer. The primary pressure will decrease and Safety Injection (SI) signal may be actuated. As a consequence of the nuclear power increase in combination with a pressure decrease, overcooling accidents (with no protective functions) can result in fuel temperature increase and departure from nuclear boiling (DNB) which can ultimately lead to fuel damage. The necessary protection against the overcooling accidents is provided by reactor trip that will reduce the core power to decay heat and the fuel temperature to no load values. The second protective action consists of the stopping the excessive heat extraction from the primary side and depends on the initial event (feedwater malfunction or excessive steam load). The reactor protection system will actuate the reactor trip on any of the following trip signals: a) Power range high neutron flux, b) Overpower  $\Delta T$  (OP $\Delta T$ ), c) Overtemperature  $\Delta T$  (OT $\Delta T$ ), d) Low pressurizer pressure, e) SI or f) Turbine trip signal. The OP $\Delta T$  and OT $\Delta T$  reactor trip functions are intended to provide fuel integrity protection during the overcooling accidents such as feedwater system malfunction or excessive steam load increase as well as during a number of overpower and overtemperature events (e.g., rod withdrawal at power and uncontrolled boron dilution).

The measured narrow range (NR) temperature signals are used in plant protection system (the setpoints for OP $\Delta T$  and OT $\Delta T$  reactor trip), as well as in a number of plant control systems (automatic rod control system, steam dump, pressurizer level control). During the 2013 outage the NPP Krško has undergone the Resistance Temperature Detector Bypass Elimination (RTDBE) project to improve operation and maintenance. The Resistance Temperature Detectors (RTD) bypass manifold system for the NR temperature measurement has been removed and the fast-response thermowell (TW) RTDs were embedded in the thermowell structure as a part of the primary loop wall. The response time of TW RTDs is slower due to thermal inertia of the additional metal mass attached to the RTD than the response time of the directly immersed RTDs. On the other hand, for TWs, there is no delay due to loop transport or thermal lag. The RCS temperature measurement response time is accounted for in reactor protection system set points as well as in plant control system settings. The OP $\Delta T$  protection function has been modified as part of RTDBE. In the old pre-RTDBE implementation the compensated measured temperature difference  $\Delta T$  was calculated by applying the lead-lag on measured temperature difference. In the new implementation, different compensations were applied for the measured hot and cold leg temperature. For overcooling accidents the OP $\Delta T$  trip protects the core due to the increasing compensated measured temperature difference  $\Delta T$  whereas the OP $\Delta T$  trip set point does not change from its steady state value. The safety concern for the overcooling

accidents is that after RTDBE the response time of the OPAT may increase thus decreasing the margin to DNB.

Two overcooling accidents for NPP Krško were analyzed using RELAP5/mod 3.3 for NPP Krško: 1. Feedwater Malfunction-Decrease in Feedwater Temperature (FM DFT) and 2. Hot Full Power Main Steam Line Break (HFP MSLB). In the analyses different concepts for coolant temperature compensation in OPAT protection set point were studied and the adequacy of the protection functions were investigated.

## 2. CALCULATION MODEL FOR NPP KRŠKO

The RELAP5/mod 3.3 nodalization for NPP Krško, Figure 1, developed at Faculty of Electrical Engineering and Computing (FER) was used for transient analysis, [1] and [2]. The plant model has been updated taking into account the RTDBE project realized during the plant 2013 outage. The explicit RTD bypass manifold system for the NR Reactor Coolant System (RCS) temperature measurement was removed and it was replaced with compensated temperature signals that were modelled to take into account the thermowell structure's thermal lag. RELAP5 model consists of 481 thermal-hydraulic volumes, 518 junctions, 378 heat structures with 2107 mesh points, 733 control variables and 197 variable and 221 logical trips. It includes major modifications related to the Krško modernization project as well as RTDBE project; e.g., the model of the replacement steam generator (RSG) based on data provided by the RSG designer (Siemens), power uprate, removal of the guide tubes plugs inside the core as well as changes to the protection and plant control systems. The RELAP5 model contains the models of the NPP Krško monitoring as well as protection and control systems, e.g., the detailed models of Safety Injection (SI) system, Main feedwater (MFW) and Auxiliary feedwater (AFW) system as well as of control systems (automatic rod control, pressurizer pressure and level control, steam dump control with realistic representation of steam dump valves and steam generator level control).

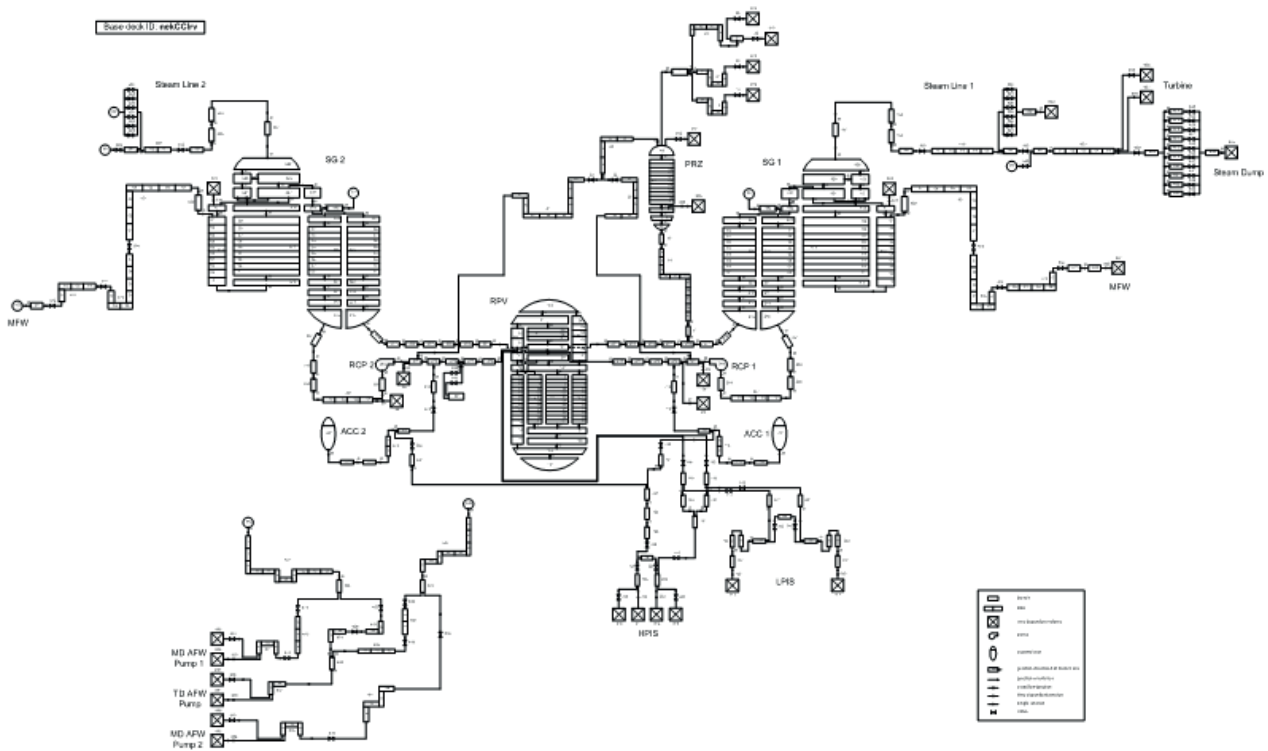


Figure 1. RELAP5/mod 3.3 nodalization scheme for NPP Krško

## 2.1 Reactor Trip Protection Functions during Overcooling Accidents

The  $OP\Delta T$  and  $OPAT$  protection functions are schematically presented in Figure 2 (Old configuration before RTDBE) and in Figure 3 (New plant configuration after RTDBE).

At the plant, the set point for  $OP\Delta T$  trip is continuously calculated by solving the following equation:

$$OP\Delta T_{setpoint} = \Delta T_0 \left[ K_4 - K_5 \left( \frac{\tau_3 s}{1 + \tau_3 s} \right) \left( \frac{1}{1 + \tau_7 s} \right) T_{avg} - K_6 \left( T_{avg} \left( \frac{1}{1 + \tau_7 s} \right) - T_{avgref} \right) \right] \quad (1)$$

Where:

$OP\Delta T_{setpoint}$  - Overpower  $\Delta T$  set point

$\Delta T_0$  - Indicated  $\Delta T$  at nominal thermal power

$T_{avg}, T_{avgref}$  - Measured and indicated loop average temperature at nominal thermal power

$K_4$  - Set point bias

$K_5, K_6$  - Constants that depend on dynamic behaviour of the measured  $T_{avg}$

$\tau_3$  - Time constant (s) of dynamic signal compensator (impulse)

$\tau_7$  - Time constant (s) in the measured  $T_{avg}$  lag compensator

$s$  - Laplace transform variable ( $s^{-1}$ )

$OP\Delta T_{setpoint}$  is limited to the value calculated at nominal  $T_{avg}$  ( $T_{avgref}$ )

The calculated  $OP\Delta T_{setpoint}$  is compared with two sets of loop temperature difference measurements ( $\Delta T$ ) per loop. The  $OP\Delta T$  reactor trip function will trip the reactor on coincidence of two out of four signals satisfying the condition below:

$$OP\Delta T_{setpoint} \leq \Delta T \quad (2)$$

In the old plant configuration (before RTDBE, Figure 2) the lead-lag compensation was applied after measured temperature difference  $\Delta T$  was formed. For the current post-RTDBE plant configuration, the measured compensated  $\Delta T$  for the  $OP\Delta T$  protection function is calculated by subtracting the compensated  $T_{cold}$  signal from the compensated  $T_{hot}$  signal. The hot leg temperature is compensated by a lag element in order to suppress the oscillations in the hot leg measurement due to hot leg streaming (lag element, time constant= $\tau_8$  in Figure 3). The compensation of the cold leg temperature that has a rather uniform distribution across the pipe is directed to fulfil the efficiency of the  $OP\Delta T$  protection function for overcooling accidents. Among the available options, the lead-lag compensation (with greater lead time constant) as well as the lag compensation was considered. The lead-lag element for  $T_{cold}$  has shown to be very sensitive to the outside electromagnetic disturbances thus leading to unnecessary reactor trips.

Finally, at the plant, the measured compensated  $\Delta T$  will be calculated using the following equation:

$$\Delta T = T_{hot} \frac{1}{1 + \tau_8 s} - T_{cold} \frac{1}{1 + \tau_5 s} \quad (3)$$

where  $\tau_5 < \tau_8$ . Thus, the increase of the compensated measured  $\Delta T$  is accelerated for overcooling accidents since the cold leg temperature decreases due to excessive heat removal in steam generators. Due to the fact that  $OP\Delta T_{setpoint}$  is limited to the value at nominal power since the RCS average temperature decreases during the overcooling accidents, the  $OP\Delta T$  trip may be actuated due to increasing measured temperature difference ( $\Delta T$ ), Eqs. (2) and (3).

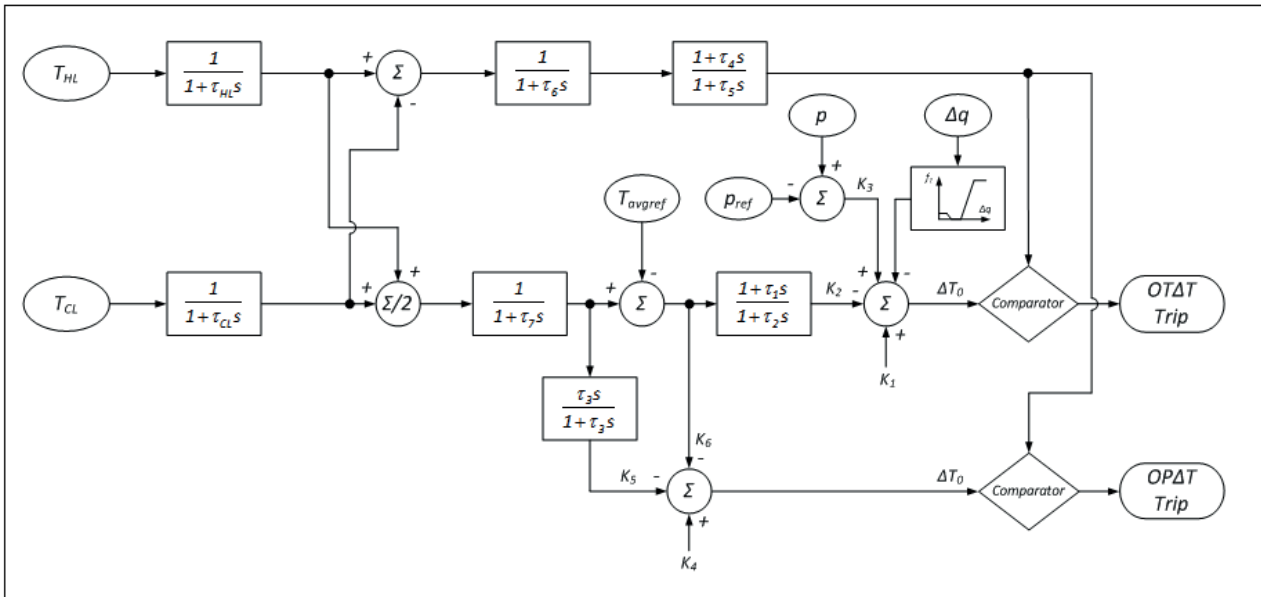


Figure 2. Old (before RTDBE) OTΔT/OPΔT control block scheme

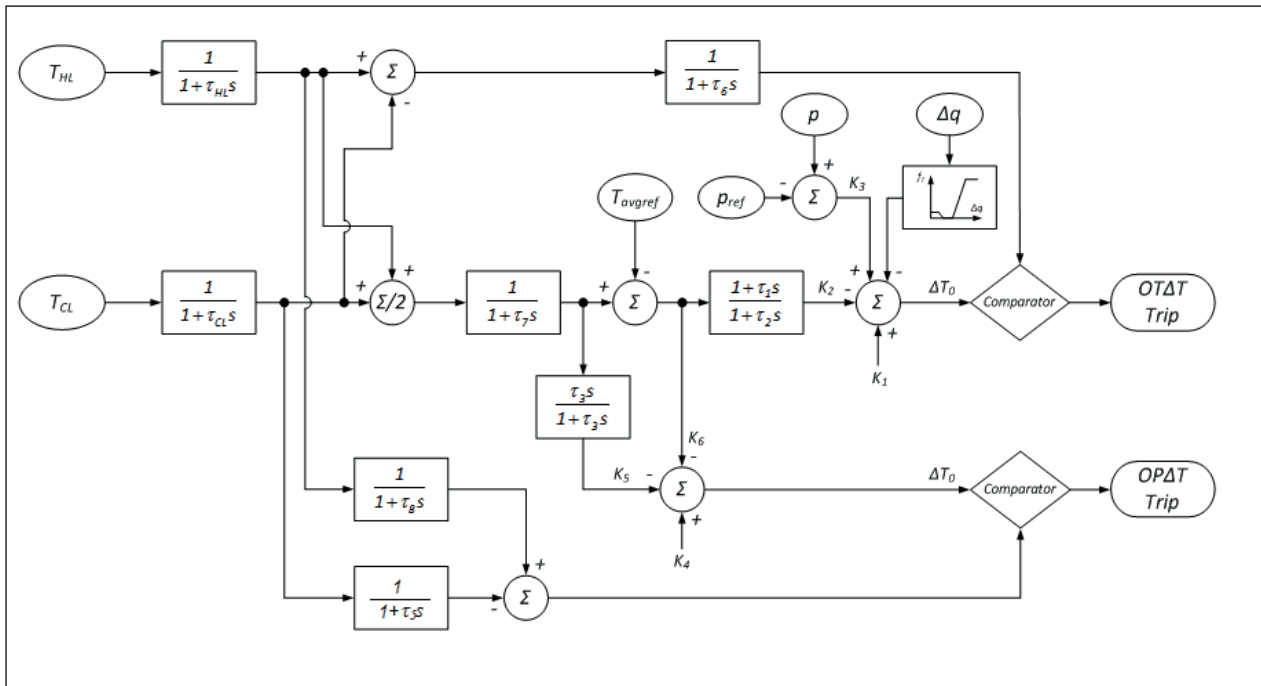


Figure 3. New (post-RTDBE) OTΔT/OPΔT control block scheme

### 3. ANALYSIS OF OVERCOOLING ACCIDENTS FOR OPΔT OPTIMIZATION

The typical overcooling accidents that are used for an assessment of the efficiency of OPΔT protection function are the Feedwater Malfunction – Decrease in Feedwater Temperature (FM DFT) and the Hot Full Power Main Steam Line Break (HFP MSLB). Both accidents were analyzed using RELAP5/mod 3.3 code. In order

to make an assessment of the adequacy of the OP $\Delta$ T protection, sensitivity study calculations were performed with different concepts for coolant temperature measurement and OP $\Delta$ T set point calculation. For the base case best-estimate calculation the current post-RTDBE NPP Krško configuration, cycle 26, and with the cold leg temperature compensation with lag element (time constant=2 s) in measured  $\Delta$ T signal was used. The End of Cycle (EOC) conditions with maximum negative moderator temperature reactivity coefficient were assumed. The power range high neutron flux trip was not credited in the analysis. Steam line pressure signal for steam line isolation and safety injection is compensated by lead-lag element introduced along with RTDBE with lead and lag time constant equal to 48 s and 8 seconds, respectively.

### **3.1 Analysis of Feedwater System Malfunction – Decrease in FW Temperature (FM DFT)**

The accident is simulated by a step decrease in the feed water temperature from the initial full power (492.7 K) to a minimum credible value (414.55 K). There are a number of events that can cause the feedwater temperature decrease, e.g., the opening of the feedwater heater bypass valve, a spurious trip of the heater drain pumps, or the break of steam flow to the high pressure heaters. The results for the base case best-estimate calculation with the lag element (time constant=2 s) for the cold leg temperature compensation in OP $\Delta$ T function are presented in Figure 4 through Figure 7. As a consequence of feedwater temperature decrease and the fact that the flow to the turbine remained constant, the heat transferred in the steam generators will increase and the coolant temperature on the primary side will decrease, Figure 4 and Figure 5. In the presence of negative moderator reactivity coefficient, decrease in moderator temperature will result in an increase in core power and fuel temperature increase. The Doppler reactivity coefficient is negative and it will reduce the total reactivity due to fuel temperature increase, Figure 6. If the automatic control system is in operation, decrease in coolant temperature may cause control rod withdrawal in an attempt to maintain the average coolant temperature at its programmed value. This may cause a further increase of nuclear power and fuel temperature. The decrease in coolant temperature will result in coolant density increase, causing the outsurge from the pressurizer and the subsequent decrease in the primary pressure. The necessary protection against the FM DFT accident is provided by reactor trip that will reduce the core power to decay heat and the fuel temperature to no load values. Further, the feedwater that causes the cooldown on the primary side will be isolated on either the low average RCS temperature in combination with reactor trip or by safety injection signal that may be actuated due to low pressurizer pressure. The reactor trip can be actuated on either of the following signals: Power range high neutron flux, OP $\Delta$ T or OT $\Delta$ T, Low pressurizer pressure and Turbine trip (on High-high SG water level). The OP $\Delta$ T provides the specific protection against two major concerns during FM DFT, i.e. the high neutron flux and low DNB ratio (DNBR). Both the nuclear power increase and the DNB are managed by the measured compensated temperature difference, whereas the OP $\Delta$ T set point is limited to its steady state value since the average temperature decreases in the transient. In our case, the OPDT trip trips

the reactor (44.3 s after transient begin) before the temperature error in the Automatic rod control system increased above the value for control rod movement, Figure 6 and Figure 7. In order to estimate the influence of different RCS temperature measurement concepts and OP $\Delta$ T set point calculation the sensitivity study calculations have been performed. Five groups of FM DFT cases have been analyzed:

1. RTDBE base case best-estimate calculation, OP $\Delta$ T cold leg temperature compensation: lag (time constant=2 s). Two cases have been analyzed:
  - a) dft\_be\_00\_auto (Automatic rod control system active) and
  - b) dft\_be\_00\_manual (Automatic rod control system not active)
2. RTDBE best-estimate calculation, OP $\Delta$ T cold leg temperature compensation: lag (time constant=7 s). The aim of the sensitivity calculation is to estimate the influence of cold leg temperature lag time constant. Two cases have been analyzed:
  - a) dft\_be\_01\_auto (Automatic rod control system active) and
  - b) dft\_be\_01\_manual (Automatic rod control system not active)
3. RTDBE best-estimate calculation, OP $\Delta$ T cold leg temperature lead-lag compensation with lead and lag time constants equal to 30 s and 10 s, respectively. Only the case with automatic rod control system not active was analyzed: dft\_be\_02\_manual.
4. RTDBE conservative calculation with the assumptions from the referent literature, e.g., ref. [5]: 1) The Safety Analysis Limit (SAL) for OP $\Delta$ T set point calculation with  $K_4=1.15$  instead of 1.08, 2) Conservative moderator (maximum) and Doppler (minimum) reactivity feedback coefficients, 3) Turbine trip on reactor trip not credited, 4) Maximum feed water flow (feedwater flow=steam flow until feedwater isolation), 5) The minimum initial SG mass (10% less than nominal), 6) The maximum initial RCS average temperature (580.55 K) and 7) The feed water temperature decreases instantaneously at the very entrance of the steam generator (without delay from feedwater header). OP $\Delta$ T cold leg temperature compensation lag time constant=2 s. Two cases have been analyzed:
  - a) dft\_sal\_auto (Automatic rod control system active) and
  - b) dft\_sal\_manual (Automatic rod control system not active)
5. RTD best-estimate calculation. The case represents the configuration before the RTDBE modification, i.e., with RTD bypass. Two cases have been analyzed:
  - a) dft\_rtd\_auto (Automatic rod control system active) and
  - b) dft\_rtd\_manual (Automatic rod control system not active)

The results for the FM-DFT analysis for the sensitivity study are summarized in Table I. For an assessment of fuel integrity the maximum nuclear power and the maximum core heat power were observed. The comparison of the two base cases (after and before RTDBE- cases 1 and 5) shows the slower response of the OP $\Delta$ T protection function for the new post-RTDBE than for the old pre-RTDBE configuration and correspondingly the higher maximum core heat power for the former case. For the post-RTDBE the OP $\Delta$ T trip is actuated 4.1 s later than for the pre-RTDBE and the maximum values for the core heat power for the post-RTDBE and pre-RTDBE are equal to 109.5% and 107.69%, respectively. The sensitivity

study calculation for the post-RTDBE configuration has shown a relatively small difference between the two lag compensations (2 s and 7 s); i.e., the maximum values for heat power are equal to 109.5% and 111.9%, respectively. The case 3 has resulted in a considerably faster reactor trip and the maximum core heat power was only slightly above the nominal value (103.4%). However, as already mentioned, the lead-lag compensation for  $T_{\text{cold}}$  will not be used because under normal operational conditions it causes unnecessary reactor trips. In general, for best-estimate cases the transient was terminated before the temperature error in the Automatic rod control system rose above the value to start the control rod movement. For the conservative calculation (Case 4) the resulting temperature error was even negative due to significant increase of nuclear power and the control rods were inserted into the core thus reducing the nuclear power. A very good agreement between RELAP5 analysis (case 4) and referent literature (ref. [5]) was obtained. The maximum core heat power in RELAP5 analysis and in ref. [5] were obtained for the case with manual rod control (117.8% and 118.6%).

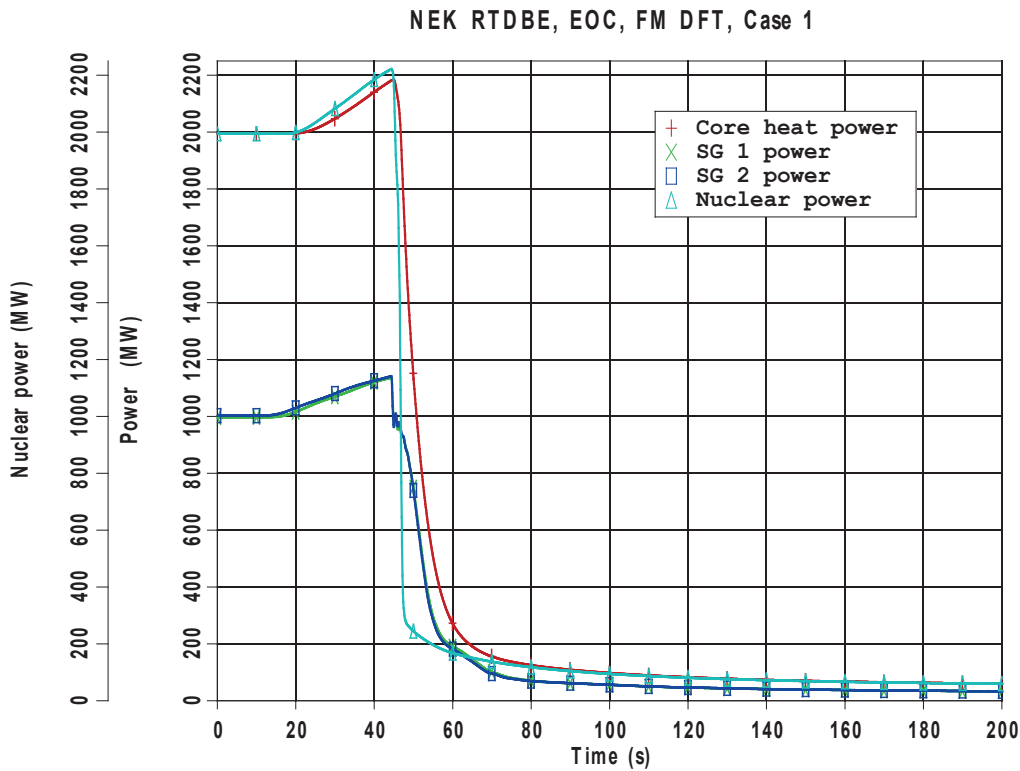


Figure 4. FM DFT analysis, base case, Nuclear and core heat power and power transferred in SGs

NEK RTDBE, EOC, FM DFT, Case 1

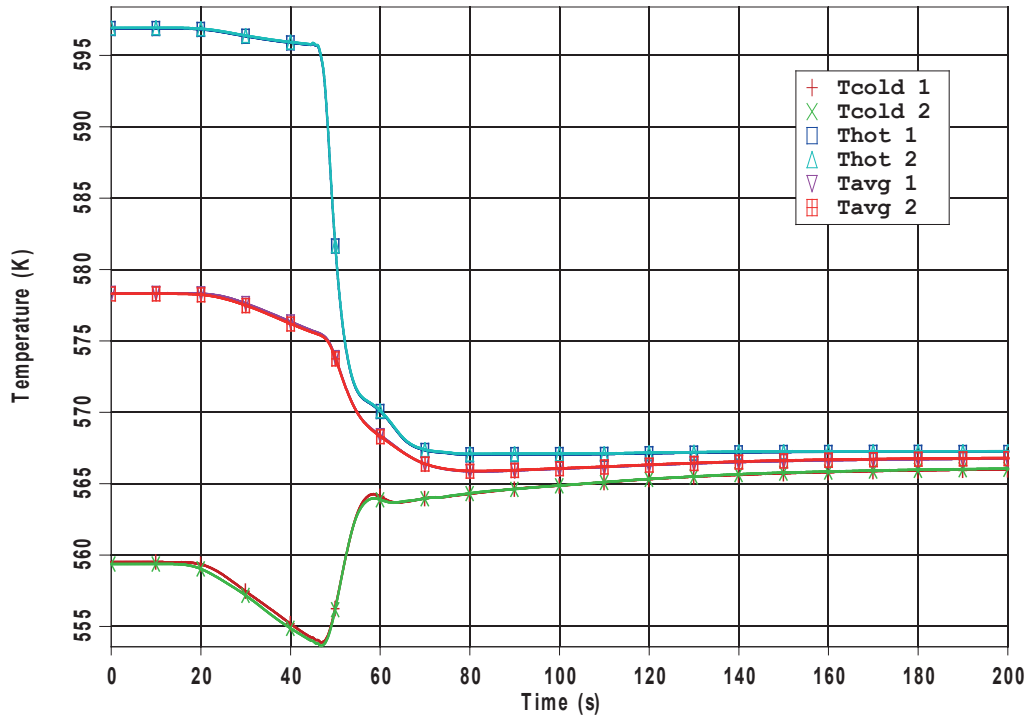


Figure 5. FM DFT analysis, base case, RCS loop temperature and RCS average temperature

NEK RTDBE, EOC, FM DFT, Case 1

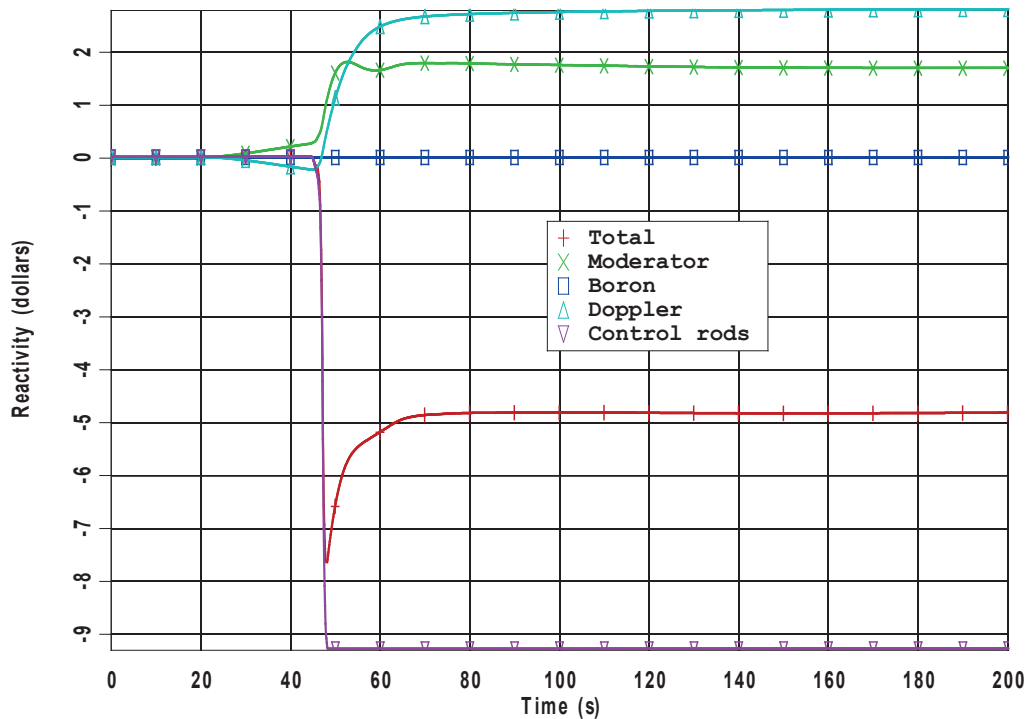


Figure 6. FM DFT analysis, base case, Reactivity

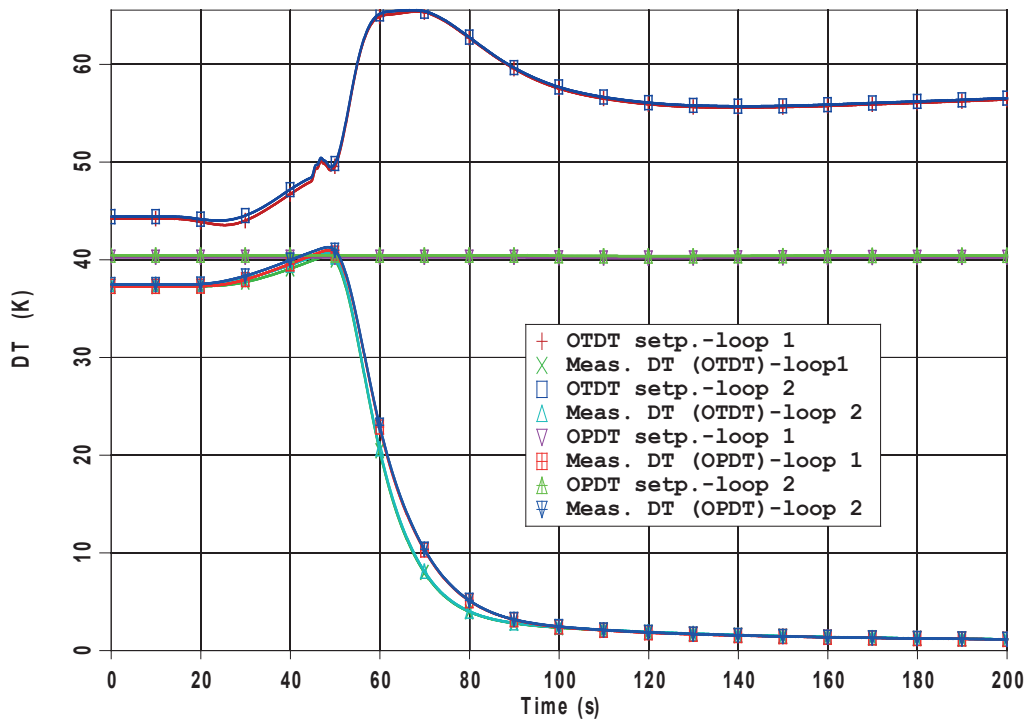


Figure 7. FM DFT analysis, base case, OPAT and OTAT set points

### 3.2 Analysis of Hot Full Power Main Steam Line Break (HFP MSLB)

Steam line break can result from a rupture of the main steam piping or branch steam piping. Depending on the location of the break the steam flow from one or both steam generators will increase. In the analysis it was conservatively assumed that the break is located upstream of the main steam isolation valve in the steam line 2 (loop without pressurizer). Further, it was assumed that the flow to the turbine remained constant and equal to the steady state value, Figure 8. The steam flow of both steam generators therefore increase and the extracted heat from the primary system increases thus resulting in a decrease of temperatures on the primary side. In the presence of the negative moderator reactivity feedback the nuclear power and the fuel temperature will increase. The combination of increased heat production on one side and the decreased margin to DNB due to lower primary pressure may lead to fuel damage if the heat production in the core is not stopped. For larger breaks, the low steam line pressure signal will actuate the safety injection signal that will actuate reactor trip. For smaller breaks the OPAT protection may be required to trip the reactor. Similarly to the FM DFT, the OPAT trip provides the protection for this transient due to increased compensated measured temperature increase in reactor vessel whereas the set point will not change. The same conservative assumptions as for the FM DFT accident were used in the analysis, i.e., the end of cycle when the moderator reactivity coefficient has the maximum negative value. The results for the secondary pressure and compensated steam line pressure for two break areas leading to OPAT trip (0.0221

m<sup>2</sup>) and to SI (0.0222 m<sup>2</sup>) are shown in Figure 9. For 0.0222 m<sup>2</sup> break, the main steam line isolation is actuated together with the safety injection. From that point onward, the pressure of the two steam generators decouple after steam line isolation. For the 0.0221 m<sup>2</sup> break, the two steam generators continue to discharge its inventory through the break after reactor and turbine trip as it is also illustrated in Figure 8.

Table I. RELAP5 results for FM DFT accident

Case	Time of reactor trip (OPΔT)	Max. nuclear power (%)	Max. core heat power (%)
1. Base case best-estimate, cold leg temp. compensation (OPΔT): lag (2 s)			
a) dft_be_00_auto (Automatic rod control)	44.3 s	111.4% (44.3 s)	109.5% (44.9 s)
b) dft_be_00_manual (Manual rod control)	44.3 s	111.4% (44.3 s)	109.5% (44.9 s)
2. Base case, cold leg temperature compensation (OPΔT): lag (7 s)			
a) dft_be_01_auto (Automatic rod control)	50.34 s	113.49% (50.3 s)	111.86% (50.8 s)
b) dft_be_01_manual (Manual rod control)	50.34 s	113.49% (50.3 s)	111.86% (50.8 s)
3. Base case, cold leg temperature compensation (OPΔT): lead-lag (30s, 10 s)			
dft_be_02_manual (Manual rod control)	31.62 s	105.17% (31.4 s)	103.4% (31.8 s)
4. Conservative calculation, ref. [5], cold leg temp. compensation (OPΔT): lag (2 s)			
a) dft_sal_auto (Automatic rod control)	48.32 s; (43.8 s, ref. [5])	117.95% (48.3 s)	117.04% (48.4 s); (118.1% (44.2 s), ref. [5])
b) dft_sal_manual (Manual rod control)	45.3 s; (33.1 s, ref. [5])	118.44% (45.2 s)	117.8% (45.0 s); (118.6% (33.5 s), ref. [5])
5. Best-estimate calculation for configuration before RTDBE			
a) dft_rtd_auto (Automatic rod control)	40.22 s	110.13% (40.2 s)	107.69% (40.4 s)
b) dft_rtd_manual (Manual rod control)	40.24 s	109.7% (40.2 s)	107.64% (40.9 s)

Similarly to the previous analysis for FM DFT, a number of sensitivity study calculations were performed to assess the effectiveness of protective functions. Seven groups of HFP MSLB analyses have been performed:

1. RTDBE base case best-estimate calculation, OPΔT cold leg temperature compensation: lag (time constant=2 s). Four cases have been analyzed:
  - a) mslb\_be\_00\_notrip (the largest break where no reactor trip signal is actuated)
  - b) mslb\_be\_00\_first\_trip (the smallest break where reactor trip signal is actuated)

- c) mslb\_be\_00\_opdt (the largest break where the safety injection signal is not actuated, the OPΔT signal trips the reactor)
  - d) mslb\_be\_00\_si (the smallest break where the safety injection signal actuates reactor trip)
2. RTDBE base case best-estimate calculation, OPΔT cold leg temperature compensation: lag (time constant=2 s). Steam line pressure signal for steam line isolation and safety injection was compensated by lead-lag element as for the pre-RTDBE with lead and lag time constant equal to 50 s and 5 seconds, respectively. The aim of the analysis is to evaluate the influence of the new RTDBE OPΔT protection as well as of steam line pressure compensation on transient results. Two cases have been analyzed:
- a) mslb\_be\_00\_opdt\_1 (the largest break where the safety injection signal is not actuated, the OPΔT signal trips the reactor).
  - b) mslb\_be\_00\_si\_1 (the smallest break where the safety injection signal actuates reactor trip).
3. RTDBE best-estimate calculation, OPΔT cold leg temperature compensation: lag (time constant=7 s). The aim of the sensitivity calculation is to estimate the influence of cold leg temperature lag time constant. Four cases have been analyzed:
- a) mslb\_be\_01\_notrip (the largest break where no reactor trip signal is actuated)
  - b) mslb\_be\_01\_first\_trip (the smallest break where reactor trip signal is actuated)
  - c) mslb\_be\_01\_opdt (the largest break where the safety injection signal is not actuated, the OPΔT signal trips the reactor)
  - d) mslb\_be\_01\_si (the smallest break where the safety injection signal actuates reactor trip)
4. RTDBE best-estimate calculation, OPΔT cold leg temperature lead-lag compensation with lead and lag time constants equal to 30 s and 10 s, respectively. Three cases have been analyzed:
- a) mslb\_be\_02\_notrip (the largest break where no reactor trip signal is actuated)
  - b) mslb\_be\_02\_opdt (the largest break where the safety injection signal is not actuated, the OPΔT signal trips the reactor)
  - c) mslb\_be\_02\_si (the smallest break where the safety injection signal actuates reactor trip)
5. RTDBE conservative calculation with the assumptions from the referent literature, e.g., ref. [6]: 1) The SAL limit for OPΔT set point calculation with  $K_4=1.15$  instead of 1.08, 2) OPΔT trip actuation if the set point is reached in both loops, 3) Conservative moderator (maximum) and Doppler (minimum) reactivity feedback coefficients, 4) Feed water flow =steam flow until feed water isolation and 5) The maximum initial RCS average temperature (580.55 K). OPΔT cold leg temperature compensation lag time constant=2 s. Three cases have been analyzed:
- a) mslb\_sal\_notrip (the largest break where no reactor trip signal is actuated)
  - b) mslb\_sal\_opdt (the largest break where the safety injection signal is not actuated, the OPΔT signal trips the reactor)
  - c) mslb\_sal\_si (the smallest break where the safety injection signal actuates reactor trip)
6. RTD best-estimate calculation. The case represents the configuration before the RTDBE modification, i.e., with RTD bypass. Low steam line pressure signal for steam line isolation and safety injection was compensated by the pre-RTDBE lead-

lag element with lead and lag time constant equal to 50 s and 5 seconds, respectively. Four cases have been analyzed:

- a) mslb\_rtd\_notrip (the largest break where no reactor trip signal is actuated)
- b) mslb\_rtd\_first\_trip (the smallest break where reactor trip signal is actuated)
- c) mslb\_rtd\_opdt (the largest break where the safety injection signal is not actuated, the OPΔT signal trips the reactor).
- d) mslb\_rtd\_si (the smallest break where the safety injection signal actuates reactor trip).

7. RTD best-estimate calculation. The case represents the configuration before the RTDBE modification, i.e., with RTD bypass. Steam line pressure signal for steam line isolation and safety injection was compensated by the post-RTDBE lead-lag element with lead and lag time constant equal to 48 s and 8 seconds, respectively. Two cases have been analyzed:

- a) mslb\_rtd\_opdt\_1 (the largest break where the safety injection signal is not actuated, the OPΔT signal trips the reactor).
- b) mslb\_rtd\_si\_1 (the smallest break where the safety injection signal actuates reactor trip).

The results for the maximum nuclear and maximum core heat power are summarized in Table II. The comparison of the two base case calculations for the new and old configuration (Cases 1 and 2 and Cases 6 and 7) has shown the influence of both the change in OPΔT set point and the change of the low steam line pressure set point for safety injection actuation. In the pre-RTDBE original configuration the SI signal on low steam line pressure was more sensitive and it was actuated for smaller break size (0.0186 m<sup>2</sup>) than for the new RTDBE configuration (0.0222 m<sup>2</sup>). Among the base case best estimate cases (Case 1 and Case 6) the earliest reactor trip for the smallest break for SI actuation was actuated for the pre-RTDBE and consequently the maximum core heat power (102.14%) was the minimum for these two groups. For the largest break for the OPΔT calculation (base case) post-RTDBE (Case 1c-0.0221 m<sup>2</sup>) the larger maximum core heat power (109.02%) than for the corresponding pre-RTDBE case (107.13% , Case 6c-0.0185 m<sup>2</sup>) was obtained. On one side, for larger breaks more adverse conditions on the primary side result before reactor trip than for the smaller break areas. Secondly, the OPΔT response for the post-RTDBE is slower for the post than for the pre-RTDBE configuration. The sensitivity analysis for the post-RTDBE and steam line compensation as for pre-RTDBE (Case 2a) and for the same break area as for the corresponding pre-RTDBE case (Case 6c) has shown that the post-RTDBE OPΔT function is slower than the pre-RTDBE OPΔT function (5.65 s later response). The resulting difference for the maximum heat flux between these two cases (108.63% and 107.13%) is slightly less than between the cases 1c and 6c due to smaller break size in the former case. However, the obtained differences for the maximum heat flux between these two base cases are small (less than 2%). A smaller difference for the response time of the OPΔT function (4.77 s) between the post and pre-RTDBE was obtained for larger break area (0.0221 m<sup>2</sup>) when comparing the base post-RTDBE case (1c) with the pre-RTDBE sensitivity case 7a. Again, the difference for the maximum heat power between these two cases is rather small (1.65%). The similar results were obtained for the FM-DFT analysis, e.g., by comparing the cases

1a and 5a (Table I) the post-RTDBE has a slower response (4.1 s) than the pre-RTDBE and correspondingly the higher maximum core heat power (1.8%).

For the post-RTDBE with the pre-RTDBE steam line compensation (Case 2) the similar results as for the base case pre-RTDBE were obtained for the smallest break area for SI actuation (Case 2b; reactor trip at time=10.21 s due to SI signal resulting in a low maximum core heat power=101.87%). The calculated differences for the maximum core heat power between the base case post-RTDBE and the base case pre-RTDBE are small for both groups of break areas leading to either OPAT trip or to the trip due to SI. The results for the core heat power are presented in Figure 10. For the RTDBE Case 3 (cold leg temperature lag compensation time constant=7 s) the maximum core heat power was larger (110.76%) than for the base case 1 (109.02%) since the OPAT trip was actuated later. Similarly to the FM DFT analysis, for the Case 4 (lead-lag compensation) a fast response for the OPAT trip has resulted in a considerably smaller maximum core heat power (103.5%) than for the base case. The largest break area for which no trip is actuated is almost identical for all the analyzed best-estimate cases (0.0085 m<sup>2</sup> for the Case 4 and 0.0088 m<sup>2</sup> for the rest of the cases). The maximum core heat power for that break area has stabilized at approx. 107.63% that corresponds to the value at which the total removed power on the secondary side (turbine and break) are equal to the elevated core power. The smallest break area for which the OPAT trip is actuated was equal to 0.0089 m<sup>2</sup> for both the base pre and post-RTDBE calculations (cases 1b and 6b). As expected from the previous discussion, the OPAT trip was actuated earlier for the pre-RTDBE than for the post-RTDBE case (172.15 s vs. 190.8 s). However, for this limiting small break, the maximum core heat power is close to the no-trip case and it was equal for both cases (107.7%). For conservative calculation, a good agreement between RELAP5 analysis and referent literature (ref. [6]) was obtained. The similar values for the maximum core heat power for RELAP5 analysis and ref. [6] were obtained (123.21% and 122.1%) and for the slightly larger break area for RELAP5 calculation (0.03198 m<sup>2</sup> vs. 0.0307 m<sup>2</sup>). For the maximum core heat power greater than 118% detailed nuclear analysis is performed (not presented here) in order to demonstrate that the limiting acceptance criteria are met. The nuclear analysis presented in ref. [6] has shown that the minimum margin to minimum DNBR is greater than 9%.

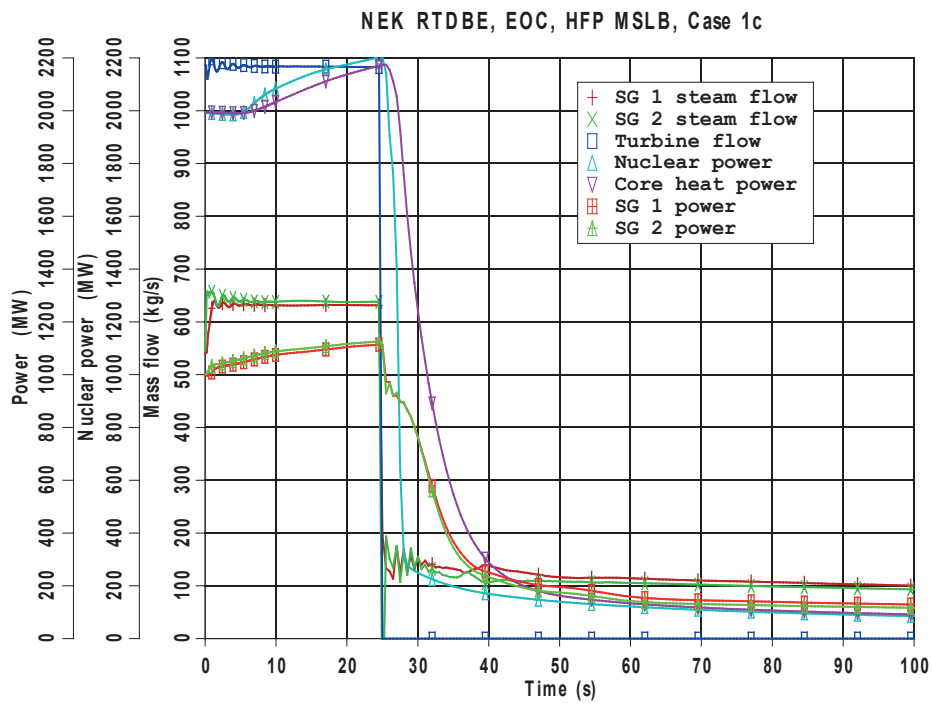


Figure 8. HFP MSLB analysis, base case, Case 1c (0.0221m<sup>2</sup> break), Steam flow, nuclear power, core heat power and power transferred in SGs

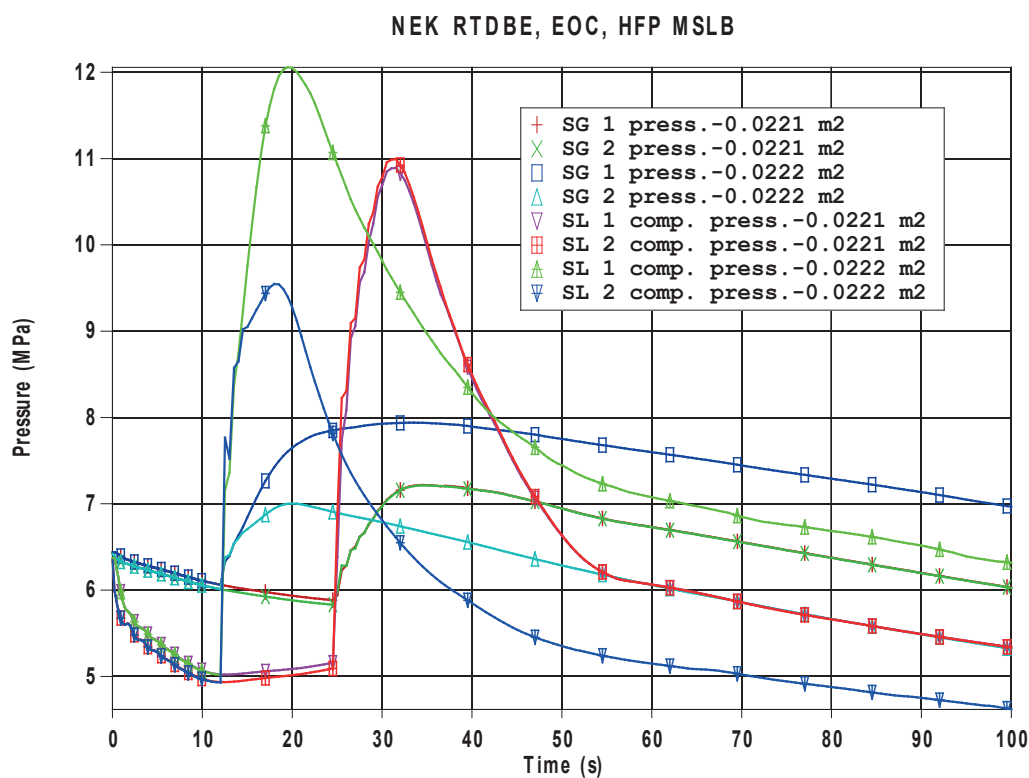


Figure 9. HFP MSLB analysis, secondary pressure and compensated steam line pressure signal, sensitivity calculations for RTDBE (Case 1c vs. Case 1d)

Table II. RELAP5 results for HFP MSLB accident

Case	Break area (m <sup>2</sup> )	Time of reactor trip	Max. nuclear power (%)	Max. core heat power (%)
1. Base case best-estimate (RTDBE), cold leg temp. compensation (OPAT): lag (2 s)				
a) mslb_be_00_notrip	0.0088	-	107.63% (208 s)	107.63% (216 s)
b) mslb_be_00_first_trip	0.0089	190.8 s (OPAT)	107.7% (190.8 s)	107.7% (190.8 s)
c) mslb_be_00_opdt – last OPAT	0.0221	24.86 s (OPAT)	110.41% (24.8 s)	109.02% (25.5 s)
d) mslb_be_00_si	0.0222	12.2 s (on SI)	105.76% (12.2 s)	103.41% (12.8 s)
2. RTDBE, steam line pressure compensation as for before RTDBE				
a) mslb_be_00_opdt_1 – last OPAT	0.0186	28.78 s (OPAT)	109.66% (28.7 s)	108.63% (29.0 s)
b) mslb_be_00_si_1	0.0187	10.21 s (on SI)	103.81% (10.2 s)	101.87% (10.5 s)
3. RTDBE, cold leg temp. compensation (OPAT): lag (7 s)				
a) mslb_be_01_notrip	0.0088	-	107.63% (208 s)	107.63% (216 s)
b) mslb_be_01_first_trip	0.0089	194.9 s (OPAT)	107.7% (194.9 s)	107.7% (195 s)
c) mslb_be_01_opdt – last OPAT	0.0221	31.59 s (OPAT)	111.78% (31.5 s)	110.76% (31.8 s)
d) mslb_be_01_si – identical to mslb_be_00_si	0.0222	12.2 s (on SI)	105.76% (12.2 s)	103.41% (12.8 s)
4. RTDBE, cold leg temp. compensation (OPAT): lead-lag (30 s, 10 s)				
a) mslb_be_02_notrip	0.0085	-	107.38% (200 s)	107.38% (216 s)
b) mslb_be_02_opdt – last OPAT	0.0221	12.27 s (OPAT)	105.75% (12.2 s)	103.5% (12.8 s)
c) mslb_be_02_si – identical to mslb_be_00_si	0.0222	12.2 s (on SI)	105.76% (12.2 s)	103.41% (12.8 s)
5. Conservative calculation, ref. [6], cold leg temp. compensation (OPAT): lag (2 s)				
a) mslb_sal_notrip	0.01826; (0.0195, ref. [6])	-	115.78% (100 s)	115.76% (100 s); (116.1% in ref. [6])
b) mslb_sal_opdt – last OPAT	0.03198; (0.0307, ref. [6])	28.48 s (OPAT); (27.15 s, ref. [6])	125.77% (28.4 s)	123.21% (28.8 s); (122.1% (27.6 s), ref. [6])
c) mslb_sal_si	0.03199	12.49 s (on SI)	112.92% (12.4 s)	107.68% (13.0 s)
6. Best-estimate calculation for configuration before RTDBE				
a) mslb_rtd_notrip	0.0088	-	107.64% (208 s)	107.64% (216 s)
b) mslb_rtd_first_trip	0.0089	172.15 s (OPAT)	107.7% (172 s)	107.7% (172 s)
c) mslb_rtd_opdt – last OPAT	0.0185	23.13 s (OPAT)	108.5% (23.1 s)	107.13% (23.4 s)
d) mslb_rtd_si	0.0186	10.72 s (on SI)	104.1% (10.7 s)	102.14% (11.2 s)
7. Best-estimate calculation for configuration before RTDBE, steam line pressure compensation as for RTDBE				
a) mslb_rtd_opdt_1 - last OPAT	0.0221	20.09 s (OPAT)	109.15% (20.0 s)	107.37% (20.5 s)
b) mslb_rtd_si_1	0.0222	12.2 s (on SI)	105.76% (12.0 s)	103.41% (12.8 s)

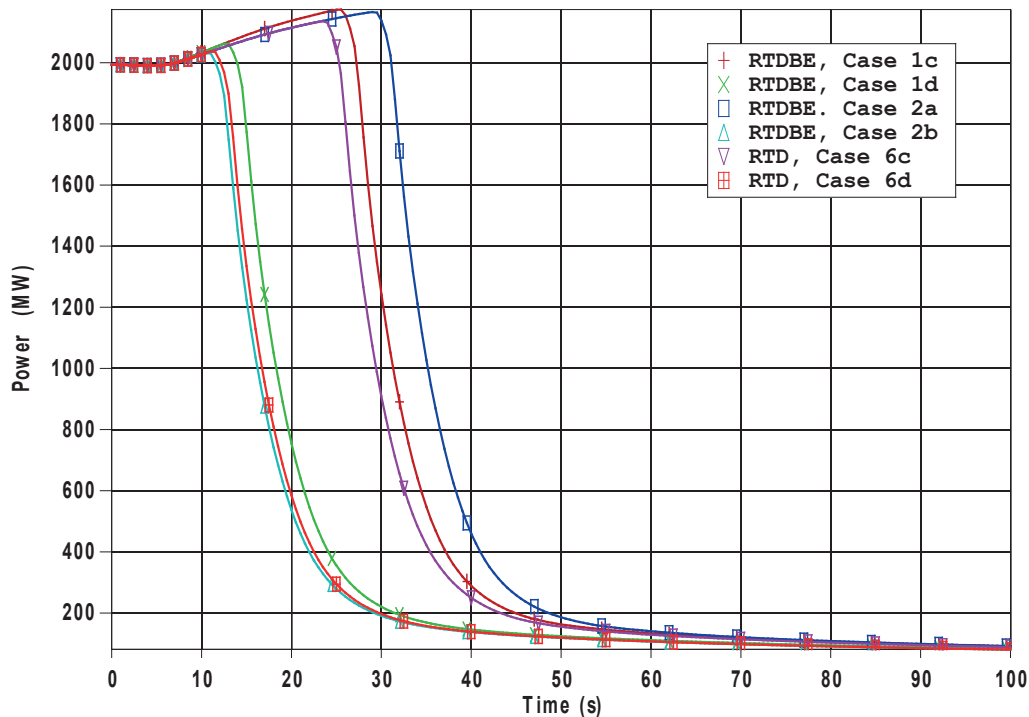


Figure 10. HFP MSLB analysis, core heat power, sensitivity calculations for RTDBE and pre-RTDBE (RTD)

#### 4. CONCLUSION

NPP Krško has changed way of RCS coolant measurement from RTD bypass to thermowell mounted RTDs as part of RTDBE project aimed to improve operation and maintenance. The compensation of the signal representing the coolant temperature increase ( $\Delta T$ ) in reactor vessel for the OPAT protection function has been modified as part of the RTDBE. In the paper, different concepts for coolant temperature compensation were studied for the decrease of feedwater temperature (FM DFT) and main steam line break at hot full power (HFP MSLB). Following conclusions can be drawn from the performed RELAP5 analyses:

- The cold leg temperature compensation for the base case post-RTDBE configuration (lag compensation, time constant=2 s) results in a delayed response of the OPAT trip when compared with the pre-RTDBE configuration. However, the obtained differences for the maximum heat power between the post and pre-RTDBE concepts are small (less than 2% for both accidents).
- By increasing the lag compensation for the cold leg temperature from 2 s to 7 s the maximum core heat power for the analyzed accidents would increase by less than (2-3)%.

- The sensitivity calculation with lead-lag compensation for the cold leg temperature with greater lead time constant (30 s vs. lag time constant=10 s) would result in fast response of the OPAT trip for both accidents and in the considerably lower maximum core heat power than for the pre-RTDBE configuration. That concept has shown to be sensitive to electromagnetic disturbances and it would cause unnecessary reactor trips.
- The analysis for the main steam line break has shown that the change of the steam line pressure compensation has a significant influence on the minimum break size for safety injection actuation. The change of the lead-lag compensation (48 s and 8 s vs. 50 s and 5 s) introduced along with the RTDBE leads to an increase of the minimum break size (0.0222 m<sup>2</sup> vs. 0.0186 m<sup>2</sup> for the pre-RTDBE).
- For both the FM DFT and the HFP MSLB accident similar values for the maximum nuclear power and the maximum core heat power values for the cases where OPAT signal is actuated were obtained (e.g., the maximum core heat power for the base case post-RTDBE configuration: 109.5% for the FM DFT and 109.02% for the HFP MSLB). The obtained maximum values are acceptable and demonstrate the adequacy of the selected post-RTDBE OPAT protection concept (cold leg temperature lag compensation, time constant= 2s) to protect the core during overcooling accidents.

## 5. REFERENCES

- [1] NEK RELAP5/MOD 3.3 Post-RTDBE Nodalization Notebook, NEK ESD-TR-02/13, Revision 0, Krško 2013.
- [2] NEK RELAP5/MOD 3.3 Post-RTDBE Steady State Qualification Report, NEK ESD-TR-03/13, Revision 0, Krško 2013.
- [3] Precautions, Limitations and Setpoints for Nuclear Steam Supply System (2000 MWt Rating), Revision 26, Krško, May 2012.
- [4] D. Grgić, V. Benčik, S. Šadek, N. Čavlina, “Relap5 Modeling of PWR Reactor RTD Bypass”, Proceedings of the 8<sup>th</sup> International Conference on Nuclear Option in Countries with Small and Medium Electricity Grids, Dubrovnik, Croatia, 16-20 May 2010.
- [5] Krško Modernization-UPR with RTDBE Impacts, Increase in Heat Removal by the Secondary System, SSR-NEK-7.1, Revision 5, March 2014.
- [6] Krško RTD Bypass Elimination, Hot Full Power Steam Line Break, RTDBE-NEK-AR-02, Revision 2, January 2014.

**ŽELJKO TOMŠIĆ**

[zeljko.tomsic@fer.hr](mailto:zeljko.tomsic@fer.hr)

**University of Zagreb, Faculty of Electrical Engineering  
and Computing**

**TOMO GALIĆ**

[galiczg@gmail.com](mailto:galiczg@gmail.com)

**INA Industrija nafte d.d.,**

## **ANALYSIS OF FUEL CELL TECHNOLOGIES FOR MICRO- COGENERATION DEVICES IN THE HOUSEHOLDS AND SERVICE SECTOR**

### **SUMMARY**

Present-day fuel cells for combined heat and power (CHP), even when fuelled with natural gas, are a promising technology in residential and commercial sectors because of their efficiency and carbon benefits. Using micro-cogeneration devices in fuel cell technologies could play a significant role in reducing harmful emissions into the environment in the building sector at a national level. This paper presents different technological solutions for fuel cells in the building sector, and reviews their applications and their technical characteristics. These characteristics are the basis for their comparison with competitive low-carbon technologies. In addition, a common benchmark for comparison of different technologies through appropriate methodology is described, considering how these devices work when they are connected to an electric power system, while using real data of comparable devices.

This paper presents evidence and methods required for comparison of fuel cells with conventional systems for production of heat and electricity, as well as for competing with low-carbon technologies. A common way to compare fuel cell directly to heat pumps is developed, primarily through calculation of the equivalent coefficient of energy efficiency. The intensity of carbon emissions from electricity production is calculated using replacement methods, and a logical extension for calculating the intensity of carbon emissions from production of thermal energy for comparison to heat pumps is proposed.

**Key words:** fuel cell, micro-cogeneration, households and service sector, combined heat and power

## 1 INTRODUCTION

The simultaneous production of electricity and heat using devices in fuel cell technology (hereinafter: fuel cells) is one of the most effective low-carbon ways of producing energy in the building sector today. For this reason, such a way of producing electricity and heat has not been adequately represented in energy plans, and in addition, discussions on sustainable production of thermal energy by using heat pumps which are powered by low-carbon electricity contributed to the slow development and application of fuel cells technology in the building sector [1, 2]. Despite its high energy efficiency and significantly lower harmful emissions to the environment, compared with other technologies, the prevalent view is that, since fuel cells are fuelled by natural gas, they represents a technology that can only be a bridging technology; therefore, it is another step on the way to "truly" sustainable production of heat and electricity [3,4]. This paper will present a simple and powerful method for comparing energy efficiency and carbon emissions intensity of fuel cells over competing technologies, such as internal combustion engines in cogeneration mode (CHP engines) and heat pumps that are powered by electricity or gas. It incorporates a high quality research that considered saving carbon emissions from those technologies [eg. 10-13], but done individually for each technology. Those studies that have dealt with the comparison of different technologies relied on significant simplification [2, 14-16] or carried out numerical simulations and load characteristics of buildings [17-20], which cannot accurately convey the real challenges and the diversity of life and business in buildings. This paper will present the latest data on the characteristics of certain technologies that replace par-declared characteristics of equipment with empirical data frame from the real use of different technologies. The focus is directed towards the research of fuel cell technologies since those technologies have the least amount of empirical operational data to date.

This paper will present two new general methods of comparing different technologies, namely: the equivalent coefficient of energy efficiency (COP), which has not been applied to fuel cell technology, and the intensity of carbon emissions in the production of thermal energy, which is largely neglected in relation to carbon emissions in the production of electricity. These methods can be used in any country and for different technologies without the need for corrective calculations, and can be used to confirm whether fuel cell technologies can produce thermal energy with greater energy efficiency

than with the best heat pumps, and if so, can the heat produced be reasonably classified as carbon neutral or even carbon negative.

## 2 THE TECHNOLOGY OF FUEL CELLS AND THEIR CHARACTERISTICS

Fuel cells convert chemical energy into electricity and heat without combustion. A series of packages of individual cells are located in the device's heart, which are interconnected in order to ensure the desired power of the device. The cells provide a thorough conversion of hydrogen into electricity and must be interconnected with a number of auxiliary systems to ensure operation of the cogeneration system, including:

- The fuel processor that transforms natural gas or other fuels into hydrogen,
- Subsystem for the reception of heat and hot water production,
- Exchanger and a voltage regulator to convert DC to AC electricity and ensuring synchronization of alternating electrical energy to the electricity network to which the fuel cell is connected,
- Extra gas boiler in order to meet peak demand for heat energy,
- Control and security subsystems and others.

Most stationary fuel cells are fuelled by natural gas because of its availability and low cost compared to other fuels. Fuel cells can also operate on liquefied petroleum gas (LPG), kerosene and gas from renewable energy sources such as landfill biogas and other types of biogas from various types of plant and animal waste. If hydrogen was available using renewable energy sources, rather than hydrocarbons, fuel cells could be in a much more competitive position than other technologies, and thus would also:

- Halve the complexity of the system and its prices due to the removal of the fuel processor,
- Improve system efficiency by 15-20%.
- Transform fuel cells from being a technology in transition to being the main technology for low-carbon energy systems.

There are different types of fuel cells, depending on the type of material used and depending on the operating temperature at which they work, which results in the type of fuel that is accepted and auxiliary equipment that is required. However, all types of fuel cell technologies have high energy efficiency, very few moving parts, operate quietly and have low emissions. The four most common technologies in fuel cell cogeneration implementation used today in these sectors are: PEMFC - proton exchange membrane fuel cells (hereinafter: PEMFC), SOFC - solid oxide fuel cells (hereinafter: SOFC), MCFC - molten carbonate fuel cells (hereinafter: MCFC) and PAFC - phosphoric acid fuel cells (hereinafter: PAFC). Low temperature fuel cells in PEMFC technology, with operating temperature from 0 to 100 degrees Celsius, are the most advanced fuel cell technology, and represent about 90% of all fuel cells [23]. A decade of research and development of fuel cells resulted in their high efficiency and long lifetime, while costs fell significantly due to increased production [21]. High-temperature fuel cells in the SOFC technology, with operating temperature from 500 to 1000 degrees Celsius, are known for the greatest degree of

electrical efficiency and greater flexibility to fuels, but cannot be operatively-dynamically managed as PEMFC technology can because of the high operating temperature [24]. Fundamental researches try to achieve the goal in the field of lifetime and stabilization of the temperature, with the trend towards medium temperatures from 500 to 750 degrees Celsius [25]. This would allow a wider range of materials that could be used, reducing production costs and improving dynamic characteristics. High-temperature fuel cells in MCFC technology are used for industrial cogeneration and power plants connected to the electricity system (3-60 MW), and become the leader in the market for large stationary applications [23]. Fuel cells in PAFC technology were the first such technology to be used for the production of thermal energy, and began being used in the 1970s in the service sector, in cogeneration systems [28]. Typical for fuel cells in PAFC technology is their long lifetime and high reliability, but also slightly lower efficiency than with other technologies [22].

## 2.1 Fuel Cells for Household Needs

Fuel cells for households in PEMFC and SOFC technologies are made up of a comprehensive system for heating and electricity supply, with a rated power of 0.75-2 kW of electric power and 1-2 kW of heat power, and are integrated into a unified energy system for household, together with a gas boiler and a hot water tank. The fuel cells systems are physically larger than gas boilers, typically located on the floor and installed outside the house or in the basement. The system weighs 150-250 kg and occupies two square meters of space, including a hot water tank and an auxiliary boiler, but smaller models are also being developed which can be mounted on the wall. Micro-cogeneration systems for household needs in large numbers began being installed in residential areas in 2009 in Japan. In 2012, for the first time, cogeneration systems in the technology of fuel cell cogeneration systems surpassed the technology of internal combustion engines with 28,000 sets built worldwide [31]. Leading manufacturers are Panasonic, Toshiba, Sanyo and Kyocera; CFCL; Baxi, Viessmann and Hexis; GM and FCPower. Japan leads in the implementation with 60,000 pieces of complete systems sold in the last four years [32]. Europe and South Korea are lagging behind Japan 6-8 years, but all regional markets increase around twice a year. This growth is expected to continue, and the Government of Japan plans to install 1.4 million fuel cells by 2020, while the European goal is 50,000 fuel cells, most of them in Germany [32, 33].

The program of the Japanese government, together with Japanese companies called ENE-FARM, has allowed the installation of over 120,000 units in households and is a good example of public-private partnerships in the development of new technologies. New models, which have arrived on the market in 2015, are smaller, more energy efficient, less expensive and a lot of them are easier to install than previous models. Models have also been developed for apartments and houses. The new models can be operated independently of the electricity grid; this is a reaction of the Japanese government to the concerns of end-customers about the reliability of the electricity grid after the events in Fukushima. Many companies in Japan participated in the development of new devices in fuel cells technologies, and among major companies that now produce commercial fuel cells for household are Panasonic and Toshiba, which offer market fuel cells in PEM technology, and

AisinSeiki that offers fuel cells in SOFC technology. Units in PEM technology have an extremely long life, with more than 60,000 hours in the pouring operation, which a few years ago was unthinkable. Panasonic claims that their model from 2015 achieved 95% of the overall energy efficiency. These units operate in parallel with the electricity grid, turning on and off in accordance to the demand for household electricity and heat. The result is the reduction of CO<sub>2</sub> emissions in households up to 50% and reduction of costs of electricity from 60,000 to 75,000 Japanese yen. The intention of the Japanese Government for hydrogen technology is 1.4 million units for households by 2020 and 5.3 million units by 2030 (about 10% of Japanese houses).

The company called Ceramic Fuel Cells Limited (CFCL) is a world leader in the development of fuel cell technology that produces highly efficient and low-carbon electricity from natural gas. The CFCL company sells fuel cells in the SOFC technology in micro-cogeneration performance called BlueGen, which produces electricity from natural gas, to major energy companies and other customers in Germany, the UK, Switzerland, the Netherlands, Belgium, France, Italy, Poland, South Korea, Japan, Australia and the United States. CFCL is also developing fully integrated products for the production of electricity and heat with leading energy companies such as E.ON in the UK, GdF Suez in France and EWE in Germany. CFCL in February 2015 announced that their product called BlueGen achieved a leading electrical efficiency at a global level in an extremely wide load range. BlueGen fuel cell produces 1.5 kW of electricity with the electrical efficiency of 60% or greater, as shown in Figure 1 [5].

The green line is the standard electrical efficiency of BlueGen units, while the blue line represents the optimistic operating mode for improved BlueGen unit. With such improved operating characteristics, BlueGen unit achieves electrical efficiency greater than 60% within the operational workforce of 0.8 kW to 1.5 kW. The electrical efficiency greater than 50% is achieved already at 0.5 kW workforces or about 30% of its rated output power.

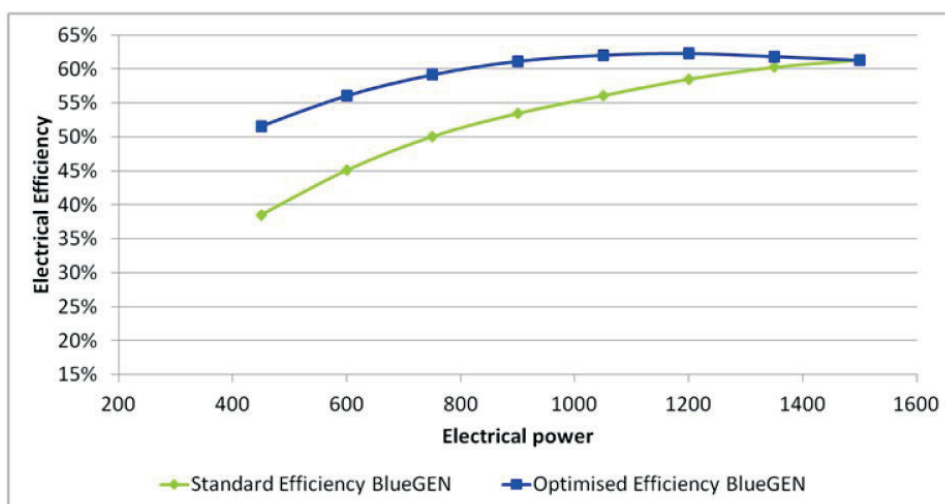


Figure 1: Electrical efficiency fuel cell BlueGen [5]

Such characteristics of BlueGen units will allow that the device operates in very harsh conditions, requiring the flexibility of the output of electric power, while maintaining high electrical efficiency within the declared operating mode. This significantly increases the commercial viability of production units in a variety of applications and different potential markets. A further focus of the development will be to reduce costs and to improve the production unit programs, and if possible, further develop of the characteristics of the commercial production units.

## **2.2 Fuel cells for service sector**

Shops, offices, healthcare facilities and other commercial buildings used in the service sector are the next significant market for fuel cells in cogeneration mode [1.35]. The demand for thermal energy in a number of business premises has a lot smoother profile than consumption demand in individual houses and is therefore much more acceptable for fuel cell technology. Fuel cells for the commercial sector are in the electrical power range from 100 to 400 kW and typically operate in parallel with the existing system of thermal energy production. The development of stationary fuel cell is driven through various programs in the European Union (EU) countries, and so the year 2015 was recorded as the last year of the German program called Callux programme, a program that encouraged the development of fuel cells through several companies of the EU, primarily German companies. More than 500 production units have been installed all over the country through this program. Compared to a relatively large number of companies that have developed micro-cogeneration fuel cells in EU Member States, the number of companies that have develop commercial and industrial fuel cells is very small. A continuous collaboration is underway between EU companies and companies from the USA, Canada, Japan and China to develop new joint solutions for fuel cell of small, medium and large size. Examples include the company Fuel Cell Energy Solutions GmbH (FCES), which is part of the US Company Fuel Cell Energy Inc. Business, which imports the modules from the USA and then develops them into finished projects in Germany. Also, in July of 2015, FCES Company announced an agreement with E.ON Connecting Energies and Friartec AG for the delivery of 1.4 MW fuel cell in cogeneration mode for production plant of the company Friartec AG in Germany.

## **3 PERFORMANCE FUEL CELLS AND THEIR CHARACTERISTICS**

### **3.1 Technical characteristics**

Technical characteristics of the individual fuel cell technology and the individual performance of fuel cell are shown in Table 1. The values for electrical and thermal efficiency are reported for the net calorific value (LHV), and can be expressed in the gross calorific value of fuel (HHV) by dividing the values with 1,109 (for natural gas).

Table 1: Summary of declared technical characteristics of fuel cells [6]

Application		PEMFC	SOFC	PAFC	MCFC
		Residential		Commercial	
Electrical capacity	(kW)	0.75-2		100-400	300+
Thermal Capacity	(kW)	0.7-2		110-450	450+
Electrical efficiency a	(LHV)	35-39%	45-60%	42%	47%
Thermal efficiency a	(LHV)	55%	30-45%	48%	43%
System lifetime	'000 h	60-80	20-90	80-1 30	20
	years	10	3-10	15-20 c	10 c
Degradation rate b	Per year	1%	1-2.5%.	0.5%	15%

<sup>a</sup> Rated specifications when new which are slightly higher than the averages experienced in practice.

<sup>b</sup> loss of peak power and efficiency .

<sup>c</sup> Includes overhaul of the fuel cell stack half - way through life.

### 3.2 Operational energy efficiency

Electrical and overall energy efficiency is relevant to cogeneration systems, but the major focus is on electrical efficiency since electricity is a much more valuable output of the system than are others. Fuel cells provide the highest electrical efficiency compared to any other technology that works in a cogeneration mode, and even small micro-CHP fuel cells are more efficient in relation to the best competitive conventional power plants [6].

Leading performance of fuel cell in the SOFC technology, for households, but also for those larger in size, have declared electrical efficiency of 45-60%, and the overall energy efficiency of 85-90% [7, 38]. The transformation of fuel for fuel cells PEMFC technology causes higher losses and lower electrical efficiency (up to 39%), but the overall energy efficiency is higher (95%) [8, 30]. Performance of European fuel cells for homes currently lags behind the leading Japanese and Australian models, with the current electrical efficiency within 30-35% for SOFC and PEMFC technologies [29].

Higher performance fuel cell PAFC technology has electrical efficiency at the level of 42% for electrical efficiency and 90% for the total energy efficiency [50], while fuel cells MCFC technology is at the level of 47% for electrical and 90% for overall energy efficiency [37]. Electrical efficiency is reduced during its lifetime due to degradation-decay of series of articles, resulting in an average electrical efficiency throughout its lifetime of 39% for PAFC technology and 42% for MCFC technology, while overall energy efficiency remains stable [39, 40]. Performance characteristics are in accordance with the manufacturer-declared characteristics since the building of the service sector provided largely continuous demand for energy.

System operation of fuel cell in real conditions in households, the achieved energy efficiency of small PEMFC and SOFC technology systems is less than the declared value, derived from laboratory tests, due to electricity for their own needs, because of reduced energy efficiency due to the load type, due to the energy required for starting the cycle of the device and loss of excess heat during the summer

because of reduced demand [22, 29]. The general trend is that higher energy efficiency is achieved in homes with higher demand for thermal energy [41, 42]. The engines in cogeneration mode and heat pumps have similar experience when using the imperfections in households due to specific operational conditions [9, 43, and 44].

Table 2 provides information on electrical and overall energy efficiency of 11 performance fuel cells for households, information about how the system works in real conditions and the information provided by the manufacturer according to factory tests as part of the manufacturing process, which are declared data. Comparative data shows that the difference is about one-tenth compared to the declared default data.

Table 2: Electrical and overall energy efficiency of fuel cells under real operating conditions [6]

			Rated Specifications <sup>a</sup>	Field Performance <sup>b</sup>	Real-world performance gap
PEMFC	Panasonic & Toshiba	2014	38.5–39% <sub>el</sub> / 94–95% <sub>tot</sub>	?	-
	(EneFarm)	2010	35–37% <sub>el</sub> / 81–89% <sub>tot</sub>	32.1% <sub>el</sub> / 73.2% <sub>tot</sub>	8-13%
	GS, FCPower & Samsung	2012	34-36% <sub>el</sub> / 82–86% <sub>tot</sub>	?	-
SOFC	Vaillant, Baxi & Hexis <sup>c</sup>	2012	31-35% <sub>el</sub> / 90–96% <sub>tot</sub>	30.5% <sub>el</sub> / 88.0% <sub>tot</sub>	8-9%
		2009	26-32% <sub>el</sub> / 90–96% <sub>tot</sub>	24.2% <sub>el</sub> / 84.1% <sub>tot</sub>	16%
	Aisin Seiki & JX (EneFarm-S)	2014	43-46.5% <sub>el</sub> / 87-90% <sub>tot</sub>	?	-
		2011	42-45% <sub>el</sub> / 77-85% <sub>tot</sub>	40.0% <sub>el</sub> / 82.1% <sub>tot</sub>	5-12%
	CFCL	2011	60% <sub>el</sub> / 85% <sub>tot</sub>	51-56% <sub>el</sub>	7-15%

<sup>a</sup> Electrical and total efficiency referred to as % el and % tot, against LHV.

<sup>b</sup> Referred to as “utilisation efficiency” or “capacity factor” to distinguish from gross generating efficiency under ideal laboratory conditions.

<sup>c</sup> Data is only available aggregated over three manufacturers of both PEMFC and SOFC.

Fuel cells are characterized by very high energy efficiency at partial loads because the voltage series of articles increases with decreasing density. However, at the level of the overall system, reducing efficiency are caused by parasitic losses, which is why efficiency falls towards the real function, as shown in Figure 2. The individual performance of fuel cells differ depending on the type of series of articles: electrical efficiency falls much faster for SOFC technology, while thermal efficiency increases at partial load.

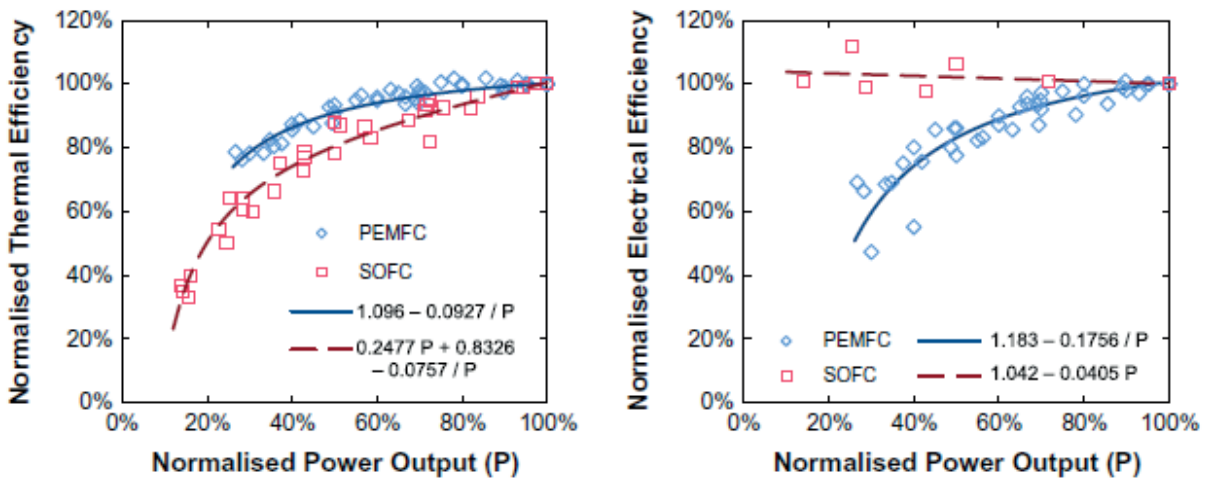


Figure 2: Electrical and thermal efficiency fuel cells for household [6]

### 3.3 The service life of the system

The duration of the system has been a key feature which slowed down the application of fuel cells and has been well below the critical 40,000 hours or about 10 years of work in household systems (about 5,000 h per year) [22]. System improvements in the last years were significant and so the lifetime values range as follows: Japanese fuel cell in PEMFC technology today guarantees 60-80,000 h of work [8, 30], and in SOFC technology up to 90,000 h [38]. Systems for households in Europe and other countries are trying to catch up with those standards, but the lifetime of their devices is around 10-20,000 h [29, 48].

The diagrams in Figure 3 show the improvement of the life of the system based on the manufacturer's warranty and results on the ground. Exponential growth characterizes each technology, suggesting the average industrial growth of the system's lifetime of 16-22% per year since the beginning of the century.

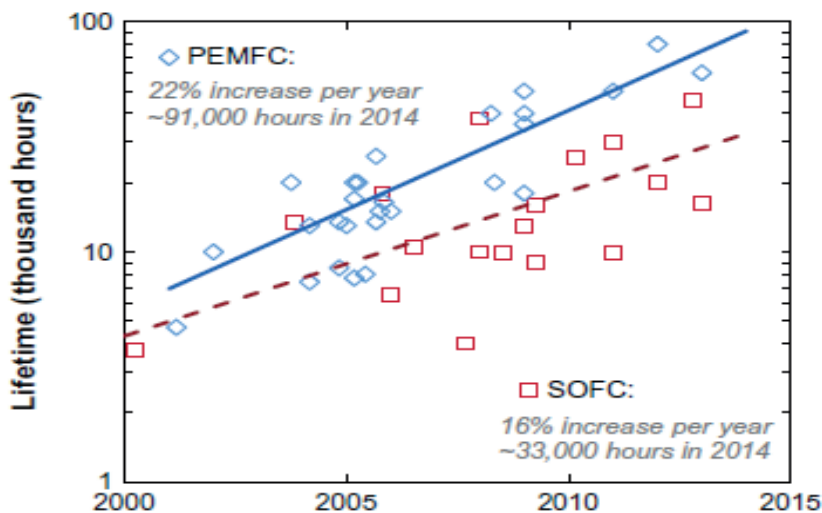


Figure 3: The service life of fuel cell PEMFC and SOFC technology [6]

Commercial fuel cells PAFC technology worked for decades, and the current system guarantees 80-130,000 hours (12 to 20 years, around 6,500 h per year), but with the need for outage after the first 10 years [52,76]. Fuel cells MCFC technology, on the other hand, is still battling with lifetime length due to aggressive chemistry of numerous articles and leakage [26, 49]. Since the system is expected to operate for 10 years, the average time for replacing a series of articles increases initial costs by about 15% [27].

### 3.4 System reliability

Conventional technologies for the production of thermal energy have a very high degree of reliability, approaching up to 99.9%, or about an outage every three years. Like all new technologies, fuel cell technologies are also struggling to achieve such a high standard. Fuel cell systems for household show a reliability of about 97%, according to a study conducted by Callux project tests in Germany. Mean time between failure (MTBF) is about 1,700 h (one failure every four months) [45]. MTBF has doubled since 2008 and the trend is expected to continue with the new generations. Similarly to that study, 90% of the unit from the first-generation project EneFarm suffered from failure in their first year during the period from 2004 to 2007, but these early problems were overcome and now only 5% of all systems fall short in the first years [8], which is comparable with the gas boilers. In both tests conducted, failures were distributed between the different components as follows: a series of articles, the converter of fuel circulation pump and system power management.

By reaching maturity, large fuel cells with PAFC and MCFC technologies moved to a higher level of reliability and their average value has been at 95% for more than a decade [27, 50]. This is the upper value that is achieved with conventional power plants [51], and is comparable with commercial engines in cogeneration mode [52].

### 3.5 Aging technology

All technologies suffer from deterioration characteristics over time, from gas turbines and wind turbines to solar photovoltaic panels [53]. But for the fuel cells this is a specific problem. Until recently, cell voltage falling was 0.5-2% per 1000 hours, which resulted in the decline of power output and electrical efficiency of 2.5-10% per year [22]. This problem is partially replaced by increasing the thermal efficiency as losses of energy transformed into heat energy.

In the previous period, the level of aging is reduced to 0.5-1.5% per year in leading PEMFC and PAFC technologies [29, 54], 2% per year in MCFC [27] and 1.0 to 2.5% per year in SOFC technologies [46, 55, 56]. End of life is often proclaimed if output falls 20% below the rated power, which nowadays happens after 10-20 years of operation.

## 4 ENERGY PERFORMANCE OF COMPETING TECHNOLOGIES

Energy sector is a sector with rapid changes and characteristics of various technologies are constantly improving, which means that comparative technology

must be based on the most recent and reliable data. It also declared that the production characteristics are not necessarily representative of the real operating conditions of complete systems. Three technologies are competing with the technology of fuel cells on the market for households and service sector: internal combustion engines in cogeneration mode, and heat pumps driven by electricity or gas. The thermal energy obtained from biomass is the fourth option, but assessing energy efficiency, practicality, and sustainability of different options, requires a special in-depth assessment [34, 57 and 58].

#### **4.1 Internal Combustion Engines**

Internal combustion engines in cogeneration mode are less energy efficient than fuel cells due to the losses in the conversion of heat energy into mechanical or electrical energy, although thermal efficiency increased as a result of the conversion. Engine from the manufacturer Honda, model Honda ECOWILL is the most effective model for the size needed for the household (26% electrical efficiency, 66% thermal efficiency) [59]. Electrical efficiency grows with the capacity by using large cylinders, low-speed engines with higher compression [60]. Systems for domestic and small service business premises (1 power 10 kW) achieved electrical efficiency of 25-30% of net calorific value of natural gas, followed by 30-35% for larger service premises (power 20-200 kW) and of 36-40% for industry and energy companies (power of 0.5-5 MW) [52,60,61]. Thermal efficiency drops with time and much faster in the rated capacity, which means that the total energy efficiency fall is in the range from 85-92% to 73-84%. Results from independent laboratory testing show that the electrical efficiencies are close to the values that are declared by the producers; however, the overall energy efficiency is about 5% smaller [62]. At least three field tests have shown that these characteristics are similar in the building sector, provided that there is a consistent demand that will allow many working hours [12, 63 and 64].

External combustion and Stirling engines have similar overall energy efficiency but significantly lower electrical efficiency of around 12-18% for households and 20-25% for larger service areas [61]. However, several studies have shown electrical efficiency of only 6-10% if the technology is very sensitive to the working conditions and working hours [12,65-67]. Small houses recorded small electrical efficiencies, where electricity produced is less than the consumption of the system control unit [12].

#### **4.2 Heat pumps on electric power**

Heat pumps are characterized by their heat pump coefficient of performance (COP), which is obtained by dividing the quantity of heat provided by the electricity used to operate the pump under certain specified conditions. The values of the coefficient often moves within the value of 3 or 4, and in some practical research in households, as well as demonstration projects, the values obtained are in the range from 3.0 to 3.5 for a heat pump with air as a heat source (ASHPE) and 3.3 -4.2 with ground source heat (GSHP) [9]. However, the characteristics depend strongly on the temperature of the heat collectors, the outside air temperature for ASHPE or

temperature below ground or water for GSHP, while the coefficient of efficiency is reduced by 0.1 for every one degree Celsius fall of the outside temperature [9].

A better measure of efficiency is therefore seasonal coefficient of performance (SPF), which represents an annual coefficient of efficiency of the heat pump for a particular location, counting the temperature changes throughout the year [9]. SPF also account for the amount of energy used for circulation pump and auxiliary heating (as heat pumps normally have as a backup option resistive heating to electricity for peak loads) [9, 68].

In large practical researches in Germany, for systems of heat pumps of ASHPE type installed in households, the average seasonal coefficient of efficiency, on an annual basis, was measured in the range of 2.6 to 3.0, while the systems of heat pumps type GSHP achieved an average SPF of 3.3-4.0 [69, 70]. Two studies in the UK achieve the SPF value of 2.4-2.6 and 3.0-3.2 for ASHPE for GSHP [99,100], which is lower than the results in Germany due to colder and wetter climate in the UK, and due to certain problems which are caused by the installation, sizing system and mode [71, 72]. Heat pumps are particularly sensitive to work conditions and need more trained installers to achieve standards as prescribed in Germany [9].

#### 4.3 Heat pumps with gas

Two technologies of heat pumps prefer to drive using gas rather than electricity. Heat pumps that use gas internal combustion engines to power the compressor, which exploit waste heat from the cogeneration process by which electrical energy is produced [73-75]. Gas engines also power the heat-driven adsorption and absorption reactions, using chemical reaction of water-ammonia and zeolite instead of vapour compression cycle [73-75]. Although small engines are less energy efficient than electric power units, processing of waste heat increases the overall output efficiency to 30%, which is especially useful in colder climates [75, 76]. Unfortunately, data on the effectiveness of the field is not available.

## 5 TEMPERATURE DEPENDENCE OF FUEL CELL

For fuel cells and other technologies, the quantity, and efficiency of heat output falls as temperatures rise. Air/water of higher temperature has higher energy content and therefore cannot be produced in an efficient manner. The decline is minimal conventional technology because the flame temperature in a combustion engine is a few hundred degrees Celsius, while in other technology without burning the drop is even higher. This is most evident with heat pumps that rely on the temperature difference between ambient temperature and heat that provides for the needs of the household.

Figure 4 shows data from a variety of tests on the ground and different variations of different technologies. The average levels of efficiency losses are:

- 1-2% for 10 degrees Celsius at the micro-CHP system;
- 6-9% for 10 degrees Celsius with micro-CHP fuel cell;
- 14-19% for 10 degrees Celsius with a heat pump.

This highlights the importance of using low-temperature heat distribution for space heating applications and explains why high-temperature industrial processes are the hardest for decarbonisation.

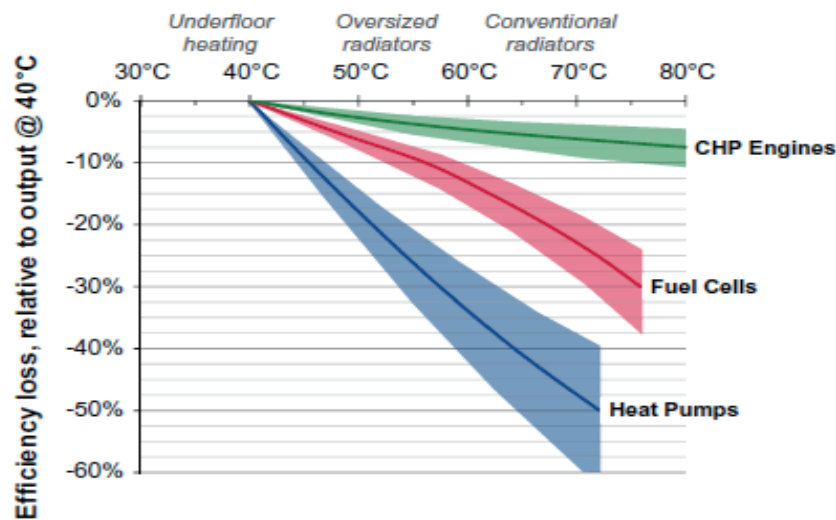


Figure 4: The influence of the outside temperature on the efficiency of thermal energy [6]

## 6 METHODS OF COMPARING ENERGY EFFICIENCY OF DIFFERENT TECHNOLOGIES

### 6.1 Comparison of efficiency through technology

Comparing the efficiency of fuel cell devices with other low-carbon technologies is not easy due to their structural diversity. For example, heat pumps consume electricity, while technology operating in cogeneration mode producing electricity. It is necessary to properly define the values of energy efficiencies, as electrical and thermal efficiency are used for cogeneration systems, and the coefficient of energy efficiency is used for heat pumps, providing a ratio of thermal energy that we get and the electricity that we provide.

MacKay explained in [3] that there is no simple cogeneration system which can be compared with the characteristics of the heat pump, which produces 3-4 units of heat per unit of electricity. This is acceptable for a medium-efficient cogeneration engine, but not for fuel cells. These technologies in different countries may be compared by calculating the electrical opposite the thermal efficiency in order to show their differences as in [3]. Primary energy efficiency of the heat pump depends on the heat pump and electricity used for its operation. The most efficient gas turbine with a combined cycle (CCGT) works with the gross energy efficiency of 60% [77], but its own parasitic consumption and time wear reduces the efficiency by 7% [53], while further transmission and distribution losses bring an additional 7% reduction of the efficiency, in the example of the UK [78]. In the last five years, a group of gas CCGT type power plants achieved an average net efficiency of 52%, which implies efficiency from the burner to the load port in the socket [78].

## 6.2 The calculation of the equivalent coefficient of energy efficiency for the system with fuel cell

By adopting measures that are used to determine the energy efficiency of heat pumps, different methods for comparison of different technologies can occur, which are based on the following ratio of input and output values in the energy system: the ratio of heat output and the amount of energy used at the entrance of a given energy system. Li et al. was the first to introduce the COP for cogeneration turbine of a large sizes [118], calculating the amount of electricity that is not produced when it produces only electricity in relation to cogeneration mode [79]. Lowe then introduced a similar method of determining the energy efficiency of cogeneration plants [120], and considerations of this problem by MacKay, which are used in the Heat energy strategy of the UK [80]. These methods are suitable for high power, such as 100 MW cogeneration power plants, but they cannot be applied to electrochemical systems such as fuel cells, which can not only produce electricity. The development of the new method is based on the adaptation of this concept to fuel cells, considering the process of enlargement of the systems which is used in lifecycle assessment methodology (LCA). By extending the model onto the entire electricity sector, the COP equivalent for the fuel cells could be calculated by dividing its heat output by the electrical output which was realized in the consumption of gas in the fuel cell (probably much more energy efficient), instead of in the CCGT power plant (best alternative technology).

Equivalent COP is calculated from the thermal efficiency fuel cell ( $\eta_{\text{heat}}$ ) divided by the difference between the electrical efficiency of fuel cell ( $\eta_{\text{elec}}$ ) and electrical efficiency of alternative power ( $\eta_{\text{CCGT}}$ ) that is extra electrical power that can be generated by the gas used in the gas plant instead of the fuel cell:

$$Eq_{\text{COP}} = \frac{\eta_{\text{heat}}}{\eta_{\text{CCGT}} - \eta_{\text{elec}}} \quad (1)$$

## 6.3 The calculation of the intensity of carbon emissions to the generated heat and electricity

By producing electricity and heat at the point of consumption, the fuel cell in the cogeneration process achieves significant CO<sub>2</sub> emission savings compared to centralized produced electricity and conventionally produced heat energy. There are several methods for determining the value of carbon emissions of the produced electricity in the cogeneration process, as the total emissions from the system must be allocated between the output value of electricity and heat [60, 81]. A typical fuel cell emits 500-600 g of CO<sub>2</sub> while producing 1 kWh of electricity and 1.5 kWh of thermal energy. These emissions can be assigned to each output product equally, weighted by its economic value or estimating net emissions by requiring the production of a single output of the product [82].

For example, if 1.5 kWh of heat is not produced using a fuel cell, it may be created using a different technology, so-called "reference technology". The common method for the allocation of the reference technology is therefore to assess how much fuel reference technology will spend to deliver such a large amount of heat

energy, and take away the resulting amount of fuel consumption of the fuel cell in order to get the net amount of fuel that is used solely to produce electricity.

Similarly, the intensity of carbon emissions for electricity produced can be calculated by assigning production of heat in the cogeneration process with an avoided production of thermal energy by using a condensing boiler. The intensity of carbon emission fuel cell to produce electricity is equal to the total amount of carbon emissions due to the production of one kWh of electricity reduced emissions that are avoided due to the simultaneous production of thermal energy. The total amount of emissions is equal to the intensity of carbon emissions flare gas ( $C_{fuel}$ ) divided by the electrical efficiency of fuel cell ( $\eta_{elec}$ ). Avoided carbon emissions are equal to the intensity of carbon emissions due to the replacement of produced heat ( $C_{boiler}$ ) multiplied by the amount of generated heat with each produced kWh of electricity, which gives the ratio of thermal efficiency ( $\eta_{heat}$ ) and electrical efficiency of fuel cell.

$$C_{FC}^{elec} = \frac{C_{fuel}}{\eta_{elec}} - (C_{boiler} \cdot \frac{\eta_{heat}}{\eta_{elec}}) \quad (2)$$

The method of equation (2) is relatively standard, used in the US EPA as a measure of "effective electrical efficiency" [60] and promotes commercial cogeneration systems [50, 37]. Less widely discussed indicator measuring the intensity of carbon emissions due to the production of thermal energy, in contrast to the intensity of carbon emissions due to electricity production. The only real application of these measurement indicators is the government standard procedural assessment of the UK when calculating the emissions of CO<sub>2</sub> when heating in local communities [83], as well as a special option for the calculation of emission factors for the offered heat or steam [81]. This method is not suitable for individual cogeneration plants or micro-cogeneration, and has not raised great, if any, attention in the academic literature. The equation (3) gives the calculation of the intensity of carbon emissions for the production of thermal energy:

$$C_{FC}^{heat} = \frac{C_{fuel}}{\eta_{elec}} - (C_{boiler} \cdot \frac{\eta_{heat}}{\eta_{elec}}) \quad (3)$$

The intensity of carbon emission fuel cells for the production of thermal energy  $C_{FC}^{heat}$  is equal to the total emissions to produce one kWh of thermal energy less emission avoided due to the simultaneous production of electricity. Total emissions are equal to the intensity of carbon emissions of gas divided by the thermal efficiency of fuel cells and the emissions that are equal to the intensity of carbon emissions for electricity from the power supply ( $C_{grid}$ ) multiplied by the amount of electricity that is produced by one kWh of thermal energy.

Impartially speaking, it is estimated that usually the best standard and available technology is the gas water heater. The intensity of carbon emissions of natural gas was 205 g/kWh (LHV), and the latest condensing boilers with an average of  $94 \pm 4\%$  of energy efficiency, in real conditions of use, produce thermal energy with emissions of 218 gCO<sub>2</sub>/kWh [44, 84].

## 6.4 The importance of the production of the average and marginal electricity

The intensity of carbon emissions due to electricity generation from the mains is open to evaluation because it is different from country to country, dependent on the season and time of the day. In the UK, the central electricity production has an average intensity of carbon emissions in the range from 500-520 g/kWh [78]. However, the average intensity varies over time as the energy-mix plants in operation (on an hourly basis) change in relation to the demand for electricity. Emission intensity is lower during the night, since nuclear power plants work in an almost constant operating regime with regard to power, which means that the fossil fuel plants reduce their work strength or shut down.

That's why we use the marginal emissions rather than the average ones when calculating the impact of distributed electricity generation. Changes in demand for electricity, caused by heat pumps that use electricity or fuel cells that generate electricity, will not cause the same reaction in the planning of power plants in the electricity system (EES). Some plants in the power system are not flexible to change of power (nuclear) or are largely unpredictable regarding the labour power (wind), leaving the remaining gas, coal and hydro power plants, which can be used to react to changes in the demand. Typical power plant (a combination of power plants) which can be engaged in response to changing demand, is known as the marginal plant, and connected with that is the marginal emission intensity which determines the actual reduction of emissions of CO<sub>2</sub>. While the intensity of average emissions in the UK is around 510 g/kWh, the intensity of the marginal emissions had an average of 690 g/kWh from 2002 to 2009 [85], and 640 g/kWh from 2009 to 2012 [127], which is around the mean between CCGT-gas plant (410 g/kWh) and coal plants (950 g/kWh) [34]. Determining the value of marginal emissions is a controversial issue and that is why average emissions are used in order to obtain the central results in this research.

## 7 THE RESULTS OF THE RESEARCH

### 7.1 Comparison of energy efficiency fuel cells and heat pumps

Figure 5 shows data on energy efficiency for conventional and low-carbon systems listed above, which are based on the characteristics of individual devices in real operating conditions, facing given producer characteristics.

Conventional - traditional systems were first presented as follows:

- Electricity from an average combination of power plants (according to data from the UK with 38.6% energy efficiency [78]), and the heat from the condensing boiler (94% energy efficiency [44]);
- The conventional - traditional technological limit is connected with a dashed line, whose technologies must be surpassed in order to offer a minimal improvement of energy efficiency.

Then "the best" low-carbon systems are considered, as follows:

- Electricity from the most efficient power plants (CCGTs with 52%) [78], and thermal energy from heat pumps based on the underground energy

sources installed in accordance with the highest standards (COP 3.3 to 4.0) [69,70];

- Intersection of technologies that use electricity is increased by efficient CCGT power plants, such as the COP 4 for heat pumps which produces 2.08 units of heat energy from one unit of natural gas burnt in the CCGT;
- The green line that connects all of these points is the limit of electricity, which represents the best available set up low-carbon solutions of the best energy efficiency, while shaded areas cover potential heat pump based on underground sources of energy, energy efficiency seen in a real use.
- Finally, the energy efficiencies of cogeneration systems that use gas are shown:
- Cogeneration with motors from 1 kW to 5 MW [52, 60, 61], with the overall efficiency reduced by 5%, which was used in the calculation in order to increased losses of the devices tested in real working conditions around the world [12, 62];
- Fuel cells based on the characteristics of real use systems around the world shown in Table 2.

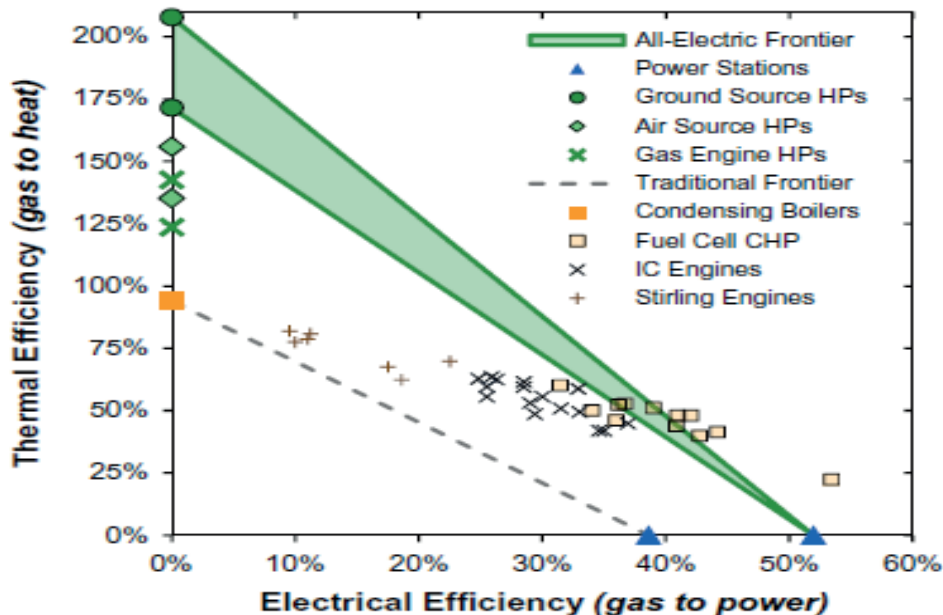


Figure 5: The energy efficiency of different technologies under real operating conditions [6]

As expected, all forms of low-carbon heating exceed the characteristics of the gas condensing boiler. The engines in cogeneration mode and gas heat pumps are slightly below the low-carbon limit, according to the MacKay, and have a similar performance compared to the current heat pump based on energy from the ambient air. However, fuel cells are around or above the threshold, implying that the best fuel cells (SOFC and MCFC generally) are much more efficient than the best heat pump even when these heat pumps are supplied with the most power from the mains.

In practice, it is not possible to guarantee that the heat pump be powered solely from a CCGT type power plant, a combination of power, gas and low efficient coal,

usually covering marginal power they can act in response to changes in demand [85]. Less optimistic assumption can move the entire border electricity on the left in Figure 5 (as production efficiency falls).

## 7.2 The equivalent ratio of energy efficiency fuel cells

Continuing with the assumption that centralized power plants are composed only of type CCGT power plants, with a 52% energy efficiency, equivalent COP for fuel cells PEMFC technology ranges from 2.8 to 3.4, and for PAFC and MCFC technology ranges from 4.1 to 4.8, while the best Japanese SOFC technology reaches 5.3. The system with a fuel cell called BlueGen of CFCL is equivalent to the heat pump with infinite COP, since its electrical efficiency is greater than the gas CCGT power plant and delivers useful heat. For comparison, the CHP engines shown in Figure 5 have an equivalent COP of 2.3 to 2.8, which is lower than both heat pumps, based on the energy in the air from the environment and energy from the ground [3]. Equivalent COP depends on the effectiveness of both the fuel cell and the power plant used instead of it. Figure 6 shows this sensitivity to a variety of fuel cell technologies. If fuel cells are replaced by the power, in equal parts, from the CCGT plant type (52% efficiency) and from standard coal boilers (40% efficiency), the equivalent COPs are significantly higher: 4.3 to 5.5 for PEMFC; 8.4 to 12.0 for PAFC and MCFC; and 14.4 - infinity for SOFC.

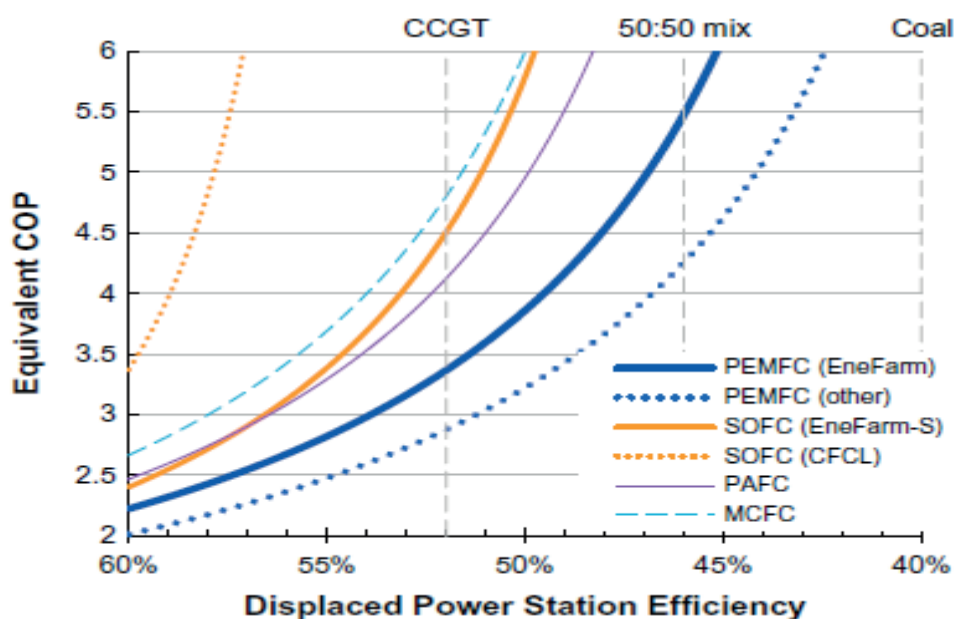


Figure 6: Sensitivity equivalent COP fuel cell on the electrical efficiency of the power system

Equivalent COP is a very sensitive characteristic of the fuel cell since the two conditions from the denominator ( $\eta_{CCGT} \times \eta_{elec}$ ) in the equation 1 are extremely close in value. Table 3 shows how the equivalent COP grows when declared efficiency is used in the area of real characteristics, calculated according to 52% efficient CCGT type power plants. As an example, we can take a 5% difference in relation to the

declared data on energy efficiency to the experience of Aisin Seiki EneFarm-S [46, 47], which reduces its equivalent COP of 8.0 to 5.3, according to Table 3.

Table 3: Equivalent COP for fuel cells with 52% efficiency power system [6]

	Field performance	Rated specifications
Panasonic & Toshiba (Enefarm)	3.31 - 3.44	4.13 - 4.32
GS, FCPower & Samsung	2.79 - 2.88	
Vaillant. Baxi & Hexis (Callux)	2.78 - 3.08	3.19 - 3.53
AisinSeiki & JX (EneFarm S)	3.94 - 5.32	5.14 - 7.98
CFCL	$\infty$	$\infty$
Purecell	3.94	4.82
Fuji	4.34	4.92
FuelCell Energy	4.82	8.69

### 7.3 The potential for mitigating carbon emissions

It is very difficult to generalize about the absolute savings of CO<sub>2</sub> derived from the use of fuel cells as they vary from country to country, mainly due to the intensity of carbon emissions from centralized power plants in the electrical network [86]. In Japan and Germany, manufacturers advertised 0.7 to 1 kW systems that generate savings from 1.3 to 1.9 TCO<sub>2</sub> per year in households with four members (reduction of 35-50%) [8, 30, 38, 129], while 1.5 kW CFCL BlueGen in Australia saves about 3 tons per year [7]. Slightly larger commercial systems (350-400 kW) offer savings of 700-1300 tCO<sub>2</sub> per year in Germany and the United States [27, 50]. There has been a general consensus that in countries with a common power system that is rich in carbon emissions, fuel cells (depending on the technology) can realize savings from 1.5 to 2 tons of CO<sub>2</sub> per year per kW of installed capacity. In other low-carbon technologies (e.g. photovoltaic panels and nuclear power plants), these savings can be additionally balanced with respect to carbon emissions generated during the production and/or construction of the power plant. The savings of carbon emissions for fuel cells are larger and more significant than for gas boilers that replace and require catalysts of nickel and platinum, which are extremely energy-intensive to produce.

Several lifetime estimates have taken into account the estimation of these carbon emissions, known as carbon footprint, discussing how fuel articles are produce, how much energy and which materials they require and how these materials are produced. The production of 1 kW cogeneration system for household emits 0.5 to 1 TCO<sub>2</sub>, while a 400 kW commercial system emits 100 to 400 tons of CO<sub>2</sub> [86,87-90]. If we reduce these emissions to average values by lifetime of those systems, they range from 10-20 gCO<sub>2</sub> per kWh (g/kWh) for electricity generation or 8-16 g/kWh of thermal energy production [86]. For comparison, the intensity of carbon emissions during construction is widely estimated at 40-80 g/kWh for photovoltaic sources of electricity and 10-30 g/kWh for nuclear power plants, from which we can conclude that the fuel cells technology has a relatively low environmental impact.

#### 7.4 The intensity of carbon emission fuel cells in the production of electricity

To avoid ambiguity caused by the diversity of national combinations of power plants to produce electricity, we can calculate the intensity of carbon emissions (g/kWh) instead of the absolute emission reductions. It then depends only on the characteristics of the fuel cell and heating system which it replaces. When the thermal energy is supplemented from the condensing gas boiler, then the intensity of carbon emissions, due to electricity from the fuel cell, is in the range from 240-280 g/kWh for the combination of about 2/3 CCGT plant type and 1/4 coal plant. Electricity from fuel cell has therefore significantly lower emissions than even the average or marginal emissions of power plants in most national electricity systems. The above values are based on the operational energy efficiency from the real conditions of use, and if the declared value were used (without penalization shown in Table 2), the intensity of carbon emissions would fall to 215 - 265 g/kWh.

Taking as an example the Panasonic EneFarm model that is in use in Japanese homes,  $\eta_{elec} = 36.7\%$  and  $\eta_{heat} = 52.6\%$ . For every kWh of electricity produced, 2.73 kWh fuel is consumed and 559 gCO<sub>2</sub> is emitted. Fuel cell also produces 1.43 kWh of thermal energy, for which, otherwise, 1.52 kWh of gas would need to be burned in a condensing boiler, and therefore the emissions would need to be reduced by 313 g. Therefore, the net intensity of carbon emissions is 246 g/kWh, which is similar to the one for fuel cells with PAFC technology (225 g/kWh) and fuel cells with MCFC technology (238-308 g/kWh) [36, 37].

Figure 7 shows the intensity of carbon emissions as a function of their electrical and thermal efficiency, showing fuel cells in parallel with an internal combustion engine (which averaged 255 to 315 g/kWh) and Stirling engines (240-340 g/kWh). There is considerable overlap between the intensity of carbon emissions from the electric power of each technology and electrical and thermal efficiency that are nearly balanced in a ratio of 1:1.

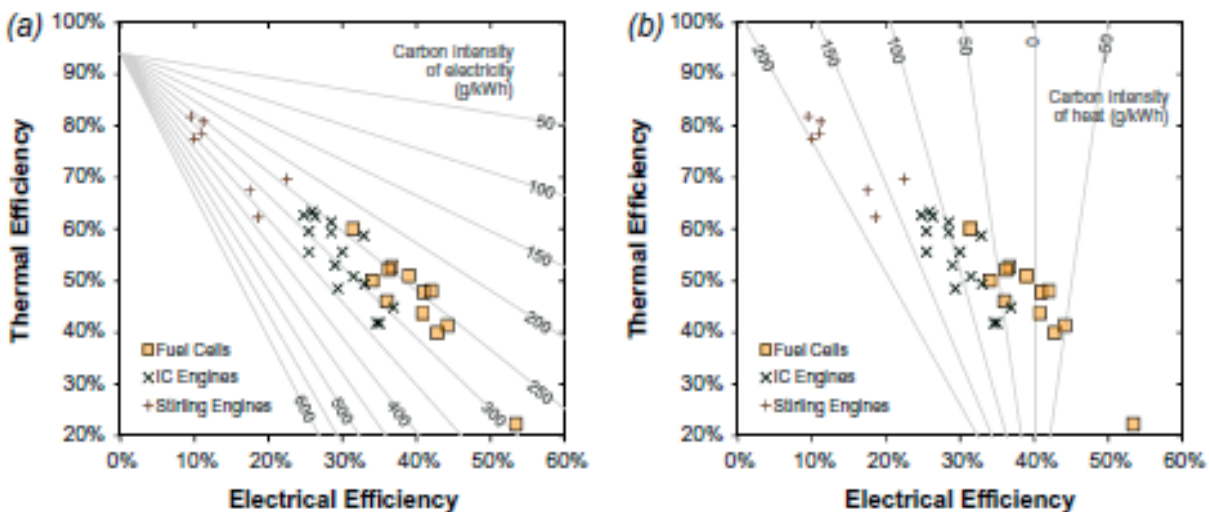


Figure 7: The intensity of carbon emission fuel cells and other technologies when the heat is replaced from condensing boiler and electricity from the power system

UK

## 7.5 The intensity of carbon emissions due to heat from the fuel cell

If electricity from fuel cells is responsible for escaped centralized electricity production, the intensity of carbon emissions due to the resulting thermal energy is around zero in the UK. Using the previously mentioned example, PEMFC fuel cell technology produced 1.43 kWh of thermal energy, emitted into the environment 559 g of CO<sub>2</sub>, while simultaneously producing 1 kWh of electricity and reducing national emissions of CO<sub>2</sub> to about 510 g/kWh (with an estimate of the average network energy mix); therefore, thermal energy has a net carbon intensity of 34 g/kWh ( $559 \times 510 / 1.43$ ), which means a six times increase compared to modern condensing boilers. By repeating the calculation with a much more efficient AisinSeiki SOFC ( $\eta_{\text{elec}} = 44.2\%$  and  $\eta_{\text{heat}} = 41.3\%$ ) outputs thermal energy that is carbon negative, with the intensity of -49 g/kWh.

It may seem counter-intuitive that a technology that uses fuel gas can produce thermal energy that is carbon neutral, but it is possible if electricity with lower emissions than emissions in the electricity grid is produced, and the thermal energy is also being used and is not thrown away. Any technology with gas combustion, with the electrical efficiency greater than 40%, has a lower emission than the average emission in the electricity grid of Great Britain; therefore, fuel cells SOFC and MCFC technology also fall into that category, while fuel cells PAFC and better PEMFC technology are not so far behind. Figure 7b shows the intensity of carbon emissions of heat from cogeneration systems whose values are: fuel cells emission average from -110 to 85 g/kWh; internal combustion engines from 70 to 120 g/kWh; Stirling engines from 155 to 200 g/kWh. For comparison, due to heat generation from heat GSHP type pumps, which use electricity exclusively from CCGT plant type, emit an average of 100 to 120 g/kWh, with an increase to 130 - 150 g/kWh for ASHPE type heat pump. If the heat pumps were to use electricity with the average formation of power plants in the UK, data on emissions for those heat pumps would be greater by 30%.

Fine lines in Figure 7b move to the right if the intensity of carbon emissions from the grid for electricity produced fall, reducing the attractiveness of cogeneration gas. If the network carbon emissions were to be halved to 255 g/kWh, then the electricity from centralized production would become equally valuable to the one produced from cogeneration technologies, as calculated in the previous section. The intensity of carbon emissions of heat from all cogeneration technologies would then converge towards the values that were obtained for burning gas in condensing boilers; then cogeneration would no longer provide benefits in carbon emissions. It is expected that the average carbon emissions in Great Britain's network, according to the latest calculations of carbon emissions, would fall to that level in the early 2020s, but it should be remembered that one cannot expect that the intensity of the marginal emissions would fall below 400 g/kWh (due to modern CCGT plant type) until the question of flexibility and manageability of low-carbon technologies is resolved.

A global review shows that the demand for heat energy rises to the level of half of the total energy consumption and CO<sub>2</sub> emission, but the reduction of carbon emissions in the production of thermal energy attracted relatively little attention compared to electricity and transport [4]. Since many countries are using gas for heat production in a highly-efficient way, it is still not yet a cost-effective low-carbon alternative. Fuel cells are not highly emphasized in the EU Decarbonisation Strategy, and are still losing against heat pumps.

This paper provides evidence and methods required for comparing conventional fuel cell systems for heat and electricity production and for competing with low-carbon technologies. A common way to compare fuel cells (and other cogeneration technology) directly to heat pumps is developed, primarily through calculation of the equivalent coefficient of energy efficiency. The intensity of carbon emissions for electricity production is calculated using replacement methods, and a logical extension is proposed in order to calculate the intensity of carbon emissions for the production of thermal energy for comparison with heat pumps.

Currently, the best solutions in the fuel cell cogeneration mode for the needs of households and the service sector, which made the analysis, reveal some key points:

- Electrical and thermal efficiency are declaratively large, but when the system works in real conditions, frequently switching the device on and off, then these values are different,
- Energy efficiency demonstrated in households is up to 10% less than the declared values, which reflects very similarly with the experience gained with heat pumps and engines in cogeneration mode,
- The service lifetime and reliability are significantly improved by the standards of competitive micro-cogeneration technology.

Even with optimistic assumptions that all electricity is produced from highly energy efficient CCGT type plants, equivalent COP fuel cells range from 2.8 to 5.3, and for the system with the best features, such as fuel cells with SOFC technology, the equivalent COP is infinite, since fuel cells with SOFC technology require less gas to produce electricity than CCGT type power plants would; and, in addition, it additionally provides thermal energy as an additional benefit. When the average energy mix for the UK was being considered (which is a distinctive energy mix for a country of higher national income), the equivalent COP grew to between 4 and 14, significantly higher than is achievable with electric or gas-powered heat pumps.

The intensity of fuel cell carbon emission can be summarized as follows:

- The equivalent thermal energy from a condensing boiler and electricity from the UK mains, with an average energy mix (two-thirds of the best CCGT power plant), is produced with half the intensity of carbon emissions from fuel cells; or
- Electricity from the power network of the UK with an average energy mix and heat energy that is carbon neutral or even carbon negative.

The development of common criteria for the comparison of different technologies, and respecting how they work within the interconnected power system, shows that the fuel cells provide heat with a higher energy efficiency than can be obtained with the best heat pumps and the heat leads to equal or even net reduced national

emissions of CO<sub>2</sub> from the use of electricity from the electricity grid, which has a higher carbon emission. Efforts to de-carbonise the power system with renewable energy sources and nuclear power plants will not significantly affect these conclusions since renewable energy sources can still quickly and easily respond to changes in demand, and are not likely to ever become marginal sources of electricity.

Fuel cells with the best characteristics in terms of energy efficiency should undoubtedly be treated as carbon neutral technologies for thermal energy. Just as heat pumps are classified as renewable technologies, despite consuming electricity from the mains, the same logic can lead to the claim that the most efficient fuel cells can be classified as renewable energy, despite consuming natural gas. So far, fuel cells have been excluded from these discussions, and as an example the definition of renewable heat in the EU directive for renewable energy can be used, which includes an electrical energy heat pump from the electricity grid, which has high carbon emissions, but excludes cogeneration systems that can offer similar or better value energy efficiency and lower carbon emissions.

There is a strong opportunity for fuel cells to contribute to low-carbon heating worldwide, by combining high efficiency, large annual energy output and wide applicability in building sector. Fuel cells can play a major role in national decarbonisation and energy policy strategies which should ensure access to this promising technology [4].

## 9 REFERENCES

- [1] DECC, 2013, The Future of Heating: Meeting the challenge: Department of Energy and Climate Change. <<http://tinyurl.com/decc-future-heat>>.
- [2] International Energy Agency, 2014, Energy Technology Perspectives. Paris: OECD/IEA.
- [3] MacKay DJC, 2008, Sustainable Energy – without the hot air. Cambridge: UIT. <[www.withouthotair.com](http://www.withouthotair.com)>.
- [4] Dodds PE, Hawkes A, McDowall W, Li F, et al., 2014, The role of hydrogen and fuel cells in providing affordable, secure low-carbon heat. London: H2FC SUPERGEN.
- [5] Bob Kennet, February 2015, Market Announcement, Technology Update: Efficiency maintained over extreme operating range; Ceramic Fuel Cells Limited.
- [6] Iain Staffell, 2015, Applied Energy- Zero carbon infinite COP heat from fuel cell CHP. Imperial College Business School, Imperial College London, Level 2 Tanaka Building, London SW7 2AZ, UK
- [7] Föger K, 2011, CFCL: Challenges in Commercialising an Ultra-efficient SOFC Residential Generator. Presented at IPHE Workshop on Stationary Fuel Cells. Tokyo. <<http://tinyurl.com/82eqw7h>>.

- [8] Nagata Y, 2013, Toshiba Fuel Cell Power Systems \_ Commercialization of Residential FC in Japan. Presented at FCH-JU General Assembly. Brussels. <<http://tinyurl.com/q8ov9td>>.
- [9] Staffell I, Brett D, Brandon N, Hawkes A. A review of domestic heat pumps. *Energy Environ Sci* 2012;5(11):9291–306.
- [10] Peacock AD, Newborough M. Impact of micro-CHP systems on domestic sector CO<sub>2</sub> emissions. *Appl Therm Eng* 2005;25(17–18):2653–76.
- [11] Dorer V, 2007, Review of Existing Residential Cogeneration Systems Performance Assessments and Evaluations. A Report of Subtask C of FC +COGEN-SIM. International Energy Agency, Annex 42.
- [12] Carbon Trust, 2007, Micro-CHP Accelerator: Interim Report. <<http://tinyurl.com/3ahxkqw>>.
- [13] Bianchi M, Branchini L, De Pascale A, Peretto A. Application of environmental performance assessment of CHP systems with local and global approaches. *Appl Energy* 2014; 130:774–82.
- [14] Cockroft J, Kelly N. A comparative assessment of future heat and power sources for the UK domestic sector. *Energy Convers Manage* 2006; 47(15–16):2349–60.
- [15] Pehnt M, Fischer C, 2006, Environmental Impacts of Micro Cogeneration, in *Micro Cogeneration: Towards Decentralized Energy Systems*, Pehnt M, Cames M, Fischer C, Praetorius B, et al., Editors. Springer: Berlin.
- [16] Dodds PE. Integrating housing stock and energy system models as a strategy to improve heat decarbonisation assessments. *Appl Energy* 2014; 132: 358–69.
- [17] Dorer V, Weber A. Energy and CO<sub>2</sub> emissions performance assessment of residential micro-cogeneration systems with dynamic whole-building simulation programs. *Energy Convers Manage* 2009; 50(3):648–57.
- [18] Cooper SJG, Hammond GP, McManus MC, Ramallo-Gonzalez A, Rogers JG. Effect of operating conditions on performance of domestic heating systems with heat pumps and fuel cell micro-cogeneration. *Energy Build* 2014; 70: 52–60.
- [19] Rogers JG, Cooper SJG, O’Grady Á, McManus MC, et al. The 20% house – an integrated assessment of options for reducing net carbon emissions from existing UK houses. *Appl. Energy* 2015; 138:108–20.
- [20] Mohamed A, Hasan A, Sirén K. Fulfillment of net-zero energy building (NZEB) with four metrics in a single family house with different heating alternatives. *Appl Energy* 2014; 114:385–99.
- [21] Staffell I, Green R. The cost of domestic fuel cell micro-CHP systems. *Int J Hydrogen Energy* 2013; 38(2):1088–102.
- [22] Staffell I, 2010, Fuel cells for domestic heat and power: Are they worth it? PhD Thesis, University of Birmingham. <<http://tinyurl.com/fcchp-worth-it>>.

- [23] Fuel Cell Today, 2013, The Fuel Cell Industry Review.
- [24] Kendall K, Singhal SC, 2003, Solid Oxide Fuel Cells: Elsevier Science.
- [25] Brett DJL, Atkinson A, Brandon NP, Skinner SJ. Intermediate temperature solid oxide fuel cells. *Chem Soc Rev* 2008; 37(8):1568–78.
- [26] Farooque M, 2009. FuelCell Energy – DFC Opportunities. Presented at US Department of Energy MCFC and PAFC R&D Workshop. Palm Springs, CA. <<http://tinyurl.com/oybpc4f>>.
- [27] Ullrich K, 2013. Fuel cells (MCFC) – the solution for self-sufficient industrial applications (CHP) with less CO<sub>2</sub>. Presented at SHFCA – Fuel Cells for large and small distributed generation. Edinburgh. <<http://tinyurl.com/mj77tb3>>.
- [28] Ferro J, 2009, PAFC History and Successes. Presented at MCFC and PAFC R&D Workshop. Palm Springs, CA.
- [29] Callux, 2013, Field Test of Residential Fuel Cells – Background & Activities. <<http://www.callux.net/home.English.html>>.
- [30] Panasonic, 2013, Launch of New ‘Ene-Farm’ Home Fuel Cell Product More Affordable and Easier to Install.
- [31] Delta-ee, 2013, Micro-CHP Annual Roundup 2012. <<http://www.delta-ee.com/research-consulting-services/micro-chp-service>>.
- [32] Hara I, 2013, Current Status of H<sub>2</sub> and Fuel Cell Programs of Japan. Presented at 20th IPHE Steering Committee Meeting. Fukuoka, Japan. <<http://tinyurl.com/pj5pee6>>.
- [33] Riddoch F, 2013, Ene.field European-wide field trials for residential fuel cell micro CHP. Presented at FCH-JU Programme Review. Brussels. <<http://tinyurl.com/nu5gudn>>.
- [34] Staffell I, Brett DJL, Brandon NP, Hawkes AD. Domestic microgeneration: renewable and distributed energy technologies, policies and economics. London: Routledge; 2015.
- [35] International Energy Agency, 2012, World Energy Balances: ESDS International, University of Manchester. <<http://dx.doi.org/10.5257/iea/web/2012>>.
- [36] ClearEdge Power, 2014, PureCell Model 400 Fuel Cell System Datasheet. <<http://tinyurl.com/oqxqebn>>.
- [37] FuelCell Energy, 2013, DFC300 Datasheet. <<http://tinyurl.com/oh9pl9j>>.
- [38] Kuwaba K, 2013, Development of SOFC for Residential Use by Aisin Seiki. Presented at 9th FC Expo. Tokyo.
- [39] Gummert G and Suttor W, 2006, Stationare Brennstoffzellen. Technik und Markt. (Stationary fuel cells. Technologies and Markets.): C.F. Muller Verlag.

- [40] Kumar A, 2012, Achieving 10 year cell stack durability in Phosphoric Acid Fuel Cell applications. Presented at Hannover Messe. <<http://tinyurl.com/pj5y6oc>>.
- [41] New Energy Foundation, 2010, (Solid Oxide Fuel Cell Empirical Research). <[http://sofc.nef.or.jp/topics/pdf/2010\\_sofc\\_houkoku.pdf](http://sofc.nef.or.jp/topics/pdf/2010_sofc_houkoku.pdf)>
- [42] New Energy Foundation, 2009, (Report data from the Large Scale Residential Fuel Cell Demonstration Project in 2008). p. 9, 38. <<http://happyfc.nef.or.jp/pdf/20fc.pdf>>.
- [43] Carbon Trust, 2011, Micro-CHP Accelerator: Final Report. <<http://tinyurl.com/7m2gkop>>.
- [44] Staffell I, Baker P, Barton JP, Bergman N, et al. UK microgeneration. Part II: technology overviews. Proceedings ICE – Energy 2010; 163(4):143–65.
- [45] Callux, 2014, Field Test of Residential Fuel Cells – Background & Activities. <<http://www.callux.net/home.English.html>>.
- [46] Iwata S, 2014, Status of Residential SOFC Development at Osaka Gas. Presented at FC EXPO. Tokyo.
- [47] New Energy Foundation, 2011, (Solid Oxide Fuel Cell Empirical Research). <<http://www.nef.or.jp/sofc/share/pdf/h22y.pdf>>
- [48] Ballhausen A, 2013, BlueGen: Vom Feldversuch in den Markt (From Field Tests to Market). Presented at NIP General Assembly. Berlin. <<http://tinyurl.com/psvs3av>>.
- [49] Hawkes A and Brett D, 2013, IEA ETSAP 13 – Fuel Cells for Stationary Applications. International Energy Agency.
- [50] Montany N, 2011, UTC Power – Commercialization of Fuel Cells. Presented at Fuel Cell Seminar & Exposition. Orlando, FL. <<http://tinyurl.com/ns249ce>>.
- [51] National Grid, 2013, Electricity Ten Year Statement. <<http://tinyurl.com/pgdoscu>>.
- [52] Lako P, 2010, IEA ETSAP 04 – Combined Heat and Power. International Energy Agency.
- [53] Staffell I, Green R. How does wind farm performance decline with age? Renewable Energy 2014; 66:775–86.
- [54] UTC Power, 2012, Energy Reinvented: Stationary Fuel Cells. Presented at Hannover Messe. <<http://tinyurl.com/pj5y6oc>>.
- [55] Knibbe R, Hauch A, Hjelm J, Ebbesen SD, Mogensen M. Durability of solid oxide cells. Green 2011; 1(2):127–240.
- [56] Haart LGJd, 2012, SOFC-Life. Presented at FCH-JU Programme Review Day. Brussels. <<http://tinyurl.com/pxnv7dp>>.

- [57] Saidur R, Abdelaziz EA, Demirbas A, Hossain MS, Mekhilef S. A review on biomass as a fuel for boilers. *Renew Sustain Energy Rev* 2011; 15 (5):2262–89.
- [58] Evans A, Strezov V, Evans TJ. Sustainability considerations for electricity generation from biomass. *Renew Sustain Energy Rev* 2010; 14(5):1419–27.
- [59] Tanaka H, Suzuki A, Yamamoto K, Yamamoto I, et al., 2011. New Ecowill – A New Generation Gas Engine Micro-CHP. Presented at International Gas Union Research Conference. Seoul. <<http://tinyurl.com/aw7s6bl>>.
- [60] EPA, 2008, Catalog of CHP Technologies. U.S. Environmental Protection Agency Combined Heat and Power Partnership. <<http://tinyurl.com/b4z7qer>>.
- [61] Darcovich K, Balslev P, Angrisani G, Roselli C, et al., 2014, A Market Overview of Commercialized Equipment for Residential Microgeneration Systems. IEA Annex 54 Subtask A.
- [62] Thomas B. Benchmark testing of Micro-CHP units. *Appl Therm Eng* 2008; 28 (16):2049–54.
- [63] Onovwiona HI, Ugursal VI. Residential cogeneration systems: review of the current technology. *Renew Sustain Energy Rev* 2006; 10(5):389–431.
- [64] Teekaram A, 2005, Installation and Monitoring of a DACHS Mini CHP unit at BSRIA. Presented at BSRIA/CIBSE CHP Group Seminar. London.
- [65] Entchev E, Gusdorf J, Swinton M, Bell M, et al. Micro-generation technology assessment for housing technology. *Energy Build* 2004; 36(9):925–31.
- [66] Woude Rvd, Haaken Et, Zutt S, Vriesema B and Beckers G, 2004, Intermediate Results of the Enatec Micro Cogeneration System Field Trials. Presented at International Stirling Forum. Osnabrück, Germany. <<http://tinyurl.com/ycnb7cw>>.
- [67] Veitch DCG, Mahkamov K. Assessment of economical and ecological benefits from deployment of a domestic combined heat and power unit based on its experimental performance. *Proc IMechE Part A J Power Energy* 2009; 223 (7):783–98.
- [68] Zottl A, Nordman R, Coevoet M, Riviere P, et al., 2011, SEPEMO WP4: Concept for evaluation of SPF Version 2.0.
- [69] Miara M, Günther D, Kramer T, Oltersdorf T and Wapler J, 2011, Wärmepumpen Effizienz (Heat Pump Efficiency). Fraunhofer ISE. <<http://wpeffizienz.ise.fraunhofer.de/>>.
- [70] Russ C, Miara M, Platt M, Günther D, et al., 2010, Feldmessung Wärmepumpen im Gebäudebestand (Monitoring Heat Pumps in Existing Buildings). Fraunhofer ISE. <<http://www.wp-im-gebaeudebestand.de/>>.
- [71] Dunbabin P and Wilkins C, 2012, Detailed analysis from the first phase of the Energy Saving Trust's heat pump field trial London, DECC. <<http://tinyurl.com/82tpk9y>>.

- [72] Dunbabin P, Charlick H and Green R, 2013, Detailed analysis from the second phase of the Energy Saving Trust's heat pump field trial. Department of Energy & Climate Change.
- [73] Wongsuwan W, Kumar S, Neveu P, Meunier F. A review of chemical heat pump technology and applications. *Appl Therm Eng* 2001; 21(15):1489–519.
- [74] Promelle J, 2011, Gas heat pumps: product overview. Presented at Gas Heat Pumps Workshop. Paris. <<http://tinyurl.com/cyjdww2>>.
- [75] Bakker E-J, Garde Jvd, Jansen K, Traversari R and Wagener P, 2010, Gas Heat Pumps: Efficient heating and cooling with natural gas. Groningen, The Netherlands: GasTerra/Castel International. <[http://www.gasterra.com/\\$resource/800](http://www.gasterra.com/$resource/800)>.
- [76] Hepbasli A, Erbay Z, Icier F, Colak N, Hancioglu E. A review of gas engine driven heat pumps (GEHPs) for residential and industrial applications. *Renew Sustain Energy Rev* 2009; 13(1):85–99.
- [77] Beedie M, 2007, GE's H-Series Breaks 60% Fuel Efficiency Barrier. <<http://tinyurl.com/y17qlcd>>.
- [78] MacLeay I, Harris K and Annut A, 2013, Digest of UK Energy Statistics. National Statistics.
- [79] Li H, Burer M, Song Z-P, Favrat D, Marechal F. Green heating system: characteristics and illustration with multi-criteria optimization of an integrated energy system. *Energy* 2004; 29(2):225–44.
- [80] DECC, 2012, The Future of Heating: A strategic framework for low carbon heat in the UK.
- [81] DECC, 2014, 2014 Government GHG Conversion Factors for Company Reporting: Methodology Paper for Emission Factors. <<http://tinyurl.com/owlt46z>>.

**Viktor Milardić**

**Ivica Pavić**

[viktor.milardic@fer.hr](mailto:viktor.milardic@fer.hr)

[ivica.pavic@fer.hr](mailto:ivica.pavic@fer.hr)

**University of Zagreb Faculty of Electrical Engineering  
and Computing**

## **ANALYSIS OF SURGE ARRESTERS FAILURES IN THE INSTALLATION OF BROADCASTING TRANSMITTER**

### **SUMMARY**

In the operation of the broadcasting transmitter, during a lightning storm, comes to frequent surge arrester failures in the switchgear of the broadcasting transmitter and along the 10 kV supply cable (surge arresters in the cable section boxes). Analysis of lightning strokes to the broadcasting transmitter is given in the paper. EMTP simulation of surge arresters loading was conducted. The energy overload of surge arresters is due to lightning flash with more than one lightning strokes or more lightning flashes in short time. Recommendations were also given for improvement of existing surge protection and reduction the number of surge arresters failures.

**Key words:** broadcasting transmitter, lightning stroke, overheating, surge arrester failure

## 1. INTRODUCTION

Broadcasting transmitters like all other tall objects (tall buildings, wind turbines) are exposed to frequent lightning strokes [1]. The average annual number of lightning strokes in such facilities can be hundreds of times [2]. Every lightning stroke in the facility may result in some damage. Lightning protection systems and surge protection seeks the probability of damages reduced to an acceptable value. Analysis of lightning strokes in the broadcasting transmitter (BT), analysis of surge arresters (SAs) failures in the switchgear of BT and along the route of the 10 kV supply cable and recommendations for improving the existing surge protection is given in this paper.

## 2. LIGHTNING STROKES IN THE BT

### 2.1. The BT

In the operation of the BT, located at 1762 m above sea level, Figure 1, during a lightning storm, comes to frequent SA failures in the switchgear of BT, Figure 2 and along the 10 kV supply cable (SAs in the cable section boxes). BT is power supplied from 35/10 kV transformer substation using 10 kV cable line length 8.455 km. The cable is sectioned by four cable boxes (CB1, CB2, CB3 and CB6), Figure 3. In every CB are installed 2 disconnectors and 3 SA (one in phase). The SAs in CBs are  $U_C=14$  kV, line discharge class 4.

SA failures have occurred in the switchgear of BT and in the cable boxes CB6 and CB3.



Figure 1. BT on Biokovo maintain 1762 m above sea level



Figure 2. Overloaded SA

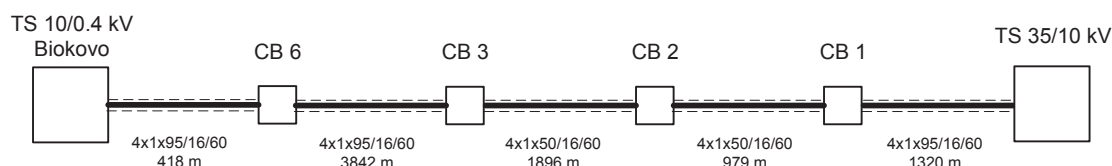


Figure 3. Schematic diagram of the 10 kV cable line

## 2.2. Statistical analysis of lightning flashes

In the Lightning Location System (LLS) [2], data were collected on lightning strokes at location of the BT. LLS data were collected over a period of six years, from 14th January 2009 to 5th January 2015. Lightning strokes were collected inside 2 km radius around the BT using LLS. LLS was collected a total of 3939 lightning strokes, with an average flash multiplicity of 1.63 gives the 2417 lightning flashes. The analysis of data on lightning strokes provided the following summary results, Table I.

Table I. Lightning flashes at location of BT [2]

Area [km <sup>2</sup> ]	Number of lightning strokes to ground	Average flash multiplicity	Number of lightning flashes to ground	Lightning flash density [1/km <sup>2</sup> year]
12.56	3939	1.63	2416	32.05

If we compare lightning flash density at the location of the BT 32.05 [1/ km<sup>2</sup>year], with the map of mean lightning flash density it is clear that the BT is many times more exposed to lightning flashes. On maps of mean lightning flash density the highest values are up to 4 [1/km<sup>2</sup>year] in Italy [3] to 6 [1/ km<sup>2</sup>year] in Spain [4] and to 4.84 [1/km<sup>2</sup>year] in Germany [5]. It should be additionally noted that the lightning flash density has been calculated for the circle radius of 2 km (12.56 km<sup>2</sup> area) around the BT. If we take the minor radius, e.g. 1 km, we will receive even greater lightning flash density, because lightning flashes are concentrated in the BT.

The analysis of the distribution of the peak values of the lightning current (3939 lightning strokes) gets the cumulative distribution shown in Figure 4.

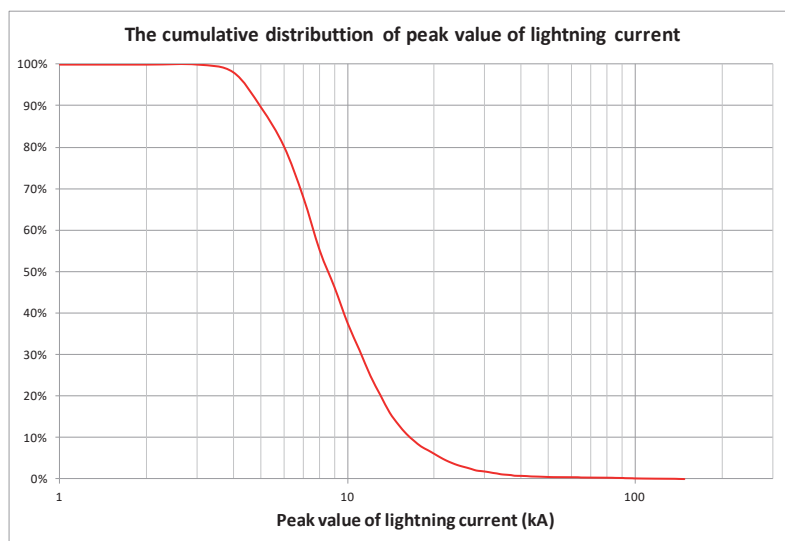


Figure 4. The cumulative distribution of peak value of lightning current (3939 lightning strokes) [2]

From Figure 4 can be read that 37.6% of all lightning strokes have a peak value greater than 10 kA. Less than 10% of lightning strokes have a peak value greater than 17 kA, and the peak value of lightning strokes greater than 37 kA, is less than 1%. The maximum peak value of lightning strokes (148.9 kA) was measured on 19<sup>th</sup> December 2011. This statistical analysis shows that the peak value of lightning strokes significantly deviating from those stated in Table A.1 in the IEC 62305-1 [6].

As previously stated, the BT like all other tall objects is exposed to frequent lightning strokes. As an example, lightning strokes from 4 PM 22<sup>nd</sup> November 2013 to 4 PM 23<sup>rd</sup> November 2013 and concentration of lightning strokes in the BT are shown in Figure 5. Lightning strokes inside 2 km radius around the BT in time between 23:26:24 and 24:00:00, 22<sup>nd</sup> November 2013 are in Table II. From Table II, we can see:

- a) There are not lightning strokes with high peak value of current;
- b) There are a large number of lightning strokes in a very short time interval.

Table II. Lightning strokes inside 2 km radius around BT in time between 23:26:24 and 24:00:00, 22<sup>nd</sup> November 2013 [2]

TIME (UTC)	CURRENT
22/11/2013/ 23:26:24,6370000	-7,3
22/11/2013/ 23:26:24,6760000	-19,2
22/11/2013/ 23:26:24,8530000	-15,8
22/11/2013/ 23:26:24,8880000	-13,2
22/11/2013/ 23:26:24,8960000	-9,8
22/11/2013/ 23:26:24,9200000	-6,2
22/11/2013/ 23:26:24,9750000	-5,5
22/11/2013/ 23:26:24,9970000	-10,1
22/11/2013/ 23:26:25,0500000	-17,6
22/11/2013/ 23:26:25,1010000	-4,8
22/11/2013/ 23:26:25,1450000	-15,1
22/11/2013/ 23:29:34,3230000	-9,3
22/11/2013/ 23:29:34,3610000	-7,7
22/11/2013/ 23:29:34,4050000	-10,7
22/11/2013/ 23:29:34,5020000	9,3
22/11/2013/ 23:30:57,0220000	4,1
22/11/2013/ 23:30:57,0320000	-9,6
22/11/2013/ 23:32:23,5520000	-3,9
22/11/2013/ 23:32:23,6190000	-5,7
22/11/2013/ 23:32:23,6340000	-14,9
22/11/2013/ 23:32:23,6430000	-6,8
22/11/2013/ 23:32:23,6500000	-9,5
22/11/2013/ 23:50:14,2110000	-9,9
22/11/2013/ 23:50:14,2520000	-9,2
22/11/2013/ 23:50:14,2660000	-4,5
22/11/2013/ 23:50:14,2810000	-4,5
22/11/2013/ 23:51:12,7370000	-4,2
22/11/2013/ 23:51:12,7690000	-4,5
22/11/2013/ 23:51:12,7810000	-3,9
22/11/2013/ 23:51:12,7930000	-4,5
22/11/2013/ 23:51:12,8090000	-9,2
22/11/2013/ 23:51:12,8330000	-4,1
22/11/2013/ 23:51:12,8560000	-5,0
22/11/2013/ 23:51:12,9170000	-9,0
22/11/2013/ 23:51:12,9200000	-9,7
22/11/2013/ 23:51:12,9420000	-8,4
22/11/2013/ 23:51:12,9670000	-9,6
22/11/2013/ 23:51:12,9850000	-7,9
22/11/2013/ 23:51:13,0250000	-21,9
22/11/2013/ 23:51:13,2310000	-4,4
22/11/2013/ 23:55:27,9280000	-10,4
22/11/2013/ 23:55:27,9450000	-4,7
22/11/2013/ 23:55:27,9630000	-4,7
22/11/2013/ 23:59:28,0590000	-8,2

Figure 6 shows the concentration of lightning strokes for a longer period of time. The different colors in Figure 6 indicate the range of peak value of lightning currents obtained from Linet LLS:

- ✕  $I \leq 3 \text{ kA}$
- ✕  $3 \text{ kA} < I \leq 5 \text{ kA}$
- ✕  $5 \text{ kA} < I \leq 10 \text{ kA}$
- ✕  $10 \text{ kA} < I \leq 16 \text{ kA}$
- ✕  $I > 16 \text{ kA}$

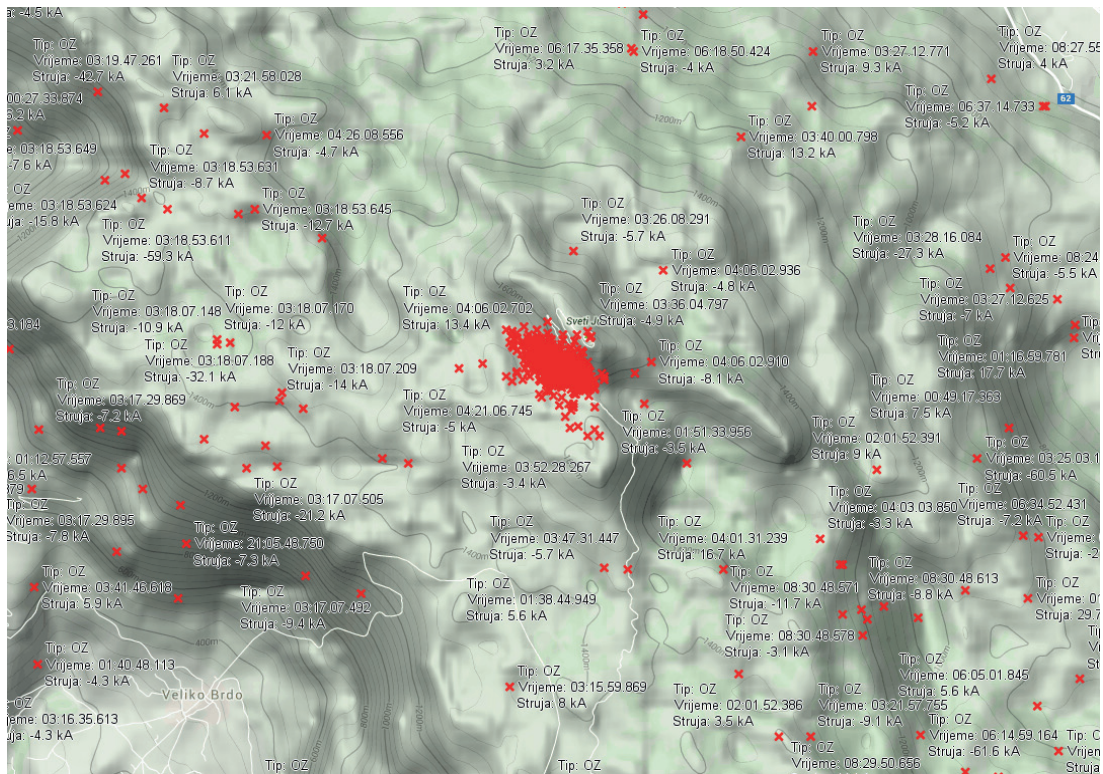


Figure 5. Concentration of lightning strokes in the BT, from 4 PM 22<sup>nd</sup> to 4 PM 23<sup>rd</sup> November 2013 [2]

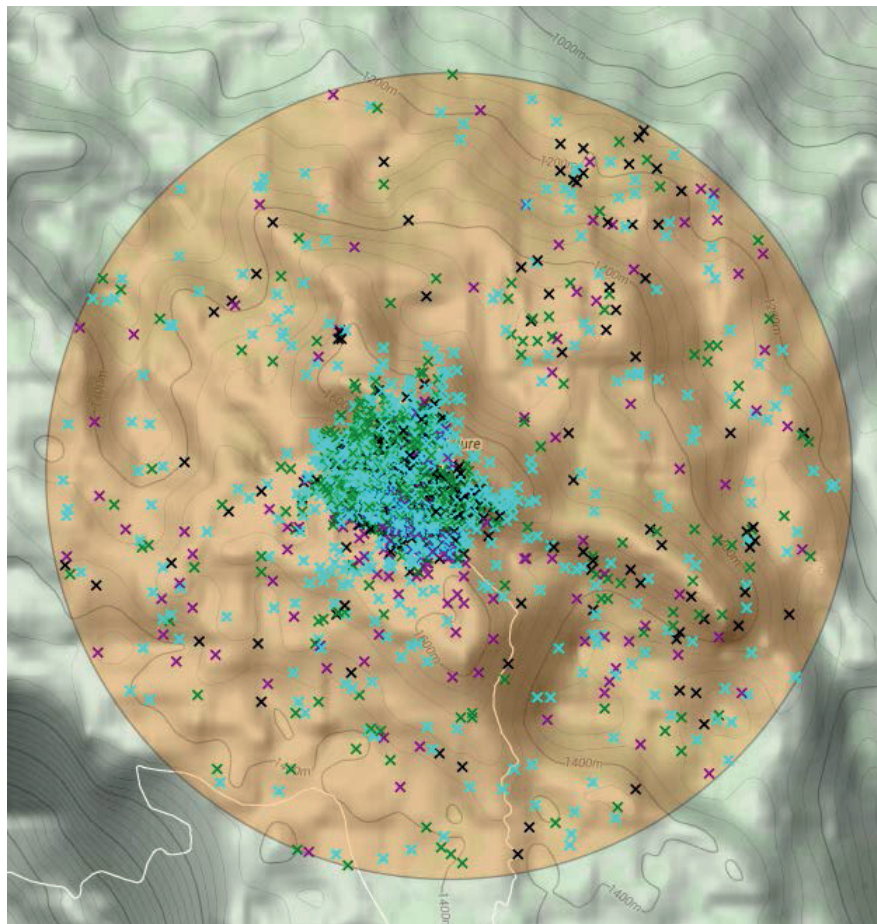


Figure 6. Concentration of lightning strokes in the BT from 14<sup>th</sup> January 2009 to 5<sup>th</sup> January 2015 [2]

Analysis of lightning strokes by months is following. Lightning strokes were collected inside 2 km radius around the BT using LLS [2]. Figure 7 shows the average monthly number of lightning flashes calculated using an average multiplicity 1.63. Lightning strokes were collected in the period January 2009 until January 2015. It can be concluded that the greatest number of lightning flashes in the BT were in October, November, December and May, Figure 7. Accordingly, the largest number of SAs failures was in those months.

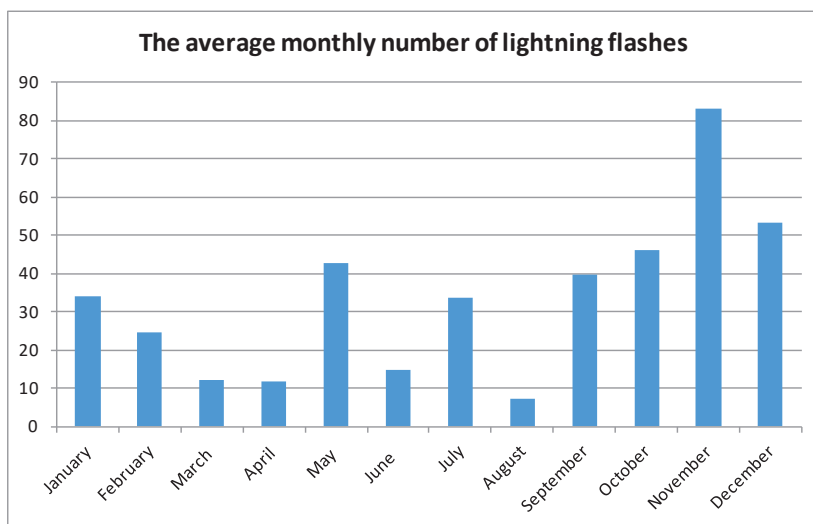


Figure 7. The average monthly number of lightning flashes

The average yearly number of lightning flashes inside 2 km radius around the BT is shown on Figure 8. It is clear that the number of lightning flashes varies considerably from year to year, and that 2013 was an extreme year by lightning flashes at the location of the BT.

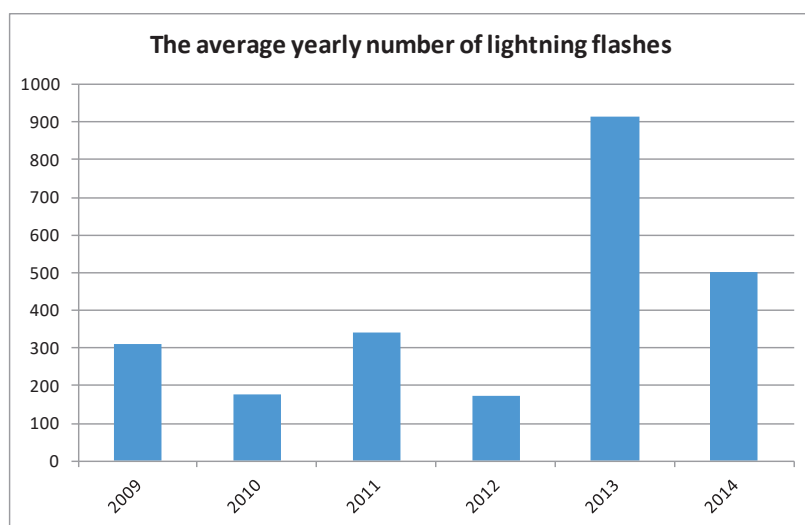


Figure 8. The average yearly number of lightning flashes

### 3. SAs FAILURES IN THE INSTALLATION OF BT

#### 3.1. Theoretical analysis

When lightning strikes BT, the lightning current flows through the earth electrode of BT and increase its potential to the reference earth. The occurrence of high transient potential of the earth electrode creates the transient voltage between the earth electrode and the phase conductors of 10 kV cables. Installed SAs limit the transient voltage conducting a part of lightning current from the earth electrode of BT to the phase conductors of 10 kV cables. In this way, the main insulation of 10 kV cables is protected. SA is heated by passing current through it. Thermal energy absorption capability is defined as the maximum level of energy injected into the SA at which it can still cool back down to its normal operating temperature. Figure 9 explains the problem of the thermal stability of SA. The electrical power loss resulting from the continuously applied power-frequency voltage is temperature-dependent. It rises over proportionally as the temperature increases. On the other hand, because of its design, the SA can only dissipate a certain limited amount of heat into the surroundings. Indeed, this heat-flow value also rises with the temperature, however, not nearly as much as the electrical power loss does. Both power curves have two common points of intersection. The left one is stable operating point. At this point exactly as much heat is dissipated to the outside, as is produced in the MO resistors i.e. a thermal balance prevails. A discharge operation disturbs this balance. The energy which is introduced increases the temperature of MO resistors rapidly, and the operating point moves to the right on the power loss curve, as is shown with an arrow in Figure 9. As long as the right point of intersection of the curves is not reached, the heat generated by electrical power loss can easily be dissipated, and the SA can return to the stable operating point. If, however, the right point of intersection is reached or exceeded, then cooling is no longer possible. The SA then becomes thermally unstable and heats up until it self-destructs. This point of intersection, therefore, represents the thermal stability limit. The thermal energy absorption capability is specified in such a way that the related temperature increase bring the SA to a temperature which exhibits an adequate safety margin to the thermal stability limit. The actual thermal stability limit depends on the overall design of SA and has a value of typically between 170 °C and 200 °C. Generally speaking, SA with molded polymeric housing dissipates the heat of the MO resistors better into the surrounding (comparing to porcelain-housed SA) and therefore its thermal stability limit is at slightly higher temperatures. On the other hand, the characteristics of MO materials (electrical losses and their temperature dependence) have an impact.

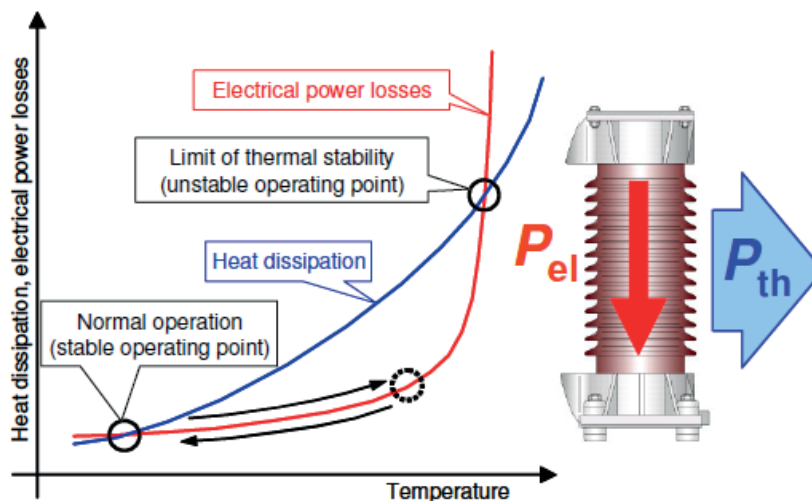


Figure 9. Explanation of the thermal stability of SA [7]

Failure of the SAs occurs by heating above the thermal stability limit. Therefore, if the SA is heated above the thermal stability limit, it leads to the thermal destruction of the SA and ultimately to earth fault (line-to-earth fault). Thermal destruction of SAs in the switchgear of BT occurs as a result of large number of lightning strokes in a very short time interval, table II. Every lightning stroke increases the temperature of MO resistors. There is not enough time for cooling of MO resistors between the lightning strokes or to return to a stable operating point. It leads to overheating and thermal destruction of the SA.

### 3.2. EMTP-ATP analyze

ATPDraw [8] simple model, shown in Figure 10, is formed for simulation of lightning stroke in the BT. Lightning stroke is simulated as the injected current. SAs of continuous operating voltage  $U_C = 14$  kV and  $U_C = 12$  kV, line discharge class 4, are modeled with their protective characteristics, Table III. SA can absorb about 186 kJ ( $U_C = 14$  kV) and about 160 kJ ( $U_C = 12$  kV). The connections of SAs to the earth electrodes are modeled as  $R=1$  m $\Omega$  and  $L=1$   $\mu$ H (or  $L=2$   $\mu$ H in dependence of their length). MV cables are modeled using JMarti model and electrical and geometrical parameters of the cable. Earth electrode resistances of the BT and of the CBs are not known. They had been measured but the sheath and the armor of the cables had not been disconnected. Because of that, resistances of certain earth electrode are not known. The assumption is that the earth electrode resistances of each one CB is 10  $\Omega$  and the earth electrode resistances of the BT is considered as parameter: 5  $\Omega$ , 10  $\Omega$  and 20  $\Omega$ . The earth electrode resistance of the BT is not necessary to modeled as nonlinear [9] according to equation (1) because the limiting current to initiate sufficient soli ionization, equation (2), in given case are: 159.16 kA ( $R=20$   $\Omega$ ), 636.6 kA ( $R=10$   $\Omega$ ) i 2546.5 kA ( $R=5$   $\Omega$ ).

$$R_i = \frac{R_0}{\sqrt{1 + \frac{I}{I_g}}} \quad (1)$$

$$I_g = \frac{\rho \cdot E_0}{2 \cdot \pi \cdot R_0^2} \quad (2)$$

In accordance to Figure 4 lightning strokes with so large peak value of current are unlikely.

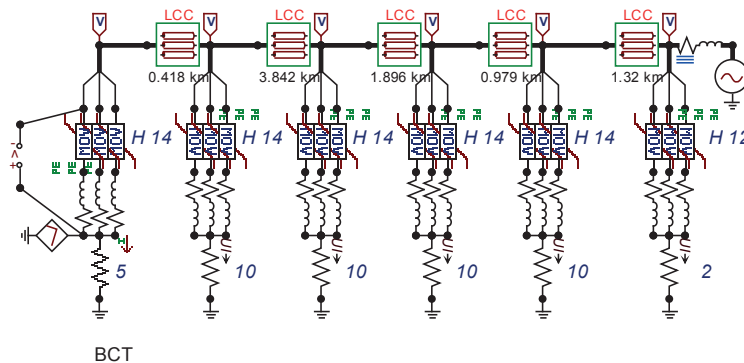


Figure 10. ATPDraw model

The lightning current 200 kA, 10/350  $\mu$ s is simulated according to [6] and the absorbed energy of SAs in all three phases are calculated. Obtained values are in Table IV (for SAs in BT), Table V (for SAs in CB6) and Table VI (for SAs in CB3). SA with  $U_C = 14$  kV, line discharge class 4, can absorb about 186 kJ, as previously was told. It is clear that energy-overload of all three SAs (in the switchgear of BT) will occur for any value of earth electrode resistance in the range (5-20)  $\Omega$ . Energy-overload of all three SAs (in CB6) will occur for value of earth electrode resistance in range just above 5  $\Omega$ . Such case of failure of all three SAs in the switchgear of BT has not been occurred.

Table III. Protective characteristics of SAs:  $U_C = 14$  kV AND  $U_C = 12$  kV, Line discharge Class 4

SAs with $U_C$	14 kV	12 kV
I (A)	U (kV)	U (kV)
0.001	19.8	16.97
0.01	22.5	19.28
0.1	25.2	21.58
1	27.9	23.89
10	30.6	26.19
100	33.3	28.50
1000	36.0	30.80
2000	37.1	31.80
5000	38.9	33.40
10000	40.6	34.80
20000	44.3	38.00
40000	49.6	42.50

Table IV. Absorbed energy of SAs in the Switchgear of BT (Lightning stroke 200 kA, 10/350)

Earth electrode resistance of BT ( $\Omega$ )	Absorbed energy of SA in phase A (kJ)	Absorbed energy of SA in phase B (kJ)	Absorbed energy of SA in phase C (kJ)
20	920	939	941
10	755	780	787
5	534	562	572

Table V. Absorbed energy of SAs in CB6 (Lightning stroke 200 kA, 10/350)

Earth electrode resistance of BT ( $\Omega$ )	Absorbed energy of SA in phase A (kJ)	Absorbed energy of SA in phase B (kJ)	Absorbed energy of SA in phase C (kJ)
20	303	323	334
10	238	254	262
5	161	169	175

Table VI. Absorbed energy of SAs in CB3 (Lightning stroke 200 kA, 10/350)

Earth electrode resistance of BT ( $\Omega$ )	Absorbed energy of SA in phase A (kJ)	Absorbed energy of SA in phase B (kJ)	Absorbed energy of SA in phase C (kJ)
20	117.1	118.2	117.7
10	94.3	91.6	89.8
5	65.6	60.6	58.7

Lightning current 37 kA, 10/350  $\mu$ s is simulated next, because less than 1% of peak value of lightning strokes are greater than 37 kA according to Figure 4. The absorbed energy of SAs in the switchgear of BT are calculated, Table VII. Different values of absorbed energy in phases occur due to different values of the power-frequency voltage at the time of stroke. From Table VII it is clear that the energy overload of SAs in case of one lightning stroke is unlikely. Therefore, the energy overload of SAs is due to lightning flash with more than one lightning stroke or more lightning flashes in short time.

Table VII. Absorbed energy of SAs in all three phases (Lightning stroke 37 kA, 10/350)

Earth electrode resistance of BT ( $\Omega$ )	Absorbed energy of SA in phase A (kJ)	Absorbed energy of SA in phase B (kJ)	Absorbed energy of SA in phase C (kJ)
20	114.0	127.0	130.7
10	80.0	94.0	98.0
5	39.3	53.0	56.7

There are 44 lightning strokes in less than 34 minutes, Table II. Every lightning stroke causes the current through the SAs and increases the temperature of MO resistors. There is not enough time for cooling of MO resistors between the lightning strokes or to return to a stable operating point. Such events can cause the overload of one or more SAs.

### 3.3. Recommendations

What can be done to avoid failures of SAs or minimize the number of failures?

Solutions are as follows:

1. Reduction of earth electrode resistance of the BT, what increases the part of the lightning current flowing through the earth electrode and decreases the part of the lightning current flowing through the SAs. This solution requires considerable financial costs. It includes the rehabilitation of the earth electrode of the BT, replacement of existing and laying new earth rods in adequately prepared channels.
2. Increase the thermal energy absorption capability of SAs (several SAs of the same type in parallel). One set of 3 SAs are installed directly at the power

transformer and the second set of 3 SAs at the point of arrival of 10 kV cable to the BT. These SAs are approximately in parallel, in phases. For this application SAs must be selected and tested in the factory accordingly to verify equal current distribution among them. For example, if the protective characteristics of parallel connected SAs differ only 1% one SA will absorb 64.45 kJ and other one 68.77 kJ (in one scenario of lightning stroke). Therefore, the protective characteristics of SA must be different under 1% in order to ensure equal current distribution in two parallel connected SAs.

3. Increase the cooling of SA (avoid squeezed closed spaces as places for installation).

In the described case, recommendations 2 and 3 are implemented. In the further monitoring of the BT operation will be decided whether to reduce the earth electrode resistance.

#### 4. CONCLUSION

Recommendations for improvement of existing surge protection of the switchgear of BT and reduction the number of SAs failures are:

- Reduction of earth electrode resistance of the BT;
- Increase the thermal energy absorption capability of SAs (two SAs of the same type in parallel pro phases);
- Increase the cooling of SAs;
- Further monitoring of the surge protection of the switchgear of BT and the 10 kV supply cable.

#### 5. REFERENCES

- [1] IEC 61400-24 ed. 1.0 (2010), Wind turbines - Part 24: Lightning protection
- [2] Lightning Location System <http://lls.zvne.fer.hr/lls/>
- [3] CEI 81-3 : "Valori medi del numero dei fulmini a terra per anno e per chilometro quadrato dei Comuni d'Italia, in ordine alfabetico." Maggio 1999.
- [4] [www.arqui.com/ayuda/Tekton3D/Modulos/Capitulos/SU8/Datos/MapaDensImpac.htm](http://www.arqui.com/ayuda/Tekton3D/Modulos/Capitulos/SU8/Datos/MapaDensImpac.htm)
- [5] DEHN: Lightning Protection Guide, 2nd updated edition, 2007.
- [6] IEC 62305-1 ed. 2.0. (2010-12) Protection against lightning – Part 1: General principles
- [7] V. Hinrichsen: MO Energy Handling Capability, V1.1., 10.3.2009.
- [8] ATPDraw, Windows version 5.6p6, NTNU/SINTEF, Norway.
- [9] IEEE Working Group: A Simplified method for estimating lightning performance of transmission Lines, *IEEE Transactions on Power Apparatus and Systems*, vol. 104, no. 4, July 1985.

**JURAJ HAVELKA ANTE MARUŠIĆ IGOR KUZLE  
HRVOJE PANDŽIĆ TOMISLAV CAPUDER**

[juraj.havelka@fer.hr](mailto:juraj.havelka@fer.hr) [ante.marusic2@fer.hr](mailto:ante.marusic2@fer.hr) [igor.kuzle@fer.hr](mailto:igor.kuzle@fer.hr)  
[hrvoje.pandzic@fer.hr](mailto:hrvoje.pandzic@fer.hr) [tomislav.capuder@fer.hr](mailto:tomislav.capuder@fer.hr)

**University of Zagreb Faculty of Electrical Engineering  
and Computing**

## **HANDS-ON EXPERIENCE WITH POWER SYSTEMS LABORATORY UPGRADE**

### **SUMMARY**

This paper addresses the challenges of developing a modern power system laboratory at the Faculty of Electrical Engineering and Computing, University of Zagreb. Focused on problem-based learning, the laboratory, developed together by professors and students, is a key to practical teaching of power system design, analysis and control.

**Key words:** Power system laboratory, power system design, SCADA, intuitive demonstration, laboratory education.

### **1. INTRODUCTION**

The Zagreb University Faculty of Electrical Engineering and Computing, with its 5000 currently enrolled students, offers BSc MSc and PhD degrees in field of

Electrical Engineering and Computing. At all three academic levels, the Department of Power Systems has approximately 500 students.

In the training laboratory for Power Systems at the Department of Power Systems, the practical classes of the courses Electrical Power Plants [1], Dynamics and Control of Power Systems [2] and Distribution Systems are carried out and lectured on. The purpose of practical classes and training is to enable the students to master the needed practical skills in controlled environment. Besides, the Laboratory also provides the possibility of performing various types of experiments that would otherwise be either too expensive or practically almost impossible to carry out in real electrical power systems [3]. The Laboratory consists of the following plant models: hydroelectric and thermal power plants that can operate in parallel; power system network; power loads; and substation with circuit breakers, feeder disconnectors, busbars and a number of transformers. Due to the size of the Laboratory (200 m<sup>2</sup>) and shortage of finances the Laboratory has been poorly maintained during the past years and is therefore rather outmoded. Hence the efforts have been put into the fund raising for its modernization and purchasing the essential equipment; at the same time part of the equipment was donated by sponsors. Few younger professors engaged students into revitalizing the laboratory.

## 2. GENERAL INFORMATION

The Laboratory is conceived as a miniature electrical power system (Fig. 1 and 2) that consists of the following:

- The model of thermal power plant (E1) with primary equipment: the motor simulating thermal turbine, generator, generator busbars, generator circuit breaker and feeder disconnector (serving to connect with the Faculty power system); and secondary equipment: measuring current and voltage transformers, protective relays, and power plant control system, including also the network synchroscope.
- The model of run-of-river hydro power plant (E2) with a Pelton turbine ( $Q_n=27$  l/s). At the level beneath the hydroelectric power station there is a 7000 liter water reservoir and a pump that pumps the water into the pipe leading to the turbine, thus simulating the penstock (simulated head is 60m). The hydroelectric power plant is equipped similar to the thermal power plant regarding the primary and secondary equipment. In addition to that, the important elements in this power plant are the automatic voltage regulator and the automatic generator control governor [4], [5].
- The rigid network (busbar E3) is the real external electric power network, which the two power plant models can be synchronized with; this enables the students to see the operation of the model power plant in the Croatian electric power system.
- Transformer substation with three winding transformer to which the loads can be connected. The transformer substation is fully equipped

with circuit breakers, feeder disconnectors, measuring current and voltage transformers, protection devices and control circuits.

- Different types of loads connected to power system model. These can be active and reactive (inductive and capacitive) loads, or their various combinations. They are used for simulation the dynamic operation of power plants and for changing the power plant parameters depending on connections of different types of loads [6].

The model of high voltage substation; it is discussed in further text.

A series of main lines models with circuit breakers and feeder disconnectors simulating a high voltage power system network that can be connected with or disconnected from the mentioned objects in different combinations.



Figure 1. Part of power system laboratory

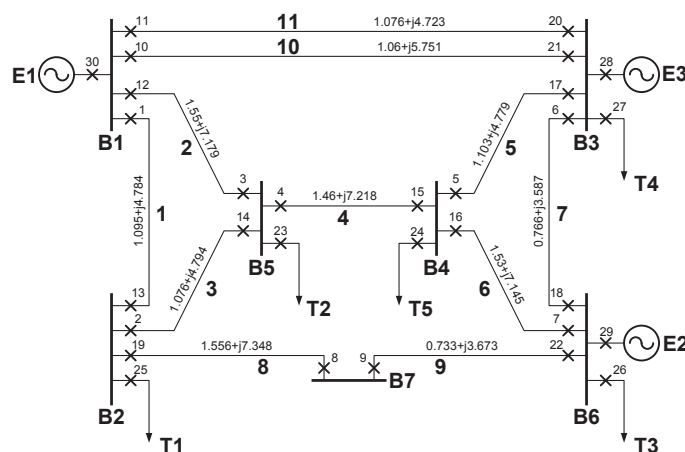


Figure 2. Part of power system laboratory

The conception of power system laboratory is based on real Croatian power system where approximately 50% of power is produced in hydro power plants and the other 50 % in thermal power plants.

### **3. THE PROBLEM**

The traditional construction of Laboratory, with no means of communication between single elements, provided challenge in its reconstruction. There was a need to equip laboratory with the most recent technologies and modern solutions used in everyday practice [7] so the students could gain the maximum benefit from practical classes. In order to improve the situation, decision was made to find the appropriate model of financing the reconstruction of the Laboratory supported by the entire Department of Power Systems staff. The very concept of the Laboratory has not been changed for it is general opinion that the model of power system is equally interesting and needed as before, today even more, since in this way the students gain the necessary practical knowledge about how the system operates.

The financing model is a topic per se, and it will not be discussed in detail. Suffice it to say that it has been agreed upon with the industrial companies interested in collaboration with our Department.

As for the new elements, the building of another thermal power plant and renewal energy sources has been planned. Besides, when all the legal requirements are satisfied, the State authorities will be asked for permission to authorize the Laboratory to test and issue certificates of operation for relay protection devices.

The reconstruction began with the simplest part: one line bay of substation. These activities have been fully completed and will be focused upon in our paper. The hydro power plant is currently being reconstructed in terms of full automation, from voltage and speed governor, various measurements, digital protection relays to automatic synchronization with the rest of electrical power system [8].

It should also be pointed out that the reconstruction of the Laboratory is designed in terms of full automation of all objects and remote control by OPC technology [9], [10]. Hence, the final objective is to design the central SCADA system for complete control of the Laboratory and to enable all those who are interested in these activities to follow up the operation of laboratory elements via the Faculty intranet [11] enabling distant learning for students. The idea is to inform all those who are interested in our activities about the reconstruction of the Laboratory, our experiences, and final outcomes. At the same time all the suggestions and ideas of those with similar experiences are highly welcomed.

### **4. RECONSTRUCTION OF THE SUBSTATION MODEL**

The model one line bay of substation has been designed in order for the students to learn how to correctly manipulate circuit breakers and feeder disconnectors in the substation [3], [12]. The major problem when dealing with the one line bay is that the feeder disconnectors do not serve to break the power circuits and should not be used for that purpose, since the circuit breakers are meant for that. However, for the more complex configuration of the substation the greater is the probability that someone might press the wrong button and instead of using the circuit breakers the power circuit is broken by feeder disconnector. It is indeed the model of a simple substation that has been installed in our Laboratory that clearly shows the mode of feeder disconnector blockage to prevent the undesired manipulation in substation and therefore possible unwanted power circuit breaking with feeder disconnector.

A single line scheme of the substation is shown in Fig. 3 (it is a three-phase system).

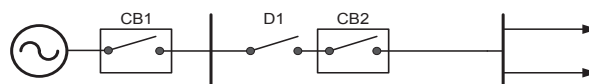


Figure 3. Single line scheme of substation, simple configuration

The substation is supplied on one side only, while on the other side there are output lines for loads. The mode of the feeder disconnectors blockage is explained to the students by using a simple substation configuration (Fig. 3), while as a task they are given a complex configuration (Fig. 4) so they can themselves produce the blockage of disconnectors.

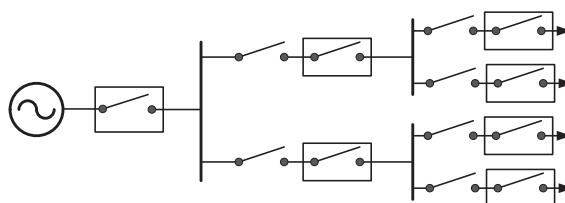


Figure 4. Single line scheme of substation, complex configuration

Before the reconstruction of Laboratory began, the practical classes were carried out on the model of substation (Fig. 5 and 6) of a rather simple configuration (Fig. 3).

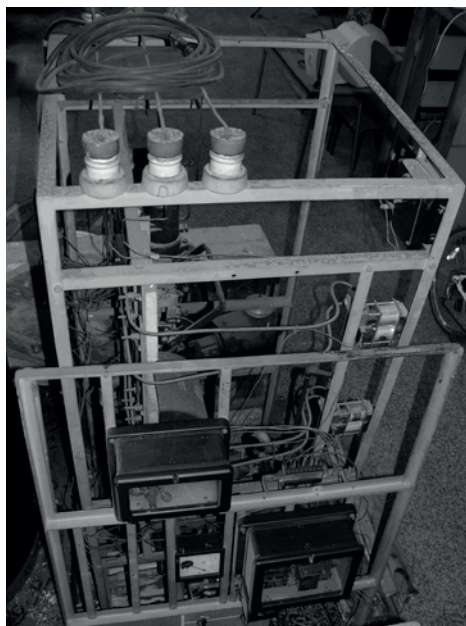


Figure 5. Part of old substation – busbars

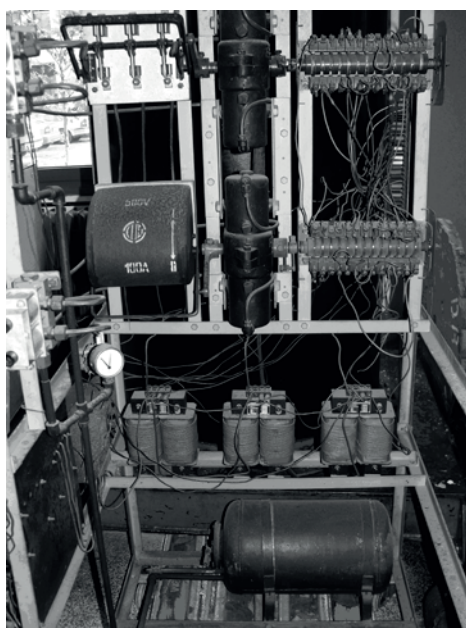


Figure 6. . Part of substation – feeder disconnecter(1), circuit breaker(2) and transformers(3)

The mere view at the above figures is sufficient without any comment as to the need for laboratory reconstruction. Fig. 5 clearly shows three busbars on top of the model high voltage substation to which the cables lead down to the feeder disconnecter, shown in Fig. 6, leading to the circuit breaker and current transformers (three transformers at the bottom of the Fig. 5). At the bottom, as shown on Fig. 6, there is also a pressurized air container connected with a compressor that maintains constant pressure. It served as a system of compressed

air which was used to control the circuit breaker and the feeder disconnecter. The control buttons were connected to the pneumatic system. The control push buttons and mode of feeder disconnecter blockage are shown in Fig. 7.

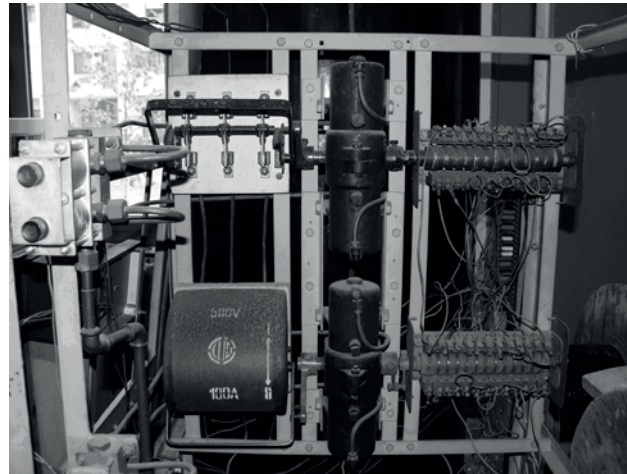


Figure 7. Control buttons(1) and blockage logic(2) in old substation

The wires and conductor rings, visible on the right side of the Fig. 7, were the logic that served to block the feeder disconnecter and circuit breaker, i.e. they responded to a simple question of whether the disconnecter should be blocked or not [13]. The operating principle was in that the conductor rings were mechanically connected to the disconnecter and circuit breaker, while they were inter-connected with wires and electrical circuits of the control push buttons. Depending on the conductor rings position, determined by the position of circuit breaker and feeder disconnecter, the electrical circuit of the control push button was either open or closed. When the feeder disconnecter control circuit was open it was not possible to operate the disconnecter with push buttons and it was blocked. Reversely, when the circuit breaker was open control circuit was closed, by pushing the control button it was possible to operate the disconnecter which then was not blocked.

The objective of practical class was to show the students how to prevent the operating staff in a substation to erroneously manipulate the disconnecters and circuit breakers [3], [12]. The described model was severely outdated, i.e. such a mode of blockage is no longer applied in modern plants [7], [23]. There was also a danger of causing injuries to students by electric shock. Other shortcomings were absence of complete measurement of currents, voltages and other parameters, and the inability to communicate with the other substation elements (no possibility of remote control), which resulted in the fact that it was not compliant with the SCADA system.

These are the principal reasons why modernization of the Laboratory was urgently needed. The Fig. 8 and Fig. 9 show the new model of substation.

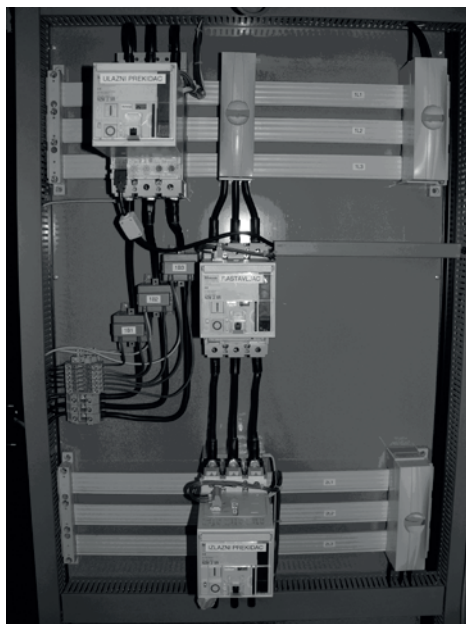


Figure 8. Model of high voltage segment

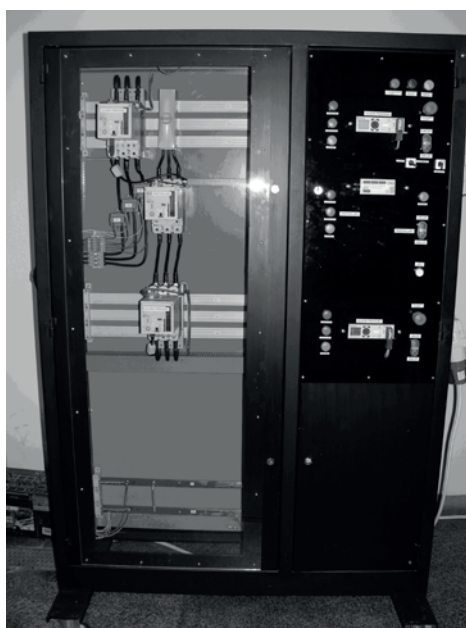


Figure 9. Model of new substation with high voltage segment and control and automation segment

It is divided (realized) into two segments. The left segment contains the model of one line bay, while the control segment with the movable control board is located on the right (Fig. 9). Since the device serves for the simulation of a high voltage plant, the model is realized by using the low voltage equipment; a careful view of Fig. 8 reveals that there is no return line, but only the three phases. Of course, there is a return line, only it is hidden so that the students can get better idea of the high voltage plant. Naturally, they are told that this is only the model

plant, while upon completion of practical class they are shown the real 10 kilovolt transformer substation that supplies the Faculty and is located within it, so that they can see the real circuit breakers, disconnectors, busbars and transformers. The developed model does not clearly differentiate the feeder disconnector from the circuit breaker as they are almost identical in appearance (using the same hardware); this is not the case in real substation, since the disconnector serves to the safety of the staff and it visibly separates the part of the plant under voltage from the voltage free segment. The students are informed about these facts in due time.

The controlling of the circuit breakers and disconnectors is simple and is performed in two ways: local - by push buttons located in the model substation, or remote - by computer serving as remote control station. If push buttons on the model are used then manual, or local, operation is employed and it is adjusted on the model itself by rotary cam switch. When automatic operation is desired (SCADA computer program) the rotary cam switch on the model should be turned from manual to automatic operation mode. The purpose is to show the students how safety at work is ensured in the substation [14] since, if it were not the case, the remote control would be possible even if some of the staff are present in the substation, which could be a life threatening situation.

The blockage of disconnector is designed in two ways. Fig. 10 shows the right segment of the model containing the control logic and automation. The first blockage mode refers to control by push buttons on the control board. This is achieved through a series of relays located at the bottom of the model, as shown in Fig. 10.

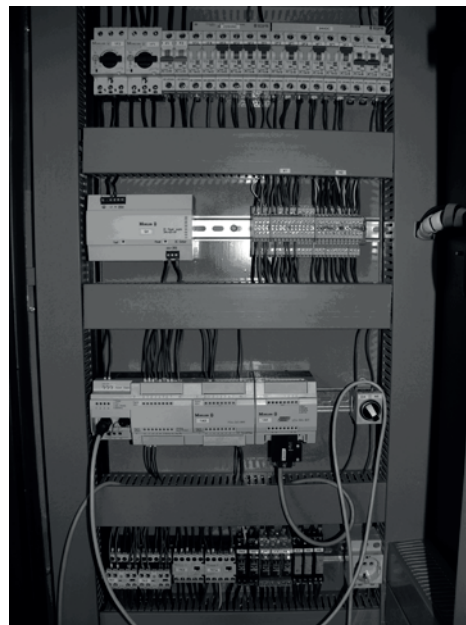


Figure 10. Relays used for disconnector blockage

They are connected with auxiliary contacts from the circuit breakers and disconnectors, which also pass across the control push buttons, allowing or not the control of the disconnectors. The relays are adjusted in the way that if the breaker 2 (Fig 3) is on, it prevents the control of disconnector 1 in a way that the electrical circuit on the push buttons for disconnector control remains open. If the breaker 1 opens then the relays close the control circuit that passes across the control push buttons for disconnector and its control is possible. In the same way functions the blockage of the mentioned disconnector if the circuit breaker no. 2 and the disconnector are open. The blockage serves to prevent the disconnector to be switched on if the breaker no. 2 is closed. If there were no blockage there would be the possibility of user connecting to the power system through the disconnector, which is not allowed.

The students learn when and how to employ blockage of the disconnector by analyzing all combinations.

Although in practice another type of blockage procedure is currently used [7], the students are shown the one using relays in order for them to learn more about the mode of blockage itself. As shown in Fig. 10, the other mode of blockage is designed by using the PLC. On its right side there is rotary cam switch which enables the selection of the desired mode of blockage: either by relays or by PLC. There is also a possibility of using both blockages simultaneously (the rotary cam switch is in neutral position). The PLC communicates with circuit breakers and disconnectors by auxiliary contacts. Every disconnector and circuit breaker has its own communication module that is connected with PLC and sends data on circuit breaker and disconnector faults and other conditions concerning the diagnostics.

A PLC contains software solutions for blockage of any disconnector. Through the serial connection the PLC is connected to the computer with SCADA software for controlling circuit breakers and disconnectors. If the software does not allow for manipulation with a certain disconnector, it is then impossible to open the desired UI in SCADA meant for controlling the given disconnector. In case of the program error in terms of possibility to open UI for control of a blocked disconnector, it is still not possible to perform control for the PLC would not allow it; during such effort the modal screen of SCADA system appears on display informing the user that at the moment it is not possible to control the disconnector and which actions should be undertaken to make it possible. It is important to know that the SCADA system for this substation model is designed by OPC technology [9], [10].

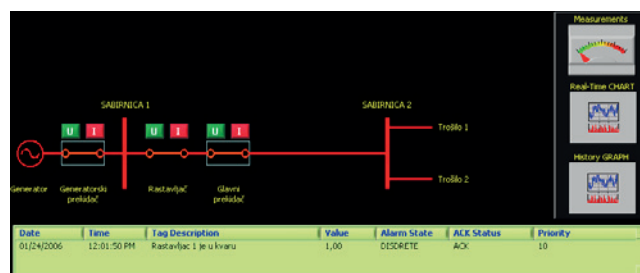


Figure 11. Single line diagram in SCADA system

Fig. 11 shows a single line diagram (from SCADA software) of the substation which can be computer controlled by the students (simpler configuration from Fig. 3). Parts of the substation without voltage are denoted by green color while the red ones have voltage. If there is a fault in either the disconnecter or the circuit breaker it blinks yellow and the alarm appears in table shown in Fig. 10 informing about the type of fault, time of its occurrence and its site (with all additional information about whether the alarm is confirmed, who has confirmed it, whether it has passed, etc.).

The students can themselves design a single line diagram for control of the configuration shown in Fig. 4 [15]. They themselves program the logic for disconnectors blockage and can check on the substation the efficacy of their programs without fear of destroying the substation and the equipment. If the student is not yet capable of programming the PLC, the software support can be designed to block the disconnectors on the computer, and then the PLC serves only as interface for collecting data from the substation and sending data to the substation from computer [16], [17]. Following data analysis, based on the program designed by the student, the computer sends command via the OPC server to the PLC.

In the substation various measurements are also performed so that the voltage, current and power in the substation can readily be seen. The measurements are made by employing voltage and current measuring transformers that are connected to digital multimeter instrument that measures and calculates all essential values (phase currents, phase and line voltages, active power, reactive power, total power per phase, sum of all powers, frequency, total harmonic distortion, etc.) [18]. The instrument is located in the center of the control board and is shown in Fig. 12. In this way the students can see at the very site the values of various substation parameters in real time.

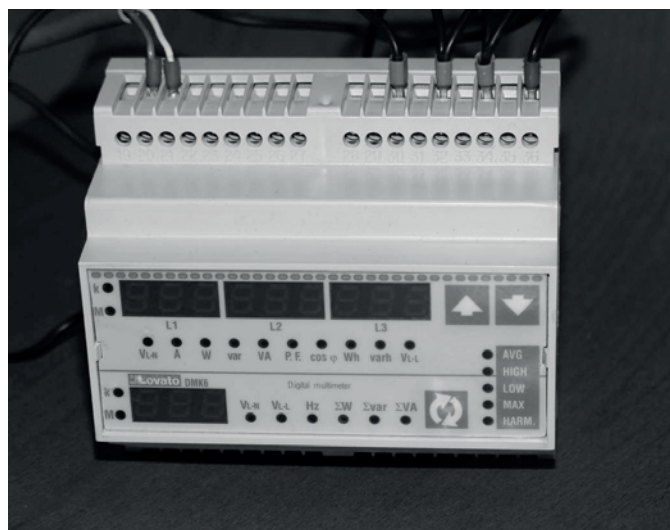


Figure 12. Digital multimeter on control board

A driver has been written for the multimeter instrument that enables communication between PLC and the instrument, by which all the measured values are automatically available to the PLC linked with the central computer. Hence the SCADA program does not serve only to control the plant, but to collect all the measured values into the database so that they can be reviewed by SCADA interface and reports made for the desired time periods if wanted (Fig. 13).

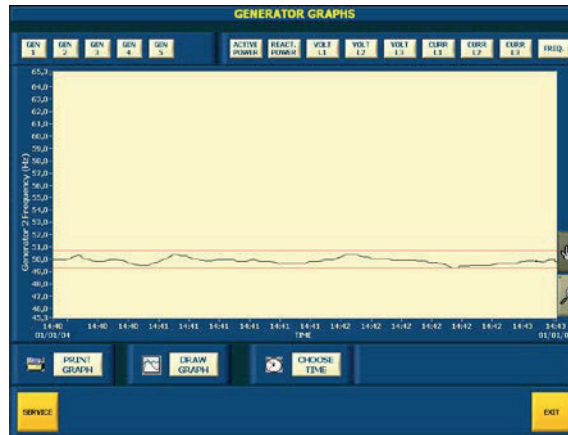


Figure 13. History viewer

With the multimeter on site it is also possible to see the real time values of all substation measured parameters remotely in the same SCADA system. Fig 14 shows UI programmed for that purpose.



Figure 14. UI showing measured real-time values and control buttons

In this way the students get the overall view of measurements in the substation, both the real time measurements and the historical measurements and therefore historical values of all measured signals as well.

It should also be pointed out that the technology of the SCADA system is entirely based on OPC technology, while the database is ODBC compatible [19], which enables the access to all data via the local network or the internet. Provided the needed licenses are obtained the students can perform certain experiments from their homes as well.

## **5. EDUCATION**

Educational approach in practical classes consists of three key elements [20]. First, the practical class is organized to discuss one topic only. Second, theory lectures focus on a given practical class topic in a way that discusses the details relevant to successful completion of a given topic only. Third, following both, the theory and practical classes, a visit is organized to the real substation where the substation staff demonstrate all that the students have learned during theory lectures and practical classes (laboratory environment). In this way close connection is achieved between the theoretical part (lectures), practical classes (laboratory), and real world application (visit to the substation). Such an approach ensures the students' great interest in the curriculum and contributes to more comprehensive knowledge about the course.

### **5.1. Lecture**

Theoretical lectures covering each practical class take 4 teaching hours weekly. During the lectures the students are given explanations on substation and its functioning [3], [21]. Further explanations are given on the construction blueprints of a substation, automation and SCADA system implementation together with proper management and operation of the substation [12]. When discussing the operation and management of the substation special emphasis is given to proper operation with the disconnectors and circuit breakers in the manner in which blockage of disconnector is made with the PLC and SCADA system. The principal objective of theoretical lectures is to enable the students to understand, at a theoretical level so far, the methods of construction planning, operation and management of the substation.

### **5.2. Laboratory classes**

The laboratory classes consist of three parts, or sections. The first two sections

take place in one day, while the third one is conceived as a homework, which the students should complete by the end of the week.

1) The first part is a demonstration class during which the students are presented with the elements of substation model and are given explanations on the methods of selecting the elements during the planning of substation construction, their purpose and how each single element works. Then the operation of substation is demonstrated, starting with proper management in order to prevent life threats, working with the circuit breakers and disconnectors locally and remotely with SCADA system, and current, voltage and power measurements are also demonstrated locally and remotely. During the final part of demonstration class the students are shown how various reports are made about the measurements in certain time periods and other reports, like e.g. alarm and event reports. A special point during the demonstration class refers to simulation of certain faults, for instance busbar short circuit and circuit breakers failures [3]. In this way the students obtain an overall picture about the substation.

2) The second part is for the students to independently design a disconnector blockage by PLC for a simple substation configuration (fig. 3). After the computer program is designed, it is tested on a substation model to find out whether it is appropriate or not. Since it is all about the substation model there is not danger for the students or the equipment in case of error in computer programming. Following the testing and corrections, if any is needed, the students control the operation of the substation locally and remotely; the control consists of the voltage, current and power measurements and of manipulation with disconnectors and circuit breakers. At the end the students make reports of events and failures in the substation and reports about measurements in given time periods in which different electrical power users were connected to or disconnected from the substation. This part of laboratory classes enables the students to gain practical knowledge based on lecture classes and on the first part of the laboratory classes.

3) The third part consists of the homework during which the students should independently design the SCADA control system for circuit breakers and disconnectors and for the measurement of electrical values. The SCADA system is designed for the complex configuration (fig. 4). Following the computer program design, the students get remotely connected to the substation and can thus check whether the program has been properly designed. This is the final part of laboratory classes during which the students are enabled to independently apply their theoretical knowledge and the knowledge gained during the first and second parts of laboratory classes. While the second section is mostly focused on team work, the third one emphasizes independent action, which is often the case in some key events in real world.

### **5.3. Real world application**

Upon completion of theoretical and laboratory classes, the students go to a one-day visit to real high voltage substation where the staff show them how it works, similar to laboratory environment, only now it is not a model substation but rather a real world one. In this way the connection is achieved between the theory,

the model, and the real world. Hence the students obtain a complete picture of the substation and are able to link the knowledge gained so far as a whole.

## 6. CONCLUSION

The new model of substation gives the students a significantly greater opportunity to get the idea of its functioning than the previous model does, starting from the possibility of one's own programming various types of disconnecter blockages, depending on the substation configuration, either by relays or PLC, or a personal computer. The students are able to change configuration of substation from a simple one toward a more complex one and vice versa. The possibility of parameter measurements and their changes depending on supply, load and condition of the substation, provides the detailed insight into the situation of real high voltage substation. The developed model enables quite a number of experiments to be conducted in controlled conditions and without any danger to the students and the plant, which would otherwise not be possible in a real high voltage substation. The examples of experiments are: inducing a three-phase short circuit on a generator terminals in thermal power station, performed on the model of thermal power station in our Laboratory, and then the analysis of the electrical plant events by the recorded waveforms of current, voltage, excitation and speed of turbine rotation prior to the fault, at the moment of fault, and after the fault. The simulation power plant is equipped with digital protective relays, enabling the analysis of their trip depending on adjustments, and coordination with other protective relays. This is only one of the many experiments that can be performed in laboratory settings.

The major difference between the previous and the current model, beside appearance and complete automation, is the possibility of communication with the substation by OPC technology. This is indeed what makes it possible for the students to program their own system and compare it with the existing SCADA one, in order to gain the feeling what this is all about. It should also be emphasized that the plant can be controlled via the network. Finally, but not the least important, the use of OPC technology enables the link between this plant and the entire laboratory supervisory control and data acquisition system (also based on OPC technology), when our Laboratory will be completely reconstructed. This means that any additional element is a modular one, making it possible to add new elements or change the old ones without interfering with the functional baseline.

## 7. ACKNOWLEDGEMENT

This work was supported by the Croatian Science Foundation under project "FENISG – Flexible Energy Nodes In Low Carbon Smart Grid" (grant no. IP-2013-11-7766).

## 8. REFERENCES

- [1] I. Kuzle, J. Havelka, H. Pandžić, T. Capuder, Hands-On Laboratory Course for Future Power System Experts, *IEEE Transactions on Power Systems*, vol. 29, no. 4, July 2014, pp. 1963-1971
- [2] I. Kuzle, K. Jurković, H. Pandžić, Development of the Power System Simulations Laboratory (in Croatian), 12. HRO CIGRE Session, Šibenik, November 08-11, 2015, C6-06, pp. 1-7
- [3] H. Požar, High Voltage Substations, 4th ed., Zagreb, Croatia, Tehnička Knjiga, 1984
- [4] F. H. Raven, Automatic Control Engineering, 5th ed., New York, McGraw-Hill, 1995.
- [5] N. Kehtarnavaz, Real-Time Digital Signal Processing, Burlington, MA, 2005
- [6] V. Venikov, Transient Processes in Electrical Power Systems, 5th ed., Moscow, Mir Publishers, 1980
- [7] N. Srb, A. Torre, B. Kosorčić, Zbirka propisa za polaganje stručnog ispita iz elektrotehničke struke: Tehnička regulativa, Zagreb, Croatia, Electrotechnical Society Zagreb, 2007.
- [8] R. Wolf, Osnove električnih strojeva, 4th ed., Zagreb, Croatia, Školska Knjiga, 1995.
- [9] F. Iwanitz, J. Lange, OLE for Process Control: Fundamentals Implementation and Application, Hüthig Verlag Heidelberg, 2001.
- [10] OPC Foundation documents, Available: <http://www.opcfoundation.org/Downloads.aspx?CM=1&CN=KEY&CI=283>
- [11] J. Travis, Internet Applications in LabVIEW, Upper Saddle River, NJ, Prentice Hall PTR, 2000.
- [12] R. W. Smeaton, W. H. Ubert, Switchgear and Control Handbook, 3rd ed., McGraw-Hill, New York, 1998.
- [13] V. Pinter, Osnove elektrotehnike (Electric Circuits), vol. 2, 4<sup>th</sup> ed., Zagreb, Croatia, Tehnička Knjiga, 1987.
- [14] N. Srb, A. Torre, B. Kosorčić, "Zbirka propisa za polaganje stručnog ispita iz elektrotehničke struke: Regulativa zaštite osoba, okoliša, materijalnih i kulturnih dobara", Zagreb, Croatia, Electrotechnical Society Zagreb, 2007.
- [15] D. J. Ritter, LabVIEW GUI Essential Techniques, New York, McGraw-Hill, 2002.
- [16] J. Travis, J. Kring, LabVIEW for Everyone, 3rd ed. Upper Saddle River, NJ, Prentice Hall PTR, 2006.

- [17] G. W. Johnson, *LabVIEW Graphical Programming*, 2nd ed., New York, McGraw-Hill, 1997.
- [18] V. Bego, *Mjerenja u elektrotehnici (Electrical Measurements)*, Zagreb, Croatia, Tehnička Knjiga, 2003.
- [19] R. M. Riordan, *Microsoft ADO.NET 2.0 Step by Step*, Microsoft Press, Redmond, Washington, 2006.
- [20] L. G. Huettel *et al.*, *Fundamentals of ECE: A Rigorous, Integrated Introduction to Electrical and Computer Engineering*, *IEEE Transactions on Education*, vol. 50, no. 3, August 2007, pp. 174-181
- [21] L. L. Grisby *et al.*, *The Electric Power Engineering Handbook*, CRC Press in cooperation with IEEE Press, Boca Raton, FL, 2001.

**Ivica Pavić      Frano Tomašević      Ivana Damjanović**  
[ivica.pavic@fer.hr](mailto:ivica.pavic@fer.hr) [frano.tomasevic@fer.hr](mailto:frano.tomasevic@fer.hr) [ivana.damjanovic@fer.hr](mailto:ivana.damjanovic@fer.hr)  
**University of Zagreb Faculty of Electrical Engineering and  
Computing**

## APPLICATION OF ARTIFICIAL NEURAL NETWORKS FOR EXTERNAL NETWORK EQUIVALENT MODELING

### SUMMARY

In this paper an artificial neural network (ANN) based methodology is proposed for determining an external network equivalent. The modified Newton-Raphson method with constant interchange of total active power between internal and external system is used for solving the load flow problem. A multilayer perceptron (MLP) with backpropagation training algorithm is applied for external network determination. The proposed methodology was tested with the IEEE 24-bus test network and simulation results show a very good performance of the ANN for external network modeling.

**Key words:** External Network Equivalent, Load Flow Analysis, Artificial Neural Network

### 1. INTRODUCTION

Power system measurement and signalization data exchange between interconnected systems still represents a significant problem for security analysis of observed power system. Inability to access needed data from the neighbouring power systems, as well as speed in processing the data to obtain satisfactory results, represent the main reasons of this. Even if the data from the neighbouring power system is accessible, considering that power systems belong to different states or countries, considerably larger problem remains the speed of obtaining the data, and achieving the simultaneity of complete data. Problem of stability and speed of

extended real-time calculation should also be taken into consideration.

Problems associated with the acquisition of external network data, and with the influence of external network on the internal network state, are most commonly solved using the steady-state external equivalents. The most popular are static equivalents known as WARD and REI equivalents, and some of their variations [1], [2], [3]. However, they often do not give acceptable results, considering that operating and switching states of external network are often unknown and therefore have to be assumed.

More complex, and thus often more accurate methods which use unreduced models of external network [4], such as state estimation or load flow based unreduced models, have also the problem of lack of information from the external network. Because of the increase of the used data, more inaccuracies in obtained data exist, and therefore there is a greater possibility of error in load flow analysis and security assessment of power systems [5], [6].

Relatively new approach in solving the problems of power system analysis is the use of ANN's, as they have provided successful results in different fields of science. So, they present a next step forward in external network modelling [7], security analysis [8] and short-term load forecasting of power systems [9]. Well trained ANN has a potential advantage over other conventional methods of equivalencing external network in significantly improving the accuracy in pattern recognition [10]. When adequately trained, ANN can quickly understand nonlinear relationship between input and output data, and apply the trained process online.

## 2. CLASSICAL METHODS OF EXTERNAL NETWORK MODELLING

### 2.1. External equivalent methods

There are two classical approaches of solving the problem of external network modeling for the needs of extended real-time calculation:

- the external equivalent approach,
- the external solution approach.

Application of external equivalent methods can be generally described in the following way:

- a) Equivalent multipoles (branches) of external network are calculated in the boundary buses for different switching states.
- b) Using the voltages in boundary buses, which are calculated using the state estimation, equivalent real-time power injections in external network are determined.

Two basic types of external network equivalents which can be gained using the afore-mentioned procedure are WARD and REI equivalent. Other methods are modified versions of these two.

Construction of WARD equivalent is based on external network data, and it is possible to represent it in two basic steps:

- a) Determination of equivalent admittance ( $Y_{equ}$ ) of external network using Gaussian elimination on bus admittance matrix of complete network (external

network is reduced to boundary buses). Given equivalent is the same for certain switching state of external network and its different operating states.

- b) Determination of additional power injections in boundary buses of WARD equivalent.

Taking into account that the power injections in the boundary buses are determined by its voltages, WARD equivalent will not give good results for the contingency analysis when an outage of internal element causes changes of those voltages. That is the reason why it is applicable, in afore-mentioned form, just for one defined switching and operating state.

Also, WARD equivalent will not give acceptable results if there are PV nodes in external network. This problem can be solved by using a modified version of basic WARD equivalent in which only the PQ nodes of external network are being reduced, and the PV nodes are kept (PV – WARD equivalent). However, for its application is necessary to know the active power and voltage magnitude in generator buses. That is why it is mostly being used for planning of transmission network. That is also a reason why a so-called extended WARD equivalent [1], [2], which can be considered a combination of basic and PV – WARD equivalent, is being used in real power systems.

Extended WARD model uses fictitious PV nodes which are added to every boundary bus to reflect the external system reactive power response to changes in the internal system. Although it gives accurate results, extended WARD equivalent is not suitable for on-line modelling of significant configuration changes of the external system since it requires all the on-line external topology information, which is very difficult to obtain.

Basic idea of REI equivalent is to concentrate all power injections from external network buses into one or more fictitious buses which are radially connected to external network. Construction of REI equivalent is possible to represent in few basic steps:

1. Power injections from external buses which are to be reduced are concentrated into fictitious node R.
2. All the boundary buses are radially connected to fictitious node G, which is connected with afore-mentioned node using the fictitious branch G – R. Admittance of the fictitious branch is determined by the power injections and voltages in the reduced buses.
3. Fictitious node G and original network buses from step 1. are eliminated.

Taking into consideration that the REI equivalent creates additional interconnections, it is preferable to use more than one equivalent. Accuracy of equivalent significantly depends on the way the external nodes are grouped into REI equivalents.

REI equivalent is considered to be suitable for contingency analysis. However, it needs to be updated constantly with information about the changes of the load and generation in the external network.

## 2.2. External solution methods

Application of external solution methods differs from external equivalent methods in two key elements:

- External network is analyzed in detail.

- External network data is extrapolated or assumed.

Therefore, external system is modeled entirely like internal system. Main disadvantage of this procedure is unavailability of all the necessary information. Unavailable information is most often estimated or extrapolated from internal system state information.

External network modeling based on power flow calculation can be demonstrated in few steps:

1. Switching and operating state of external system are determined based on the last accessible information from external network. Production of generators is determined by the principles of economic dispatching. Voltages in generator nodes are derived from assumed loads.
2. Bus loads are extrapolated based on the information about the internal network load and the entire network load.
3. Boundary buses are in power flow calculation treated as slack buses (voltage magnitude and angle are determined by state estimation of the internal network).
4. Difference between assumed and real external network information is noted as difference between power injections determined by internal network state estimation and calculation of power flows in external network.

External network modeling based on power flow calculation very often results in significant differences in boundary buses because the operating state of external network was not correctly assumed.

Better way for minimizing those differences is undoubtedly method based on state estimation. In fact, the goal of state estimation program is to determine, using the minimizing procedure, the most probable system state based on the measurements and signals.

In this case also, only a small number of measurements in external network is available, and the rest of the information needs to be assumed. Depending on how some information is gained, by assuming or by measurements, and also how accurate the measurements are, they are associated with a certain weight factor.

### 2.3. Modified Newton-Raphson method of power flow calculation

Partially modified numerical method Newton – Raphson is used for power flow calculation. Modifications of the method are necessary considering that there is another bus with regulating generator in the external network, besides the one in the internal network. In the case the inner slack bus is also a reference one, only the magnitude of voltage is known in the regulating generator bus of external network, and its voltage angle is unknown. Key information for the feasibility of the power flow calculation in that case is the interchange between two systems, which is constant and known in advance.

In *Fig 1.* is shown a simplified scheme of a network which is constituted of internal and external system. Following assumptions are made:

- Internal network has  $n$  buses altogether, of which buses marked as  $t_1-t_{int}$  are boundary buses.
- External network has  $m$  buses altogether, of which buses marked as  $s_1-s_{ext}$  are boundary buses.
- Bus marked as  $n$  is a slack bus of internal network and also a reference bus.

- Bus marked as  $n+m$  is a regulating generator bus of external network.
- There are  $g_{int}$  PV buses in the internal network and  $g_{ext}$  in the external network.
- PQ buses in internal network are marked with numbers  $1, 2, \dots, (n-g_{int}-1)$ , and in external network with numbers  $n+1, n+2, \dots, (n+m-g_{ext}-1)$ .
- PV buses in internal network are marked with numbers  $(n-g_{int}), (n-g_{int}+1), \dots, (n-1)$ , and in external with numbers  $(n+m-g_{ext}), (n+m-g_{ext}+1), \dots, (n+m-1)$ .
- Total interchange between two systems, marked as  $P_T$ , is constant.
- Parameters of all tie lines are known.

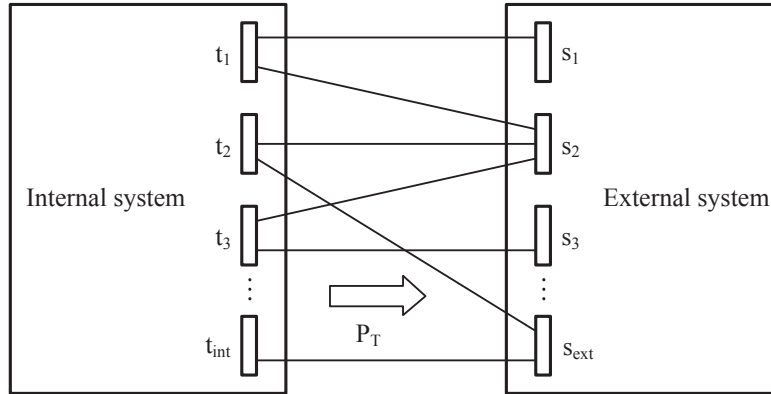


Fig. 1. Interconnected power system

As in standard Newton – Raphson method, procedure starts with assuming voltage magnitudes and angles at all PQ buses and angles at all PV buses. Voltage angle at external regulating generator bus is also assumed considering it is unknown. Assumed voltages are updated in every iteration by adding the corresponding changes to the previous values, as described in the following part.

Bus voltages are used for calculating real power injections in PV and PQ buses, and reactive power injections in PQ buses in every iteration:

$$P_{calc_i}^{(k)} = \sum_{j=1}^{n+m} |\bar{V}_i^{(k)}| \cdot |\bar{V}_j^{(k)}| \cdot |\bar{Y}_{ij}| \cdot \cos(\delta_i^{(k)} - \delta_j^{(k)} - \Theta_{ij}), \quad i = 1, 2, \dots, n-1, n+1, n+2, \dots, n+m-1 \quad (1)$$

$$Q_{calc_i}^{(k)} = \sum_{j=1}^{n+m} |\bar{V}_i^{(k)}| \cdot |\bar{V}_j^{(k)}| \cdot |\bar{Y}_{ij}| \cdot \sin(\delta_i^{(k)} - \delta_j^{(k)} - \Theta_{ij}), \quad i = 1, 2, \dots, n-g_{int}-1, n+1, n+2, \dots, n+m-g_{ext}-1 \quad (2)$$

Taking into account that the bus  $n+m$  with regulating generator in the external network is determined only by the magnitude of voltage, the calculation of power flow using the standard Newton-Raphson method would not be feasible. In modified Newton – Raphson method this problem is solved by adding the interchange of real power between two systems in the iterative calculation [12], because it is known in advance:

$$P_T^{(k)} = \sum_{i=1}^{int} \sum_{j=1}^{ext} |\bar{V}_{t_i}^{(k)}| \cdot |\bar{V}_{s_j}^{(k)}| \cdot |\bar{Y}_{t_i s_j}| \cdot \cos(\delta_{t_i}^{(k)} - \delta_{s_j}^{(k)} - \Theta_{t_i s_j}) \quad (3)$$

Calculated power injections in buses and interchange of real power are used to determine the mismatch vector. Elements of mismatch vector are defined as differences between specified and calculated real and reactive powers:

$$\Delta P_i^{(k)} = P_{spec_i} - P_{calc_i}^{(k)} \quad (4)$$

$$\Delta Q_i^{(k)} = Q_{spec_i} - Q_{calc_i}^{(k)} \quad (5)$$

As in standard Newton – Raphson method, aforementioned mismatch vector and the Jacobi matrix are used for calculating the correction vector. Correction vector determines values of voltage magnitude and angle for the next iteration.

Considering that the decoupled Newton – Raphson method is used, complete procedure is possible to separate into two parts using Jacobi submatrices  $J_1$  and  $J_4$  instead of complete Jacobi matrix:

$$[\Delta\delta]^{(k)} = \left([J_1]^{(k)}\right)^{-1} \cdot [\Delta P]^{(k)} \quad (6)$$

$$[\Delta|V|]^{(k)} = \left([J_4]^{(k)}\right)^{-1} \cdot [\Delta Q]^{(k)} \quad (7)$$

Because of the usage of the interchange power calculation of the Jacobi submatrices is also partially modified. Jacobi submatrix  $J_1$  is calculated in iteration  $k$  as:

$$[J_1]^{(k)} = \begin{bmatrix} \left(\frac{\partial P_1}{\partial \delta_1}\right)^{(k)} & \dots & \left(\frac{\partial P_1}{\partial \delta_{m+n}}\right)^{(k)} \\ \vdots & \ddots & \vdots \\ \left(\frac{\partial P_{m+n-1}}{\partial \delta_1}\right)^{(k)} & \dots & \left(\frac{\partial P_{m+n-1}}{\partial \delta_{m+n}}\right)^{(k)} \\ \left(\frac{\partial P_T}{\partial \delta_1}\right)^{(k)} & \dots & \left(\frac{\partial P_T}{\partial \delta_{m+n}}\right)^{(k)} \end{bmatrix} \quad (8)$$

For the feasibility of the calculation it is necessary to include partial derivation of real power interchange ( $P_T$ ) with respect to bus voltage angles ( $\delta_i$ , where:  $i=1, 2, \dots, n-1, n+1, n+2, \dots, n+m$ ) in the construction of Jacobi submatrix  $J_1$ , as it can be seen in (8).

Jacobi submatrix  $J_4$  is calculated in iteration  $k$  as:

$$[J_4]^{(k)} = \begin{bmatrix} \left(\frac{\partial Q_1}{\partial V_1}\right)^{(k)} & \dots & \left(\frac{\partial Q_1}{\partial V_{m+n-1}}\right)^{(k)} \\ \vdots & \ddots & \vdots \\ \left(\frac{\partial Q_{m+n-1}}{\partial V_1}\right)^{(k)} & \dots & \left(\frac{\partial Q_{m+n-1}}{\partial V_{m+n-1}}\right)^{(k)} \end{bmatrix} \quad (9)$$

Bus voltages for iteration  $k+1$  are calculated using the values of correction vector as:

$$|\bar{V}_i^{(k+1)}| = |\bar{V}_i^{(k)}| + \Delta |\bar{V}_i^{(k)}| \quad (10)$$

$$\delta_i^{(k+1)} = \delta_i^{(k)} + \Delta \delta_i^{(k)} \quad (11)$$

Iteration procedure stops when all the elements of mismatch vector are lower than the specified accuracy. Final results of calculation are voltage angles and magnitudes for all buses, from which is possible to determine power flows in both systems.

### 3. EXTERNAL NETWORK MODELING BASED ON ARTIFICIAL NEURAL NETWORKS

There are certain assumptions to be made in order for number of switching and operating states that satisfy necessary balance between power production and

consumption to be reduced to number of combinations that are relevant for power system security analysis so the power system could be optimally controlled. Load flow calculation of the whole system containing internal and external power systems are the basis in defining training sets used for neural network training algorithm.

### 3.1. Defining training sets for neural network training algorithm

In order for training set to be produced, the following assumptions are to be taken:

1. Load changes are determined based on the known daily load curve.
2. Reactive loads in all of the external network nodes are determined considering that power factor is known for all of them.
3. Availability of power production units, transmission lines and transformers is determined according to maintenance plans.
4. Taking the hydro/thermal coordination into account as well as the principles of economic dispatching, different possibilities of production management are determined to satisfy the needed load.
5. During the load flow calculation, a satisfactory voltage and reactive power regulation is obtained through assumed voltages and transformers tap-changer positions. Extreme conditions are not taken into account, because they are not present in normal operation state.
6. The load flow calculation, used for creation of training sets, tries to keep the arranged power transfer between the power systems within the agreed limits.

Next step in neural network implementation is the choice of input and output data for training. Consequently, most important variables describing interconnected power systems are to be chosen. Every power system and its external network equivalent are described through its topology and state vector, which contains voltages in all nodes. With this stated, one will come to conclusion that the output vector of neural network should contain the same data: topology and state vector which includes voltages in every node of external network. However, this approach would not yield positive results, because the same vector would contain continuous data (node voltages) and discontinuous data (topology states). Instead, important switching and operating states determined by sensitivity analysis and randomly chosen loads in external network may be taken as output training data. After that, node voltages in whole network can be determined using the load flow calculation. Input data is determined using the sensitivity analysis. Active power flows through interconnected transmission lines between internal and external network, and transmission lines close to them were designated as data most sensitive to changes in the external network, and therefore were used as input data for training sets.

### 3.2. Multilayer neural network with backpropagation training algorithm

Multilayer neural network has one input layer, one or more hidden layers and one output layer. It has three significant attributes:

1. Every neuron, basic element of neural network, contains some type of activation function. Most common used functions are logistic, tangency, hyperbolic, etc.

2. Multilayer neural network has one or more hidden layers whose purpose is to select from variety of existing hidden layers those who are important and forward them to the output layer.
3. Neurons from neighbouring layers are interconnected with weight factors, often referred to as synapses.

Multilayer neural network with backpropagation training algorithm was used in this paper. This type of neural network is characterized with double passage through the network. The first passage is forwards, when neurons are activated in particular layers on the basis of information used as input data, giving the output data as result. Then, second passage is backwards, when the weight factors between particular neurons are corrected on the basis of error calculation. Error is defined as difference between real output and expected output data. In this paper, a method of fastest gradient descent is used for error correction. With this method used, the weight factor correction is proportional to the partial derivation of the sum of  $n$  quadratic errors in  $n$ -th training example. Sigmoidal function is used as activation function, because it is commonly used for nonlinear problem solving. In addition, a learning rate  $\eta$  is used for ensuring sufficiently fast convergence to a response of weight factors, and acceleration factor  $\alpha$  is used for correction of expression that defines weight factor correction.

### 3.3. Application of artificial neural networks for power system equivalent modeling

There is a variety of scenarios that define the behavior of external network for an operating or switching state. These scenarios can be significantly different between themselves topologically and operationally, and this can complicate and slow down training process. Very often, before applying the controlled training process, training examples are grouped into clusters. Clusters are constituted from examples whose input vectors are not significantly different between themselves and therefore every switching and operating state can be observed as a cluster.

After finishing the grouping process of all prepared examples, the training process starts. All examples used for training represent the input data vector for classification of switching states. Then, for every switching state a classification of operating states is determined. Only after finishing these two processes, a recognition process can be carried out for any combination of switching and operating states. For this methodology it is typical that the process is fragmented into several levels, and the system is composed of several neural networks [11].

After the classification of switching and operating states the training process resumes with the process of recognizing the active power flows through transmission lines of external network for every single combination of switching and operating states. Considering that this data is to be very specific, an accuracy factor is very significant.

Training process is considered finished when error taken from set of examples used for random examination of neural network parameters is minimal. Also, default accuracy factor can be observed as the training stop criterion. Accuracy factor criterion is satisfied when all neurons in output layer have satisfactory accuracy factor, for all training examples.

When training process is running, a training trend and speed must be taken into account. If training process has begun with unsatisfactory starting values of

weight factors or the saturation process started too soon, training has to restart with whole new set of weight factor values. Also, if the training process has reached its local minimum, a process for abandoning the local minimum must be used, such as “simulated annealing”. If the training process is too slow, learning rate and acceleration factor must be corrected, so the process can be much faster.

Testing of trained artificial neural network is needed before using the same network for recognizing the new states. Power flows are being calculated for known input-output data that was not used for the training process. Given results are being compared with results gained by artificial neural network. If the differences between these two are within limits defined in the training process it can be stated that the artificial neural network is deciding correctly, and that it can satisfactorily reconstruct external network using the determined weight factors and measurements in internal network.

#### 4. CONCLUSION

Instead of conventional numerical methods the ANN can be successfully used for external network modeling. The planned power generation, bus loads, line outages in external network and power interchange between internal and external network are used for learning process. Once trained, an ANN is able to make decision in negligible time, because the output is obtained by simple arithmetic operations. From this reason the ANN based methodology could replace the conventional methods for external network modeling in real time operation.

#### 5. REFERENCES

- [1] F. F. Wu, A. Monticelli, Critical Review of External Network Modelling for Online security Analysis, *Electrical Power and Energy Systems*, vol.5, no.4, October, 1983, pp. 222-235.
- [2] A. Bose, Modelling of External Networks for On-Line Security Analysis, *IEEE Transactions on Power Apparatus and Systems*, vol.PAS-103, no.8, August 1984., pp. 2117-2125.
- [3] A. Monticelli, S. Deckmann, A. Garcia, B. Stott, Real Time External Equivalents for Static Security Analysis, *IEEE Transactions on Power Apparatus and Systems*, vol.PAS-98, no.2, March/April 1979., pp. 498-508.
- [4] S. Deckmann, A. Pizzolante, A. Monticelli, B. Stott, Studies on Power System Load Flow Equivalencing, *IEEE Transactions on Power Apparatus and Systems*, vol.PAS-99, no.6, November/December 1980., pp. 2301-2310.
- [5] J. F. Dopazo, M. H. Dwarakanath, J. J. Li, A. M. Sasson, An External System Equivalent Model using Real-Time Measurements for System Security Evaluation, *IEEE Transactions on Power Apparatus and Systems*, vol.PAS-96, no.2, March/April 1977., pp. 431-446.
- [6] K. L. Lo, L. J. Peng, J. F. Macqueen, A. O. Ekwue, D. T. Y. Cheng, An extended Ward Equivalent Approach for Power System Security Assessment, *Electric Power Systems Research*, vol.42, no.3, September 1997., pp. 181-188.

- [7] H. H. Muller, M. J. Rider, C. A. Castro, Artificial Neural Networks for Load Flow and External Equivalent Studies, *Electric Power Systems Research*, vol.80, no.9, September 2010, pp. 1033-1041.
- [8] K. Warwick, A. Ekwue, R. Aggarwal, *Artificial Intelligence Techniques in Power Systems* (The Institution of Electrical Engineers, London 1997).
- [9] Z. H. Ashour, M. A. Farahat, A New Artificial Neural Network Approach With Selected Inputs for Short Term Electric Load Forecasting, *International Review of Electrical Engineering (IREE)*, vol. 3 n. 1, February 2008, pp. 32 – 36.
- [10] T. Masters, *Practical Neural Network Recipes in C++* (Academic Press, San Diego, 1993).
- [11] Z. H. Ashour, S. R. Hashem, H. A. Fayed, A New Approach for Combining Neural Networks During Training for Time Series Modeling, *International Review of Electrical Engineering (IREE)*, vol. 2 n. 1, October 2007, pp. 745 – 750.

**ZORAN ZBUNJAK**

[zoran.zbunjak@hops.hr](mailto:zoran.zbunjak@hops.hr)

**HOPS Croatian Transmission System Operator Ltd.**

**HRVOJE BAŠIĆ HRVOJE PANDŽIĆ IGOR KUZLE**

[hrvoje.basic@fer.hr](mailto:hrvoje.basic@fer.hr) [hrvoje.pandzic@fer.hr](mailto:hrvoje.pandzic@fer.hr) [igor.kuzle@fer.hr](mailto:igor.kuzle@fer.hr)

**University of Zagreb Faculty of Electrical Engineering  
and Computing**

## **PHASE SHIFTING AUTOTRANSFORMER, TRANSMISSION SWITCHING AND BATTERY ENERGY STORAGE SYSTEMS TO ENSURE N-1 CRITERION OF STABILITY**

### **SUMMARY**

Since the portion of non-dispatchable renewable generators in the system is increasing, several challenges to the safety and stability of the power system have arisen. The focus of this paper is analyzing local congestion effects in the system by using three distinct methods: phase shifting autotransformer, transmission switching and battery energy storage system. This work includes a review of the congestion management techniques and the results of simulations that utilize phase shifting autotransformer to reduce power flows in the network, and transmission switching and battery energy storage system in order to ensure N-1 stability criterion in case of malfunction of the integrated autotransformer. Power system is modelled and simulated using Power Transmission System Planning Software, a software tool for electric transmission system analysis and planning. Results of simulations are presented, a thorough analysis of the results is performed and justification of investments in proposed methods is elaborated.

**Key words:** Battery energy storage, N-1 criterion, phase-shifting autotransformer, transmission switching.

## 1. INTRODUCTION

Generally, high penetration of non-dispatchable renewable generation calls for more reserves to control frequency and perform voltage regulation in the system. Locally, it is more difficult to ensure N-1 stability criterion in areas with low consumption and high renewable generation because of increased power flow through transmission lines. Increased power flow issues can traditionally be solved by building new transmission lines or by revitalizing the existing transmission lines with new lines of higher transmission capacity. This solution can be considered as a long-term solution, but several constraints of power network can make it inefficient or even technically infeasible. In areas with rare or occasional high power flow, additional transmission lines can cause higher losses because of underloaded transmission lines, resulting in higher inductions of reactive power and very high voltage levels in the network. Additionally, building a new transmission lines can be complicated because of geographical constraints and legal affairs.

Because of all the above, different solutions to mitigate high power flow issues are presented in this work: integration of phase shifting autotransformer to redirect power flow, usage of transmission switching and integration of battery energy storage systems in order to ensure N-1 stability in case of an outage of any single network element.

Case studies presented in this study are based on a real part of Croatian power system, where a complex combination of variations in power flow, generation from hydroelectric and wind power plants and non-consistent consumption during the year makes this area challenging to operate.

The following section provides a literature review on the existing research and practical solutions in applications of phase shifting autotransformer, transmission switching and integration of battery energy storage systems. Region of the Croatian power system observed in this work is described in section Description of modelled region of the Croatian power system. In section Model description, the model of network transmission system is presented. Simulations of methods to reduce power flow and ensure n-1 criterion are presented and analyzed in section Simulation of different case studies, through four case studies. Model of network transmission system is modelled and simulated using Power Transmission System Planning Software (PSS®E) [1], a software tool for electric transmission system

analysis and planning. A thorough analysis is performed and some relevant conclusions are duly drawn.

## **2. TECHNICAL WORK PREPARATION**

### **2.1. Phase Shifting Autotransformer**

Transformers in power systems are primarily used to transport electric power between two different voltage levels. Their ability of regulating voltage magnitude and voltage phase angle between two different voltage levels ensures them a significant role in regulation of the power system. Voltage magnitude regulation transformers are used to control the reactive power flow in the system, while voltage phase angle regulating transformers are used to control the active power flow in the system. Phase shifting transformers are used in power systems to control the active and reactive power flow because they have the ability or regulating both voltage phase angle and voltage magnitude.

### **2.2. Transmission switching**

Transmission switching is a tool that can be used to solve various problems in transmission system. According to reference [2], it can be used as a corrective mechanism to tackle line overloading, voltage violations and even for co-optimal generation with network topology rescheduling. It can also be used to modify network topology after outages of lines in the network, to improve efficiency of the transmission system and reduce generation costs, to ensure N-1 criterion, and as a congestion management tool.

Reference [3] describes a mixed-integer linear program for minimizing load shedding after applying a set of contingencies that can cause violations of the operation constraints. N-1 criterion was not described, and the proposed model is proven to be the most effective for high and low transmission loading conditions.

Optimal power flow problem, formulated as a mixed-integer linear program, is often used in research and operation for mathematical modelling of networks in steady state. Its application provides reliable and usable results, but in some cases it can cause system security issues as a result of angular security. Authors in [4] extend the optimal power flow problem with N-1 and voltage constraints and binary variables to satisfy N-1 and voltage security criteria.

### **2.3. Battery energy storage systems**

The idea of integration of battery energy storage in power systems with the purpose of providing services for increasing safety has recently become relevant for real-life applications, since technologies for storing energy have become more

technologically improved and economically attractive. However, literature on integration of battery energy storage in power systems to ensure N-1 criterion is quite scarce, although there are many available information and results of research on the power system safety, N-1 criterion and integration of energy systems to provide ancillary services to the power system.

In [5] a technique for optimal integration battery energy storage system in the transmission network, based on mixed-integer linear program with lossless dc representation, is presented. A technique is divided in three stages: in the first stage optimal siting's for integration are located, in the second sizing's of battery energy storages are defined, and in the third technical characteristics, capabilities and constraints of the power system and battery energy storages are introduced.

In [6], a comparative analysis of the economic and technical benefits of energy storage and N-1 network security in transmission expansion planning, based on mixed-integer linear programming approach, is performed. This analysis indicates that investment costs and generator operating costs can be reduced by integration of energy storage system into the network planning procedure, while respecting the N-1 criteria.

Enhancement of security-constrained optimal power flow with distributed battery energy storage for post-contingency power flow corrective control is proposed in [7]. The authors conclude that implementation of the proposed idea increases the utilization of transmission lines bringing them closer to their economic optimum. In [8], the authors extend the security-constrained optimal power flow model from [7] with utility-scale storage units to the unit commitment model, aiming to reduce operating costs by using storage units to reduce operating costs and for corrective control actions. Security-constrained optimal power flow is formulated as a large two-stage mixed-integer programming problem and solved using Benders' decomposition method.

Based on the literature review, dealing with increased power flows and congestion issues is a well-known problem in research community. The specific contribution of this paper is in evaluating different combinations of the proposed solutions, comparison of benefits and drawbacks of each solution and simulation of the proposed solution on a model of part of a real power system.

### **3. DESCRIPTION OF MODELLED REGION OF THE CROATIAN POWER SYSTEM AND MODEL DESCRIPTION**

The main characteristic of the Croatian power transmission system are high power flows from the south to the north of country, especially in hydrologically favorable conditions. Large hydroelectric power plants are located in the south of the country, while most of thermal power plants are located in the north, continental part of the country. Scheme of the modelled region of the Croatian power system is shown in Fig. 1. Wind farm Vrataruša, with a total installed capacity of 42 MW, is situated in the described south-north corridor. Its variable

and heavily planned generation can cause certain issues in the 110 kV part of the power transmission network. Wind power plant Vrataruša is located on an already heavily loaded 110 kV corridor between two hydroelectric power plants Senj (210 MW) and Vinodol (85 MW). With full engagement of hydro power plant Senj and wind power plant Vrataruša, 110 kV transmission line Crikvenica - Vrataruša can be overloaded. Different scenarios for mitigating this problem are analyzed through the rest of paper.

The focus of this work is mitigation of local congestion caused by non-dispatchable renewable generators and ensuring N-1 criterion.

A real part of the Croatian power system with existing problems of ensuring N-1 security criterion after integration of wind generation in the area is modelled and simulated in PSS®E.

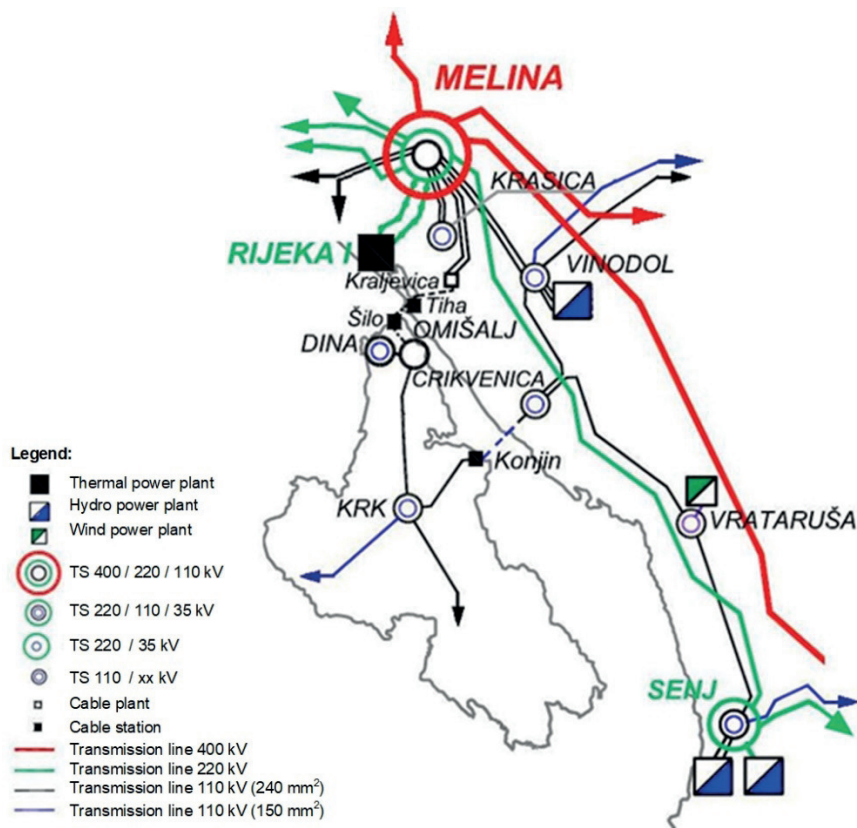


Figure 1. Power system scheme

#### 4. SIMULATION OF DIFFERENT CASE STUDIES

The base case is representing the worst scenario captured in the real world, with the highest active power flow through transmission lines in the area, caused by high generation of hydro and wind generators in the area. Case study 1 presents

the long-term solution to possible congestions in transmission lines, integration of phase shifting autotransformer. Since n-1 criterion would not be ensured in case of outage of the integrated autotransformer, possible scenario of violation of n-1 criterion is shown in case study 2. Several solutions to reduce active power ensure n-1 criterion after outage of the autotransformer are presented in case studies 3, 4 and 5, as shown in Table I.

Table I. Case studies

Case study	Description
Base case study	The worst scenario from the real world, with the highest active power flow through transmission lines
Case study 1	Integration of phase shifting autotransformer to reduce active power flow
Case study 2	Example of N-1 criterion violation – outage of the autotransformer
Case study 3	Transmission switching to ensure N-1 criterion after outage of the autotransformer
Case study 4	Integration of battery energy storage to ensure N-1 criterion after outage of the autotransformer
Case study 5	Combination of integration of battery energy storage and transmission switching to ensure N-1 criterion after outage of the autotransformer

#### 4.1. Base case study

In the base case, the transformer is operating in the voltage magnitude regulation mode, battery energy storage at busbar Vrataruša is not connected and all transmission lines are in operation, so power flow from/to other areas is fully enabled. Active power flow through transmission power lines in the presented area is shown in Fig. 2. It is shown that transmission line 110 kV Vrataruša – 110 kV Crikvenica is loaded at 108,1 MW (89,2 %) and that N-1 criterion is not ensured in case of failure of a bulk element in the area.

As mentioned in introduction, building a new transmission line or increasing the capacity of the existing line is not considered as an economically feasible solution because it would operate in underloaded mode most of the time, thus already high voltages in this area of the network would further increase. Therefore, we consider integration of phase shifting autotransformer, integration of battery energy storage and performing transmission switching.

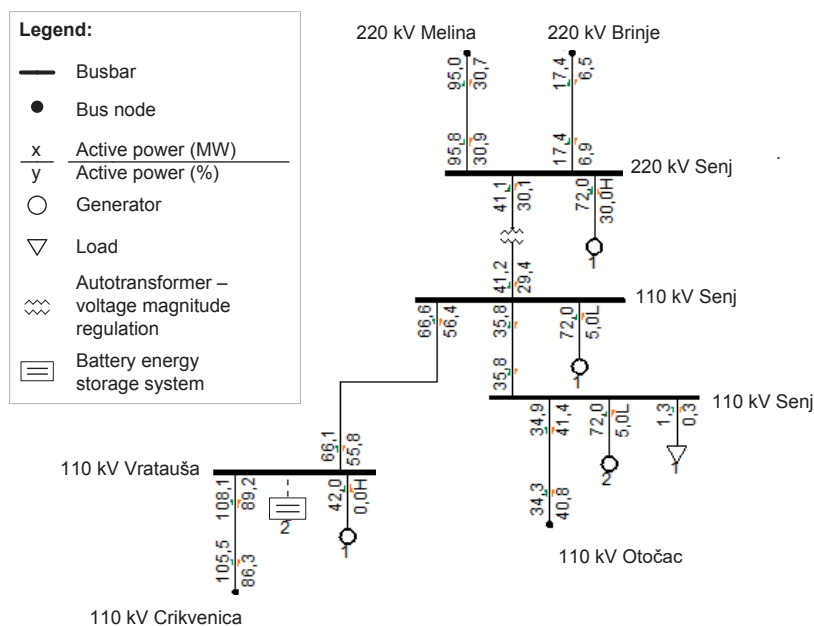


Figure 2. Active power flow in transmission power lines in the considered sub-network (base case)

#### 4.2. Case study 1

Integration of a phase shifting autotransformer is presented as a good solution to reduce active power flow in transmission lines. In Fig. 3, the results show that a high percentage of active power flow is redirected from the highly loaded 110 kV to the 220 kV network, and thus possible congestion and violation of N-1 criterion in 110 kV network are reduced. Active power flow through the endangered transmission line reduces from 108,1 MW (89,2 %) to 54,8 MW (48,8 %). It is important to notice that the N-1 criterion issue is still present in case of an outage of the phase shifting autotransformer or in case of increased power flows in 220 kV network.

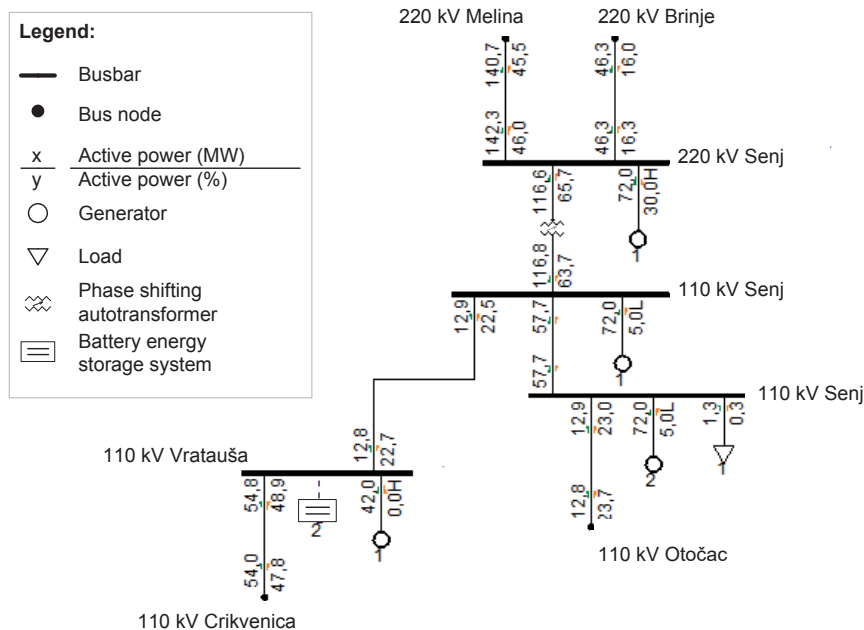


Figure 3. Integration of phase shifting autotransformer to reduce active power flow in 110 kV transmission network (Case study 1)

#### 4.3. Case study 2

Active power flow in the presented area after an outage of the phase shifting autotransformer is shown in Fig. 4, where endangered transmission line 110 kV Vrataraša – 110 kV Crikvenica is overloaded at 137,2 MW (111,8 %).

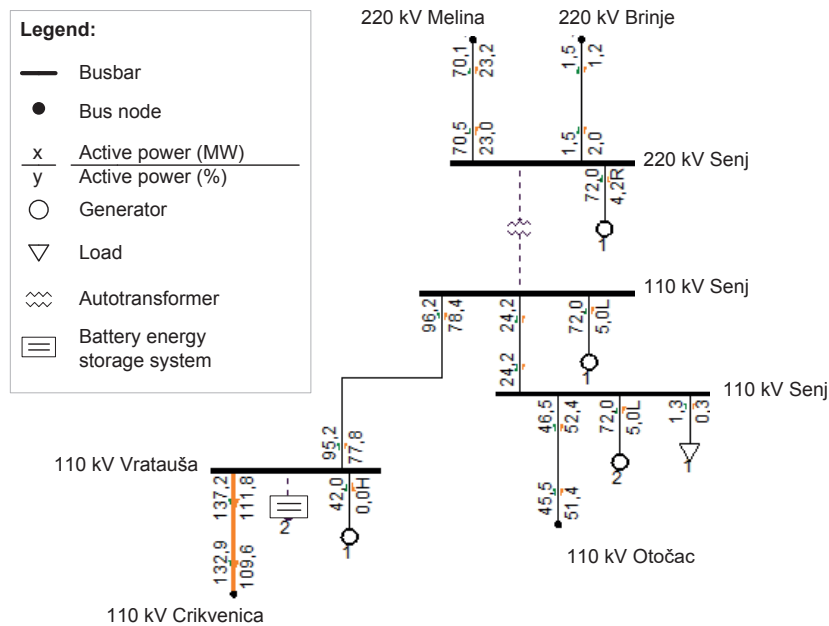


Figure 4. Example of a violation of the N-1 criterion - congestions of active power flow in transmission power lines after an outage of the autotransformer (case study 2)

There are several possible solutions to ensure N-1 criterion in the area. Replacing or upgrading the existing transmission lines with lines of higher capacity would resolve the issues of congestion and even N-1 criterion, but it would cause additional losses during most of the operating hours. In this work, two other solutions to ensure N-1 criterion are analyzed: transmission switching and battery energy storage.

#### 4.4. Case study 3

In Fig. 5, performing transmission switching after an outage of the autotransformer (shown in Fig. 4) is presented. After separation of busbars, power flows are modified according to the Kirchhoff's voltage law, where load of transmission line 110 kV Vratauša – 110 kV Crikvenica is reduced to 113,4 MW (92,4 %). Even though the results are satisfactory, transmission switching can only be used in limited number of cases when conditions in network allow, thus it cannot be considered as the long-term solution.

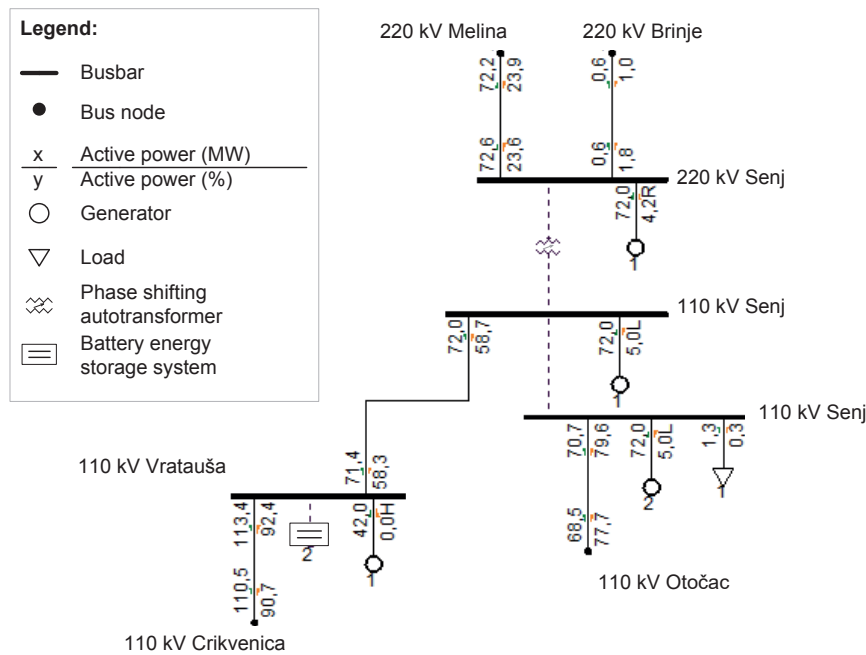


Figure 5. Transmission switching after an outage of the autotransformer to ensure N-1 criterion (case study 3)

#### 4.5. Case study 4

Integration of 20 MW battery energy storage system at one end of transmission line 110 kV Vrataruša – 110 kV Crikvenica after an outage of the autotransformer, to ensure N-1 criterion, is shown in Fig. 6. Battery energy storage in this case operates as a consumer that stores limited amount of energy. Thus, battery storage system capacity should be carefully dimensioned according to history data and future plans of generation and consumption in the area. Detailed and optimal calculation of the capacity of the battery energy storage is not a part of this work because only static analysis of power flow is simulated. It is shown that battery energy storage system reduces the loading of transmission line 110 kV Vrataruša – 110 kV Crikvenica to 121,7 MW (99,3 %).

#### 4.6. Case study 5

Combination of integration of 20 MW battery energy storage at one end of transmission line 110 kV Vrataruša – 110 kV Crikvenica and performing transmission switching after an outage of the autotransformer, to ensure N-1 criterion, is shown in Fig. 7. It is shown that this combination reduces the loading of transmission line 110 kV Vrataruša – 110 kV Crikvenica to 93,4 MW (76,1 %).

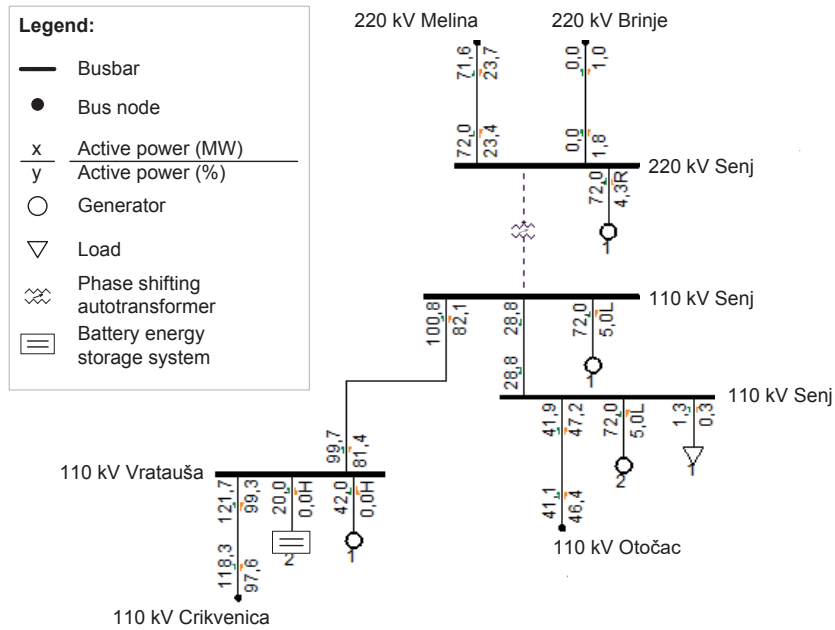


Figure 6. Integration of battery energy storage system after an outage of the autotransformer to ensure N-1 criterion (case study 4)

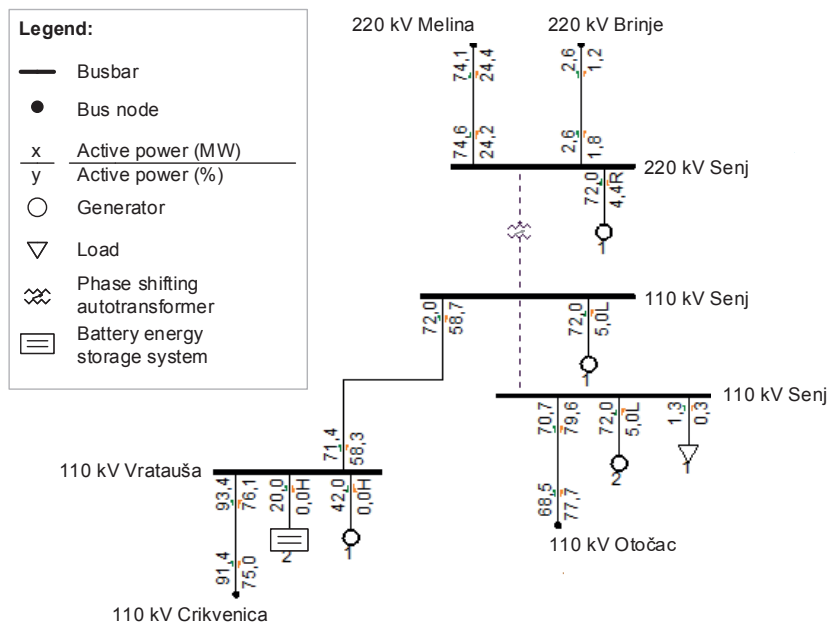


Figure 7. Combination of integration of battery energy storage system and transmission switching after an outage of the autotransformer to ensure N-1 criterion (case study 5)

#### 4.7. Analysis of the simulation results

Results from simulations of all case studies are presented in Table II, where the endangered transmission line 110 kV Vrataruša – 110 kV Crikvenica is bolded.

Table II. Active power flow for all simulated case studies

Transmission line	Active power flow (%)					
	Base case study	Case study 1	Case study 2	Case study 3	Case study 4	Case study 5
220 kV Melina – 220 kV Senj	- 30,7	-45,5	- 23,2	- 23,9	- 23,7	- 24,4
220 kV Brinje – 220 kV Senj	- 6,5	- 46,3	1,2	0,6	0	1,2
220 kV Senj – 110 kV Senj 1	- 30,1	- 65,7	0	0	0	0
Bus coupler 110 kV Senj	- 23,86	- 38,47	- 16,13	0	- 19,2	0
110 kV Senj 1 – 110 kV Vrataruša	56,4	22,5	78,4	58,7	100,8	58,7
110 kV Vrataruša – 110 kV Crikvenica	89,2	48,8	111,8	92,4	99,3	76,1
110 kV Vrataruša – Battery energy storage system	0	0	0	0	- 100	- 100
110 kV Senj 2 – 110 kV Otočac	41,4	23,0	52,4	70,7	47,2	79,6

After integration of the phase shifting autotransformer in case study 1 more power is evacuated through transmission lines 220 kV Melina – 220 kV Senj and 220 kV Brinje – 220 kV Senj, which reduces the loading of the endangered transmission line 110 kV Vrataruša – 110 kV Crikvenica. Still, after an outage of the integrated autotransformer, transmission line 110 kV Vrataruša – 110 kV Crikvenica is overloaded at 111,8 % of nominal power flow. In case studies 3 and 4, usage of transmission switching and integration of battery energy storage system used separately reduces power flow through the endangered transmission line below 100 %. Combination of transmission switching and integration of battery energy storage in case study 5 gives the best result since the power flow through the endangered transmission line is reduced to 76,1 %.

Approximate investment costs based on the existing studies and evaluations are presented in Table III.

Table III. Investment costs for all case studies

Case study	Approximate investment costs (€)
Base case study	7.500.000
Case study 1	3.000.000
Case study 2	/
Case study 3	0

Case study 4	56.000.000
Case study 5	56.000.000

Investment costs for battery energy storage are based on [9], where the investment costs are evaluated to 2.800 € per 1 kW. Therefore, the 20 MW battery energy storage the investment cost is estimated to 56.000.000 € in case studies 4 and 5. Investment costs in the base case scenario, for building new transmission lines, are evaluated based on information from [10], where the costs are evaluated at 2.500.000 € per 10 km of 110 kV transmission line. Transmission line 110 kV Vrataruša – 110 kV Crikvenica is approximately 30 km long, so overall costs for building new transmission line are evaluated at 7.500.000 €. It is important to notice that investment costs for increasing transmission capacity by only replacing the existing conductors with more efficient high-temperature conductors, based on real investment, are evaluated at 2.000.000,00 €. Transmission switching, in case scenarios 3 and 5, can be used in the existing network, so no additional costs are necessary.

Investment in phase shifting autotransformer (Case study 1) is high, but in this case it provides a long-term solution for managing power flow in the area, so the investment is justified. N-1 criteria violation issues can be efficiently solved by integration of battery energy storage system and possible usage of transmission switching. High investment costs for integration of battery energy storage can be justified by using battery energy storage in providing additional ancillary services in regulation of power system, such as primary and secondary frequency regulation, peak shaving, etc., in times when N-1 criterion is not endangered.

## 5. CONCLUSION

Managing power flow in the power system network is a complex assignment. It is necessary to maintain the safety of the network in means of ensuring the possibility of transmitting all generated power to consumers without overloading the transmission equipment, while maintaining the most efficient and economical generation schedule. Integration of non-dispatchable renewable generation makes this assignment even more challenging.

In this work, alternate solutions to increase the capacity of transmission lines are presented and elaborated through simulations of part of a real power system. In a specific area of the Croatian power system, where 110 kV network is highly loaded, especially after integration of wind power plants, integration of phase shifting autotransformer with possibility of redirecting power flow to more stable and less loaded 220 kV network is presented as the long-term solution. However, N-1 criterion can be violated in case of an outage of this autotransformer, so integration of battery energy storage in the area is presented as a good solution to preserve N-1 criterion, especially in combination with transmission switching, which yields the best results. High costs of battery energy storage can be justified by utilizing it in providing ancillary services to the power system.

## 6. REFERENCES

1. <http://w3.siemens.com/smartgrid/global/en/products-systems-solutions/software-solutions/planning-data-management-software/planning-simulation/Pages/PSS-E.aspx>
2. Hedman, K. W., Oren, S. S. and O'Neill, R. P., A review of transmission switching and network topology optimization, in 2011 IEEE Power and Energy Society General Meeting, 2011, pp. 1–7.
3. Khorram, S. A. T., Fard, A. A. T., Fotuhi-Firuzabad, M. and Safdarian, A., Optimal transmission switching as a remedial action to enhance composite system reliability, in *2015 Smart Grid Conference (SGC), 2015*, pp. 152–157.
4. Khanabadi, M., Ghasemi, H. and Doostizadeh, M., Optimal Transmission Switching Considering Voltage Security and N-1 Contingency Analysis, *IEEE Trans. Power Syst.*, vol. 28, no. 1, pp. 542–550, Feb. 2013.
5. H. Pandzic, Y. Wang, T. Qiu, Y. Dvorkin, D. Kirschen, "Near-optimal method for siting and sizing of distributed storage in a transmission network", *IEEE Trans. Power Syst.*, vol. 30, no. 5, pp. 2288-2300, Sep. 2014.
6. Obio, E. B. and Mutale, J., A comparative analysis of energy storage and N-1 network security in transmission expansion planning, *Power Engineering Conference (UPEC), 2015 50th International Universities*, INSPEC Accession Number: 15649955, DOI: 10.1109/UPEC.2015.7339947
7. Wen, Y., Guo, C., Kirschen, D. S. and Dong, S., Enhanced Security-Constrained OPF With Distributed Battery Energy Storage, *IEEE Trans. Power Syst.*, vol. 30, no. 1, pp. 98–108, Jan. 2015.
8. Wen, Y., Guo, C., Pandžić, H. and Kirschen, D. S., Enhanced Security-Constrained Unit Commitment With Emerging Utility-Scale Energy Storage, *IEEE Trans. Power Syst.*, early access.
9. <http://www.renewableenergyworld.com>
10. Yli-Hannuksela, J., The Transmission Line Cost Calculation, University of Applied Science, 2011.

Journal  
of Energy

ENERGY